CENTRO INTERNACIONAL DE ESTUDOS
DE DOUTORAMENTO E AVANZADOS
DA USC (CIEDUS)

DOCTORAL THESIS

DEVELOPMENT OF NANOCARRIERS FOR INTRACELLULAR DELIVERY OF PROTEIN DRUGS

Andrea Gonella

INTERNATIONAL DOCTORAL SCHOOL
DOCTORAL PROGRAM IN DRUG RESEARCH AND DEVELOPMENT

SANTIAGO DE COMPOSTELA
2019

USC
UNIVERSIDADE
DE SANTIAGO
DE COMPOSTELA

CENTRO INTERNACIONAL DE ESTUDOS
DE DOUTORAMENTO E AVANZADOS
DA USC (CIEDUS)

TESIS DE DOCTORADO

DESARROLLO DE NANOTRANSPORTADORES PARA LA LIBERACIÓN INTRACELULAR DE PROTEÍNAS

Andrea Gonella

ESCUELA DE DOCTORADO INTERNACIONAL
PROGRAMA DE DOCTORADO EN I + D DE MEDICAMENTOS

SANTIAGO DE COMPOSTELA
2019

USC
UNIVERSIDADE
DE SANTIAGO
DE COMPOSTELA

AUTHORIZATION OF THE THESIS SUPERVISORS

Development of nanocarriers for intracellular delivery of protein drugs

Prof. Maria José Alonso Fernández, Full professor of the Department of Pharmacology, Pharmacy and Pharmaceutical Technology at the University of Santiago de Compostela

Prof. Dolores Torres López, Associate Professor of the Department of Pharmacology, Pharmacy and Pharmaceutical Technology at the University of Santiago de Compostela

REPORT

That the present thesis, corresponds to the work carried out by Mr. Andrea Gonella, under our supervision, and that we authorize its presentation considering it gathers the necessary requirements of article 34 of the USC Doctoral Studies regulation, and that as supervisors of this thesis, it does not incur in the abstention causes established by the law 40/2015.

At Santiago de Compostela, on July 2019.

Sig.: **Maria José Alonso Fernández**

Sig.: **Dolores Torres López**

USC
UNIVERSIDADE
DE SANTIAGO
DE COMPOSTELA

AUTORIZACIÓN DEL DIRECTOR / TUTOR DE LA TESIS

Desarrollo de nanotransportadores para la liberación intracelular de proteínas

Dña. **Maria José Alonso Fernández,** Catedrática del Departemento de Farmacología, Farmacia y Tecnología Farmacéutica de la Universidad de Santiago de Compostela

Dña. **Dolores Torres López,** Profesora Titular del Departemento de Farmacología, Farmacia y Tecnología Farmacéutica de la Universidad de Santiago de Compostela

INFORMAN:

Que la presente tesis, corresponde con el trabajo realizado por Don Andrea Gonella, bajo nuestra dirección, y autorizamos su presentación, considerando que reúne los requisitos exigidos en el Reglamento de Estudios de Doctorado de la USC, y que como directoras de ésta no incurre en las causas de abstención establecidas en Ley 40/2015.

En Santiago de Compostela, Julio de 2019

Fdo.: **Maria José Alonso Fernández**

Fdo.: **Dolores Torres López**

USC
UNIVERSIDADE
DE SANTIAGO
DE COMPOSTELA

PhD CANDIDATE STATEMENT

Development of nanocarriers for intracellular delivery of protein drugs

Mr. Andrea Gonella

I submit my Doctoral thesis, following the procedure according to the Regulation, stating that:

1) This thesis gathers the results corresponding to my work

2) When applicable, explicit mentions is given to the collaborations the work may have had

3) The present document is the final version submitted for its defense and coincides with the document sent in electronic format

4) I confirm that this thesis does not incur in any plagiarism of any other authors or documents submitted by me for obtaining other degrees

At Santiago de Compostela, on July 2019

Sig.: **Andrea Gonella**

USC
UNIVERSIDADE
DE SANTIAGO
DE COMPOSTELA

DECLARACIÓN DEL AUTOR DE LA TESIS

Desarrollo de nanotransportadores para la liberación intracelular de proteínas

D. .Andrea Gonella

Presento mi tesis, siguiendo el procedimiento adecuado al Reglamento, y declaro que:

1) *La tesis abarca los resultados de la elaboración de mi trabajo.*
2) *En su caso, en la tesis se hace referencia a las colaboraciones que tuvo este trabajo.*
3) *La tesis es la versión definitiva presentada para su defensa y coincide con la versión enviada en formato electrónico.*
4) *Confirmo que la tesis no incurre en ningún tipo de plagio de otros autores ni de trabajos presentados por mí para la obtención de otros títulos.*

En Santiago de Compostela, Julio de 2019

Fdo.: **Andrea Gonella**

USC
UNIVERSIDADE
DE SANTIAGO
DE COMPOSTELA

Conflict of interest

I declare that there is no conflict of interest with the topics or materials discussed in this thesis

Sig.: Andrea Gonella

USC
UNIVERSIDADE
DE SANTIAGO
DE COMPOSTELA

Declaration of the author

All the images presented in this thesis were made by the author of the thesis. In case of images reused from other manuscripts, permission has been asked to the publishers and the mode of legal use has been indicated at the bottom of the figures.

USC
UNIVERSIDADE
DE SANTIAGO
DE COMPOSTELA

Abstract/Resumen

USC
UNIVERSIDADE
DE SANTIAGO
DE COMPOSTELA

Abstract

Cancer is one of the main causes of death in the developed countries, being the chemotherapy the main therapeutic option to treat this kind of diseases. Unfortunately, the efficacy of these treatments is often limited and the associated side effects are remarkable. To solve this problem, researchers have looked at multiple strategies, some of which involve the use of proteins and monoclonal antibodies. Proteins are highly selective and specific drugs, better tolerated by the human body, and monoclonal antibodies-based anticancer therapies are among the most promising. However, several limitations related to their low penetration into the tumor mass, the development of resistance mechanisms and their toxicity, have limited their full exploitation.

The nanoencapsulation of monoclonal antibodies appears as a promising solution to overcome these problems. Indeed, the use of a nanocarrier may facilitate the targeting and penetration of proteins across the tumor tissue, enhancing their accumulation at the target site, even at the intracellular level. It could also help to overcome the typically observed resistance mechanisms triggered by the tumor cells.

The objective of this work was to develop and characterize a new nanocarrier with the capacity to deliver monoclonal antibodies not only in the tumor extracellular matrix but also inside the cancer cells. Different nanocarriers were produced, all of them having in common two key components, i.e. the cationic surfactant ethyl lauroyl arginate (LAE) and hyaluronic acid (HA). LAE was chosen due to its amphiphilic properties and, hence, for the possibility of interacting with proteins through hydrophobic and electrostatic forces. HA was selected as the main biomaterial of the nanocarrier due to its excellent safety profile and the capacity to target the CD44 receptors.

Bevacizumab (BVZ) was selected as a model monoclonal antibody designed to target the vascular endothelia growth factor-A (VEGF-A). The nanocarriers could allow the targeting of both the extracellular, surface localized, and the intracellular pool of VEGF-A, enhancing the effect of the therapy and reducing the resistance to BVZ-based therapies

Several formulation strategies were developed using model proteins (i.e. bovine serum albumin, BSA, and a model IgG) and the knowledge generated was applied to the encapsulation of BVZ. The prototype which resulted more suitable as BVZ nanovehicle consisted of nanocomplexes of BVZ with HA and the surfactant LAE, enveloped by a HA shell. The enveloped nanocomplexes (ENCPs) were able to associate BVZ (~50% association efficiency) and were stable for 24 hours in SBF (PBS supplemented with FBS). The ENCPs provided a bi-phasic release of BVZ, with an initial burst followed by the absence of release for at least 24 hours, and they could be freeze-dried while preserving their physicochemical properties.

Cell viability studies on MDA-MB-231 breast cancer cells indicated that the ENCPs interacted with the cells and possibly facilitated the internalization of the antibody. *In vivo* studies performed in a MDA-MB-231 tumor-bearing mice model, showed that the efficacy of the free antibody was not significantly different from the encapsulated one. This limited efficacy could be attributed to a variety of reasons including, the modality of administration and dosing protocol, a potential inefficient biodistribution and/or the necessity of a combination therapy.

Resumen

El cáncer es una de las principales causas de muerte en los países desarrollados, siendo la quimioterapia la principal opción terapéutica para tratar este tipo de enfermedades. Sin embargo, la eficacia de estos tratamientos resulta a menudo limitada, ya que los efectos secundarios asociados son notables. Para resolver este problema, los investigadores han desarrollado múltiples estrategias, algunas de las cuales implican el uso de anticuerpos monoclonales. Éstos son fármacos altamente selectivos y específicos, que están dando lugar a resultados muy prometedores. Sin embargo, determinadas limitaciones de los anticuerpos monoclonales como su baja penetración en tumor, el desarrollo de mecanismos de resistencia y su toxicidad limitan todavía su explotación.

La nanoencapsulación de anticuerpos monoclonales aparece como una solución prometedora para superar estos problemas. De hecho, el uso de un nanotransportador puede facilitar el direccionamiento y la penetración en el tejido tumoral, aumentando la acumulación del monoclonal en el lugar diana, incluso a nivel intracelular. También podría ayudar a superar los mecanismos de resistencia típicamente activados por las células tumorales.

El objetivo de este trabajo ha sido el desarrollo y caracterización de un nuevo nanotransportador con capacidad para liberar anticuerpos monoclonales no solo en la matriz extracelular del tumor sino también en el interior de las células cancerosas. Para ello, se han desarrollado diferentes nanotransportadores, cuyos componentes clave son el tensoactivo catiónico, lauril arginato de etilo (LAE) y el ácido hialurónico (HA). Se eligió el LAE por sus propiedades anfifílicas y, por lo tanto, por la posibilidad de interactuar con proteínas mediante fuerzas hidrófobas y electrostáticas. El HA se seleccionó por su excelente perfil de seguridad y la capacidad de *targeting* hacia los receptores CD44.

El Bevacizumab (BVZ), cuyo *target* es el factor A de crecimiento del endotelio vascular (VEGF-A), fue el anticuerpo utilizado. Los nanotransportadores podrían facilitar el *targeting* hacia el *pool* de VEGF-A localizado tanto a nivel extracelular, como en el interior de las células tumorales, lo que aumentaría el efecto de la terapia y reduciría los fenómenos de resistencia.

Se diseñaron distintas formulaciones utilizando proteínas modelo (albúmina de suero bovino; BSA, y una IgG modelo) y el conocimiento generado se aplicó a la encapsulación del BVZ. El prototipo que resultó más adecuado como nanovehículo del BVZ estaba constituído por nanocomplejos de BVZ con HA y el tensoactivo LAE, recubiertos por una película de HA. Los nanocomplejos recubiertos (ENCPs) mostraron una asociación adecuada de BVZ (~50% de eficacia de asociación) y se mantuvieron estables durante 24 horas en fluidos biológicos simulados (PBS suplementado con FBS). Los ENCPs dieron lugar a un perfil de liberación bifásico de BVZ, con un *burst* inicial seguido por la ausencia de liberación durante al menos 24 horas. Los nanocomplejos recubiertos se pudieron liofilizar convenientemente, manteniendose sus propiedades fisicoquímicas.

Los estudios de viabilidad celular en células de cáncer de mama MDA-MB-231 indicaron que los ENCPs interaccionaban con las células pudiendo, aparentemente, facilitar la penetración del anticuerpo a nivel intracelular. Los resultados del estudio de eficacia *in vivo* en un modelo de ratón con tumor MDA-MB-231 mostraron que la eficacia del BVZ, en su forma libre o asociado a ENCPs era

similar. Esta limitada eficacia podría atribuirse a distintas razones, entre ellas, la modalidad de administración y el protocolo de dosificación, una posible biodistribución ineficaz y/o la necesidad de una terapia de combinación.

USC
UNIVERSIDADE
DE SANTIAGO
DE COMPOSTELA

Resumen *in extenso*

USC
UNIVERSIDADE
DE SANTIAGO
DE COMPOSTELA

1. Introducción

El cáncer sigue siendo uno de los principales problemas en Salud Global, con 18.1 millones de nuevos casos diagnosticados sólo en 2018 y causante de 9.6 millones de muertes) [1,2]. La Agencia Internacional para la Investigación del Cáncer (IARC) ha estimado que uno de cada cinco hombres y una de cada seis mujeres a nivel mundial desarrollarán cáncer durante su vida [3]. Entre los diferentes enfoques para tratar el cáncer, la cirugía y la radioterapia son los tratamientos de elección para los tumores locales y no metastásicos, mientras que la quimioterapia sigue siendo, pese a todos los avances terapéuticos, la opción principal para los tumores metastáticos [4–6]. En este sentido, la búsqueda de terapias más específicas que actúen de forma selectiva sobre las células cancerosas evitando así los numerosos efectos secundarios causados por su distribución indiscriminada a otros tejidos, sigue siendo uno de los objetivos prioritarios en la investigación oncológica.

Las proteínas y los péptidos terapéuticos son fármacos altamente específicos y selectivos cuya importancia ha aumentado de manera exponencial en el mercado farmacéutico durante la última década [7]. Así entre 2011 y 2016, el 26% de las proteínas terapéuticas aprobadas pertenecían al ámbito de la oncología, siendo alrededor del 48% de estos fármacos aprobados, anticuerpos monoclonales (mAbs), lo que indica el enorme potencial de estas biomoléculas [7]. De hecho, los mAbs ofrecen ventajas en términos de especificidad, potencia, tolerancia y frecuencia de dosificación, en comparación a la quimioterapia convencional. Además, su buen perfil de seguridad en comparación con el de los quimioterapéuticos ha contribuido a su rápida comercialización, todo ello potenciado por las notables mejoras en su proceso de producción, que han permitido su fabricación a gran escala [8].

Sin embargo, para que las proteínas terapéuticas consigan maximizar su eficacia en la lucha contra el cáncer, son muchos los problemas que aún quedan por resolver. Centrándonos en los anticuerpos monoclonales (mAbs), quizás los principales inconvenientes en la terapia están relacionados con su baja penetración tumoral, el desarrollo de mecanismos de resistencia, su incapacidad para bloquear antígenos intracelulares (debido a la limitada permeabilidad de la membrana celular) y su inmunogenicidad. De hecho, aunque los anticuerpos humanizados son menos inmunogénicos que los murinos, desarrollados iniciamente, aún pueden activar el sistema inmunológico [15–18].
Por otra parte, además del problema de estabilidad por agregación de la proteína en contacto con el plasma, la limitada vida media de alguna de estas moléculas sigue siendo un importante inconveniente a superar.

La nanoencapsulación de mAbs se presenta como una solución prometedora para vencer muchos de estos problemas. De hecho, el uso de un nanotransportador puede facilitar el direccionamiento y la penetración del anticuerpo en el estroma tumoral, aumentando su acumulación en el tejido diana, llegando incluso a nivel intracelular. También, las nanoestructuras ayudarían a vencer los mecanismos de resistencia desarrollados típicamente por las células tumorales para ocultarse del efecto de las distintas terapias [19–22]. Demás, si la superficie está decorada con ligandos específicos, podría favorecer la orientación de las proteínas terapéuticas hacia las células tumorales. En particular, la nanoencapsulación de bevacizumab (BVZ) se ha estudiado como una de las estrategias

más prometedoras para superar los inconvenientes que aparecen en la terapia con el fármaco libre [23–28].

Tabla 1. Ventajas que aporta la nanoencapsulación de proteinas antitumorales. Se indican en la tabla tanto las mejoras conseguidas, como los mecanismos mediante los cuales se alcanzan

Objetivo consegido	Mecanismo	Referencias
Targeting y penetración tumoral	*Targeting*: con la utilización de polímeros o ligandos que reconocen el tumor de manera selectiva. Penetración: posiblemente evitando que las proteinas tumorales se queden atascadas en la periferia del tumor.	[22,24,29,30]
Targeting intracelular	Si son adecuadamente decorados en superficie, los nanotransportadores pueden favorecer el *targeting* de antígenos intracelulares, aumentando la eficacia de la terapia o permitiendo el *targeting* de nuevos antígenos.	[20,21,31,32]
Protección frente a la degradación enzimática	Protección física de las proteínas frente a la degradación enzimática, que puede también aumentar la inmunogenicidad de la proteína.	[33,34]
Reducción de la inmunogenicidad	Las nanopartículas, si son elaboradas con polímeros específicos, pueden reducir la inmunogenicidad de las proteinas terapéuticas, evitando la adhesión de proteínas inflamatorias (*protein corona*) al fármaco proteico	[35,36]
Aumento de la vida media	En el caso de proteinas cuya vida media es corta, los nanotransportadores pueden aportar protección, propiedades *stealth*, reducir su excreción y favorecer una liberación controlada.	[37,38]

El objetivo principal de este trabajo se ha dirigido al desarrollo de nuevos nanotransportadores constituídos por ácido hialurónico (HA), con la capacidad de asociar proteínas, fundamentalmente anticuerpos, para ser liberadas en las células tumorales, y vencer los distintos obstáculos que presentan estas biomoléculas en la terapia antitumoral.

Este objetivo se ha cubierto a través de las siguientes etapas experimentales:

Desarrollo de nuevos nanosistemas constituídos por HA para la liberación de proteínas a nivel intracelular

1. Desarrollo de nanocomplejos de HA y el tensoactivo catiónico LAE, recubiertos por una capa protectora de polímero.
2. Asociación de dos proteínas modelo (BSA e IgG) a los nanocomplejos desarrollados y evaluación de su estabilidad estructural durante el proceso de formulación, así como la estabilidad y la liberación en fluidos biológicos simulados.
3. Evaluación de la estabilidad en almacenamiento de los nanotransportadores en diferentes condiciones.

Los resultados correspondientes a esa etapa se mostrarán en el Capítulo III: “Nanocomplejos de ácido hialurónico para la liberación de proteínas en las células tumorales "

Desarrollo de nanosistemas constituídos por HA para la liberación intracelular de BVZ

1. Desarrollo de nanocomplejos de HA/LAE conteniendo BVZ (HA ENCPs).
2. Evaluación de la eficacia de asociación y estabilidad funcional de BVZ.
3. Estudio de la estabilidad de los nanocomplejos en fluidos biológicos simulados y de liberación del BVZ tras la dilución del nanosistema en los mismos medios.
4. Evaluación de la estabilidad de los nanocomplejos conteniendo BVZ en su almacenamiento en diferentes condiciones.
5. Comprender la interacción de los nanotransportadores conteniendo BVZ con una línea celular de cáncer de mama. Se realizarán experimentos de toxicidad, internalización y expresión génica.
6. Evaluación de la eficacia *in vivo* de la formulación desarrollada.

Los resultados de estos estudios se presentarán en el Capítulo IV: “Nanocomplejos envueltos en ácido hialurónico cargados con bevacizumab para el tratamiento del cáncer de mama”
Este trabajo se realizó en colaboración con el Instituto Galien Paris Sud (Université Paris Sud) y Sylentis S.A. (Madrid).

2. Resultados y discusión

Se diseñaron y evaluaron diferentes tipos de nanotransportadores, teniendo todos ellos en común los componentes que constituían el núcleo del sistema, es decir, el polímero HA y el tensoactivo LAE (lauroil arginato de etilo). Se eligió el HA por su capacidad para interactuar con los receptores CD44, sobreexpresados en la superficie de algunas líneas celulares de cáncer, ya que esta interacción podría favorecer la internalización celular de los nanotransportadores mediante endocitosis [39,40]. El tensoactivo LAE se seleccionó por su carga positiva, para promover su interacción con el polímero cargado negativamente, y por sus propiedades anfifílicas y, por lo tanto, la posibilidad de interactuar con proteínas a través de fuerzas hidrófobas y electrostáticas [41].
Se desarrollaron diferentes estrategias de formulación aplicadas a proteínas modelo (BSA e IgG), utilizando el conocimiento generado en el estudio para la encapsulación del mAb bevacizumab (BVZ). El objetivo final fue comprobar el éxito en el *targeting* del anticuerpo a la diana del anticuerpo, el factor de crecimiento del vascular VEGF-A (localizada tanto a nivel extra como intracelular)

Inicialmente, se investigaron dos procedimientos diferentes, la hidratación del *film polimérico* y la técnica de inyección, para la producción de los nanocomplejos de HA, sin molécula activa. Posteriormente, se evaluó el recubrimiento de los nanocomplejos, ya conteniendo proteínas modelo, con polímeros adicionales, como una estrategia para mejorar la estabilidad de los nanosistemas en contacto con fluidos biológicos (*layer-by-layer PArg/HA ENCPs*). La técnica de inyección se eligió sobre la hidratación del *film polimérico* por ser menos agresiva (sin disolventes) y sencilla. Se

seleccionaron a continuación las cantidades adecuadas de HA y LAE (criterios: ausencia de agregados, potencial zeta negativo y tamaño alrededor de 200 nm o inferior), el orden de adición y los medios de formulación adecuados (agua MilliQ o tampón fosfato). Como proteínas modelo, se incorporaron a los nanosistemas la BSA y una IgG modelo. Como resultado, se obtuvieron tres prototipos diferentes: (i) nanocomplejos de HA conteniendo BSA (ii) nanocomplejos de HA conteniendo IgG y BSA, y (iii) una tercera formulación en la que estos últimos complejos se recubrieron con una doble capa polimérica de PArg (poli-L-Arginina) y HA, denominada *layer-by-layer* PArg/HA ENCPs (Tabla 2).
Las estrategias de formulación se adaptaron a las características de cada proteína específica. Por ejemplo, en el caso de la formulación de nanocomplejos conteniendo IgG, se hizo necesaria la presencia de BSA para estabilizar los sistemas en fluidos bilógicos simulados (SBF) conteniendo sales. Cuando el protocolo utilizado, se aplicó a la asociación de BVZ, se obtuvieron agregados. La adaptación del procedimiento, disminuyendo la cantidad de HA y recubriendo los nanocomplejos con una capa adicional de HA (Figura 1) ayudó a preservar su estabilidad.

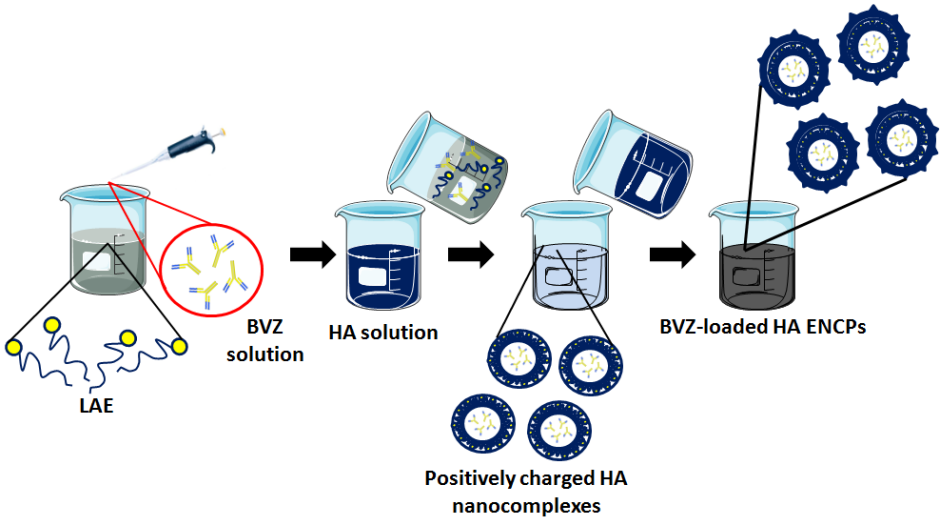

Figura 1. Representación esquemática de la formación de los ENCPs de HA cargados con BVZ (BVZ-loaded HA ENCPs).

Tabla 2. Comparación de las características de los nanocomplejos de HA cargados con BSA, nanocomplejos de HA cargados con BSA/IgG, ENCPs de PArg/HA layer-by-layer y ENCPs de HA con BVZ (BVZ-loaded HA ENCPs). En la tabla se indican el medio de formulación, las cantidades y volúmenes de LAE y HA y las propiedades fisicoquímicas de las formulaciones.

Prototipo de formulación	Medio de formulacion	Cantidad de LAE (mg)	Volumen de LAE (µL)	Cantidad de HA (mg)	Volúmen de HA (µL)	II capa de HA	Tamaño (nm)	ζ (mV)	% AE	% LC
Nanocomplejos de HA cargados con BSA	Tampón fosfato pH 7.2	2	250	2	500	No	292 ± 36	-31±4	97	33
Nanocomplejos de HA cargados con BSA/IgG	Agua MilliQ	2	250	2	500	No	220 ± 22	-26±4	98*	2.4*
ENCPs de PArg/HA *layer-by-layer*	Agua MilliQ	2	250	2	500	Yes**	191±16	-25±1	85*	1.7*
ENCPs de HA cargados con BVZ	Agua MilliQ	2	250	0.25	500	Yes***	179±8	-27±1	42 or 48****	7.3 or 1.5****

AE (%) = eficacia de asociación (%); LC (%) = capacidad de carga (%) (experimental); BSA= albúmina sérica bovina; BVZ = bevacizumab; ENCPs = nanocomplejos recubiertos; MQ: nanocomplejos formulados en agua milliQ; BP: nanocomplejos formulados en tampón fosfato.

**AE and LC están calculadas en relación a la IgG;*

*** Los nanocomplejos de HA cargados con BSA/IgG se recubrieron con una primera capa de poli-L-arginina (PArg) y una segunda capa de HA: se añadieron 450 µL de poli-L-arginina sobre 450 µL de los nanocomplejos de HA cargados con BSA/IgGs y posteriormente, se añadieron 200 µL de de una solución de HA (3.1 mg/mL) sobre 200 µL de los nanocomplejos recubiertos con PArg.*

****Se añadieron 500 µL de una solución de HA (2 mg/mL) sobre 500 µL de los nanocomplejos cargados con BVZ.*

***** Se han utilizado ENCPs de HA con dos contenidos iniciales de BVZ diferentes: 75 µg (correspondientes a una carga proteica final de 1.5%) y 375 µg (correspondientes a una carga proteica final de 7.3%).*

Los nanotransportadores desarrollados se caracterizaron en cuanto a sus propiedades fisicoquímicas, eficacia de encapsulación, estabilidad en fluidos biológicos simulados, estabilidad en el almacenamiento y liberación. También se realizaron estudios relacionados con la estabilidad estructural de las proteínas encapsuladas para evaluar la funcionalidad de la proteína.

Tamaño de los nanosistemas

La Tabla 2 presenta las principales diferencias entre las propiedades de los sistemas obtenidos de acuerdo con las distintas estrategias. Destaca por ejemplo el diferente tamaño de los prototipos evaluados. Así, la presencia de sales en los medios de formulación aumenta el tamaño de los nanocomplejos (como es el caso de los nanocomplejos de HA conteniendo BSA, elaborado en tampón fosfato). La presencia de iones apantalla las cargas tanto de LAE como de HA, y conduce a la co-precipitación de la proteína y los polímeros en forma de complejos mas grandes [42–44].

Curiosamente, cuando se utilizó BSA, se formó un complejo entre la proteína y el LAE, mientras que esto no sucedió con el BVZ. Ello se debe probablemente a las diferentes propiedades de las proteínas y, por lo tanto, a su diferente interacción con los polímeros. A pH neutros, la BSA tiene una mayor tendencia que los anticuerpos a interactuar con la cabeza catiónica del LAE (por ejemplo, el pI de BSA es 4.7, mientras que el de BVZ es 8.3). Además, la BSA puede interactuar también a través de fuerzas hidrófobas [45].

La formación de múltiples capas en torno a los nanocomplejos (ENCPs de PArg/HA *layer-by layer*) dio lugar a una reducción del tamaño de los mismos. Esto se debe probablemente a la compresión electrostática ejercida por las capas de polímero adheridas a la superficie, lo que conduce a la formación de una estructura más compacta, como ya se observó con otras nanopartículas de múltiples capas [46,47]. Curiosamente, los ENCPs de HA cargados de BVZ mostraron el menor tamaño, probablemente debido a la ausencia de BSA y a la menor cantidad de HA utilizada para formar el núcleo de los nanocomplejos.

En la Figura 2, se puede apreciar el aspecto de los nanocomplejos de HA con BSA, y de los diferentes ENCPs de HA en las imágenes tomadas por STEM y TEM. En todos los casos, interacción entre LAE y HA dio lugar a sistemas esféricos, independientemente de la estrategia de formulación utilizada.

Estabilidad de los nanosistemas en fluídos biológicos simulados (SBF)

Se han detectado también diferencias entre formulaciones relacionadas con su estabilidad en SBF. De hecho, la BSA resultó fundamental para conferir estabilidad a los nanocomplejos de HA que encapsulaban IgG, tras su dilución en SBF conteniendo sales (PBS). Una posible hipótesis que

explique este comportamiento es que la BSA podría formar una cubierta protectora alrededor de los nanocomplejos (similar a la bien conocida corona proteíca) y funcionar como un ancla para ambos, la IgG y el LAE. De hecho, debido a sus propiedades anfifílicas, la BSA podría interactuar con las colas hidrófobas del tensoactivo, formando un núcleo más compacto, estabilizando así la formulación en SBF [48].

El recubrimiento con la doble capa polimérica (ENCPs con tecnología l*ayer-by-layer*) se desarrolló para estabilizar las partículas en un medio más complejo conteniendo proteínas (10% de suplemento de FBS). En el caso del prototipo HA ENCPs conteniendo BVZ, el tamaño disminuyó tras la dilución en el SBF suplementado; sin embargo, el tamaño se mantuvo estable durante al menos 24 horas sin la necesidad de BSA o de capas múltiples.

Todas estas observaciones sugieren que las propiedades fisicoquímicas de la proteína y, potencialmente, la configuración de la proteína, son críticos en el proceso de formulación.

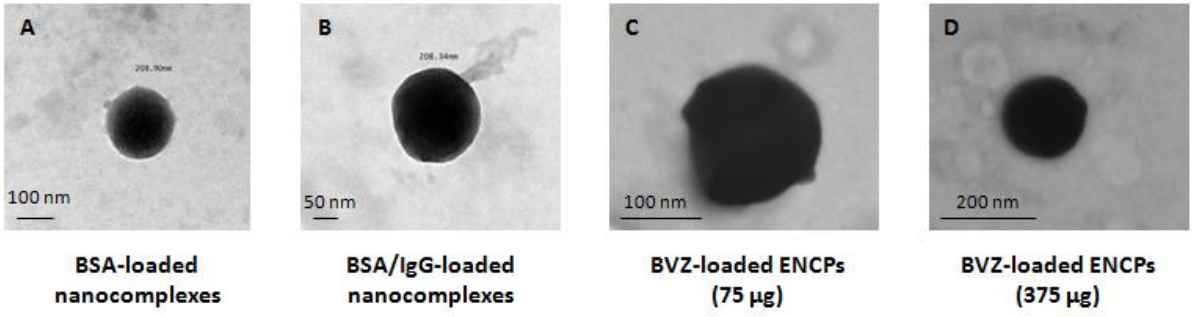

Figura 2. Imágenes de microscopia electrónica STEM y TEM de los prototipos desarrollados. (A) nanocomplejos de HA cargados con BSA (TEM); (B) nanocomplejos de HA cargados con BSA/IgG (TEM); (C) ENCPs de HA cargados con BVZ (75 µg) (STEM); (D) ENCPs de HA cargados con BVZ (375 µg) (STEM). Desafortunadamente, las fotos de microscopia de los ENCPs de PArg/HA layer-by-layer no están disponibles.

Asociación de las proteínas y capacidad de carga de los nanosistemas

Se ha podido apreciar una fuerte influencia de la composición de la fase acuosa en la que se incorporan las proteínas sobre la eficacia de asociación y la capacidad de carga de los nanosistemas. De hecho, se observó por ejemplo que cuando la IgG se disolvía en la solución acuosa de HA, se obtenían cargas de proteína más bajas en comparación con las obtenidas cuando la proteína se disolvía en la solución acuosa de LAE. Se hace evidente, por lo tanto, que la IgG interacciona más favorablemente con el LAE que con él HA. Ello se debe probablemente a la capacidad del anticuerpo de interaccionar con el LAE a través de fuerzas hidrófobas y electrostáticas, mientras que con él HA no es posible que se establezcan dichas interacciones. A este respecto, se han utilizado alternativas similares para formar micelas autoensambladas que asociaban lisozima o trastuzumab a polímeros modificados hidrofóbicamente[22,49].

Finalmente, las eficacias de encapsulación obtenidas incorporando las proteínas en la solución de LAE resultaron elevadas para la BSA (97%) y la IgG (98 y 85%),

En el caso del BVZ, se desarrollaron ENCPs conteniendo cantidades diferentes de BVZ (75 μg y 375 μg), tal y como indica la Tabla 2. En ambos casos, la eficacia de asociación experimentó una reducción, situándose en torno al 42-48%, respectivamente. En este caso, además de las características del BVZ, de las que cabe esperar una menor interacción con el LAE, hay que considerar que la formulación comercial de BVZ que se utilizó en la formulación, contenía diferentes componentes, entre ellos sales, que pueden alterar también la interacción.

Liberación de las proteínas a partir de los nanosistemas

Con respecto a la liberación de las moléculas modelo, se obtuvo un perfil bifásico caracterizado por una liberación *burst* inicial seguida de un proceso muy lento de liberación. El efecto *burst*, observado típicamente en nanotransportadores conteniendo proteínas, podría atribuirse al desprendimiento de las moléculas de situadas cerca de la superficie de los nanosistemas [50,51]. La alta osmolaridad del medio de liberación, favorecería este proceso. Esto corrobora la idea de que la interacción de la proteína con el nanotransportador estaría, al menos en parte, mediada por fuerzas electrostáticas [52,53]. Sin embargo, otro tipo de interacciones (hidrófobas, enlaces de hidrógeno, interacciones dipolo-dipolo, etc.) podrían participar en la formación de los nanosistemas, ya que el tamaño estable se mantuvo durante al menos 24 horas.

Estabilidad estructural y funcional de las proteínas asociadas

Conociendo la capacidad de los tensoactivos iónicos para desestabilizar la estructura de las proteínas [54,55], evaluamos la estabilidad estructural y funcional de las proteínas formuladas en forma de nanocomplejos utilizando el dicroismo circular y la técnica ELISA. Los resultados indicaron que la estabilidad estructural de la BSA no se vio afectada por las diferentes estrategias de formulación. De forma similar, se encontró que la estabilidad funcional de BVZ no se modificó al asociarse con los nanosistemas.

Liofilización de los nanosistemas

Teniendo en cuenta la necesidad de preservar la estabilidad de las formulaciones en el almacenamiento [56], las formulaciones se liofilizaron utilizando diferentes crioprotectores. La trealosa resultó ser la más adecuada para todos los prototipos, sin embargo, en el caso de los ENCPs de HA conteniendo BVZ (375 μg) (formulación con la mayor carga de anticuerpo), fue necesario agregar PEG-400 para preservar su estabilidad.

Estudios *In vitro* en cultivos celulares

La toxicidad y la internalización de las ENCPs de HA conteniendo BVZ, se evaluaron en una línea celular de cáncer de mama (MDA-MB-231). Los ENCP con el mayor contenido en BVZ (7.3%) fueron las formulaciones sometidas al estudio.

Los resultados indicaron una disminución significativa en la viabilidad celular cuando las células se expusieron a las ENCPs-BVZ a concentraciones de BVZ superiores a 15 μg/mL (127 μg/mL de nanotransportador) durante 72 horas. La toxicidad se debió probablemente a la presencia del tensoactivo cargado positivamente, ya que se mostraron perfiles de toxicidad muy similares cuando las células se trataron con los ENCP sin fármaco o con el LAE solo. De hecho, es frecuente que los

tensoactivos catiónicos exhiban una cierta citotoxicidad, normalmente atribuida a su capacidad para alterar la membrana celular [41,57–61].

Está bien documentado que el depósito intracelular de VEGF-A es fundamental para el crecimiento, la migración y la invasión de las células cancerosas [62,63], así como para el reclutamiento de células madre derivadas de la médula ósea, una posible fuente de resistencia a los tratamientos con BVZ [64,65]. Basándonos en esto, nuestra hipótesis ha sido que la asociación de BVZ a un nanotransportador puede facilitar el acceso al VEGF-A intracelular. Hasta ahora se han hecho varios intentos para alcanzar este objetivo, y algunos de ellos han dado resultados positivos. Por ejemplo, cuando el BVZ se incorporó en liposomas y se administró junto con un agente fotosensibilizante [25,65], se observó una disminución en el crecimiento del tumor. Los autores plantearon la hipótesis de que la administración intracelular de BVZ podría bloquear la cascada de señales antes de su iniciación, evitando la regeneración del tumor y superando el efecto de los mecanismos de resistencia potenciales.

En este trabajo, hemos observado que el BVZ asociado a los ENCPs interacciona con la línea celular de cáncer de mama MDA-MB-231 (Figura 3). De hecho, tras 1 hora de incubación con las ENCP cargadas con FITC-BVZ, se pudo identificar la presencia de fluorescencia atribuible al BVZ, aparentemente, dentro de las células. Por el contrario, dicho efecto no se observó para el BVZ libre. Además, se observó que la presencia de LAE facilitaba la aparente internalización del anticuerpo libre. Sería deseable realizar experimentos adicionales dirigidos a verificar la internalización del anticuerpo y los mecanismos involucrados en el proceso, tanto in vitro como in vivo [25].

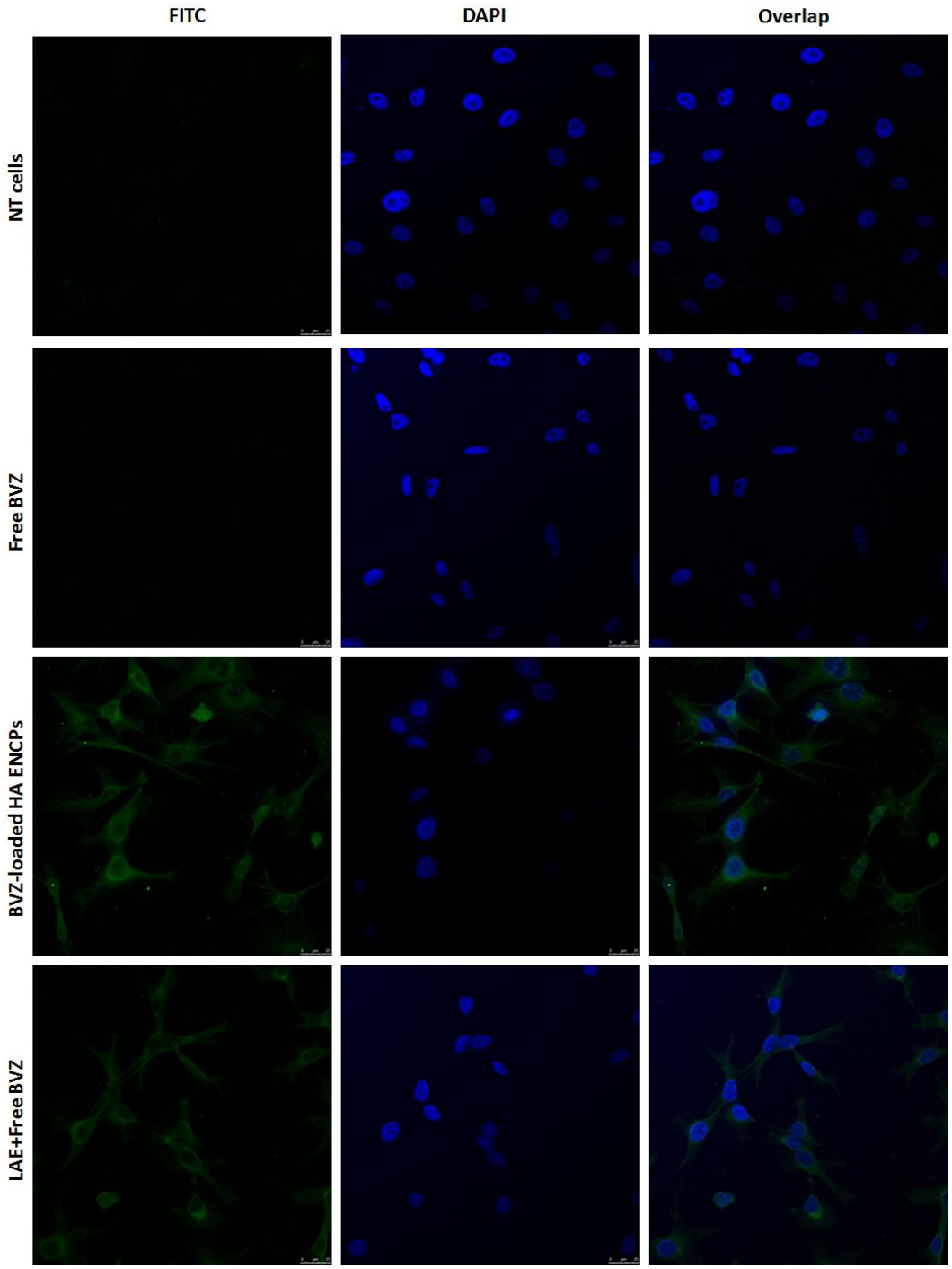

Figura 3. Estudios de internalización celular. El BVZ asociado a los ENCPs se marcó con FITC, obteniéndose las imágenes por microscopía láser confocal, tras 1 hora de incubación con células MDA-MB-231. También se muestran los controles de células no tratadas (células NT), BVZ libre y la mezcla física de BVZ y LAE (LAE + FreeBVZ). Se usó DAPI para marcar el núcleo de las células.

También se llevaron a cabo experimentos orientados a investigar la influencia de los ENCP-BVZ en la expresión de algunos de los genes involucrados en la ruta del VEGF. Incluso si el objetivo natural del BVZ es el VEGF-A, la función del VEGF-A podría ser reemplazada por los otros factores de crecimiento de la familia VEGF [66–68], por lo tanto, la expresión de los otros genes que pertenecen a la misma familia de proteínas (VEGF-B, VEGF-C y VEGF-D) también se investigaron. Los resultados no

mostraron variaciones significativas en la expresión del RNAm que pudieran atribuirse a la internalización del anticuerpo. Probablemente, el resultado más interesante de este conjunto de experimentos fue el encontrado con los ENCP-BVZ sobre la expresión de VEGF-A. Tras una exposición de 48 horas, los niveles de expresión del gen disminuyeron en comparación con el período de 24 horas, mientras que no se observó el mismo efecto para los grupos control (BVZ libre y ENCP sin anticuerpo). Sería necesario completar el estudio con más experimentos que correlacionen el gen con el patrón de expresión de proteínas, estudiando un mayor número de genes (es decir, análisis basados en chips de genes). Con ellos se podría llegar a comprender el efecto de la liberación intracelular de BVZ, y también si hay más genes involucrados en la respuesta de bloqueo al VEGF-A [69,70].

Estudios de eficacia In vivo

Finalmente, se realizó un experimento de eficacia *in vivo*. Los resultados indicaron que tras el tratamiento intraperitoneal con BVZ a ratones con tumores de mama MDA-MB-231, ya sea en forma libre o asociado a los ENCP, se observó una reducción estadísticamente significativa en el crecimiento del tumor (a partir del día 19). Sin embargo, no se observaron diferencias significativas entre los dos tratamientos (Figura 4). Como se esperaba, el crecimiento del tumor y la necrosis se mostraron más rápidos en los grupos no tratados con BVZ.

Se pueden encontrar distintas explicaciones para la respuesta limitada al tratamiento. Una de ellas podría estar relacionada con la modalidad de inyección y la dosis inyectada. En humanos, el BVZ se administra por vía intravenosa a una dosis alta (10-20 mg/kg), mientras que en el experimento que se describe se utilizó una administración intraperitoneal de una dosis relativamente baja (6.3 mg/kg). Un tratamiento a ratones en una etapa más temprana también podría ser una opción que aumentase la eficacia de la terapia. Varios artículos indican que un tratamiento con BVZ 1 o 2 días después de la inyección de células tumorales redujo significativamente el crecimiento del tumor en comparación con los grupos de control [71–73]. Por otro lado, deberán realizarse estudios de biodistribución para aclarar los posibles problemas de acceso a tumor del anticuerpo asociado al nanosistema. También, serían interesantes estudios sobre el grado de densidad vascular y la cobertura de pericitos para discernir un problema potencial de difusión a través del estroma tumoral [74,75]. Finalmente, una terapia de combinación también sería una posible alternativa para mejorar la eficacia de la terapia. De hecho, los pocos estudios *in vivo* que muestran efectos significativos con BVZ nanoencapsulado, administraron el anticuerpo junto con un agente quimioterapéutico o fotosensible, atribuyendo la mejora en la terapia a la internalización de ambos fármacos [25,65].

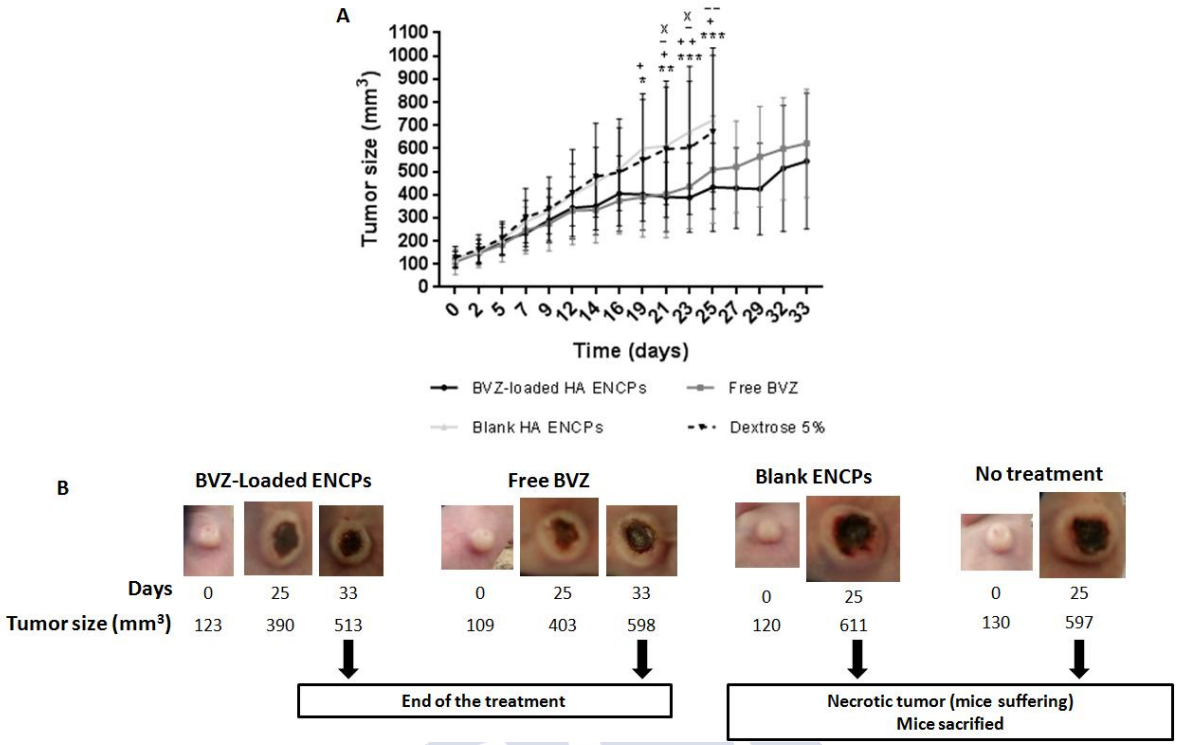

Figura 4. Crecimiento tumoral durante el tratamiento

A) Evolución del volumen tumoral en ratones con tumores MDA-MB-231 tras la administración intraperitoneal de ENCPs de HA cargados con BVZ, BVZ libre, ENCPs de HA blancos y solución de dextrosa al 5%. A continuación se señalan las diferencias significativas entre grupos:

**= ENCPs de HA con BVZ y ENCPs de HA.blancos (*p<0.05, **p<0.01 y ***p<0.001)*

+ = BVZ libre y ENCPs de HA con BVZ ($^{+}$p<0.05 and $^{++}$p<0.01)

- = ENCPs de HA con BVZ y dextrosa 5% ($^{-}$p<0.05 and $^{--}$p<0.01)

x= BVZ libre y dextrosa 5%. (^{x}p<0.05 and ^{xx}p<0.01)

No se encontró ninguna diferencia estadísticamente significativa entre los grupos ENCPs de HA con BVZ y BVZ libre al final del tratamiento

.B). Fotos del tumor durante las diferentes etapas del desarrollo (las fotos corresponden a un único ratón por grupo). El tamaño tumoral indicado se refiere a la media de los tamaños tumorales de cada grupo. El crecimiento tumoral de los grupos control (ENCPs de HA blancos y BVZ libre) fue más rápido y el tumor entró en fase de necrosis en una fase más temprana en comparación con los grupos que recibieron el tratamiento con BVZ libre o nanoencapsulado.

3. Conclusiones

El objetivo del presente trabajo consistió en el diseño y desarrollo de nuevos nanotransportadores constituídos por HA para la asociación y liberación de anticuerpos monoclonales, no solo en el estroma tumoral sino también en el interior de las células tumorales. Los resultados nos han permitieron obtener las siguientes conclusiones:

1. Se han obtenido nuevos sistemas de liberación de fármacos constituídos por nanocomplejos obtenidos mediante el simple ensamblaje de ácido hialurónico (HA) y el agente tensoactivo catiónico, lauril arginato de etilo (LAE), utilizando diferentes métodos y condiciones de formulación.

2. Los nanosistemas asociaron de manera eficaz diferentes proteínas, como las proteínas modelo BSA e IgG, y el anticuerpo monoclonal terapéutico BVZ. Las nanoformulaciones desarrolladas fueron estables al menos durante 24 horas en fluidos biológicos simulados y pudieron liofilizarse convenientemente. El mantenimiento de la estabilidad estructural y funcional de las proteínas encapsuladas se comprobó mediante el uso de técnicas de dicroismo circular y ELISA.

3. Los nanocomplejos recubiertos por HA (ENCPs) conteniendo BVZ permitieron una interacción efectiva con una línea celular de cáncer de mama, interacción no observada para el BVZ libre.

4. El uso de BVZ (libre o asociado a los ENCPs de HA) en el tratamiento de ratones con cáncer de mama consiguió disminuir el crecimiento tumoral. Sin embargo, no se observaron diferencias significativas entre los grupos de ENCPs conteniendo BVZ y el de BVZ libre. Esta eficacia limitada podría atribuirse a distintas razones, incluida la modalidad de administración y el protocolo de dosificación, una biodistribución ineficaz y/o la necesidad de una terapia de combinación.

Bibliografía

[1] https://www.nature.com/subjects/cancer/, (n.d.).

[2] F. Bray, J. Ferlay, I. Soerjomataram, R.L. Siegel, L.A. Torre, A. Jemal, Global Cancer Statistics 2018: GLOBOCAN Estimates of Incidence and Mortality Worldwide for 36 Cancers in 185 Countries, CA. Cancer J. Clin. 68 (2018) 394–424. doi:10.3322/caac.21492.

[3] Globocan, https://www.uicc.org/new-global-cancer-data-globocan-2018, (2018).

[4] E. Pérez-Herrero, A. Fernández-Medarde, Advanced targeted therapies in cancer: Drug nanocarriers, the future of chemotherapy, Eur. J. Pharm. Biopharm. 93 (2015) 52–79. doi:10.1016/j.ejpb.2015.03.018.

[5] B.A. Chabner, T.G. Roberts Jr, Chemotherapy and the war on cancer, Nat. Rev. Cancer. 5 (2005) 65–72.

[6] Metastasis: Diagnosing & Treating Metastatic Cancer, (n.d.). https://www.cancercenter.com/terms/metastasis/.

[7] H.A.D. Lagassé, A. Alexaki, V.L. Simhadri, N.H. Katagiri, W. Jankowski, Z.E. Sauna, C. Kimchi-sarfaty, Recent advances in (therapeutic protein) drug development, F1000 Res. 6 (2017) 1–17. doi:10.12688/f1000research.9970.1.

[8] D.M. Ecker, S.D. Jones, H.L. Levine, The therapeutic monoclonal antibody market, MAbs. 7 (2015) 9–14. doi:10.4161/19420862.2015.989042.

[9] R.A. Beckman, L.M. Weiner, H.M. Davis, Antibody constructs in cancer therapy. Protein Engineering Strategies to Improve Exposure in Solid Tumors, Cancer. 109 (2007) 170–179. doi:10.1002/cncr.22402.

[10] O. Casanovas, D.J. Hicklin, G. Bergers, D. Hanahan, Drug resistance by evasion of antiangiogenic targeting of VEGF signaling in late-stage pancreatic islet tumors, Cancer Cell. 8 (2005) 299–309. doi:10.1016/j.ccr.2005.09.005.

[11] P. Chames, M. Van Regenmortel, E. Weiss, D. Baty, Therapeutic antibodies: successes , limitations and hopes for the future, Br. J. Pharmacol. 157 (2009) 220–233. doi:10.1111/j.1476-5381.2009.00190.x.

[12] M.J. Miller, Cancer Immunotherapy: Present Status, Future Perspective, and a New Paradigm of Peptide Immunotherapeutics, Discov. Med. 15 (2013) 166–176.

[13] T.A.S. Aguirre, D. Teijeiro-Osorio, M. Rosa, I.S. Coulter, M.J. Alonso, D.J. Brayden, Current status of selected oral peptide technologies in advanced preclinical development and in

clinical trials, Adv. Drug Deliv. Rev. 106 (2016) 223–241. doi:10.1016/j.addr.2016.02.004.
[14] I. Santalices, A. Gonella, D. Torres, M. Jos, Advances on the formulation of proteins using nanotechnologies, J. Drug Deliv. Sci. Technol. 42 (2017) 155–180. doi:10.1016/j.jddst.2017.06.018.
[15] J.K.H. Liu, The history of monoclonal antibody development e Progress , remaining challenges and future innovations, Ann. Med. Surg. 3 (2014) 113–116. doi:10.1016/j.amsu.2014.09.001.
[16] F.C. Breedveld, Therapeutic monoclonal antibodies, New Drug Classes. 355 (2000) 735–740. doi:10.1016/S0140-6736(00)01034-5.
[17] K. Bloem, B. Hernandez-Breijo, A. Martìnez-Feito, T. Rispens, Immunogenicity of therapeutic antibodies: monitoring anti-drug antibodies in a clinical context, Ther. Drug Monit. 39 (2017) 327–332. doi:10.1097/FTD.0000000000000404.
[18] M.P. Baker, H.M. Reynolds, B. Lumicisi, C.J. Bryson, Immunogenicity of protein therapeutics The key causes , consequences and challenges, Self. Nonself. 1 (2010) 314–322. doi:10.4161/self.1.4.13904.
[19] F. Sousa, A. Cruz, P. Fonte, I.M. Pinto, M.T. Neves, B. Sarmento, A new paradigm for antiangiogenic therapy through controlled release of bevacizumab from PLGA nanoparticles, Nat. Sci. Reports. 7 (2017) 1–13. doi:10.1038/s41598-017-03959-4.
[20] S. Tangutoori, B.Q. Spring, Z. Mai, A. Palanisami, L.B. Mensah, T. Hasan, Simultaneous delivery of cytotoxic and biologic therapeutics using nanophotoactivatable liposomes enhances treatment efficacy in a mouse model of pancreatic cancer, Nanomedicine Nanotechnology, Biol. Med. 12 (2016) 223–234. doi:10.1016/j.nano.2015.08.007.
[21] A.R. Srinivasan, A. Lakshmikuttyamma, S.A. Shoyele, Investigation of the Stability and Cellular Uptake of Self-Associated Monoclonal Antibody (MAb) Nanoparticles by Non-Small Lung Cancer Cells, Mol. Pharm. 10 (2013) 3275–3284. doi:10.1021/mp3005935.
[22] J.E. Chung, S. Tan, S.J. Gao, N. Yongvongsoontorn, S.H. Kim, J.H. Lee, H.S. Choi, H. Yano, L. Zhuo, M. Kurisawa, J.Y. Ying, Self-assembled micellar nanocomplexes comprising green tea catechin derivatives and protein drugs for cancer therapy, Nat. Nanotechnol. 9 (2014) 907–912. doi:10.1038/nnano.2014.208.
[23] Y. Zhang, J. Guo, X. Zhang, D. Li, T. Zhang, Antibody fragment-armed mesoporous silica nanoparticles for the targeted delivery of bevacizumab in ovarian cancer cells, Nanomedicine. 496 (2015) 1026–1033.
[24] F. Sousa, A. Cruz, P. Fonte, I.M. Pinto, M.T. Neves-, A new paradigm for antiangiogenic therapy through controlled release of bevacizumab from PLGA nanoparticles, (2017) 1–13. doi:10.1038/s41598-017-03959-4.
[25] B. Spring, Z. Mai, P. Rai, S. Chang, T. Hasan, Theranostic Nanocells for Simultaneous Imaging and Photodynamic therapy of Pancreatic Cancer, Opt. Methods Tumor Treat. Detect. Mech. Tech. Photodyn. Ther. 7551 (2010) 1–11. doi:10.1117/12.843725.
[26] A.R. Srinivasan, A. Lakshmikuttyamma, S.A. Shoyele, Investigation of the Stability and Cellular Uptake of Self-Associated Monoclonal Antibody (MAb) Nanoparticles by Non-Small Lung Cancer Cells, Mol. Pharm. 10 (2013) 3275–3284.
[27] L. Battaglia, M. Gallarate, E. Peira, D. Chirio, I. Solazzi, S. Marzia, A. Giordano, C.L. Gigliotti, C. Riganti, C. Dianzani, Bevacizumab loaded solid lipid nanoparticles prepared by the coacervation technique: preliminary in vitro studies, Nanotechnology. 26 (2015) 255102. doi:10.1088/0957-4484/26/25/255102.
[28] Y. Tang, F. Soroush, Z. Tong, M.F. Kiani, B. Wang, Targeted multidrug delivery system to overcome chemoresistance in breast cancer, Int. J. Nanomedicine. 12 (2017) 671–681. doi:10.2147/IJN.S124770.
[29] F. Ordikhani, M. Uehara, V. Kasinath, L. Dai, S.K. Eskandari, B. Bahmani, M. Yonar, J.R. Azzi, Y. Haik, P.T. Sage, G.F. Murphy, N. Annabi, T. Schatton, I. Guleria, R. Abdi, Targeting antigen-presenting cells by anti – PD-1 nanoparticles augments antitumor immunity, JCI Insight. 3

(2018) 1–17. doi:doi: 10.1172/jci.insight.122700.
[30] G. Tripodo, A. Trapani, M. Luisa, G. Giammona, G. Trapani, D. Mandracchia, Hyaluronic acid and its derivatives in drug delivery and imaging : Recent advances and challenges, Eur. J. Pharm. Biopharm. 97 (2015) 400–416. doi:10.1016/j.ejpb.2015.03.032.
[31] A. Gdowski, A. Ranjan, A. Mukerjee, J. Vishwanatha, Development of Biodegradable Nanocarriers Loaded with a Monoclonal Antibody, Int. J. Mol. Sci. 16 (2015) 3990–3995. doi:10.3390/ijms16023990.
[32] H. Deng, K. Song, X. Zhao, Y. Li, F. Wang, J. Zhang, A. Dong, Z. Qin, Tumor Microenvironment Activated Membrane Fusogenic Liposome with Speedy Antibody and Doxorubicin Delivery for Synergistic Treatment of Metastatic Tumor, ACS Appl. Mater. Interfaces. 9 (2017) 9315–9326. doi:10.1021/acsami.6b14683.
[33] L. Li, J. Wang, H. Kong, Y. Zeng, G. Liu, Functional biomimetic nanoparticles for drug delivery and theranostic applications in cancer treatment, Sci. Technol. Adv. Mater. 19 (2018) 771–790. doi:10.1080/14686996.2018.1528850.
[34] R. Mout, M. Ray, T. Tay, K. Sasaki, G.Y. Tonga, V.M. Rotello, General Strategy for Direct Cytosolic Protein Delivery via Protein−Nanoparticle Co‑engineering, ACS Nano. 11 (2017) 6416–6421. doi:10.1021/acsnano.7b02884.
[35] P. Zhang, F. Sun, C. Tsao, S. Liu, P. Jain, A. Sinclair, H. Hung, T. Bai, K. Wu, S. Jiang, Zwitterionic gel encapsulation promotes protein stability, enhances pharmacokinetics, and reduces immunogenicity, PNAS. 112 (2015) 12046–12051. doi:10.1073/pnas.1512465112.
[36] A. Almalik, H. Benabdelkamel, A. Masood, I.O. Alanazi, M.A. Majrashi, A.A. Alfadda, W.M. Alghamdi, H. Alrabiah, N. Tirelli, A.H. Alhasan, Hyaluronic Acid Coated Chitosan Nanoparticles Reduced the Immunogenicity of the Formed Protein Corona, Sci. Rep. 7 (2017) 1–9. doi:10.1038/s41598-017-10836-7.
[37] V.P. Torchilin, A.N. Lukyanov, Peptide and protein drug delivery to and into tumors: challenges and solutions, Drug Discov. Today. 8 (2003) 259–266. doi:10.1016/S1359-6446(03)02623-0.
[38] W. Il Choi, N. Kamaly, L. Riol-blanco, I. Lee, J. Wu, A. Swami, C. Vilos, B. Yameen, M. Yu, J. Shi, I. Tabas, U.H. Von Andrian, S. Jon, O.C. Farokhzad, A Solvent-Free Thermosponge Nanoparticle Platform for E fficient Delivery of Labile Proteins, Nano Lett. 14 (2014) 6449–6455. doi:10.1021/nl502994y.
[39] D.A. Ossipov, Nanostructured hyaluronic acid-based materials for active delivery to cancer, Expert Opin. Drug Deliv. 7 (2010) 681–703. doi:10.1517/17425241003730399.
[40] G. Tzircotis, R.F. Thorne, C.M. Isacke, Chemotaxis towards hyaluronan is dependent on CD44 expression and modulated by cell type variation in CD44-hyaluronan binding, J. Cell Sci. 118 (2005) 5119–5128. doi:10.1242/jcs.02629.
[41] S. Inàcio, K.A. Mesquita, M. Baptista, In Vitro Surfactant Structure-Toxicity Relationships: Implications for Surfactant Use in Sexually Transmitted Infection Prophylaxis and Contraception, PLoS One. 6 (2011) 1–15. doi:10.1371/journal.pone.0019850.
[42] M. Lund, R. Vacha, P. Jungwirth, Specific Ion Binding to Macromolecules : Effects of Hydrophobicity and Ion Pairing, Langmuir. 24 (2008) 3387–3391. doi:10.1021/la7034104.
[43] P. Mukerjee, K. Mysels, P. Kapadan, Counterion Specificity in the Formation of Ionic Micelles — Size , Hyadration, and Hydrophobic Bonding Effect, 71 (1966) 4166–4175. doi:10.1021/j100872a702.
[44] H. Dautzenberg, Polyelectrolyte Complex Formation in Highly Aggregating Systems. 1. Effect of Salt: Polyelectrolyte Complex Formation in the Presence of NaCl, 30 (1997) 7810–7815. doi:10.1021/ma970803f.
[45] G. Van der Vusse, Albumin as Fatty Acid Transporter, Drug Metab. Pharmacokinet. 24 (2009) 300–307. doi:10.2133/dmpk.24.300.

[46] J. Crecente-Campo, S. Lorenzo-Abalde, A. Mora, J. Marzoa, N. Csaba, J. Blanco, Á. González-Fernández, M. José, Bilayer polymeric nanocapsules: A formulation approach for a thermostable and adjuvanted E. coli antigen vaccine, J. Control. Release. 286 (2018) 20–32. doi:10.1016/j.jconrel.2018.07.018.

[47] T. Ramasamy, T. Hiep, J. Yeon, H. Jun, J. Hwan, C. Soon, H. Choi, J. Oh, Layer-by-layer coated lipid – polymer hybrid nanoparticles designed for use in anticancer drug delivery, 102 (2014) 653–661. doi:10.1016/j.carbpol.2013.11.009.

[48] A. Valstar, M. Almgren, W. Brown, The Interaction of Bovine Serum Albumin with Surfactants Studied by Light Scattering, Langmuir. 16 (2000) 922–927. doi:10.1021/la990423i.

[49] K. Liang, S. Ng, F. Lee, J. Lim, J.E. Chung, S.S. Lee, M. Kurisawa, Targeted intracellular protein delivery based on hyaluronic acid-green tea catechin nanogels, Acta Biomater. 33 (2016) 142–152. doi:10.1016/j.actbio.2016.01.011.

[50] Y. Yeo, K. Park, Control of Encapsulation Efficiency and Initial Burst in Polymeric Microparticle Systems, Arch. Pharm. Res. 27 (2004) 1–12. doi:10.1007/BF02980037.

[51] Q. Gan, T. Wang, Chitosan nanoparticle as protein delivery carrier — Systematic examination of fabrication conditions for efficient loading and release, Colloids Surfaces B. 59 (2007) 24–34. doi:10.1016/j.colsurfb.2007.04.009.

[52] M. Alonso-Sande, M. Cuna, C. Remunàn-Lopez, D. Teijeiro-Osorio, J.L. Alonso-Lebrero, M. Alonso, Formation of New Glucomannan - Chitosan Nanoparticles and Study of Their Ability To Associate and Deliver Proteins, Macromolecules. 39 (2006) 4152–4158.

[53] W. Tiyaboonchai, J. Woiszwillo, R.C. Sims, C.R. Middaugh, Insulin containing polyethylenimine-dextran sulfate nanoparticles, Int. J. Pharm. 255 (2003) 139–151. doi:10.1016/S0378-5173(03)00055-3.

[54] D. Kelley, D.J. McClements, Interactions of bovine serum albumin with ionic surfactants in aqueous solutions, Kelley, D. McClements, D.J. 17 (2003) 73–85. doi:10.1016/S0268-005X(02)00040-1.

[55] D. Otzen, Protein–surfactant interactions: A tale of many states, Biochim. Biophys. Acta. 1814 (2011) 562–591. doi:10.1016/j.bbapap.2011.03.003.

[56] World Health Organization, Stability testing of active pharmaceutical ingredients and finished pharmaceutical products, 2009.

[57] N. Vlachy, D. Touraud, J. Heilmann, W. Kunz, Determining the cytotoxicity of catanionic surfactant mixtures on HeLa cells, Colloids Surfaces B Biointerfaces. 70 (2009) 278–280. doi:10.1016/j.colsurfb.2008.12.038.

[58] R.L. Grant, C. Yao, D. Gabaldon, D. Acosta, Evaluation of surfactant cytotoxicity potential by primary cultures of ocular tissues: I . Characterization of rabbit corneal epithelial cells and initial injury and delayed toxicity studies, Toxicology. 76 (1992) 153–176. doi:10.1016/0300-483X(92)90162-8.

[59] M.K. Dymond, G.S. Attard, Cationic Type I Amphiphiles As Modulators of Membrane Curvature Elastic Stress in Vivo, Langmuir. 24 (2008) 11743–11751. doi:10.1021/la8017612.

[60] B. Vieira, A.M. Carmona-ribeiro, U. De Sa, A. Lineu, P. Butanta, Cationic lipids and surfactants as antifungal agents : mode of action, J. Antimicrob. Chemother. 58 (2006) 760–767. doi:10.1093/jac/dkl312.

[61] A. Patrzykat, C.L. Friedrich, L. Zhang, V. Mendoza, R.E.W. Hancock, Sublethal Concentrations of Pleurocidin-Derived Antimicrobial Peptides Inhibit Macromolecular Synthesis in Escherichia coli, Antimicrob. Agents Chemother. 46 (2002) 605–614. doi:10.1128/AAC.46.3.605.

[62] R. Bhattacharya, F. Fan, R. Wang, X. Ye, L. Xia, D. Boulbes, L.M. Ellis, Intracrine VEGF signalling mediates colorectal cancer cell migration and invasion, Br. J. Cancer. 117 (2017) 848–855. doi:10.1038/bjc.2017.238.

[63] M. Björndahl, R. Cao, A. Eriksson, Y. Cao, Blockage of VEGF-Induced Angiogenesis by Preventing VEGF Secretion, Circ. Res. 94 (2004) 1443–50.

doi:10.1161/01.RES.0000129194.61747.bf.
[64] R. Bhattacharya, X. Ye, R. Wang, X. Ling, M. Mcmanus, F. Fan, D. Boulbes, L.M. Ellis, Intracrine VEGF Signaling Mediates the Activity of Pro-survival Pathways in Human Colorectal Cancer Cells, Cancer Res. 76 (2017) 3014–3024. doi:10.1158/0008-5472.CAN-15-1605.
[65] S. Tangutoori, B.Q. Spring, Z. Mai, A. Palanisami, L.B. Mensah, T. Hasan, Simultaneous delivery of cytotoxic and biologic therapeutics using nanophotoactivatable liposomes enhances treatment efficacy in a mouse model of pancreatic cancer, Nanomedicine Nanotechnology, Biol. Med. 12 (2016) 223–234. doi:10.1016/j.nano.2015.08.007.
[66] M. Chien, C. Ku, G. Johansson, M. Chen, M. Hsiao, J. Su, K. Hua, L. Wei, M. Kuo, Vascular endothelial growth factor-C (VEGF-C) promotes angiogenesis by induction of COX-2 in leukemic cells via the VEGF-R3/JNK/AP-1 pathway, Carcinogeneis. 30 (2013) 2005–2013. doi:10.1093/carcin/bgp244.
[67] A.J. Weickhardt, D.S. Williams, C.K. Lee, F. Chionh, J. Simes, C. Murone, K. Wilson, M.M. Parry, K. Asadi, A.M. Scott, C.J. Punt, I.D. Nagtegaal, T.J. Price, J.M. Mariadason, N.C. Tebbutt, Vascular endothelial growth factor D expression is a potential biomarker of bevacizumab benefit in colorectal cancer, Br. J. Cancer. 113 (2015) 37–45. doi:10.1038/bjc.2015.209.
[68] F. Zhang, Z. Tang, X. Hou, J. Lennartsson, Y. Li, A.W. Koch, P. Scotney, C. Lee, P. Arjunan, L. Dong, A. Kumar, T.T. Rissanen, B. Wang, N. Nagai, P. Fons, R. Fariss, Y. Zhang, E. Wawrousek, G. Tansey, J. Raber, G. Fong, H. Ding, D.A. Greenberg, K.G. Becker, J. Herbert, A. Nash, S. Yla-herttuala, Y. Cao, R.J. Watts, X. Li, VEGF-B is dispensable for blood vessel growth but critical for their survival , and VEGF-B targeting inhibits pathological angiogenesis, PNAS. 106 (2009) 6152–6157. doi:10.1073/pnas.0813061106.
[69] G. Pentheroudakis, V. Kotoula, E. Fountzilas, G. Kouvatseas, G. Basdanis, I. Xanthakis, T. Makatsoris, E. Charalambous, D. Papamichael, E. Samantas, P. Papakostas, D. Bafaloukos, E. Razis, C. Christodoulou, I. Varthalitis, P. Nicholas, G. Fountzilas, A study of gene expression markers for predictive significance for bevacizumab benefit in patients with metastatic colon cancer: a translational research study of the Hellenic Cooperative Oncology Group (HeCOG), BMC Cancer. 14 (2014) 1–10. doi:10.1186/1471-2407-14-111.
[70] M. Filali, L. V. Ly, G.P.M. Luyten, M. Versluis, H.E. Grossniklaus, P.A. Van, Bevacizumab and intraocular tumors : an intriguing paradox, Mol. Vis. 12 (2012) 2454–2467.
[71] R.S. Warren, H. Yuan, M.R. Matli, N.A. Gillett, N. Ferrara, Regulation by Vascular Endothelial Growth Factor of Human Colon Cancer Tumorigenesis in a Mouse Model of Experimental Liver Metastasis, J. Clin. Invest. 95 (1995) 1789–1797. doi:10.1172/JCI117857.
[72] Y. Okada, T. Akisue, H. Hara, K. Kishimoto, T. Kawamoto, M. Imabori, S. Kishimoto, N. Fukase, Y. Onishi, M. Kurosaka, The Effect of Bevacizumab on Tumour Growth of Malignant Fibrous Histiocytoma in an Animal Model, Anticancer Res. 30 (2010) 3391–3395.
[73] Z. Zhao, X. Li, W. Liu, X. Liu, S. Wu, X. Hu, Inhibition of Growth and Metastasis of Tumor in Nude Mice after Intraperitoneal Injection of Bevacizumab, Orthop. Surg. 8 (2016) 234–240. doi:10.1111/os.12236.
[74] M.O. Stefanini, F.T.H. Wu, F. Mac Gabhann, A.S. Popel, Increase of Plasma VEGF after Intravenous Administration of Bevacizumab Is Predicted by a Pharmacokinetic Model, Cancer Res. 70 (2010) 9886–9895. doi:10.1158/0008-5472.CAN-10-1419.
[75] N. Zhang, G. Zhang, Y. Zheng, T. Wang, H. Wang, Effect of Avastin on the number and structure of tumor blood vessels of nude mice with A549 lung adenocarcinoma, Exp. Ther. Med. 8 (2014) 1723–1726. doi:10.3892/etm.2014.1991.

Table of contents

USC
UNIVERSIDADE
DE SANTIAGO
DE COMPOSTELA

USC
UNIVERSIDADE
DE SANTIAGO
DE COMPOSTELA

Introduction

USC
UNIVERSIDADE
DE SANTIAGO
DE COMPOSTELA

Chapter I

Proteins, cancer and nanotechnology

USC
UNIVERSIDADE
DE SANTIAGO
DE COMPOSTELA

1. Nanotechnology and protein delivery in cancer therapy

1.1 Cancer and protein therapeutics

Cancer refers to diseases resulting from the unregulated proliferation of tumor cells. Once turned into malignant, these cells are no able to respond to the signals which regulate normal cells behaviors, i.e. differentiation, survival, proliferation and death [1,2]. This results in the uncontrolled growth of the tissue and the possibility for cancer cells invasion, eventually spreading through the body (metastasis). The development of cancer is a multistep process where cells accumulate genetic alterations, which confer specific advantages over normal cells that are hence outgrown. This process is called clonal selection (Figure 1) [2]. There are more than 200 different types of cancer. Only in 2018, 18.1 million new cancer cases were reported, resulting in 9.6 million deaths (Figure 2) [1,3]. The International Agency for Research on Cancer (IARC) has estimated that one-in-five men and one-in-six women worldwide will develop cancer during their life [4]. These data highlight how cancer has become a public health problem which is increasing year after year. Among the different approaches for treating cancer [5], surgery and radiation therapy are the first treatments for local and non-metastatic cancers, while chemotherapy is still the main option when tumors turn to metastatic [6–8]. Chemotherapeutic treatments are based on toxic drugs which kill both, cancer and normal cells, causing significant side effects. In this regard, finding more specific therapies which selectively act on cancer cells without affecting normal tissues would strongly improve the efficacy of the treatments.

Protein drugs are far more selective and specific compared to small chemotherapeutics and may contribute in reducing side effects. The development of protein engineering technologies also allow the modification of their properties, which can increase their activity and biological stability [9]. Since 2011, the FDA has approved 62 therapeutic proteins, 26% of them used in oncology [10] . However, problems related to their short half-life, low tumor penetration, immunogenicity and to the development of resistances by cancer cells, make the administration of therapeutic proteins challenging [9,11–13]. These problems can be faced using nanotechnology, entrapping, adsorbing or chemically conjugating the proteins to nanocarriers [13,14]. The nanosystems could favor the targeting and the penetration of the protein drugs both enhancing their half-life, favoring their extravasation at the tumor site, and avoiding their stackness at the tumor proximity (often observed with monoclonal antibodies) [15,16]. This topic will be deeper discussed in the following paragraphs. The nanoencapsulation could also favor the cell internalization of the protein drugs, with the possibility of acting on new targets considered untapped until today. This field is rapidly evolving, and several works aiming at developing nanocarriers for the intracellular delivery of proteins have been released in the last years [17–19]. Other advantages related to protein nanoencapsulation are the possibility of reducing protein's immunogenicity and protecting them from enzymatic degradation. In fact, immunogenic responses have been detected also with humanized protein therapeutics [20]. The nanoencapsulation diminishes the opsonization processes, reducing the immunogenicity of the drug [21].

A summary of the principal advantages resulting from anticancer proteins nanoencapsulation is shown in Table 1. These topics will be deeply described and commented in the following part of this chapter.

The chapter will be focused on the importance of monoclonal antibodies and nanotechnology for treating cancer. An overview of this topic will be given in the following paragraphs, focusing finally on bevacizumab and its nanoencapsulation.

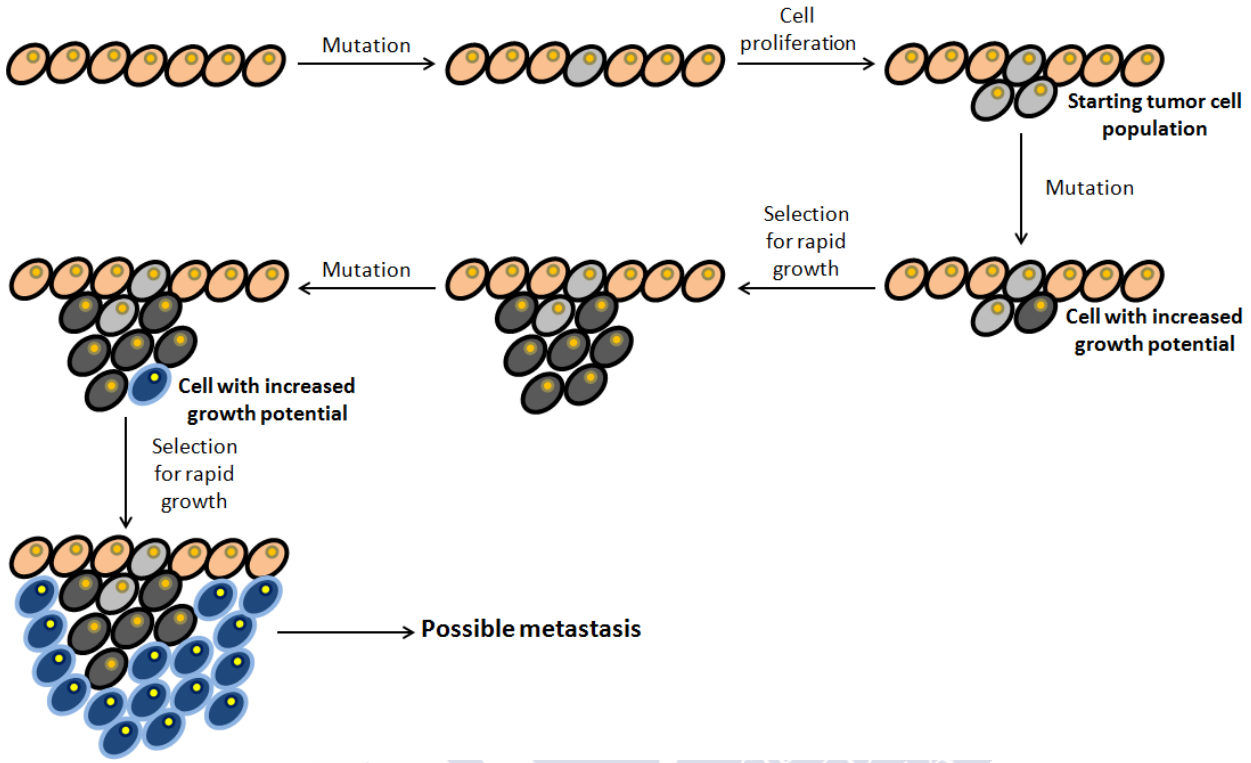

Figure 1. Clonal selection of cells with increased growth potential leading to the development of cancer.

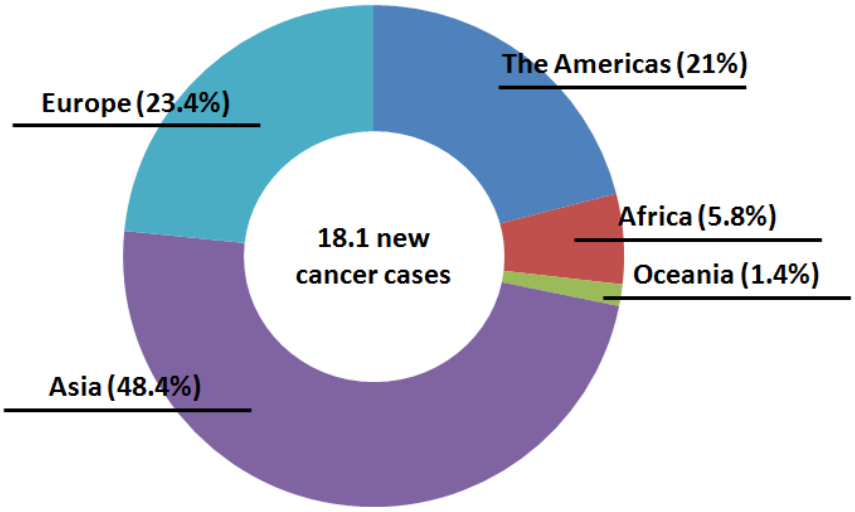

Figure 2. Cancer statistics during the year 2018 expressed by continents. 18.1 new cancer cases have been detected worldwide. Data were collected from GLOBOCAN [3,4].

Table 1. Some of the main reasons for nanoencapsulating anticancer proteins. The achievement and the mechanism of action have been indicated in the table.

Achievement	Mechanism	Reference
Tumor targeting and penetration	Targeting: through the use of polymers or ligands which specifically bind the tumor. Penetration: possibly avoiding the stackness of proteins at the tumor periphery.	[22–25]
Intracellular targeting	If surface-decorated with the proper moieties, the nanocarrier could favor the targeting of intracellular antigens, enhancing the efficacy of the therapy or allowing the targeting of new antigens.	[19,26–28]
Protection from enzymatic degradation	Protection of the protein from the enzymatic degradation at the tumor site or inside the cells (endosomes). Protein degradation could also increase its immunogenicity.	[29,30]
Reduction of the immunogenicity	If produced with the proper polymers, the nanocarrier reduces the immunogenicity of the therapeutic proteins by avoiding the attachment of inflammatory proteins (protein corona) to the drug.	[21,31]
Enhanced half-life	For specific proteins whose half-life is short. The nanocarrier confers stealth properties, protection, reduced clearance and sustained release.	[32,33]

2. Nanotechnology and monoclonal antibodies in cancer therapy

2.1. Monoclonal antibodies and cancer therapy

2.1.1 Antibodies structure and functions

Antibodies are high molecular weight proteins naturally produced by B-cells of the immune system (i.e. B-lymphocytes). They principally provide protection against viral, bacterial and fungal infections through the recognition of epitopes on the antigens of these foreign materials. Other functions attributed to antibodies include the regulation of the B-cell development, the selection of the B-cells pool and their responses, protection from cancer, vascular homeostasis maintenance, clearance of apoptotic debris and allergic suppression [34].

Antibodies are molecules with an average molecular weight of 150 kDa, with a Y shape and made by two heavy chains (average MW of 55 KDa) and two light chains (average MW of 25 KDa). Each one of the chains is composed by a constant region and an N-terminal variable region. The variable portion is fundamental for antigens recognition while the constant region has effector functions. The general structure of antibodies is shown in Figure 3.

Antibodies can be classified in polyclonal (pAbs) and monoclonal antibodies (mAbs). The pAbs are able to recognize the same antigen on different epitopes and are genetically different since produced by different B-cell clones. On the other hand, mAbs are genetically equal, because they are produced from the same clone, and are able to bind the same epitope on an antigen. This is possible thanks to some hypervariable regions of the variable portions of the light and heavy chains, called complementary determinant regions (CDR) [35,36].

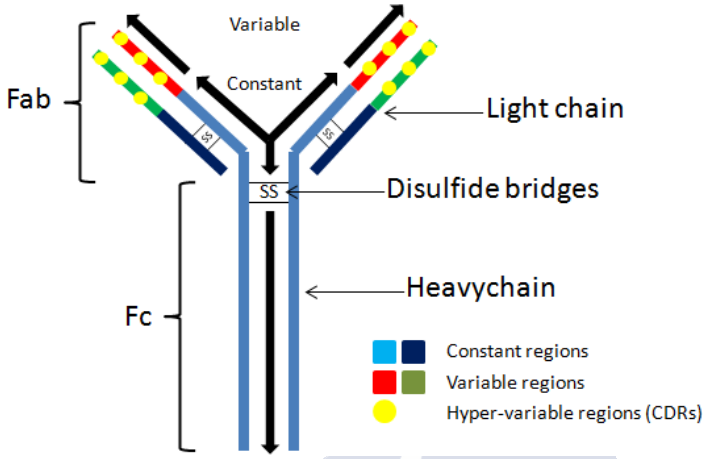

Figure 3. General structure of an antibody. The protein is made by two heavy chains and two light chains, joined by disulfide bridges. Each one of the chains is composed by one constant region and one variable region. In the variable regions the hyper-variable domains (CDRs) can be found, which are the portions responsible for the high specificity of antibodies (antigen recognition).

Upon the binding with their antigens, antibodies are recognized by Fc receptor expressing cells (e.g. macrophages, NK cells, etc.) and activate their functions, i.e. macrophages uptake of antigen-antibodies complexes, B-cells activation and antibody-dependent cell-mediated cytotoxicity (ADCC) [37].

The Fc structure is also important for defining the half-life of the antibodies in the blood. For example, the average half-life of IgG1, IgG2 and IgG4 is 23 days, while the one of IgG3 is around 2-6 days [37,38].

2.1.2 Market and production techniques of mAbs

The market of therapeutic mAbs has exploded in the last years (Figure 4). Pharmaceutical companies have decided to exploit the huge specificity of these molecules for treating several diseases and invested important amounts of resources for developing antibodies production and protein engineering techniques. Until today more than 70 mAbs have been approved by the FDA and EMA [39]. The development of the hybridoma technology in 1975 by Kohler and Milstein, allowed the production of mAbs in a reproducible and rapid way, thanks to the fusion of lymphocyte-B cells (taken from immunized mice) with murine myeloma cell lines (immortalized) [35,40]. However, the murine mAbs produced with this technique resulted highly immunogenic when administered to humans [35]. Hence, humanization of antibodies has been then achieved by substituting the mice mAbs producing genes with the ones of humans. A 95% human structure homology can be reproduced with this method, strongly reducing the immunogenicity of the proteins [41,42]. Finally, with the development of the phage display technology, fully human antibodies can be produced.

Libraries with billions of different mAbs can be created and among them, some drug candidates can be found after a rapid screening [42].

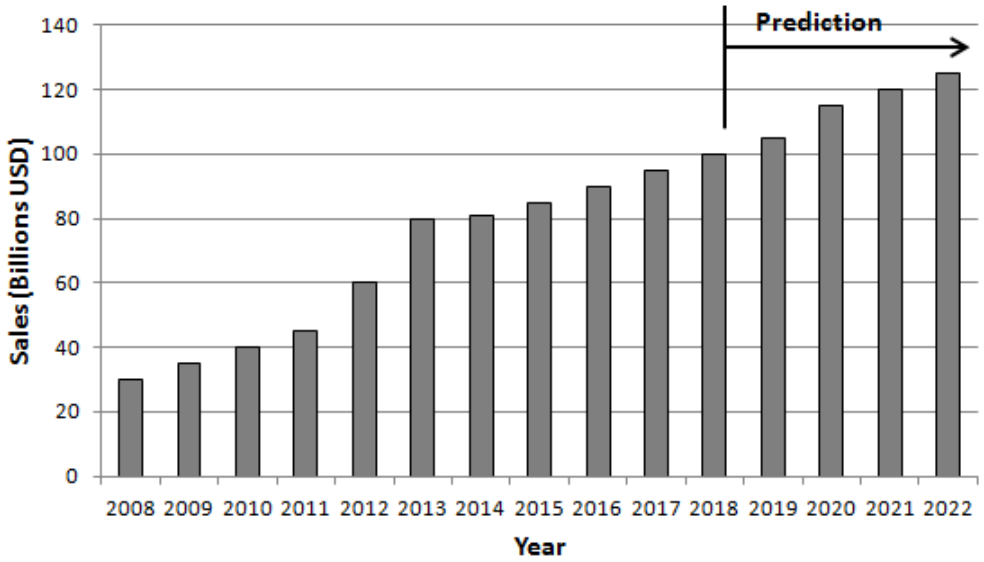

Figure 4. Evolution of the therapeutic mAbs market in the last years [43–45].

2.1.3 Monoclonal antibodies as anticancer therapeutics

The identification of tumor antigens has opened new doors in the field of anticancer treatments. The higher specificity and selectivity of mAbs compared to the normal chemotherapeutic agents, introduced huge benefits, drastically reducing the side effects of the therapies [46]. Moreover, the possibility of modulating mAbs pharmacokinetics, size, effects and immunogenicity through molecular techniques and new formulation strategies, has increased the interest around these molecules.

Therapeutic mAbs can act in different manners, i.e. as agonists or antagonists, modifying or avoiding the interaction between an antigen and its receptor, modulating the immune system response or targeting a specific drug to a particular region of the tumor [17,47]. As indicated by the American Cancer Society, FDA approved mAbs for cancer treatment can be classified in naked and conjugated. Naked mAbs, are antibodies which are therapeutically active by themselves and work boosting the immune system against cancer cells (e.g. alemtuzumab) or against the immune system checkpoints, or blocking antigens which allow tumor growth (e.g. trastuzumab and bevacizumab). Conjugated mAbs are chemically coupled to chemotherapeutic drugs or radioactive moieties. In this case, the antibodies work as targeting moieties while the active therapeutic portion is the attached molecule. Examples are ibritumomab-tiuxetan, used to treat the non-Hodgkin lymphoma, or adotrastuzumab-emtansine, for the treatment of breast cancer. Table 2 summarize the different approaches used by therapeutic mAbs for tumor cell killing [47].

Table 2. Approaches used by therapeutic mAbs for tumor cells killing.

	Naked antibodies	Conjugated antibodies
Direct antibody action	Receptor blockade	Delivery of drugs or cytotoxic agents
	General agonist activity	
	Induction of apoptosis	
	Targeting tumor vasculature and stroma	
Immune mediated cell killing	Complement dependent cytotoxicity (CDC)	
	Antibody-dependent cellular cytoxicity (ADCC)	

2.1.4 Current limitations of mAbs-based anticancer therapies

Despite the advantages provided by the use of anticancer mAbs compared to small chemotherapeutics, several problems still need to be faced. Antibodies are very expensive molecules which are repeatedly administered, often through infusion pumps (i.e. reducing patients' compliance). This makes the cost of the treatment unaffordable for most patients (up to $100000/year) [48]. As an example, rituximab, a monoclonal antibody used for the treatment of non-Hodgkin's lymphoma, can be considered. The recommended dosage per patient is 375 mg/m^2, resulting in an average price per infusion of more than $3000 [49].

Beyond these economical aspects, several limitations related to the molecules themselves and to their mechanisms of action are reported. MAbs are big molecules which just barely penetrate the tumors. It is reported that less than 20% of the administered antibody dose interacts with the tumor mass [50]. This is not only due to their size, but also to their high specificity and to their interaction with the neonatal Fc receptor (FcRn). In fact, due to their strong antigen binding affinity, mAbs could get stacked to peripheral antigens, without penetrating into the tumor (a mechanism described in literature as *binding site barrier effect*) [15]. On the other hand, the FcRn, expressed on several cells types like vascular endothelium cells, monocytes and macrophages, transports back the mAbs to the circulation once internalized, a mechanism that increases the half-life of these molecules but limits their action at the tumor site [50].

Also, the existing approved mAbs just target surface or soluble antigens, a fact that is probably due to the difficulties of developing delivery systems that can efficiently transport these molecules inside

the cells. Fortunately, efforts are now being made for developing strategies to delivery proteins into the cytoplasm of cancer cells [17,49,51].

Some limitations are also related to the intrinsic mAb's side effects. Immune reactions, such as acute anaphylaxis, serum sickness and production of neutralizing antibodies have been observed when treating patients with anticancer mAbs [48,49]. An example is given by cetuximab, directed against the epidermal growth factor receptor (EGFR) and used for the treatment of several tumors (e.g. colorectal cancer). Acute anaphylactic and anaphylactoid reactions have been described upon the treatment with this mAb, due to the production of anti-mAb antibodies [52].

Limitations related to the development of resistances have been also described in literature. The mechanisms by which tumors resist to mAbs are different based on the type of mAb. Generally, an increased (or decreased) expression of the targets, the upregulation of some signaling pathways, the expression of immune modulatory molecules and the use of alternative molecules for accomplishing the blocked function have been indicated as some of the known resistance mechanisms [53–55]. As examples, trastuzumab and cetuximab can be considered. It is reported that patients with advanced colorectal cancer do not respond to cetuximab therapies due to a mutation in the kRAS gene [56]. On the other hand, it was demonstrated that the overexpression of MUC4, a membrane associated glycoprotein, can sterically impede the recognition of HER2 by trastuzumab, leading to potential resistances [57].

2.2 The potential of nanotechnology for the delivery of mAbs

Nowadays, mAbs are among the most promising anticancer drugs due to their high specificity and activity [58,59]. However, as previously indicated, several limitations related to their pharmacokinetics and pharmacodynamics are still unsolved, and nanotechnology is emerging as a promising solution for facing these drawbacks [60,61]. Several works studying the nanoencapsulation of anticancer mAbs have been found in literature (Table 3).

The nanoencapsulation of mAbs could favor their **penetration across the tumor**. Solid tumors are abnormal masses of tissue made by tumor cells, stroma and leaking blood vessels which contribute to increase the interstitial fluid pressure at the tumor proximity, limiting mAbs penetration [62]. Additionally, the *binding site barrier effect* and the recirculation made by the *FcRn* are further restrictions [61,63–65]. When encapsulated into nanosystems, both the Fc and the antigen binding site of the mAbs could be hidden and protected inside the nanocarrier, allowing a better penetration of the drug across the tumor by reducing their interactions with other cells or proteins [24,60]. The study of Chung and co-workers, for example, demonstrated that a higher tumor accumulation of trastuzumab is obtained when the antibody is organized into micellar nanocomplexes, showing higher selectivity and anticancer effects compared to free trastuzumab [22].

Additionally, the **intracellular targeting** of antigens through endocytosis-mediated mechanisms is a further advantage of mAb nanoencapsulation. Antigens that have been considered "untargetable" so far can now be reached, thus opening doors for the development of new therapies [17–19,24,66].

For example, Deng and co-workers have shown an enhanced anticancer activity when an anti-S100A4 mAb was encapsulated into liposomes and delivered at the cytoplasm of tumor cells (in combination with doxorubicin). With this approach, the anticancer effects of both the mAb and doxorubicin was enhanced *in vivo* [27].

As endocytic pathways drive the internalized material to endosomes and lysosomes, the nanocarrier becomes also fundamental for **protecting** the internalized mAb from enzymatic degradation, physically screening the drug and favoring its endosomal escape. It is also hypothesized that the targeting of intracellular antigens could help in **overcoming some resistance mechanisms** that tumors use for making the therapy inefficient. This is the for example the case of bevacizumab, which will be deeply analyzed in the following paragraphs [18,67].

Finally, It is important to underline the importance of nanocarriers for **reducing mAb immunogenicity** (immunogenic responses have been detected also with humanized proteins [20]) and off-target toxicity. Even if the most used strategy for reducing protein immunogenicity is PEGylation [68] studies related to the use of nanoparticles made of polymers different from PEG have been found in literature. For example, it was found that the immunogenicity of a highly immunogenic model protein (i.e. uricase) was reduced when encapsulated into zwitterionic nanogels made of polycarboxybetadine (PCB). The authors showed the superiority of this nanosystem compared to the simple PEGylation of the protein, demonstrating in vivo the production of anti-PEG antibodies but not the one of anti-PCB antibodies [31]. In another interesting work, the potential of hyaluronic acid (HA) as non-immunogenic coating polymer for nanoparticles has been assessed. The polymer is able to repel the adsorption of inflammatory proteins at the nanoparticles surface compared to non HA decorated particles [21].

Table 3. Some examples of nanocarriers used for the encapsulation of anticancer mAbs. The type of nanosystem, the released molecule and the achievement obtained (in vivo) are indicated in the table.

Type of nanocarrier	Released mAb	Achievement	Reference
AntiCD44 decorated Liposomes	anti-IL6	Inhibition of IL6R-Stat3 signalling which leads to the inhibition of breast cancer metastasis and to a delay in tumor growth compared to the free antibody or the non decorated liposomes.	[69]
Self-assembled micelles	Trastuzumab	The micelles lead to a higher trastuzumab accumulation in the tumor, higher selectivity and longer blood half-life. This results in a higher anticancer activity.	[22]
PLGA NPs	anti-PD-1	Antitumor effect measured in a murine melanoma model. The mechanism still needs to be elucidated but it was found that the anti-PD-1 was able to favor the maturation of dendritic cells to T-cells, which can attack the tumor. The prophylactic treatment with the nanoencapsulated mAb significantly reduced the tumor growth.	[23]
Liposomes	anti S100A4 antibody (combination with doxorubicin)	Delivery of both the antibody and doxorubicin in the intracellular environment of breast cancer cells. The combination of the two molecules enhances the anticancer effect of the therapy.	[27]
PLA-PEG and PLGA-PEG	anti-PD-1 (combination with docetaxel)	Enhanced antitumor efficacy (squamous non-small cell lung cancer is targeted) when docetaxel and anti-PD1 are co-delivered (in the same nanoparticle).	[70]

2.3. Bevacizumab in cancer therapy

Bevacizumab (BVZ) is a 149 kDa humanized mAb firstly approved in 2004 (in combination with 5-fluorouracil-based chemotherapy) for the treatment of colorectal metastatic cancer and, in the following years, for the treatment of some solid tumors which overexpress VEGF-A (its target) [71,72]. The 93% of its structure comes from humans, the remaining 7% is murine. The estimated half-life of the mAb is 21 days [73].

2.3.1 VEGF-A structure and its natural function

VEGFs are growth factors expressed in a lot of different cell types, e.g. endothelial cells, fibroblasts, inflammatory cells and tumor cells. The VEGF family includes different proteins, i.e. VEGF-A, VEGF-B, VEGF-C, VEGF-D and the placenta growth factor (PlGF). VEGF-A is the main protein involved in angiogenic processes and it exists in different isoforms; VEGF189 and VEGF206 are the ones associated to the cell membrane, while VEGF165 and VEGF121 are the ones secreted by cells. VEGF165 is the most abundant form and it is overexpressed in different cancer types. It is recognized

by two cell surface tyrosine kinases receptors, VEGFR-1 and VEGFR-2, also called Flt-1 and KDR. The main receptor involved in angiogenesis is KDR and upon the recognition of the growth factor activates a cascade of intracellular signals, which allows a longer survival and proliferation of vascular endothelial cells, a higher migration and invasion, and the sprouting and increased permeability of the existing vessels [71]. All these functions are fundamental for the normal processes occurring in the human body, like the development of the vascular system during embryogenesis, the growth and development of normal tissues and for wound healing and reproduction [74]. It must be underlined, that vessels in normal adult tissues are relatively independent from VEGF-A [71].

2.3.2. VEGF-A and cancer

The development of hypoxic regions in some areas of the tumor tissues is a well-known hallmark for all the solid tumors [75]. Beyond the important metabolic consequences that this implies (i.e. shifting from an oxidative to a fermentative metabolism), the lack of oxygen causes the overexpression of proangiogenic factors, like VEGF-A.

Tumor hypoxia is a consequence of the rapid growth of tumors tissues. Growing faster compared to normal tissues, tumors need new blood vessels for the delivery of nutrients and oxygen and for eliminating waste products [76]. The growth of the hematic tissue is outgrown by the rapid tumor cells proliferation, resulting in regions of the tumor masses with reduced oxygen availability. The hypoxic environment, which causes an acidification of the tumor microenvironment, allows the selection of more aggressive tumor cells which, for sustaining their growth, overexpress the hypoxia-inducible factor-1 (HIF-1). HIF-1 activates a series of downstream intracellular events, which result in the increased expression of VEGF-A. VEGF-A overexpression is also caused by the activation of some oncogenes (i.e. src, ras, p53, vhl and fos) and by the activity of hormones and cytokines such as androgens, estrogens, epidermal growth factor receptor ligands, and insulin-like growth factor-1. VEGF-A is the main source for the "angiogenic switch", the transition from an avascular phase to a vascular phase (rapid blood vessel formation), which is fundamental for tumor growth [71,74]. Since the blood vessels are "forced" in growing faster by tumor cells, the resulting new vessels present abnormalities, are more branched and chaotic, and show areas of constriction and dilatation. Besides, the formation of gaps between the endothelial cells junctions and of vessels with a tighter diameter takes place [71]. A scheme which reports the main events leading to the "angiogenic switch" is shown in Figure 5. It is reported that without a sustained angiogenesis, tumors would be unable to overcome the 100 µm of diameter. VEGF-A also promotes vessels permeability, fundamental for the intake of necessary nutrients for the growth of the tumor [71].

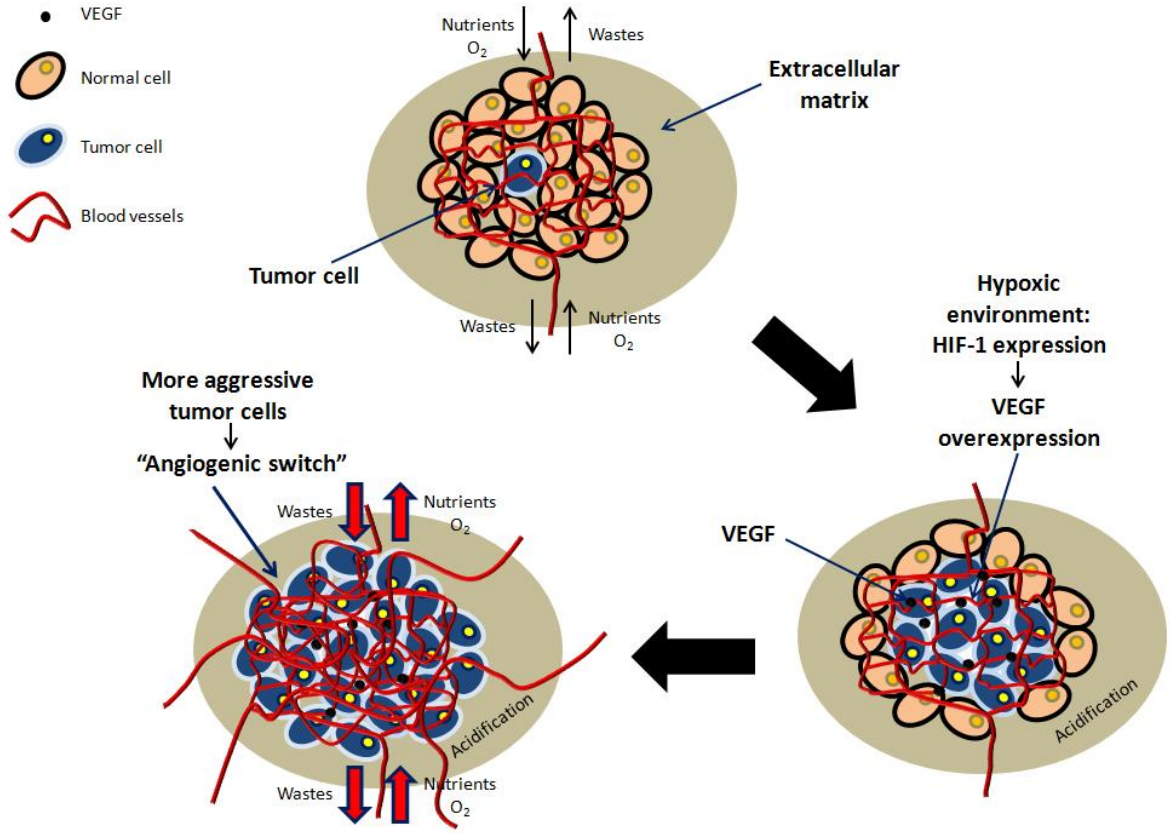

Figure 5. Tumor development and "angiogenic switch". The rapid growth of the tumor leads to the formation of hypoxic regions in the tumor mass (and to the acidification of tumor microenvironment), which induces the expression of HIF-1. HIF-1 activates a series of downstream events, which results in the increased expression of VEGF and the consequent "angiogenic switch", the rapid growth of tumor blood vessels for sustaining tumor growth.

2.3.3. BVZ therapy: tumor starvation and vessels normalization

The novel induced tumor blood vessels are structurally and functionally abnormal, with larger fenestrations and less pericytes coverage. Blood is lost through the fenestrations of the leaking blood vessels, leading to an increased interstitial fluid pressure, edema and leaking of chemotherapeutic drugs during the therapeutic treatment. The target of BVZ is the secreted VEGF-A: once administered intravenously, the antibody recognizes the growth factor, which is no more available for the recognition by its receptors, the VEGFRs. This causes the inhibition of new blood vessels growth and the regression of the existing ones, restoring the structure of the hematic tissue [74,77]. Less nutrients are available for the faster growing tumor, that is hence starved. The idea of starving the tumors blocking angiogenesis started in the beginning of the '70s and successfully ended up in 2004, with the approval by FDA of BVZ [11,71,72,78]. The regression of the tumor blood vessels to a standard condition is called "normalization" (i.e. decreased number and size of immature tumor vessels, increased pericytes coverage and reduced interstitial pressure) (Figure 6) [77]. This procedure enhances the delivery of chemotherapeutic agents and allows a better oxygenation of the tumor, which makes the therapies more effective (the effect of certain chemotherapeutic agents is based on the formation of reactive oxygen species, which are not formed in an environment with lack of oxygen, like tumor masses) [79]. In fact, BVZ is always given in combination with

chemotherapeutic drugs and no significant benefits have been measured when the antibody alone is administered [11,80].

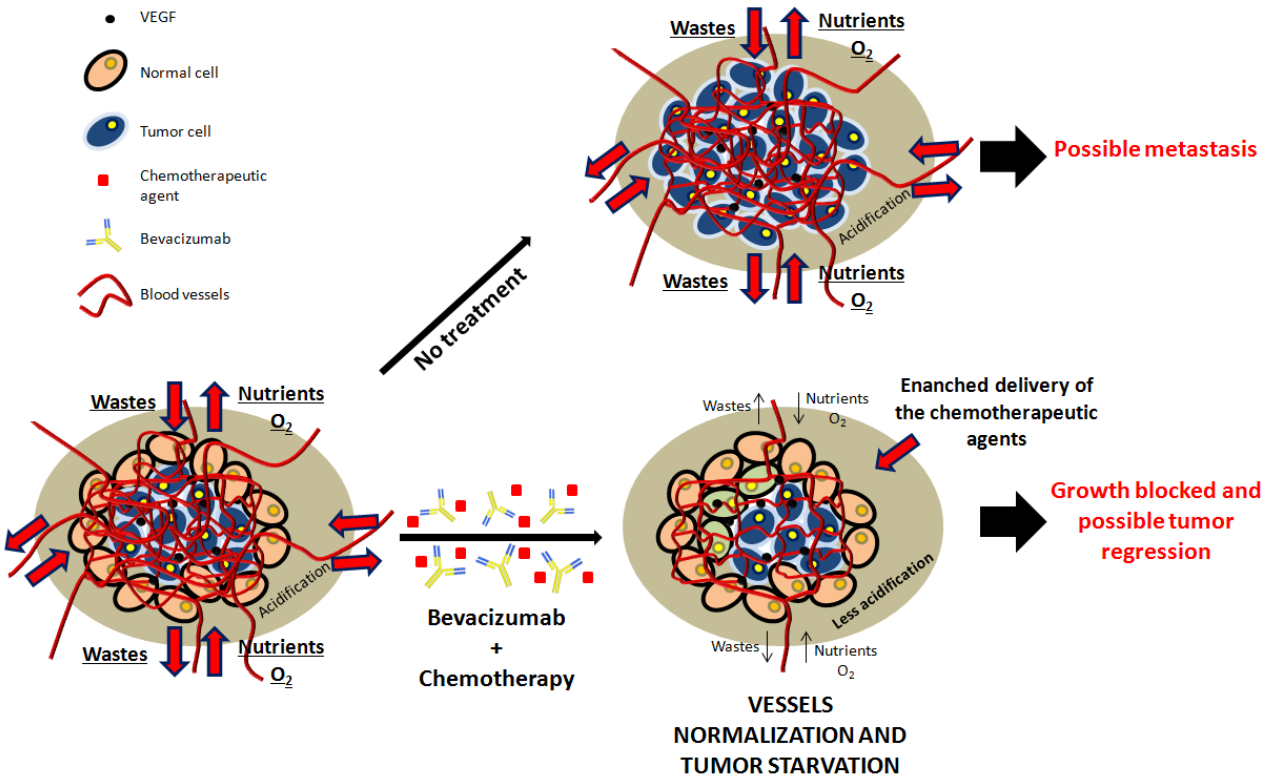

Figure 6. Schematic view of an untreated tumor and of a tumor treated with BVZ and chemotherapy. The tumor vascularization has grown thanks to the presence of pro-angiogenic factors like VEGF-A. If the tumor is not treated, it keeps growing and possible metastasis can be formed. When the tumor is treated with BVZ, blood vessels are normalized, allowing a better penetration of the chemotherapeutic agents and the starvation of tumor cells.

2.3.4. Resistance mechanisms to anti-angiogenic therapies

After the BVZ treatment, a first period of clinical benefit followed by a further tumor regrowth (within months) is often observed. This is attributed to some resistance mechanisms which tumor cells use for by-passing the effect of the anti-angiogenic therapies. A list of the known mechanisms against BVZ therapy is resumed in Table 4.

Table 4. Mechanisms used by tumor cells to resist the treatment with BVZ.

BVZ resistance mechanisms description	Reference
Use of alternative pro-angiogenic factors: the BVZ blocks the VEGF-A pathways but the cancer cells use alternative pro-angiogenic factors for favoring angiogenesis. Examples of the alternative factors are FGF1, FGF2, Bv8 and PlGF.	[54,81–83]
Recruitment of vascular progenitor cells and pro-angiogenic monocytes from the bone marrow. An example is given by TAMs (tumor associated macrophages) which are recruited due to the low levels of oxygen and by the tumor cells secretion of VEGF-A. The recruited TAMs produce pro-angiogenic factors which confer resistance to the BVZ therapies. The myeloid cells are recruited due to the release of a storm of cytokines from the healthy tissues as a consequence of the VEGF-A blockade. The newly recruited myeloid cells can also increase their production of VEGF-A (due to the hypoxic environment or transcription activation by oncogenes) [84,85].	[67,84–88]
The new vessels formation can be caused by differentiation processes, independent from the VEGF-A signal. Examples are the differentiation of tumor cells or bone-marrow derived tumor stem cells to endothelial cells. Also, the presence of pre-existing circulating endothelial progenitors which can differentiate to endothelial cells or which can secrete angiogenic cytokines, can be a cause of resistance.	[88,89]
Increased and tight pericytes coverage. After the tumor regression induced by BVZ, a "pool" of pericytes tightly associated to the remained blood vessels resist. These pericytes confer resistance to the blood vessels, which could start growing again. Also, pericytes can express VEGF-A and other pro-angiogenic factors. Endothelial cells can recruit pericytes (through the release of cytokines) which will get associated to the newly formed vessels rendering them more stable.	[88,90,91]
Intracrine production of VEGF-A by cancer cells. The intracellularly produced growth factor is able to activate the VEGF-A signal cascade which leads to cancer cell survival and promotes invasion and migration.	[92,93]

2.3.5. Nanoencapsulation of BVZ in cancer treatment: state of art

In the sparse bibliography found on nanoencapsulation of BVZ, the described advantages are generally the same as the ones previously cited for the encapsulation of mAbs. However, it is particularly significant to underline the importance of the nanoencapsulation of BVZ for hypothetically overcoming the frequently observed resistance mechanisms [54,81–89]. In fact, the nanocarriers can allow the targeting of both the extracellular, surface localized, and the intracellular pool of VEGF-A, enhancing the effect of the therapy [66,94,95]. Tangutoori and co-workers hypothesized that targeting the VEGF-A prior being released would inhibit the VEGF-A signal cascade before its activation, thus limiting or avoiding the recruitment of bone marrow-derived cells progenitors (from which TAMs are for example generated) [28]. Blocking the signal cascade before it starts would also potentially increase the BVZ action, avoiding the formation of new blood vessels, tumor invasion and metastasis formation. [18,66]. It has also been shown *in vivo* that blocking the VEGF-A secretion strongly reduces lung carcinoma growth [96]. Recent studies also demonstrated that blocking the secreted VEGF-A has no effects on the AKT or ERK1/2 phosphorilation (i.e. some of the proteins activated by the VEGF cascade and which action confers tumor cells survival), indicating the intracellular VEGF-A pool as the main source of survival for colorectal cancer [92]. Similar results have been shown for breast cancer, where the intracrine VEGF-A plays a role in cell survival by its interaction with VEGFR-1 (Flt-1) [97]. It has also been demonstrated that blocking the intracellularly produced VEGF-A significantly reduces tumor cells migration and invasion [93].

Overall, it can be concluded that targeting the intracellular VEGF-A population, delivering BVZ in the cytoplasm of tumor cells, could potentially avoid the activation of survival signals and the formation of metastasis.

It is also important to stress that the nanoencapsulation of BVZ could also reduce the toxicity issues observed upon the treatment with the free mAb. In fact, hypertension, proteinuria, gastrointestinal perforation and increased thromboembolic events have been described upon the intravenous administration of the drug. Its nanoencapsulation could decrease these side effects by reducing the off-target toxicity and immunogenicity [95,98,99].

Until now, some works have described the development of both polymer- and lipid-based nanocarriers for the encapsulation and release of BVZ [18,100,101]. Table 5, summarizes the BVZ-loaded nanosystems reported in the literature for cancer therapy. A schematic representation of the used systems is presented in Figure 7. Most of the described nanosystems have been intended to target the intracellular VEGF pool [18,94,102]. For example, Tangutoori and co-workers developed liposomes which co-deliver BVZ and BPD (a photo-inducible molecule which generates cytotoxic species when irradiated) for the treatment of pancreatic cancer. They demonstrated, the *in vitro* capacity of the system to deliver BVZ in the cytoplasm of the tumor cells, suggesting that the good results obtained *in vivo* with the combined therapy could be partially due to the intracellular VEGF-A blocking [18]. A similar approach was described by Spring and co-workers, who demonstrated that the co-delivery of BVZ and BDP in the cytoplasm of cancer cells led to a drastic reduction of the tumor burden in a pancreatic cancer bearing mice model [100]. In another work, the intracellular delivery of BVZ from mesoporous silica nanoparticles was found to correlate with a higher cancer cell mortality through apoptotic mechanisms [95]. Tang and co-workers also showed the superiority of

the treatment of breast cancer bearing mice when two types of liposomes were co-administered, one encapsulating doxorubicin (and surface decorated with an anti-HER2 antibody) and the other one containing BVZ. The co-administration of the two delivery systems significantly reduced the tumor growth compared to the controls (i.e. the liposomes administered alone or free doxorubicin) [101]. Finally, Battaglia et al. proposed the encapsulation of BVZ into solid lipid nanoparticles, for the treatment of glioblastoma. The results showed that, *in vitro*, BVZ activity increased from 100 to 200 times when encapsulated. It was also demonstrated *in vitro* that the nanoparticles allow the BVZ permeation through a blood brain barrier cell monolayer, while it was not the case of free BVZ [102].

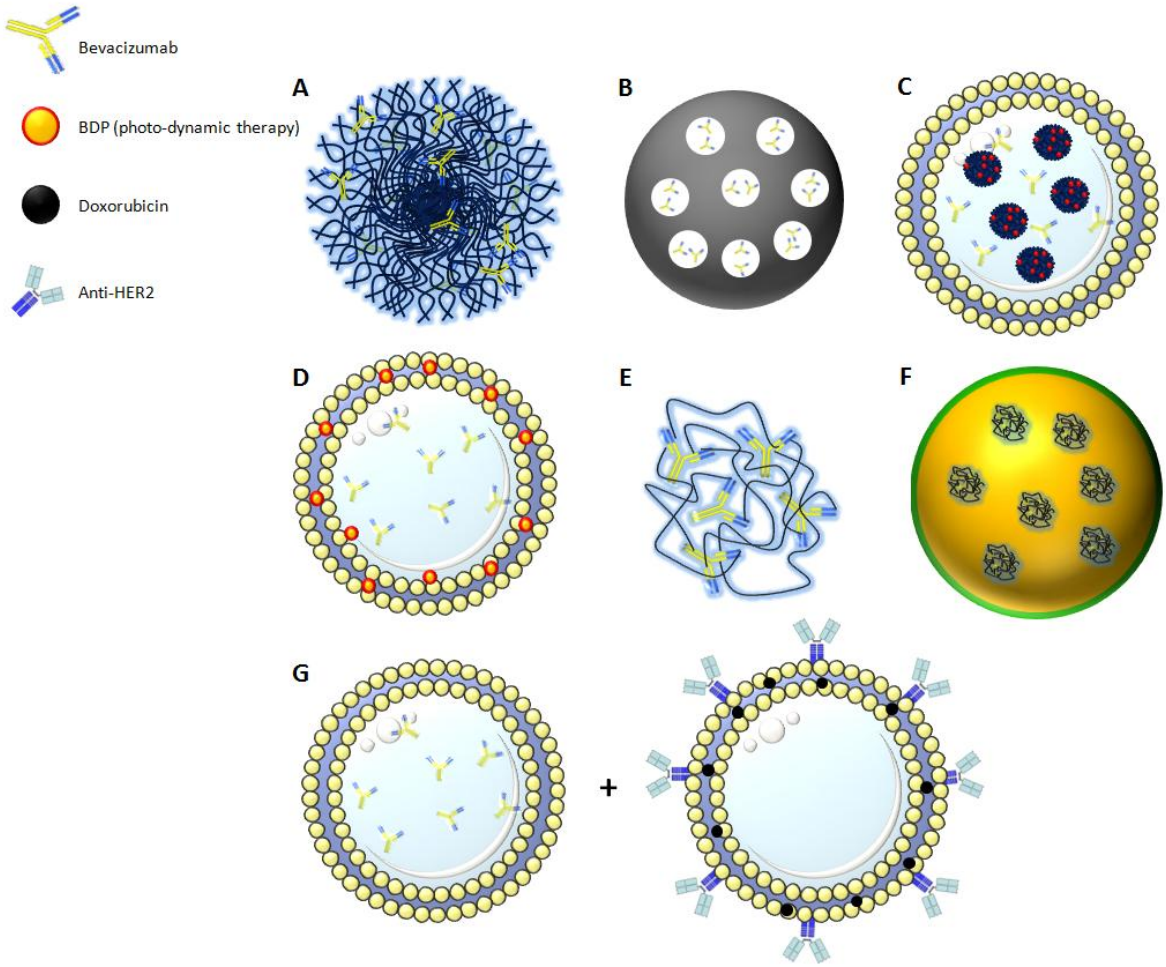

Figure 7. Schematic representation of the nanocarriers used for associating BVZ and treating different types of tumors. The figure reflects the formulation approaches described in Table 5. A) PLGA nanoparticles used by Sousa and co-workers [24]*; B) Mesoporous silica nanoparticles used by the Zhang´s group* [95]. *C) Nanocells used by Spring and co-workers: BDP loaded PLGA nanoparticles were encapsulated into BVZ containing liposomes* [100]*; D) BDP and BVZ-loaded liposomes used in the work of Tangutoori et al.* [18]*; E) Self-assembled BVZ nanoparticles used by Srinivasan et al.* [66]*; F) Battaglia's BVZ-loaded solid-lipid nanoparticles* [102]*; G) BVZ-loaded liposomes used in combination with doxorubicin-loaded anti-HER2 decorated liposomes described in the work of Tang et al.* [101].

Table 5. Bevacizumab (BVZ)-loaded nanocarriers for tumor treatment found in literature. Some experimental details are given (i.e. size of the carrier, the type of therapy, if the authors performed in vivo experiments, the obtained achievements and the ability of the nanocarrier for delivering the antibody inside the cells).

Type of nanocarrier	Size (nm)	In vivo efficacy	Type of therapy	Achievement	Target	Cellular uptake	Reference
PLGA NPs	199	Not done	Single therapy	BVZ partially loses its conformation when formulated, however once released it folds back to the native form. It was shown *in vitro* that the released antibody was still active (through viability and proliferation assays of HUVEC cells)	Tumors in general	Not done	[24]
Mesoporous silica NPs	166	Not done	Single therapy	It was demonstrated *in vitro* the superiority of the treatment with encapsulated BVZ by measuring the cytotoxicity in cancer cells. The formulation was able to control the release of the antibody up to 100 h and the presence of a targeting moiety (antibody fragment) on their surface favored the internalization of the carrier	Ovarian cancer	Yes, in vitro	[95]
Liposomes containing PLGA-PEG nanoparticles	NA	Yes	Combination of BVZ with photodynamic therapy (BDP)	It was shown the *in vivo* intracellular release of both BDP and BVZ, enhancing the anticancer efficacy of the single treatments.	Human pancreatic cancer	Yes, in vitro and in vivo	[100]
Liposomes	111-122	Yes	Combination of BVZ with photodynamic therapy (BDP)	The *in vivo* antitumor activity was enhanced when the BDP and BVZ were combined. It was also proved the *in vitro* intracellular uptake by the cancer cells and an increased in vivo BVZ tumor accumulation. It was hypothesized that the intracellular delivery of BVZ could have a role in overcoming some resistance mechanisms making the therapy more efficient.	Pancreatic ductal adenocarcinoma	Yes, in vitro	[18]
Self-assembled BVZ	370-770	Not done	Single therapy	It was shown the importance of surfactants for the mantainance of antibody's structure. The anti-VEGF effect of BVZ was maintained after being formulated and released in the cytoplasm of cancer cells	Non-small Lung cancer	Yes, in vitro	[66]
Solid lipid NPs	420	Not done	Single therapy	BVZ-associated nanoparticles surprisingly increased BVZ activity compared to the free drug. It was also shown the ability of the nanoparticles to allow the BVZ permeation through a blood brain barrier cell monolayer (hCMEC/D3 cell)	Glioblastoma	Not done	[102]
Liposomes	150	Yes	Combination of BVZ with chemotherapy (doxorubicin)	It was shown in vivo the increase of anticancer efficacy when BVZ and doxorubicin were incorporated in liposomes. The antibody and doxorubicin were encapsulated into two independent liposomes formulations. The doxorubicin-associating liposomes were surface decorated with an anti-HER2 antibody, which increased the targeting properties of the delivery system. The combined therapy increased the antitumor efficacy in comparison to the single administration of the liposomal formulations	Breasr cancer	Not done	[101]

2.4. Concluding remarks

Overall, the interest of nanotechnology for the delivery of therapeutic proteins, with emphasis on mAbs, is presented in this chapter. In the last decades, these molecules have been extensively investigated due to their high specificity and selectivity and these research efforts have led to the commercialization of a significant number of them, especially in the field of cancer [39,58,59]. However, several limitations still need to be solved, such as the poor penetration in solid tumors, the lack of intracellular antigens targeting, the development of resistance mechanisms and immunogenic reactions [60,62]. In this regard, different technologies based on mAbs-loaded nanoparticles (see Table 3) have recently been developed with the aim of improving the free mAbs-based therapies.

In this chapter, special attention has been paid to the use of BVZ for treating solid tumors and to its nanoencapsulation. BVZ acts on the tumor vasculature, normalizing the blood vessels, starving the tumor and enhancing the delivery of the common chemotherapeutics [71]. BVZ is normally administered in combination with chemotherapeutic agents [80]. Despite its efficacy, problems related to the development of resistance mechanisms (where the intracellular VEGF-A play a pivotal role) and its toxicity, have encouraged researchers to develop nanoformulations to overcome these issues (see Table 5). The strategies have generally involved the co-encapsulation of BVZ along with chemotherapeutic or photo-inducible agents. It has been claimed that the enhancement of the anticancer effect is due to the intracellular delivery of BVZ, which acts on the VEGF-A intracellular pool [18,95,100]. However, no reports have been found regarding single therapies with nanoencapsulated BVZ.

Bibliography

[1] https://www.nature.com/subjects/cancer/.
[2] G.M. Cooper, The Cell-A Molecular Approach, 2000.
[3] F. Bray, J. Ferlay, I. Soerjomataram, R.L. Siegel, L.A. Torre, A. Jemal, Global Cancer Statistics 2018: GLOBOCAN Estimates of Incidence and Mortality Worldwide for 36 Cancers in 185 Countries, CA. Cancer J. Clin. 68 (2018) 394–424. doi:10.3322/caac.21492.
[4] Globocan, https://www.uicc.org/new-global-cancer-data-globocan-2018, (2018).
[5] NIH, Cancer treatment, https://www.cancer.gov/about-cancer/treatment.
[6] E. Pérez-Herrero, A. Fernández-Medarde, Advanced targeted therapies in cancer: Drug nanocarriers, the future of chemotherapy, Eur. J. Pharm. Biopharm. 93 (2015) 52–79. doi:10.1016/j.ejpb.2015.03.018.
[7] B.A. Chabner, T.G. Roberts Jr, Chemotherapy and the war on cancer, Nat. Rev. Cancer. 5 (2005) 65–72.
[8] Metastasis: Diagnosing & Treating Metastatic Cancer,. https://www.cancercenter.com/terms/metastasis/.
[9] J.R. Kintzing, M. V. Filsinger Interrante, J.R. Cochran, Emerging Strategies for Developing Next-Generation Protein Therapeutics for Cancer Treatment, Trends Pharm. Sci. 37 (2016) 1–16.
[10] H.A.D. Lagassé, A. Alexaki, V.L. Simhadri, N.H. Katagiri, W. Jankowski, Z.E. Sauna, C. Kimchi-sarfaty, Recent advances in (therapeutic protein) drug development, F1000 Res. 6 (2017) 1–17. doi:10.12688/f1000research.9970.1.
[11] G. Bergers, D. Hanahan, Modes of resistance to anti-angiogenic therapy, Nat. Rev. Drug Discov. 8 (2008) 592–603. doi:10.1038/nrc2442.

[12] P.A. Tang, M.J. Moore, Aflibercept in the treatment of patients with metastatic colorectal cancer : latest findings and interpretations, Therap. Adv. Gastroenterol. 6 (2013) 459–473. doi:10.1177/1756283X13502637.

[13] A. Patel, K. Cholkar, A.K. Mitra, Recent developments in protein and peptide parenteral delivery approaches, Ther. Deliv. 5 (2014) 337–365. doi:10.4155/tde.14.5.

[14] I. Santalices, A. Gonella, D. Torres, M. Jos, Advances on the formulation of proteins using nanotechnologies, J. Drug Deliv. Sci. Technol. 42 (2017) 155–180. doi:10.1016/j.jddst.2017.06.018.

[15] R.A. Beckman, L.M. Weiner, H.M. Davis, Antibody constructs in cancer therapy. Protein Engineering Strategies to Improve Exposure in Solid Tumors, Cancer. 109 (2007) 170–179. doi:10.1002/cncr.22402.

[16] D. Rosenblum, N. Joshi, W. Tao, J.M. Karp, D. Peer, Progress and challenges towards targeted delivery of cancer therapeutics, Nat. Commun. 9 (2018) 1–12. doi:10.1038/s41467-018-03705-y.

[17] A. Kim, Y. Miura, T. Ishii, O. Mutaf, N. Nishiyama, H. Cabral, K. Kataoka, Intracellular Delivery of Charge-Converted Monoclonal Antibodies by Combinatorial Design of Block/Homo Polyion Complex Micelles, Biomacromolecules. (2016) 446–453. doi:10.1021/acs.biomac.5b01335.

[18] S. Tangutoori, B.Q. Spring, Z. Mai, A. Palanisami, L.B. Mensah, T. Hasan, Simultaneous delivery of cytotoxic and biologic therapeutics using nanophotoactivatable liposomes enhances treatment efficacy in a mouse model of pancreatic cancer, Nanomedicine Nanotechnology, Biol. Med. 12 (2016) 223–234. doi:10.1016/j.nano.2015.08.007.

[19] A. Gdowski, A. Ranjan, A. Mukerjee, J. Vishwanatha, Development of Biodegradable Nanocarriers Loaded with a Monoclonal Antibody, Int. J. Mol. Sci. 16 (2015) 3990–3995. doi:10.3390/ijms16023990.

[20] M.P. Baker, H.M. Reynolds, B. Lumicisi, C.J. Bryson, Immunogenicity of protein therapeutics The key causes , consequences and challenges, Self. Nonself. 1 (2010) 314–322. doi:10.4161/self.1.4.13904.

[21] A. Almalik, H. Benabdelkamel, A. Masood, I.O. Alanazi, M.A. Majrashi, A.A. Alfadda, W.M. Alghamdi, H. Alrabiah, N. Tirelli, A.H. Alhasan, Hyaluronic Acid Coated Chitosan Nanoparticles Reduced the Immunogenicity of the Formed Protein Corona, Sci. Rep. 7 (2017) 1–9. doi:10.1038/s41598-017-10836-7.

[22] J.E. Chung, S. Tan, S.J. Gao, N. Yongvongsoontorn, S.H. Kim, J.H. Lee, H.S. Choi, H. Yano, L. Zhuo, M. Kurisawa, J.Y. Ying, Self-assembled micellar nanocomplexes comprising green tea catechin derivatives and protein drugs for cancer therapy, Nat. Nanotechnol. 9 (2014) 907–912. doi:10.1038/nnano.2014.208.

[23] F. Ordikhani, M. Uehara, V. Kasinath, L. Dai, S.K. Eskandari, B. Bahmani, M. Yonar, J.R. Azzi, Y. Haik, P.T. Sage, G.F. Murphy, N. Annabi, T. Schatton, I. Guleria, R. Abdi, Targeting antigen-presenting cells by anti – PD-1 nanoparticles augments antitumor immunity, JCI Insight. 3 (2018) 1–17. doi:doi: 10.1172/jci.insight.122700.

[24] F. Sousa, A. Cruz, P. Fonte, I.M. Pinto, M.T. Neves-, A new paradigm for antiangiogenic therapy through controlled release of bevacizumab from PLGA nanoparticles, (2017) 1–13. doi:10.1038/s41598-017-03959-4.

[25] G. Tripodo, A. Trapani, M. Luisa, G. Giammona, G. Trapani, D. Mandracchia, Hyaluronic acid and its derivatives in drug delivery and imaging : Recent advances and challenges, Eur. J. Pharm. Biopharm. 97 (2015) 400–416. doi:10.1016/j.ejpb.2015.03.032.

[26] A.R. Srinivasan, A. Lakshmikuttyamma, S.A. Shoyele, Investigation of the Stability and Cellular Uptake of Self-Associated Monoclonal Antibody (MAb) Nanoparticles by Non-Small Lung Cancer Cells, Mol. Pharm. 10 (2013) 3275–3284. doi:10.1021/mp3005935.

[27] H. Deng, K. Song, X. Zhao, Y. Li, F. Wang, J. Zhang, A. Dong, Z. Qin, Tumor Microenvironment Activated Membrane Fusogenic Liposome with Speedy Antibody and Doxorubicin Delivery for

Synergistic Treatment of Metastatic Tumor, ACS Appl. Mater. Interfaces. 9 (2017) 9315–9326. doi:10.1021/acsami.6b14683.

[28] S. Tangutoori, B.Q. Spring, Z. Mai, A. Palanisami, L.B. Mensah, T. Hasan, Simultaneous delivery of cytotoxic and biologic therapeutics using nanophotoactivatable liposomes enhances treatment efficacy in a mouse model of pancreatic cancer, Nanomedicine Nanotechnology, Biol. Med. 12 (2016) 223–234. doi:10.1016/j.nano.2015.08.007.

[29] L. Li, J. Wang, H. Kong, Y. Zeng, G. Liu, Functional biomimetic nanoparticles for drug delivery and theranostic applications in cancer treatment, Sci. Technol. Adv. Mater. 19 (2018) 771–790. doi:10.1080/14686996.2018.1528850.

[30] R. Mout, M. Ray, T. Tay, K. Sasaki, G.Y. Tonga, V.M. Rotello, General Strategy for Direct Cytosolic Protein Delivery via Protein−Nanoparticle Co‑engineering, ACS Nano. 11 (2017) 6416–6421. doi:10.1021/acsnano.7b02884.

[31] P. Zhang, F. Sun, C. Tsao, S. Liu, P. Jain, A. Sinclair, H. Hung, T. Bai, K. Wu, S. Jiang, Zwitterionic gel encapsulation promotes protein stability, enhances pharmacokinetics, and reduces immunogenicity, PNAS. 112 (2015) 12046–12051. doi:10.1073/pnas.1512465112.

[32] V.P. Torchilin, A.N. Lukyanov, Peptide and protein drug delivery to and into tumors: challenges and solutions, Drug Discov. Today. 8 (2003) 259–266. doi:10.1016/S1359-6446(03)02623-0.

[33] W. Il Choi, N. Kamaly, L. Riol-blanco, I. Lee, J. Wu, A. Swami, C. Vilos, B. Yameen, M. Yu, J. Shi, I. Tabas, U.H. Von Andrian, S. Jon, O.C. Farokhzad, A Solvent-Free Thermosponge Nanoparticle Platform for E fficient Delivery of Labile Proteins, Nano Lett. 14 (2014) 6449–6455. doi:10.1021/nl502994y.

[34] N.E. Holodick, N. Rodriguez-Zhurbenko, A.M. Hernández, Defining Natural Antibodies, Front. Immunol. 8 (2017) 1–8. doi:10.3389/fimmu.2017.00872.

[35] M. Stern, R. Herrmann, Overview of monoclonal antibodies in cancer therapy : present and promise, Clin. Rev. Oncol. Hematol. 54 (2005) 11–29. doi:10.1016/j.critrevonc.2004.10.011.

[36] H. Schroeder Jr, L. Cavacini, Structure and Function of Immunoglobulins, J. Allergy Clin. Immunol. 125 (2010) 41–52. doi:10.1016/j.jaci.2009.09.046.Structure.

[37] K. Elegert, Immunology: Understanding the Immune System, 1998.

[38] A. Saxena, D. Wu, Advances in Therapeutic Fc engineering – Modulation of igG-Associated effector Functions and Serum Half-life, Front. Immunol. 7 (2016) 1–11. doi:10.3389/fimmu.2016.00580.

[39] Animal Cell Technology Industrial Platform - Monoclonal Antibodies Approved by the EMA and FDA for Therapeutic Use (status 2017), (2017). http://www.actip.org/products/monoclonal-antibodies-approved-by-the-ema-and-fda-for-therapeutic-use/.

[40] A. Coulson, A. Levy, Monoclonal Antibodies in Cancer Therapy : Mechanisms, Successes and Limitations, West Indian Med. J. 63 (2014) 650–654. doi:10.7727/wimj.2013.241.

[41] A.M. Scott, J.P. Allison, J.D. Wolchok, H. Hughes, Monoclonal antibodies in cancer therapy, Cancer Immun. 12 (2012) 1–8.

[42] J. Osbourn, L. Jermutus, A. Duncan, Current methods for the generation of human antibodies for the treatment of autoimmune diseases, Drug Discov. Today. 8 (2003) 845–851. doi:10.1016/S1359-6446(03)02803-4.

[43] A.L. Grilo, A. Mantalaris, The Increasingly Human and Profitable Monoclonal Antibody Market, Trends Biotechnol. In Press (2014) 1–7. doi:10.1016/j.tibtech.2018.05.014.

[44] D.M. Ecker, S.D. Jones, H.L. Levine, The therapeutic monoclonal antibody market, MAbs. 7 (2015) 9–14. doi:10.4161/19420862.2015.989042.

[45] Grand View Research, https://www.grandviewresearch.com/industry-analysis/monoclonal-antibodies-market.

[46] A.L. Catapano, N. Papadopoulos, The safety of therapeutic monoclonal antibodies : Implications for cardiovascular disease and targeting the PCSK9 pathway, Atherosclerosis. 228 (2013) 18–28. doi:10.1016/j.atherosclerosis.2013.01.044.
[47] A.M. Scott, J.D. Wolchok, L.J. Old, Antibody therapy of cancer, Nature. 12 (2012) 278–287. doi:10.1038/nrc3236.
[48] H. Modjtahedi, S. Ali, S. Essapen, Therapeutic application of monoclonal antibodies in cancer : advances and challenges, Br. Med. Bullettin. 104 (2012) 41–59. doi:10.1093/bmb/lds032.
[49] M.J. Miller, Cancer Immunotherapy: Present Status, Future Perspective, and a New Paradigm of Peptide Immunotherapeutics, Discov. Med. 15 (2013) 166–176.
[50] P. Chames, M. Van Regenmortel, E. Weiss, D. Baty, Therapeutic antibodies: successes , limitations and hopes for the future, Br. J. Pharmacol. 157 (2009) 220–233. doi:10.1111/j.1476-5381.2009.00190.x.
[51] A. Gdowski, A. Ranjan, A. Mukerjee, J. Vishwanatha, Development of Biodegradable Nanocarriers Loaded with a Monoclonal Antibody, Int. J. Mol. Sci. 16 (2015) 3990–3995. doi:10.3390/ijms16023990.
[52] T.T. Hansel, H. Kropshofer, T. Singer, J.A. Mitchell, A.J.T. George, The safety and side effects of monoclonal antibodies, Nat. Rev. Drug Discov. 9 (2010) 325–338. doi:10.1038/nrd3003.
[53] C.W. Shuptrine, R. Surana, L.M. Weiner, Monoclonal antibodies for the treatment of cancer, Semin. Cancer Biol. 22 (2012) 3–13. doi:10.1016/j.semcancer.2011.12.009.
[54] O. Casanovas, D.J. Hicklin, G. Bergers, D. Hanahan, Drug resistance by evasion of antiangiogenic targeting of VEGF signaling in late-stage pancreatic islet tumors, Cancer Cell. 8 (2005) 299–309. doi:10.1016/j.ccr.2005.09.005.
[55] L. Reslan, S. Dalle, C. Dumontet, Understanding and circumventing resistance to anticancer monoclonal antibodies, MAbs. 1 (2009) 222–229.
[56] A. Lièvre, J.-B. Bachet, V. Boige, A. Cayre, D. Le Corre, E. Buc, M. Ychou, O. Bouche, B. Landi, C. Louvet, T. Andre, F. Bibeau, M.-D. Diebold, P. Rougier, M. Ducreux, G. Tomasic, J.-F. Emile, F. Penault-Llorca, P. Laurent-Puig, KRAS Mutations As an Independent Prognostic Factor in Patients With Advanced Colorectal Cancer Treated With Cetuximab, J. Clin. Oncol. 26 (2019) 374–379. doi:10.1200/JCO.2007.12.5906.
[57] S.A. Price-Schiavi, S. Jepson, L. Peter, M. Arango, P.S. Rudland, L. Yee, K.L. Carraway, Rat MUC4 (sialomucin complex) reduces binding of anti-ERBB2 antibodies to tumor cell surfaces, a potential mechanism for Herceptin resistance, Int. J. Cancer. 99 (2002) 783–791. doi:10.1002/ijc.10410.
[58] J.T. Pento, Monoclonal Antibodies for the Treatment of Cancer, Anticancer Res. 37 (2017) 5935–5939. doi:10.21873/anticanres.12040.
[59] S.M. Chiavenna, J.P. Jaworski, A. Vendrell, State of the art in anti-cancer mAbs, J. Biomed. Sci. 24 (2017) 1–12. doi:10.1186/s12929-016-0311-y.
[60] F. Sousa, P. Castro, P. Fonte, P.J. Kennedy, M. Teresa, B. Sarmento, Nanoparticles for the delivery of therapeutic antibodies: Dogma or promising strategy?, Expert Opin. Drug Deliv. 14 (2017) 1163–1176. doi:10.1080/17425247.2017.1273345.
[61] M. Arruebo, Antibody-Conjugated Nanoparticles for Biomedical Applications, J. Nanomater. 2009 (2009) 1–24. doi:10.1155/2009/439389.
[62] M. Hofmann, M. Guschel, A. Bernd, J. Bereiter-Hahn, R. Kaufmann, C. Tandi, H. Wiig, S. Kippenberger, Lowering of Tumor Interstitial Fluid Pressure Reduces Tumor Cell Proliferation in a Xenograft Tumor Model 1, Neoplasia. 8 (2006) 89–95. doi:10.1593/neo.05469.
[63] P. Chames, M. Van Regenmortel, E. Weiss, D. Baty, Therapeutic antibodies : successes, limitations and hopes for the future, Br. J. Pharmacol. 157 (2009) 220–233. doi:10.1111/j.1476-5381.2009.00190.x.
[64] T.T. Kuo, V.G. Aveson, Neonatal Fc receptor and IgG-based therapeutics, MAbs. 3 (2011) 422–430. doi:10.4161/mabs.3.5.16983.

[65] R.A. Beckman, L.M. Weiner, H.M. Davis, Antibody constructs in cancer therapy - Protein Engineering Strategies to Improve Exposure in Solid Tumors, Cancer. 109 (2006) 170–179. doi:10.1002/cncr.22402.

[66] A.R. Srinivasan, A. Lakshmikuttyamma, S.A. Shoyele, Investigation of the Stability and Cellular Uptake of Self-Associated Monoclonal Antibody (MAb) Nanoparticles by Non-Small Lung Cancer Cells, Mol. Pharm. 10 (2013) 3275–3284.

[67] X. Zhao, H.Q. Liu, J. Li, X.L. Liu, Endothelial progenitor cells promote tumor growth and progression by enhancing new vessel formation, Oncol. Lett. 12 (2016) 793–799. doi:10.3892/ol.2016.4733.

[68] P. Milla, F. Dosio, L. Cattel, PEGylation of Proteins and Liposomes : a Powerful and Flexible Strategy to Improve the Drug Delivery, Curr. Drug Metab. 13 (2012) 105–119. doi:10.2174/138920012798356934.

[69] C. Guo, Y. Chen, W. Gao, A. Chang, Y. Ye, W. Shen, Y. Luo, S. Yang, P. Sun, R. Xiang, N. Li, Liposomal Nanoparticles Carrying anti-IL6R Antibody to the Tumour Microenvironment Inhibit Metastasis in Two Molecular Subtypes of Breast Cancer Mouse Models, Theranostics. 7 (2017) 775–778. doi:10.7150/thno.17237.

[70] S.E. Zale, Therapeutic nanoparticles comprising a therapeutic agent and methods of making and using same, 2017.

[71] L.M. Ellis, Mechanisms of Action of Bevacizumab as a Component of Therapy for Metastatic Colorectal Cancer, Semin. Oncol. 33 (2006) S1–S7. doi:10.1053/j.seminoncol.2006.08.002.

[72] Genentech, FDA Approves Avastin, a Targeted Therapy for First-Line Metastatic Colorectal Cancer Patients, (2004). https://www.gene.com/media/press-releases/7167/2004-02-26/fda-approves-avastin-a-targeted-therapy-.

[73] M. Ignez, J. Sabbaga, P.M. Hoff, Bevacizumab: overview of the literature, Expert Rev. Anticancer Ther. 12 (2012) 567–580. doi:10.1586/era.12.13.

[74] H. Gerber, N. Ferrara, Pharmacology and Pharmacodynamics of Bevacizumab as Monotherapy or in Combination with Cytotoxic Therapy in Preclinical Studies, Am. Assoc. Cancer Res. 65 (2005) 671–681.

[75] D. Hanahan, R.A. Weinberg, Review Hallmarks of Cancer : The Next Generation, Cell. 144 (2011) 646–674. doi:10.1016/j.cell.2011.02.013.

[76] D.M. Gilkes, G.L. Semenza, D. Wirtz, Hypoxia and the extracellular matrix: drivers of tumour metastasis, Nat. Rev. Cancer. 14 (2014) 430–439. doi:10.1038/nrc3726.

[77] M. Arjaans, T.H.O. Munnink, S.F. Oosting, A.G.T.T. Van Scheltinga, J.A. Gietema, E.T. Garbacik, H. Timmer-bosscha, M.N.L. Hooge, Bevacizumab-Induced Normalization of Blood Vessels in Tumors Hampers Antibody Uptake, Am. Assoc. Cancer Res. 73 (2013) 3347–3356. doi:10.1158/0008-5472.CAN-12-3518.

[78] J. Folkman, Tumor angiogenesis: therapeutic implications, N. Engl. J. Med. 285 (1971) 1182–1186.

[79] P. Carmeliet, R.K. Jain, Principles and mechanisms of vessel normalization for cancer and other angiogenic diseases, Nat. Rev. Drug Discov. 10 (2011) 417–427. doi:10.1038/nrd3455.

[80] R.K. Jain, Antiangiogenesis strategies revisited: from starving tumors to alleviating hypoxia, Cancer Cell. 26 (2014) 605–622. doi:10.1016/j.ccell.2014.10.006.

[81] C.H. Lieu, H. Tran, Z. Jiang, M. Mao, M.J. Overman, E. Lin, C. Eng, J. Morris, L. Ellis, J. V Heymach, S. Kopetz, The Association of Alternate VEGF Ligands with Resistance to Anti-VEGF Therapy in Metastatic Colorectal Cancer, PLoS One. 8 (2013) 1–11. doi:10.1371/journal.pone.0077117.

[82] R. Gyanchandani, M.V. Ortega Alves, J.N. Myers, S. Kim, A Proangiogenic Signature is Revealed in FGF-Mediated Bevacizumab Resistant Head and Neck Squamous Cell Carcinoma, Mol. Cancer Res. 11 (2014) 1585–1596. doi:10.1158/1541-7786.MCR-13-0358.A.

[83] A. Mitsuhashi, H. Goto, A. Saijo, V.T. Trung, Y. Aono, H. Ogino, T. Kuramoto, S. Tabata, H.

Uehara, K. Izumi, M. Yoshida, H. Kobayashi, H. Takahashi, M. Gotoh, S. Kakiuchi, M. Hanibuchi, S. Yano, H. Yokomise, S. Sakiyama, Y. Nishioka, Fibrocyte-like cells mediate acquired resistance to anti-angiogenic therapy with bevacizumab, Nat. Commun. 6 (2015) 1–15. doi:10.1038/ncomms9792.

[84] C. Stockmann, A. Doedens, A. Weidemann, N. Zhang, N. Takeda, J.I. Greenberg, D.A. Cheresh, R.S. Johnson, Deletion of vascular endothelial growth factor in myeloid cells accelerates tumorigenesis, Nature. 456 (2008) 814–819. doi:10.1038/nature07445.

[85] C. Murdoch, M. Muthana, S.B. Coffelt, C.E. Lewis, The role of myeloid cells in the promotion of tumour angiogenesis, Nature. 8 (2008) 618–631. doi:10.1038/nrc2444.

[86] S.B. Coffelt, R. Hughes, C.E. Lewis, Tumor-associated macrophages : Effectors of angiogenesis and tumor progression, Biochim. Biophys. Acta. 1796 (2009) 11–18. doi:10.1016/j.bbcan.2009.02.004.

[87] B.A. Castro, P. Flanigan, A. Jahangiri, D. Hoffman, W. Chen, R. Kuang, M. De Lay, G. Yagnik, J.R. Wagner, S. Mascharak, M. Sidorov, S. Shrivastav, G. Kohanbash, H. Okada, M.K. Aghi, Macrophage migration inhibitory factor downregulation: a novel mechanism of resistance to anti-angiogenic therapy, Oncogene. 36 (2017) 3749–3759. doi:10.1038/onc.2017.1.

[88] S. Loges, T. Schmidt, P. Carmeliet, Mechanisms of Resistance to Anti- Angiogenic Therapy and Development of Third-Generation Anti-Angiogenic Drug Candidates, Genes Cancer. 1 (2010) 12–25. doi:10.1177/1947601909356574.

[89] H. Chen, K. Wu, Endothelial Transdifferentiation of Tumor Cells Triggered by the Twist1-Jagged1-KLF4 Axis : Relationship between Cancer Stemness and Angiogenesis, Stem Cells Int. 2016 (2016) 1–10. doi:10.1155/2016/6439864.

[90] S. Becherirat, F. Valamanesh, Discontinuous Schedule of Bevacizumab in Colorectal Cancer Induces Accelerated Tumor Growth and Phenotypic Changes, Transl. Oncol. 11 (2018) 406–415. doi:10.1016/j.tranon.2018.01.017.

[91] I. Helfrich, I. Scheffrahn, S. Bartling, J. Weis, V. Von Felbert, M. Middleton, M. Kato, S. Ergün, H.G. Augustin, D. Schadendorf, Resistance to antiangiogenic therapy is directed by vascular phenotype , vessel stabilization , and maturation in malignant melanoma, J. Exp. Med. 207 (2010) 491–503. doi:10.1084/jem.20091846.

[92] R. Bhattacharya, X. Ye, R. Wang, X. Ling, M. Mcmanus, F. Fan, D. Boulbes, L.M. Ellis, Intracrine VEGF Signaling Mediates the Activity of Pro-survival Pathways in Human Colorectal Cancer Cells, Cancer Res. 76 (2017) 3014–3024. doi:10.1158/0008-5472.CAN-15-1605.

[93] R. Bhattacharya, F. Fan, R. Wang, X. Ye, L. Xia, D. Boulbes, L.M. Ellis, Intracrine VEGF signalling mediates colorectal cancer cell migration and invasion, Br. J. Cancer. 117 (2017) 848–855. doi:10.1038/bjc.2017.238.

[94] F. Sousa, A. Cruz, P. Fonte, I.M. Pinto, M.T. Neves, B. Sarmento, A new paradigm for antiangiogenic therapy through controlled release of bevacizumab from PLGA nanoparticles, Nat. Sci. Reports. 7 (2017) 1–13. doi:10.1038/s41598-017-03959-4.

[95] Y. Zhang, J. Guo, X. Zhang, D. Li, T. Zhang, Antibody fragment-armed mesoporous silica nanoparticles for the targeted delivery of bevacizumab in ovarian cancer cells, Nanomedicine. 496 (2015) 1026–1033.

[96] M. Björndahl, R. Cao, A. Eriksson, Y. Cao, Blockage of VEGF-Induced Angiogenesis by Preventing VEGF Secretion, Circ. Res. 94 (2004) 1443–50. doi:10.1161/01.RES.0000129194.61747.bf.

[97] T. Lee, S. Seng, M. Sekine, C. Hinton, Y. Fu, H.K. Avraham, S. Avraham, Vascular Endothelial Growth Factor Mediates Intracrine Survival in Human Breast Carcinoma Cells through Internally Expressed VEGFR1/ FLT1, Plos Med. 4 (2007) 1101–1116. doi:10.1371/journal.pmed.0040186.

[98] M.W.V. Henk, H.M. Pinedo, Possible molecular mechanisms involved in the toxicity of angiogenesis inhibition, Nature. 7 (2007) 475–485. doi:10.1038/nrc2152.

[99] F. Saffari, A. Jafarzadeh, B.K. Khandani, F. Saffari, S. Soleimanyamoli, M. Mohammadi, Immunogenicity of Rituximab , Trastuzumab, and Bevacizumab Monoclonal Antibodies in Patients with Malignant Diseases, Int. J. Cancer Manag. 11 (2018) 4–8. doi:10.5812/ijcm.64983.Research.

[100] B. Spring, Z. Mai, P. Rai, S. Chang, T. Hasan, Theranostic Nanocells for Simultaneous Imaging and Photodynamic therapy of Pancreatic Cancer, Opt. Methods Tumor Treat. Detect. Mech. Tech. Photodyn. Ther. 7551 (2010) 1–11. doi:10.1117/12.843725.

[101] Y. Tang, F. Soroush, Z. Tong, M.F. Kiani, B. Wang, Targeted multidrug delivery system to overcome chemoresistance in breast cancer, Int. J. Nanomedicine. 12 (2017) 671–681. doi:10.2147/IJN.S124770.

[102] L. Battaglia, M. Gallarate, E. Peira, D. Chirio, I. Solazzi, S. Marzia, A. Giordano, C.L. Gigliotti, C. Riganti, C. Dianzani, Bevacizumab loaded solid lipid nanoparticles prepared by the coacervation technique: preliminary in vitro studies, Nanotechnology. 26 (2015) 255102. doi:10.1088/0957-4484/26/25/255102.

USC
UNIVERSIDADE
DE SANTIAGO
DE COMPOSTELA

Chapter II

Polymer based nanotechnologies for protein delivery

USC
UNIVERSIDADE
DE SANTIAGO
DE COMPOSTELA

This chapter has been adapted/extracted from the review entitled "Advances on the formulation of proteins using nanotechnologies" [1].

1. An overview of the existing polymer based nanocarriers

Polymer-based nanocarriers (Figure 1) have been widely used for the delivery of proteins and peptides. Both, hydrophobic (e.g. poly(lactide-co-glycolide)) and hydrophilic (e.g. polysaccharides) polymers have been employed during the last years for the encapsulation of peptides and proteins with some promising results. Here, a brief overview of the polymers and techniques used to produce protein/peptide-loaded nanoparticles is given.

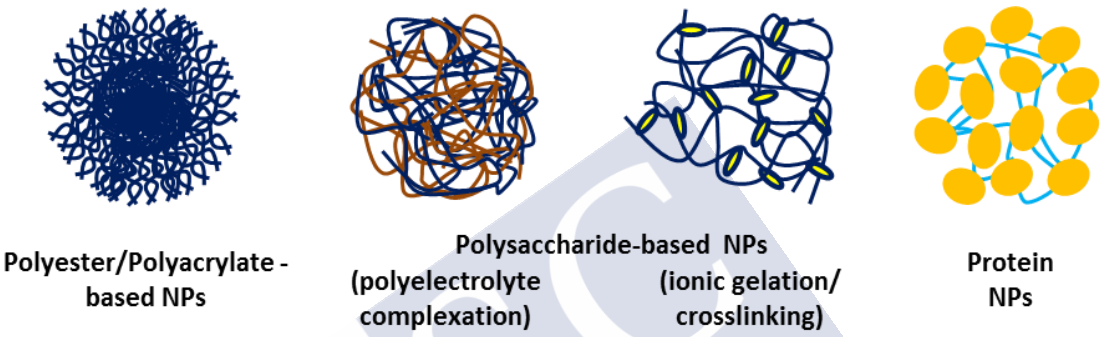

Figure 1. Illustration of the main polymer-based nanoparticles (NPs) used for protein/peptide delivery. Adapted with permission from [1] *(permitted by ELSEVIER).*

1.1. Polyesters-based nanocarriers

Polyesters such as poly(lactide-co-glycolyde) (PLGA), poly(lactide) (PLA) and poly(ε-caprolactone) (PCL), are the most commonly used polymers for pharmaceutical applications, with PLGA as principal polymer for nanoparticles production [2]. In addition, following our discovery on the positive role of the PLGA PEGylation in protein formulation, a number of studies have adopted this strategy [3,4].

PLGA is a synthetic co-polymer composed of a mixture of two structural monomer units: lactic acid and glycolic acid (the monomers which form respectively PLA and PGA). For the purpose of peptide/protein delivery using PLGA nanoparticles, the cargo can be localized either inside the polymer matrix or attached on its surface (adsorbed or covalently linked) [5,6]. The main interest of these polymers relies on the fact that they are part of a number of marketed formulations, some of them containing peptides [7].

1.1.1. Preparation techniques

Overall the principles for the formation of these nanoparticles involve the dissolution of the protein in an aqueous phase and the dissolution of the polymer in an organic solvent. The main difference among techniques resides in the nature of the organic solvent in which the polymer is dissolved, and in the composition of the external aqueous phase. In the case that the polymer is dissolved in a non-polar solvent, i.e. ethyl acetate, the protein solution forms an emulsion and this emulsion could be

subsequently emulsified in a water phase (double emulsion-solvent evaporation) or precipitated in a polar solvent external phase (emulsion-solvent diffusion). When the polymer is dissolved in a polar solvent the protein is co-dissolved in this phase, and this polar phase can be precipitated upon solvent diffusion in water (nanoprecipitation). On the other hand, a critical step in these fabrication methodologies is the mixing of the different phases. This can be achieved using minor energy sources (regular agitation) in the case of emulsion-solvent diffusion and nanoprecipitation or high energy sources in the case of double emulsion-solvent evaporation.

Finally, it is important to highlight that the microfluidics approach is currently receiving a great attention as a way to mix the phases. In fact, microfluidic devices can control the way the different phases are mixed with each other, with the possibility of tuning the physicochemical properties of the particles formed [8–10].

Table 1 gives an overview of the techniques employed to produce polyester-based nanoparticles for protein/peptide delivery.

Table 1*. Main characteristics of the most commonly used techniques to form peptide/protein-loaded polyester-based nanoparticles. Adapted with permission from* [1] *(permitted by ELSEVIER).*

Technique	Principle	Stress exposure	Organic solvents	Simplicity
Double emulsion - solvent evaporation	Double emulsion and precipitation of the polymer due to evaporation of the solvent	Homogenization/ sonication/ surfactants	Yes	+
Emulsion-solvent diffusion	Emulsification and precipitation of the polymer due to the diffusion of the solvent into a non-solvent external phase	Vortex/surfactants (if necessary)	Yes	+
Nanoprecipitation	Polymer precipitation into a non-solvent external phase	No	Yes	+

i) Double emulsion-solvent evaporation

This technique was described in the early 90's for the microencapsulation of proteins, and, a few years later, our group pioneered its adaptation to the encapsulation of proteins within nanoparticles of around 200 nm [11]. The principle involves the emulsification of an aqueous solution containing the protein/peptide into an organic non-polar solvent (i.e. methylene chloride or ethyl acetate) containing the polymer (i.e. PLGA), thereby forming a W/O emulsion. This W/O emulsion is then emulsified again in a volume of an external aqueous phase containing a surfactant (i.e. polyvinylalcohol (PVA)). The solvent present in the resulting double emulsion is eliminated by evaporation [6,11,12]. The two emulsification processes require the use of high energy sources (homogenization, sonication or high-speed vortex in the case of small volumes). A schematic view of the procedure is shown in Figure 2.

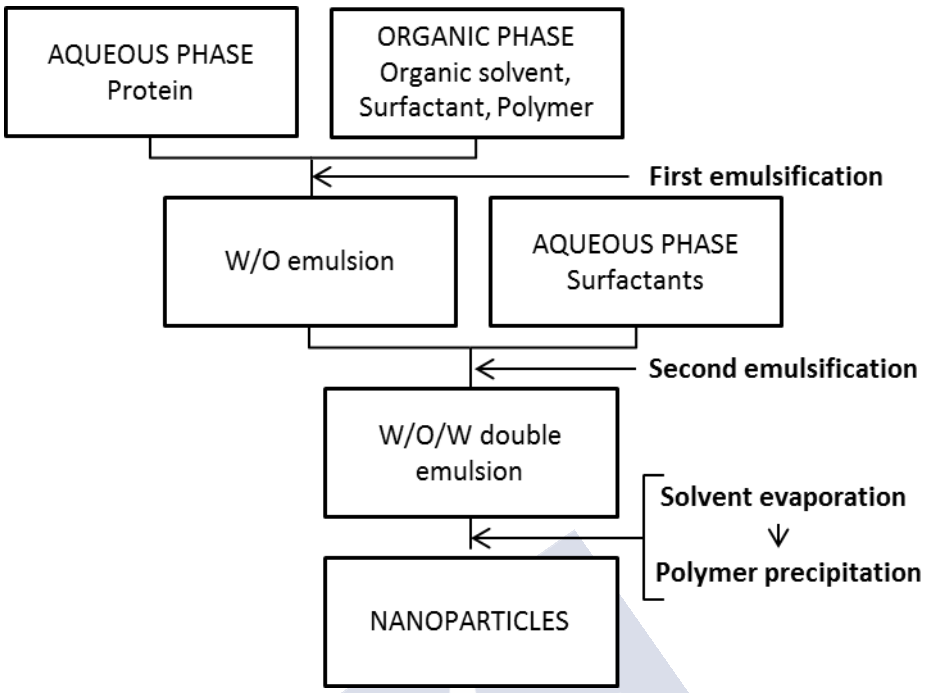

Figure 2. Schematic view of the double emulsion-solvent evaporation procedure to produce polyester-based nanoparticles. Adapted with permission from [1] *(permitted by ELSEVIER).*

ii) Emulsion -solvent diffusion

As in the previous method, an aqueous solution of the peptide/protein is emulsified in an organic non-polar phase containing the polymer and potentially some surfactants. Then, this emulsion is added to an external polar phase (a mixture of water and ethanol) in which the organic solvent is miscible. As a consequence, the polymer precipitates into the polar phase (polymer non-solvents), causing the formation of the nanoparticles (Figure 3) [13–16]. A final evaporation step is necessary to remove the organic solvents.

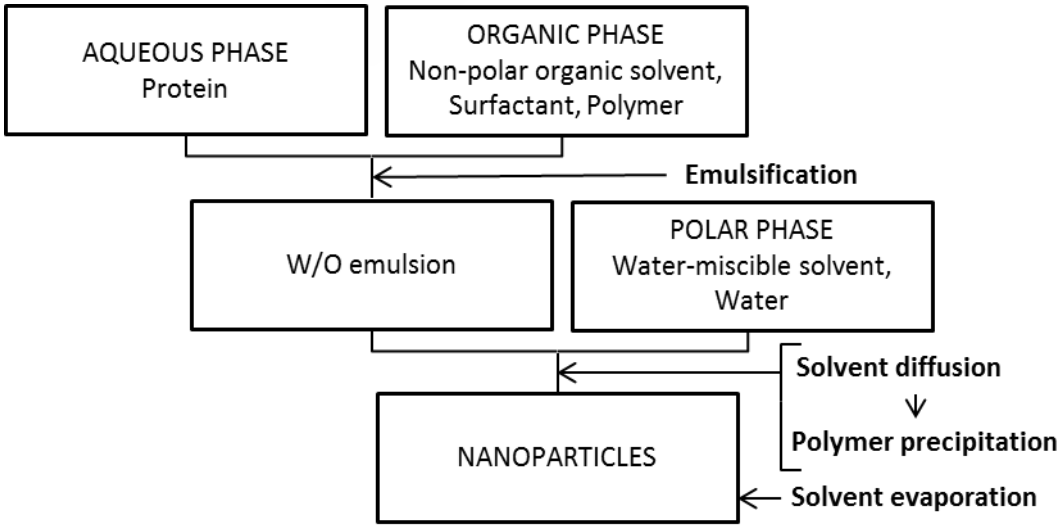

Figure 3. Schematic view of the emulsion-solvent diffusion method to produce polyester-based nanoparticles. Adapted with permission from [1] *(permitted by ELSEVIER).*

iii) Nanoprecipitation

According to this method, the polymer and the proteins are dissolved into a water-miscible organic solvent that is then added dropwise or injected into a dispersing phase in which the polymer is not soluble (Figure 4). The rapid shifting of the solvent into the water causes the nucleation of the polymer, which aggregates, forming the nanoparticles [17,18]. A final evaporation step to remove solvent traces is usually done.

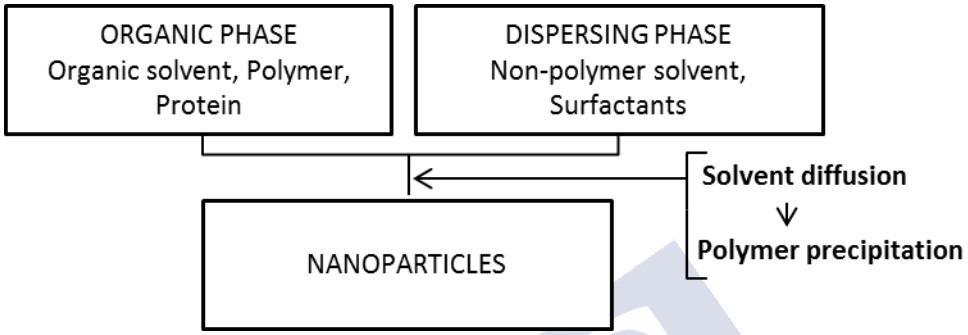

Figure 4. Schematic view of the nanoprecipitation method to produce polyester-based nanoparticles. Adapted with permission from [1] *(permitted by ELSEVIER).*

1.1.2. Characterization, peptide/protein loading, activity and release profile

- Particle size distribution: the nanoparticles production technique and the associated formulation parameters have been reported to influence the final particle size distribution. For example, in the case of the double emulsion-solvent evaporation, the size of the particles is highly dependent on the type of instrument and energy applied during the mixing of the organic and aqueous phases. Additionally, the polymer concentration and the type and amount of surfactants added to the formulation may affect the particle size distribution [19,20]. In the case of the solvent-diffusion/nanoprecipitation based techniques, the particle size is mainly determined by the polymer concentration and the rate of mixing the two phases. In general, for protein delivery purposes, particles sizes between 100 and 300 nm and negative surface charges are reported [14,16,18,21].

- Peptide/protein loading and activity: most of the articles reporting the encapsulation of peptides/proteins within PLGA nanoparticles, refer to high AE values, however the final LC is not normally reported and it is usually lower than 5 % [14,15,21]. Both, the AE and LC depend on the preparation technique and also on a number of formulation factors, which include the type of PLGA (ratio lactic/glycolic acid), its molecular weight, its concentration in the polymer solution, the presence of stabilizers or other formulation additives, as well as the type and theoretical loading of the protein. For example, the molecular weight of the polymer and its hydrophobicity have influenced the L-asparaginase loading capacity of PLGA nanoparticles, showing values ranged from 1.8 up to 4.9 % LC [22].The highest LC was achieved with high molecular weight-hydrophilic polymers, which was rationalized as follows. While the presence of free carboxylic groups in the chains of the hydrophilic polymers facilitated its interaction with the protein, the high molecular weights led to a highly viscous polymer solution, which made difficult the diffusion of the protein from the organic phase to the external aqueous medium. In a different study it was found that the

presence of mannosamine covalently attached to PLGA nanoparticles produced by double emulsion/solvent evaporation led to an increase in the association of insulin compared to the unmodified PLGA particles (68 vs 77 % AE; 3.5 vs 4 % LC), probably due to an interaction between the mannosamine residues and the protein [23]. On the other hand, the pH of the internal protein-containing aqueous phase has also been shown to influence the association of BSA to PLGA nanoparticles. Indeed, in a particular study, it was shown that a pH value near the BSA isoelectric point led to a significant increase in the BSA association due to an increase in its hydrophobicity [21].

Finally, it is important to highlight that the presence of stabilizers such as sodium bicarbonate, trehalose or poloxamer 188 in the inner aqueous phase were found to help the stability of the protein during the nanoparticles preparation procedure, although this was normally associated to a decrease in AE values [11,24]. In another case, it was shown that the presence of both, heparin and BSA, as formulation additives was fundamental to increase the association of PDGF-BB (platelet-derived growth factor) (from 35 % to 87 %) into PLGA nanoparticles produced by the solvent diffusion technique. This was attributed to the surfactant properties of BSA, which led to a reduction of the contact of the growth factor with the water/oil interface, thus increasing the association of the protein to the nanoparticles [15].

In fact, the main source of peptide/protein instability common to all the above described techniques is the presence of organic solvents, which can cause denaturation and/or aggregation. The use of stabilizing additives (e.g. methyl-β-cyclodextrins, BSA or PEG) could increase the stability of the drugs, helping them to keep their structure [15,17,18]. Sonication (for double emulsion-solvent evaporation) and the presence of surfactants (for both double emulsion-solvent evaporation and emulsion-solvent diffusion) can also affect the peptide protein/structure [17]. HPLC, ELISA and enzymatic assays have been used to evaluate both encapsulation and structural stability of peptides/proteins [15,17,24]. Direct *in vivo* evaluation of the formulation has also been reported with the same aim [24].

- Peptide/protein release: the typical protein release profile from PLGA nanoparticles consists of an initial burst followed by a sustained release that may last from days to weeks depending on the characteristics of the PLGA nanoparticles. In general, the first fraction of protein released is the one located close to the surface of the particles [14]. Then, the release of the entrapped protein is triggered by the degradation of the polymer by erosion, followed by the diffusion of the protein through the channels created in the process [25]. This erosion process is known to generate oligomers that can easily interact with the encapsulated protein leading to its denaturation [26]. Based on this finding, we have developed a variety of strategies to prevent this critical problem. These include the incorporation of surface active materials, i.e. block copolymers of poly(ethylene oxide) (PEO) and poly(propylene oxide) (PPO) [11,14], as well as the use of PEGylated PLGA [3,4]. In both situations, the presence of PEG molecules inside the PLGA matrix was found to work as a barrier for the irreversible deleterious protein-polymer interaction. Finally, although the mechanism of release is mainly driven by the degradation of the polymer, the nature of the protein may also influence its solubility, its interaction with the polymer and its diffusion across the channels generated in the polymer degradation process [4,16,21,23,27].

Table 2 shows examples of proteins associated to PLGA nanoparticles produced by different techniques.

Table 2. Examples of peptide/protein-loaded PLGA nanoparticles obtained through different preparation methods: drug loading and release properties. Adapted with permission from [1] *(permitted by ELSEVIER).*

Preparation method	Peptide/ Protein	AE (%)	LC (%)	≤1 h burst / cumulative release (time) - pH medium	Ref.
Double emulsion - solvent evaporation	BSA	70 - 80	0.7 - 0.8	n.a. / 80 % (28 d) pH 7.4	[23]
	Insulin	70 - 80	3.5 - 4	n.a. / 20 % (28 d) pH 7.4	
	Cyclosporine A	60 -90	n.a.	15 - 25 % / 70-90% (24 h) pH 7.4	[28]
	BSA	28 - 88	n.a.	n.a. / 40 - 100 % (28 d) pH 7.4	[11]
	HSA	22 - 33	1.3 - 2.6	n.a.	[29]
	Tetanus toxoid	31 - 37	n.a.	n.a. / 7 - 18 % (1 d) pH 7.4 <7 / 4 - 15 % (4 h) pH 1.2*/7.5*	[3,4]
	L-Asparaginase	15 - 40	1.8 - 4.9	n.a./15 - 95 % (21 d) pH 7.4	[22]
	Insulin	n.a.	n.a.	n.a. / 70 % (40 d) pH n.a.	[30]
	IGF-1	22 - 43	n.a.	n.a. / 78 % (40 d) pH n.a.	
Emulsion - solvent diffusion	BSA	4 - 60	1 - 4 theor.	60 - 80 % / 80 - 90 % (14 d) pH 7.4	[21]
	IgG	n.a.	1 - 4 theor.	5 - 25 % / 10-30 % (14 d) pH 7.4	
	Insulin	20 - 40	0.2 - 0.4	20 % / 80 % (14 h) pH 7.4	[14]
	PDGF-BB	87	0.01	40 % / 80 % (40 d) pH 7.4	[15]
	FGF-2	68	0.01	40 % / 80 % (40 d) pH 7.4	
Nanoprecipitation	Insulin	14 - 23	0.3 - 0.5	n.a.	[17]
	Lysozyme	35 - 91	0.7 - 1.8	n.a.	
	α-chymotrypsin	11 - 71	2 - 5 theor.	n. a.	[18]
	Cyt-c	72	3.6	n. a. / 100 % (120 d) pH 7.3	

AE: association efficiency (100 x associated peptide mass / total peptide mass); BSA: bovine serum albumin; Cyt-c: horse heart cytochrome c; FGF-2: fibroblast growth factor; HAS: human serum albumin; IGF-1: insulin-like growth factor; IgG: immunoglobulin G; LC: loading capacity (100 x peptide mass /total formulation mass); n.a.: not applicable; PDGF-BB: platelet-derived growth factor; Ref.: references; theor.: theoretical; *Enzyme supplemented.

1.2. Acrylic polymers-based nanoparticles

Following the pioneering work of P. Speiser and co-workers on the association of antigens (human immunoglobulin G and tetanus toxoid) to polyacrylamide nanoparticles in 1976 [31], different types of acrylic polymers have been used to produce nanoparticles, including polyacrylic acid, polyacrylamides, polymethylmethacrylates and poly(alkylcyanoacrylates) [32]. These synthetic polymers are considered to be biocompatible and, in some cases, biodegradable polymers [33,34]. Among them, poly(alkylcyanoacrylates) (PACA) are the most commonly used for preparing nanoparticulate systems and, in particular, for the delivery of proteins. Their nitrile and ester groups are electron attractive functional groups and this property makes the vinyl carbon of the monomer really reactive, hence, able to polymerize in the presence of an initiator. Free radical, anionic or

zwitterionic polymerization are the main approaches adopted so far for the production of PACA nanoparticles [34–36]. Overall, despite the early development and attention that these particles received in the past, only a few papers describing their use for protein delivery have been found in the literature.

1.2.1. Preparation techniques

Three main strategies (summarized in Table 3) have been described to synthesize polyacrylate-based nanostructures: the interfacial polymerization, the anionic polymerization and the free radical dispersion polymerization techniques. In last two cases, the use organic solvents is avoided, being the main source of protein instability its potential reactivity with the monomer.

Table 3. Main characteristics of the most commonly used techniques to form peptide/protein-loaded polyacrylate-based nanoparticles. Adapted with permission from [1] *(permitted by ELSEVIER).*

Technique	Principle	Stress exposure	Organic solvents	Simplicity
***"in situ"* polymerization / interfacial polymerization**	Monomers polymerization *"in situ"* at the inter-face of an emulsion	Undesirable reactions drug-monomers / Vigorous stirring	No necessarily	+
Anionic polymerization	Monomers polymerization due to OH^- groups in the medium	Undesirable reactions drug-monomers	No	+
Free radical dispersion polymerization	Monomers polymerization due to the generation of free radicals and crosslinking	Undesirable reactions drug-monomers-crosslinking agent / Free radicals / UV / Heat	No	+

i) *"In situ" p*olymerization.

In this method, which is also named as interfacial polymerization, the polymer formation occurs "in situ" at the interface of an emulsion through a fast polymerization among reactive monomers. Due to their rapid and easy polymerization, alkylcyanoacrylates have been the monomers of choice for this purpose [37,38]. Unfortunately, the potential reaction between the drug and the reactive monomers during the process constitutes a limitation of this approach [39]. Both oily core and aqueous core nanocapsules can be formed with this method.

- Interfacial polymerization in oily core nanocapsules. In this case, the organic phase is composed by the peptide/protein, the oil, the monomers and an organic solvent. The solvent needs to be water-miscible in order to promote its diffusion towards the aqueous phase, allowing the spontaneous formation of nanometric oily droplets [40]. The organic phase is usually injected into the aqueous phase, which contains at least a hydrophilic surfactant. This process is usually performed under vigorous stirring, leading to the instantaneous formation of the nanocapsules (Figure 5). An additional final step to remove the organic solvents can be performed [38,41].

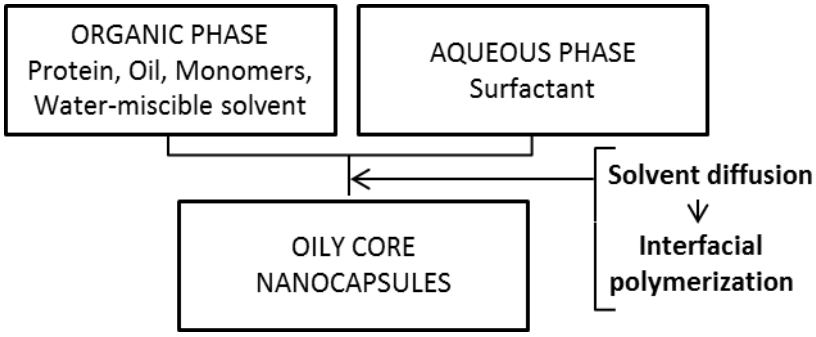

Figure 5. Schematic view of the interfacial polymerization technique to produce oily core nanocapsules. Adapted with permission from [1] *(permitted by ELSEVIER).*

- Interfacial polymerization in aqueous core nanocapsules. In this method, the aqueous phase, which contains the protein/peptide, water and sometimes water-miscible solvent, is emulsified into an organic phase consisting of an oil and a lipophilic surfactant using sonication or vigorous stirring. Once the W/O emulsion is formed, the monomers are added under mechanical stirring. This last step, triggers the polymerization at the W/O interface and leads to a final system consisting of aqueous core nanocapsules dispersed in oil (Figure 6) [42,43]. The nanocapsules are finally isolated by ultracentrifugation followed by their resuspension in water [44,45].

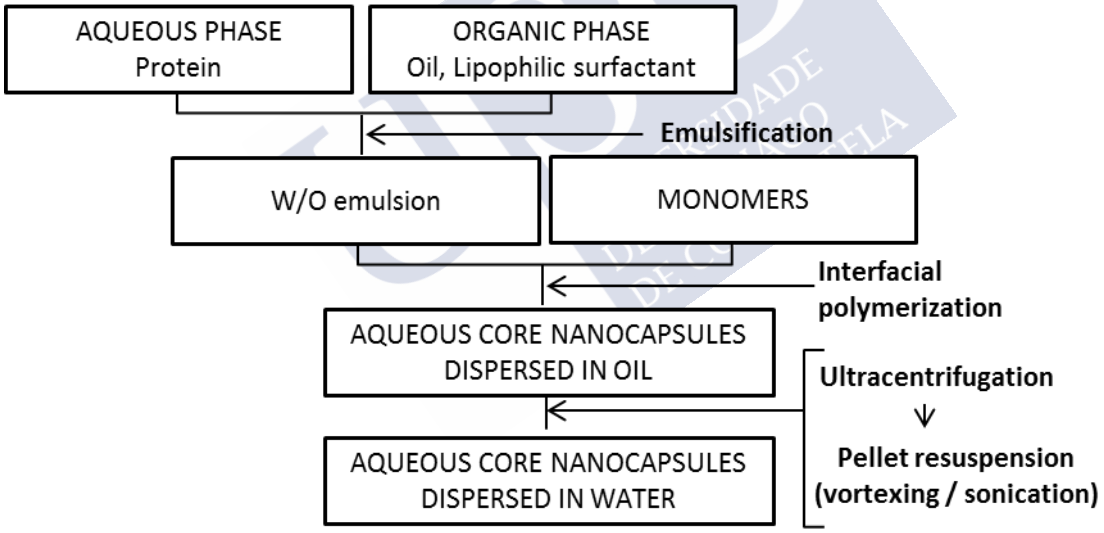

Figure 6. Schematic view of the interfacial polymerization technique to produce aqueous core nanocapsules. Adapted with permission from [1] *(permitted by ELSEVIER).*

ii) Anionic polymerization

In this technique, the acrylic monomers, a stabilizer and an initiator (OH^- in water) are necessary to form the nanoparticles. The monomers, which are poorly soluble in water, are emulsified into an acidic water solution (pH 2 - 4) containing the stabilizer (typically dextran). Once the droplets are formed, the monomer starts to polymerize thanks to the hydroxyl ions (OH^-) present in the water phase (Figure 7). The acidic pH slows down the polymerization rate, thereby controlling the process of particles formation [35,37]. Proteins can be attached onto the surface of the particles, or simply incorporated into the reaction mixture during particles formation [46–50].

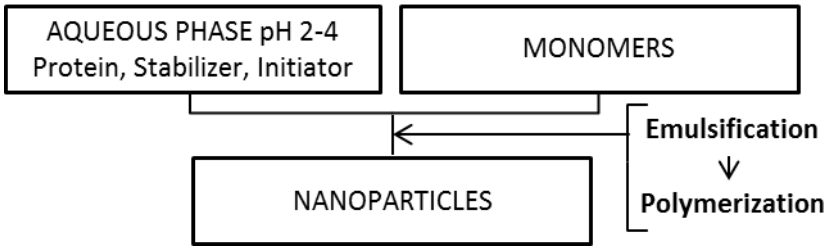

Figure 7. Schematic representation of the anionic-polymerization technique to produce polyacrylate-based nanoparticles. *Adapted with permission from* [1] *(permitted by ELSEVIER).*

iii) Free radical dispersion polymerization.

Peppas and co-workers used this technique to obtain gel nanospheres through a photo- or thermal-initiated polymerization (Figure 8). This technology involves the use of specific initiators as well as a crosslinking agent. The monomers (i.e. methacrylic acid, MAA and monomethylether monomethacrylate, PEGMA), the crosslinking agent (i.e. tetra (ethylene glycol) dimethacrylate) and the initiator (i.e., 1-Hydroxylcyclohexyl phenyl ketone) are solubilized in an aqueous phase. Once the initiator is activated (UV, heat), the formation of oligomers and crosslinks starts. Finally, since the polymer is not soluble in water, nuclei of polymerization are created leading to the formation of nanospheres (i.e. P(MAA-g-PEG)). Once the polymerization is completed, nanospheres are purified by repeated washing steps to remove the unreacted monomers and the association of the protein (i.e. insulin, OVA) is carried out in a subsequent incubation step [51,52].

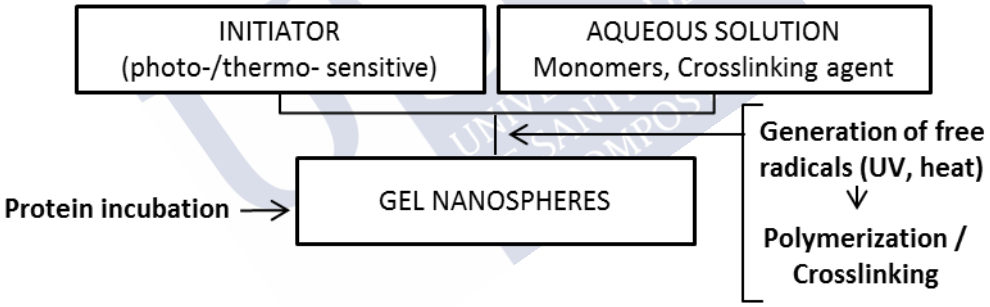

Figure 8. Schematic representation of the free radical dispersion polymerization technique to produce polyacrylate-based gel nanospheres. *Adapted with permission from* [1] *(permitted by ELSEVIER).*

1.2.2 Characterization, peptide/protein loading, activity and release profile

- Particle size distribution: in general, polyacrylate-based nanoparticles described in the literature have a size in the range of 50 nm and 500 nm and a negative surface charge [53–55]. Different parameters can affect the polymerization process and, as a consequence, the physicochemical properties of PACA nanoparticles. The most important parameter, which allows the control of the polymerization rate and, hence the particle formation is the pH, however, the monomer concentration also has a significant influence in this process. Finally, the temperature and the addition of surfactants have also been described as a way to modulate the particle size [46,55–58].

- Peptide/protein loading and activity: Table 4 gives an overview of the properties of some protein/peptide-loaded polyacrylate-based nanoparticles formulations. The AE and LC values described in the literature are very variable, ranging between 3.5 and 95 % AE and up to 26 % LC

[48,49,59]. Among the factors influencing the AE, the time at which the protein is added during the polymerization process has been found to be critical. For example, both insulin and GRF (growth hormone releasing factor) reached around 85 % AE when they were added to the polymerization medium 30 minutes after the process started [39,48].

As for the "*in situ*" polymerization method, the peptide/protein could undesirably work as a monomer during the polymerization procedure, which may result in its inactivation [49,60]. Apart from techniques like HPLC or enzymatic assays [46,60], direct *in vivo* efficacy of the formulation has often been used to test the integrity and activity of the loaded peptides/proteins [52].

- Peptide/protein release: the release of proteins from polyacrylate-based nanoparticles is mainly due to the bioerosion of the polymeric matrix [39]. Typically, these particles show an initial burst release, which can be buffered using additives. The presence of dextran into the formulation medium could, for example, delay the release of BSA from poly(α-butylcyanoacrylate) nanoparticles [49]. Protein release has also been shown to be strongly influenced by the type of PACA used. For example, the release of GRF was faster in the case of poly(isobutylcyanoacrylate), as compared to the case of poly(isohexylcyanoacrylate) nanoparticles. This was due to the different bioerosion rates of the two polymers [39]. In the particular case of the polyacrylate-based gel nanospheres (acrylic acid (AA) or methacrylic acid (MAA), they were specifically designed to exhibit a pH-dependent swelling and, hence, release behavior [52]. This control could be achieved by adjusting the polymerization and crosslinking conditions.

Table 4. Examples of peptide/protein-loaded polyacrylate-based nanoparticles prepared by anionic and free radical dispersion polymerization: drug loading and release properties. Adapted with permission from [1] *(permitted by ELSEVIER).*

Preparation method	Peptide/ Protein	AE (%)	LC (%)	≤1h burst / cumulative release (time) - pH medium	Ref.
Anionic polymerization	Insulin	87	n.a.	n.a.	[48]
	BSA	3.5	n.a.	15 - 55 % / 70- 90 % (14 d) pH 7.4	[49]
	SOD	7 - 33	n.a.	n.a.	[46]
	NR1	6 - 10	n.a.	n.a.	
	GRF	80	n.a	70 % / 80- 90 % (8 h) pH 7.4*	[39]
Free radical dispersion polymerization	Insulin	65	2.1	n.a.	[51]
		93 - 95	7	10 - 80 % / 100 % (3 h) 1h pH 3 + 2 h pH 7	[52]
	OVA	51	26	0 % / 90 - 100 % (3 h) 1.5 h pH 3 + 2 h pH 7.4	[59]

AE: association efficiency (100 x associated peptide mass / total peptide mass); BSA: bovine serum albumin; GRF: growth hormone releasing factor; LC: loading capacity (100 x peptide mass /total formulation mass); n.a.: not applicable; NR1: anti-glutamate N-methyl D-aspartate receptor 1 antibody; OVA: ovalbumin; Ref.: references; SOD: superoxide dismutase; *Enzyme supplemented.

1.3. Polysaccharide-based nanoparticles

The most commonly employed polysaccharides for protein delivery purposes are chitosan, alginate, dextran and hyaluronic acid. Chitosan, a deacetylated form of chitin, is formed by repeated units of D-glucosamine and N-acetylglucosamine [41,42,43]. Alginate is a block co-polymer made by α-guluronic acid (pKa 3.4) and β-D-mannuronic acid (pKa 3.6) residues linearly linked [63]. Like

chitosan, it can be chemically modified on the acidic functional groups to obtain the desired properties [64,65]. Dextran is made by α (1→6) glucopyranoside units [66–68]. The hydroxyl groups are the main sites used for chemical modifications, with dextran sulfate as the most common modified form for drug delivery applications [69–71]. Finally, hyaluronic acid is a linear polysaccharide made by repeated units of the disaccharide formed by N-acetyl D–glucosamine and D–glucuronic acid [72]. These natural polysaccharides have in common the property of being water-soluble; however their distinct chemistry results in different pKa and functionality in terms of their potential interaction with different targets and their capacity to be modified with different ligands. Among the polysaccharide-based nanoparticles described so far, those made of chitosan were originally developed in our lab for the association of proteins [73,74]. Since this discovery until now, chitosan nanoparticles have been classified as the polymeric delivery nanoparticles that have received the greatest deal of attention. Overall, an advantage of the techniques for the production of polysaccharide nanoparticles relies in the mildness of the procedures [75–77], with the exception of the chemical crosslinking [78], which may lead to the denaturation of the protein.

1.3.1 Preparation techniques

Different techniques have been described until now to produce polysaccharide-based nanoparticles and nanocomplexes, being the most commonly employed the ionic gelation and the polyelectrolyte complexation. General specifications of the different preparation techniques are presented in Table 5.

Table 5. Characteristics of the most commonly used techniques to form polysaccharide-based nanoparticles containing peptides/proteins. Adapted with permission from [1] *(permitted by ELSEVIER).*

Technique	Principle	Stress exposure	Organic solvents	Simplicity
Ionic gelation/crosslinking	Gelation of the particles by ionic crosslinking	Ionic interactions with the protein / Crosslinking agent	No	+ +
Polyelectrolyte complexation	Ionic interaction between polymers of opposite charge	Ionic interactions with the protein	No	+ +

i) Ionic gelation/Ionic crosslinking

Our lab pioneered the development of chitosan nanoparticles using the ionic gelation/ionic crosslinking technique [73,74], which has been later extended to other polysaccharides such as alginate and dextran [79,80]. This technique is based on the fact that some charged polysaccharides can gel in aqueous solution in the presence of small ions and crosslinking agents (Figure 9) [37,65,81]. The type of gelling agent is different based on the type of polysaccharide. For example, in the case of chitosan, tripolyphosphate (TPP) is the most commonly crosslinking agent employed, while in the case of alginates, the use of calcium salts (calcium chloride, calcium sulfate, or calcium carbonate) is the most common gelation approach [65,74,80,82–85].

Alternatively, nanoparticles can be produced using a chemical cross-linking reaction. However, this technique has not been almost explored for the association of proteins [78] due to the potential chemical reactions with the loaded protein.

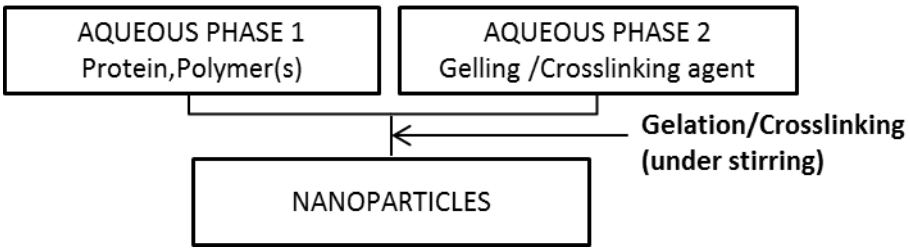

Figure 9. Schematic view of the ionic gelation/crosslinking technique to produce polysaccharide-based nanoparticles. Adapted with permission from [1] *(permitted by ELSEVIER).*

ii) Polyelectrolyte complexation

Polyelectrolytes complexes (PECs) are complexes resulting from the mixing of two oppositely charged macromolecules (i.e., polyelectrolytes). A schematic representation of the procedure is shown in Figure 10 [86,87]. The density of the charges and the charge distribution over the polymeric chains, in addition to the concentration of the two polyelectrolytes are the main parameters influencing the properties of the particles formed. The control of the ionic strength and pH of the reaction medium, which influences the degree of ionization, is also fundamental for the nanoparticles formation [88].

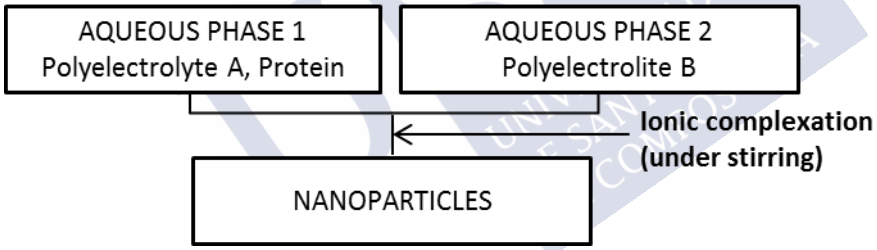

Figure 10. Schematic view of the polyelectrolyte complexation technique to produce polysaccharide-based nanoparticles. Adapted with permission from [1] *(permitted by ELSEVIER).*

1.3.2. Characterization, peptide/protein loading, activity and release profile

- Particle size distribution: the ionic gelation/crosslinking is, among the techniques described above, probably the one allowing a better control of the size. Indeed, in a report by our group [89], intended to compare the ionic crosslinking vs. the ionic complexation of chitosan and pDNA, we showed that the nanoparticles prepared by crosslinking of chitosan with TPP had a more controllable size and a lower polidispersity than those produced by ionic complexation. This result was attributed to the fact that the crosslinking with TPP led to the formation of nanogelled particles with a round and more defined structure [90,91]. Overall, the main factors influencing the particle size distribution are the ratio and the concentration of the ionically interacting species [70,74].

- Peptide/protein loading and activity: in general, particles produced by gelation or complexation are characterized by a high LC, which can reach values up to 50 % and AE values close to 100 % [70,74,91,92]. The protein association efficiency is mainly affected by the number of interacting species and their degree of ionization. For example the AE of insulin to chitosan nanoparticles

reached values close to 90 %, however the value decreased to 37 % in the case of chitosan/glucomannan polyelectrolyte complexes [91]. This was attributed to the different pHs of the protein solution and also to a competition between the protein and glucomannan for the chitosan positive sites. A similar competition phenomenon was observed for the basic peptide salmon calcitonin, which was found to compete with protamine in its association to hyaluronic acid/protamine nanoparticles [93]. These affinity/ionic competition phenomena have been taken into account for the modulation of the LC. For example, the association efficiency of insulin to chitosan-based nanoparticles could be increased from 66 % to 94 % when the anionic interacting polymers were alginate and dextran sulfate respectively. This behaviour was explained due to the strong ionic interactions between the insulin and the sulfate groups of dextran [94].

The main source of instability for the loaded peptide/protein is, in both ionic gelation and polyelectrolyte complexation, the possible ionic interaction between the peptide/protein and the polymers/crosslinking agents, which could drive to protein denaturation [92,95,96]. Additionally, the acidic pH often necessary to produce nanoparticles by ionic gelation (e.g. chitosan nanoparticles) can destabilize or affect the peptide/protein activity (e.g. pH optimum of enzymes) [97]. Both electrophoresis-based techniques (i.e. SDS-PAGE and Western blot) and ELISA assays have been used to check if the peptide/protein integrity and activity were preserved once included in polysaccharide-based nanoparticles[95,96,98]. Likewise, spectroscopy-based techniques like FTIR have been used to study the interactions between the functional groups of the peptide/protein and the polyelectrolytes [99]. In the case of enzymes, the activity was simply evaluated through enzymatic activity assays [100]. Finally, in some cases, the activity was only assessed after their *in vivo* administration [92,101].

- Peptide/protein release: from the point of view of drug release, nanoparticles produced by ionic gelation or complexation normally show an ionic strength-dependent release profile, with an initial burst release. In fact, the sensitivity of these systems to pH changes and to the presence of ions, is one of their main drawbacks [71,91]. An example of this behavior has been observed for insulin-loaded dextran sulfate/polyethylenimine (PEI) nanoparticles produced by complexation, which completely released the peptide in PBS 50 mM after 5 minutes, while just the 65 % of the peptide was released in PBS 5 mM [71].

Among the formulation factors that can be modified in order to have a certain control of the release process, the combination of different counteracting polymers and surfactants can be highlighted. For example, we have shown that the release of BSA from chitosan nanoparticles produced by ionic crosslinking was affected by the presence of poloxamer 188 in the formulation [73,74]. Similarly, Sarmento et al compared the insulin release profile from alginate/chitosan and dextran/chitosan nanoparticles [94]. They showed that the release of insulin was strongly influenced by type of polymers used, being the interaction between the protein drug and the polymers fundamental to control the release. These chitosan/alginate nanoparticles were shown to have a pH-dependent release profile, suitable for the gastric and intestinal environment. In fact, these systems were able to retain the protein at the low pH of the stomach, and release it in the intestine, when the pH increased [80,102]. Swelling, dissociation, diffusion and erosion are reported as the main

mechanisms behind protein release from the nanoparticles made by ionic gelation or polyelectrolyte complexation [70,103].

Overall, it could be concluded that polysaccharide-based nanoparticles are those leading to the highest protein loading capacity, among those indicated in this review. The challenge that remains associated to these nanoparticles is related to their limited capacity to control the release in different physiologically relevant media. Nevertheless, the combination of different biomaterials and surfactants are now seen as approaches to overcome this hurdle.

Table 6 reports examples of peptides and proteins encapsulated into polysaccharide-based nanoparticles synthesized by different strategies.

Table 6. Examples of peptide/protein-loaded polysaccharide-based nanoparticles prepared by the different methods: drug loading and release properties. Adapted with permission from [1] *(permitted by ELSEVIER).*

Preparation method	Peptide / Protein	AE (%)	LC (%)	≤ 1 h burst / cumulative release (time) - pH medium	Ref.
Ionic gelation/ crosslinking	Insulin	87 - 97	19 - 55	100 % / 100 % (2 h) pH 4/7 80 - 100 % / 100 % (2 h) pH 6.4	[92]
		40 - 90	20 - 22 theor.	15 - 90 % / 15 - 90 % (2 h) pH 7.4	[91]
	Immuno-modulatory protein P1	10 - 30	16 - 21 theor.	10 -75 % / 10 - 75 % (2 h) pH 7.4	
	BSA	5 - 80	10 - 50	n.a. / 30 - 100 % (8 d) pH 7	[74]
	Tetanus Toxoid	50	10	n.a.	[90]
	VEGF	32 - 94	0.04-0.34	80 % / > 90 % (24 h) pH 7	[98]
	PDGF	27 - 54	0.05 -0.1	n.a. / > 90 % (7 d) pH 7	
	Insulin	69	10	95 % / 95 % (2 h) pH 1.2 80 % / 80 % (2 h) pH 6.8	[94]
Polyelectrolyte complexation	BSA	70	n.a.	40 - 60 % / 40 - 60 % (7 h) pH 7.4	[99]
	Insulin	66 - 94	5 - 13	55 - 100 % / 55 - 100 % (2 h) pH 1.2 70 - 100 % / 70 - 100 % (2 h) pH 6.8	[94]
	rHBsAg	90 - 95	2.5 - 5	n.a.	[96]
	sCT	100	10 - 39	55 % / 70 - 80 % (24 h) pH 7.4	[93]
	TRIAL	n.a.	n.a.	n.a.	[101]
	ARH peptide	36 - 72	11 - 13	n.a. / 15 - 60 % (6 d) pH 7.4	[104]
	OVA	80 - 85	7 - 38	n.a.	[63]

AE: association efficiency (100 x associated peptide mass / total peptide mass); BSA: bovine serum albumin; INF-α: interferon alpha; LC: loading capacity (100 x peptide mass /total formulation mass); n.a.: not applicable; OVA: Ovalbumin; PDGF: platelet-derived growth factor; Ref.: references; rHBsAg: recombinant hepatitis B surface antigen; sCT: salmon calcitonin; theor.: theoretical; TRIAL: tumor necrosis factor-related apoptosis inducing ligand; VEGF: Vascular endothelial growth factor.

1.4. Protein-based nanoparticles

Protein nanoparticles have been proposed for a long time as drug delivery systems due to their low cost, easy production, low cytotoxicity and biodegradability [105,106]. A protein nanoparticle-based product for the delivery of paclitaxel (Abraxane®) has been approved by FDA and EMA, generating a high interest around this kind of particles. Recent works related to protein nanoparticles for protein delivery have been reported in literature, using gelatin, HSA, BSA, green fluorescent protein (GFP) and silk fibroin as starting materials to produce the particles [105].

1.4.1. Preparation techniques

The preparation method most commonly used to produce protein nanoparticles is the desolvation technique, described below.

i) Desolvation

An aqueous solution of both the therapeutic protein and the one used as a starting material to produce the particles is prepared. A desolvating agent, like acetone, ethanol or dimethyl sulfoxide (DMSO), is then slowly added to the proteins solution. After the desolvation process, nanoaggregates of the proteins are formed and a crosslinking agent, usually glutaraldehyde, is added, causing the formation of stable particles (Figure 11) [106,107]. Alternatively to the chemical crosslinking, a coating with an ionic polymer (e.g., PEI) can be done to improve the stability of the particles [108].

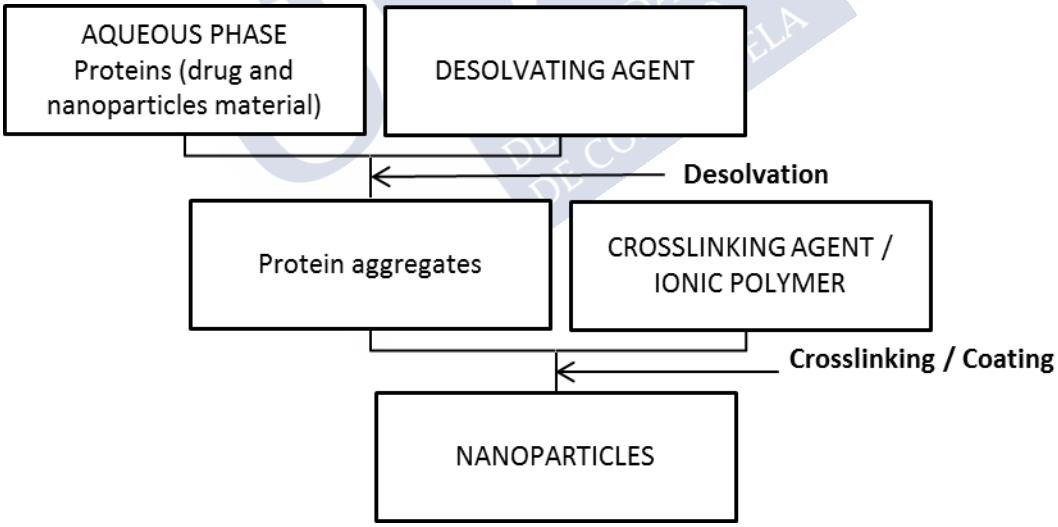

Figure 11. Schematic view of the desolvation technique to produce protein nanoparticles. Adapted with permission from [1] *(permitted by ELSEVIER).*

1.4.2 Characterization, peptide/protein loading and activity, and release profile

- Particle size distribution: the size of the protein-based nanoparticles, which usually ranges between 150 and 400 nm, depends on parameters like the type of crosslinker and the crosslinking time. Their surface charge depends on the pH of the media and the type of protein used to produce the particles [107–110].

- Peptide/protein loading and activity: although the number of references describing the use of protein nanoparticles for protein delivery is very low, in general high AE values are reported in literature (Table 7). Furthermore, the presence of a polymer coating that helps to retain the protein drug can also enhance the AE values of protein nanoparticles, as demonstrated for albumin nanoparticles prepared by desolvation with PEI forming the polymer coating [108].

The main drawback of the desolvation process is the use of organic solvents or crosslinking agents, which could denaturate the peptide/protein structure, leading to protein inactivation. In this regard, ELISA and enzymatic assays have been used to check if the peptide/protein activity was retained after the nanoparticle formation [109][106,108].

- Peptide/protein release: a first burst release followed by a sustained release profile is usually observed. The sustained release phase is associated to the degradation and dissolution of the protein matrix. Therefore, the release is highly dependent on the type of protein forming the matrix and also on its interaction with the protein cargo [108]. In the case of the PEI-coated BSA nanoparticles developed by Zhang and co-workers, it was observed that a the layer of PEI could reduce the undesired release of the protein drug (bone morphogenetic protein-2, BMP-2) from 70 % to 15 % in the first hour [108].

Table 7. Examples of peptide/protein-loaded protein-based nanoparticles: drug loading and release properties. Adapted with permission from [1] *(permitted by ELSEVIER).*

Preparation method	Peptide / Protein	AE (%)	LC (%)	≤ 1 h burst / cumulative release (time) - pH medium	Ref.
Desolvation	BSA	0 - 89	n.a.	10 % / 90 % (150 h) pH 7.4	[97]
	β-galactosidase	80 - 95	n.a.	25 - 35 % / 40 - 60 % (300 h) pH 7.4	[106]
	BMP-2	> 90	n.a.	10 - 70 % / 50- 80 % (250 h) pH 7	[108]
	VEGF	100	n.a.	5 - 85 % / 50 - 100 % (20 d) pH 7.4	[109]
	HSA	80	10	n. a. / 25 % (400 h) pH 7.4	[110]

AE: association efficiency (100 x associated peptide mass / total peptide mass); BMP - 2: bone morphogenetic protein - 2 BSA: bovine serum albumin; HSA: human serum albumin; LC: loading capacity (100 x peptide mass /total formulation mass); n.a.: not applicable; Ref.: references; VEGF: Vascular endothelial growth factor.

2. The interest of hyaluronic acid as polymer for targeting cancer and its use in nanotechnology

2.1. Biological relevance of hyaluronic acid and its importance for the targeting of cancer

Hyaluronic acid (HA) is a linear polysaccharide made by repeated units of the disaccharide formed by N-acetyl D–glucosamine and D–glucuronic acid linked through β (1→4) interglycosidic bonds (see Figure 12). The disaccharides are connected by β (1→3) linkages [72,111]. The pka of the acidic group is reported to be between 3 and 4 meaning that, in physiological conditions, the polymer is

negatively charged [72]. Within the human body, HA is abundant in the synovial fluid and in the extracellular matrix of tissues, and has an average molecular weight between 10^6 and 10^7 Da.

Natural HA has an important role in the regulation of cell functions like migration, proliferation, maintenance of cell and tissue integrity (cell-cell and cell-matrix adhesion), cell survival and apoptosis [72,112,113]. The polymer is exploiting all these functions when interacting with CD44 (i.e. Cluster Determinant 44, an 85 kDa glycoprotein), the principal HA recognizing receptor, located on cells membrane. Other important receptors involved in HA metabolism and functions are the lymphatic vessel endothelial HA receptor (LYVE-1) and RHAMM. LYVE-1 is expressed on the surface of the lymphatic endothelial cells and it is important for cells migration and for mediating immunoresposes [114,115]. RHAMM is a soluble receptor which is involved in cells cycle regulation and in the definition of cell polarity and chromosomes distribution during mitosis [115].

Due to its biodegradable and biocompatible properties, the use of HA in pharmaceutical applications have been well documented for tissue engineering, drug delivery and molecular imaging applications. In the drug delivery field HA was often used exploiting its "stealth" and cancer targeting properties [116,117]. In fact, the CD44 receptor is overexpressed in several solid tumors (e.g. lung, breast, colorectal, gastric, etc.) and the production of HA-based delivery systems could confer targeting properties to the carriers. It was also recently claimed that low MW HA may stimulate the immune system, favoring the polarization of tumor-associated macrophages (TAMs) and the formation of M1 anti-tumoral macrophages [118].
Importantly, the interaction between the CD44 and HA turns on endocytosis mediated processes, which have been exploited for targeting the intracellular environment of cancer cells [117,119–121].

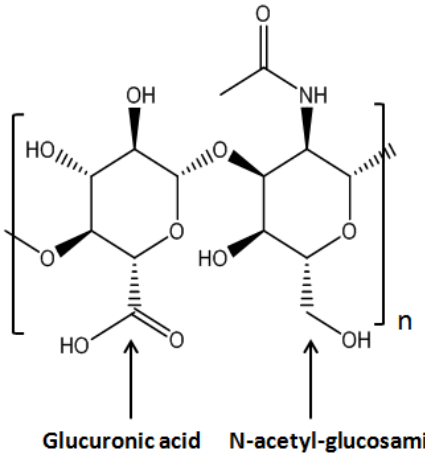

Figure 12. Chemical structure of hyaluronic acid.

2.2. HA polymer-based nanotechnologies for protein delivery

Due to its properties, HA has gained increasing importance in the field of nanotechnology, especially in nano-oncology. Its negative charge, biocompatibility and targeting properties, have made this polymer a reliable candidate in the field of material sciences [122]. As the encapsulation of proteins in HA-based nanosystems will be one of the main objectives of this thesis, the methodologies

described so far in literature for producing protein encapsulating HA-based nanocarriers will be briefly revised. In Table 8 some of the existing protein nano-delivery systems based on HA are reported.

2.2.1. HA Nanogels

Nanogels are defined as nanometric particles formed by the crosslinking of polymers, which swell in presence of a good solvent and that can respond to external stimuli like temperature or pH variations [77,123]. Two main crosslinking strategies can be used to produce nanogels, i.e. physical or chemical crosslinking. A schematic representation of nanogels formation is presented in Figure 13. Physical crosslinking is related to all those interactions which involve non-covalent bindings like hydrophobic forces, ionic interactions, hydrogen bonding or host-guest interactions, and the nanoparticles usually self-assemble in the presence of water. The physical crosslinking is usually preferred for protein encapsulation, due to the mild conditions of the procedures. Hydrophobic modified HAs which self-assemble in the presence of water are the most commonly employed polymers for protein delivery, when physical cross-linking is used. As an example, HA was modified with a hydrophobic moiety named catechin and self-assembles in the presence of polyethylenimine (PEI). The system was used for the encapsulation of the cytotoxic protein Granzyme-B. The authors proposed that the hydrophobic moieties of the protein interact with catechin, leading to a more compact structure, with a narrow size distribution compare to when the non-modified HA is used [75]. In another work, cholesterol-graft-HA was employed for producing physically crosslinked nanosystems for encapsulating bovine serum amine oxidase. The modified HA polymer was able to self-assemble in water after sonication, forming nanoparticles [76].

Chemical crosslinking involves covalent bonds between the polymers obtained by photopolymerization, Michael addition, click chemistry or native chemical ligation. Photopolymerization is based on the use of a photoinitiator, which, when exposed to UV or visible light, forms radicals. The radicals can react with functional groups like acrylate or methacrylate, leading to nanogel formation. Michael addition occurs in water at physiological pH and at room temperature, suitable conditions when a protein drug is used. It is based on the reaction of a nucleophile (like thiol or amino groups) with an alkene double bond. The click chemistry is based on the cyclo-addition of azide to alkyne using copper (Cu (I)) as catalyst. Finally, native chemical ligation is the reaction between a C-terminal thioester with an N-terminal cysteine residue [77].

Several chemical crosslinking-based nanosystems for the encapsulation of proteins have been found in literature. For example, Chen and co-workers encapsulated the proteins Cytochrome C (CC) and grandzyme-B (GrB) in nanogels produced using click chemistry coupled with photo initiation strategies [78]. Interestingly, it was shown that the produced nanogel is well able to control the release of the CC, which is significantly released only in cytoplasmic reductive conditions.

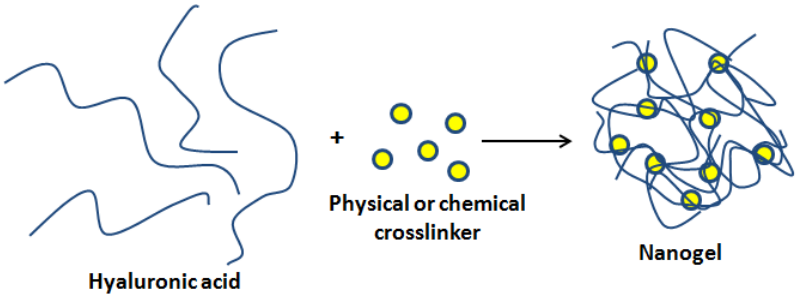

Figure 13. Schematic representation of nanogel formation. With the physical crosslinking, the nanogels are assembled in water through self-assembly mechanisms under mild conditions. On the other hand, with chemical crosslinking, covalent bonds are formed among the hyaluronic acid polymers for forming the nanogels.

2.2.2. Polyelectrolyte complexation

Due to its high charge density, HA is also able to form polyelectrolyte complexes (PECs) with positively charged polymers (Figure 14). HA-chitosan nanoparticles were investigated for the encapsulation of vascular endothelial growth factor (VEGF) and platelet derived growth factor (PDGF-BB). Nanoparticles showing 200 nm and entrapping the two proteins with high efficiencies (95 and 50%, respectively) were formed [124]. In another study the formation of nanocomplexes using HA and protamine have been shown. The system was used for the encapsulation of the recombinant hepatitis B surface antigen and salmon calcitonin, and it was found that its size and zeta potential were strongly influenced by the polymers ratio [93,96].

Generally, nanoparticles based on polyelectrolyte complexation present stability problems in physiological conditions (e.g. sensitive to high ionic strengths) due the electrostatic interactions between the polymers being the only force involved. The stability of the particles can be improved introducing covalent bonds [125].

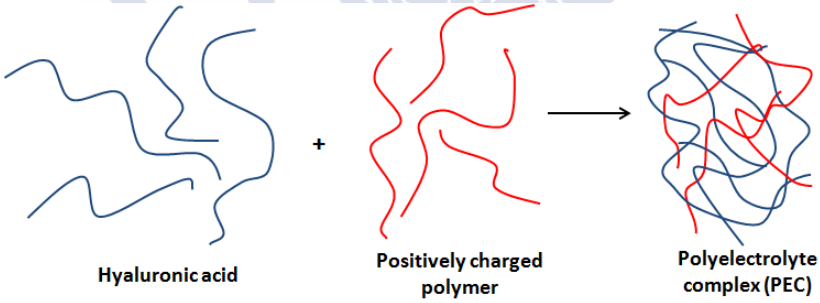

Figure 14. Schematic representation of HA-based polyelectrolyte complexes formation. Due to its high charge density, hyaluronic acid can be complexed with a positively charged electrolyte, forming nanoparticles.

2.2.3. HA-Protein bioconjugates

Even if they cannot be properly considered nanocarriers, HA bioconjugates are polymeric-based delivery systems that have been used for the delivery of proteins. They are based on the covalent conjugation of HA to bioactive molecules like proteins or peptides, a process called HAyalation (Figure 15). This approach is usually used to enhance the stability and the circulation times of the drugs into the body and to overcome the solubility problems of some pharmaceuticals. The principal drawback of using bioconjugates is the possibility of affecting the structural and functional stability of the protein, due to the type of chemistry employed for their formation [126]. The HA carboxylic, alcoholic and acetoamido groups are the ones used for the conjugation reactions with proteins,

which can occur in water [126,127]. However, the polymer is just randomly attached to the proteins, resulting in variations between different batches produced with the same reactions. Proteins like trypsin, ribonuclease A or epidermal growth factor were successfully conjugated to HA [128,129].

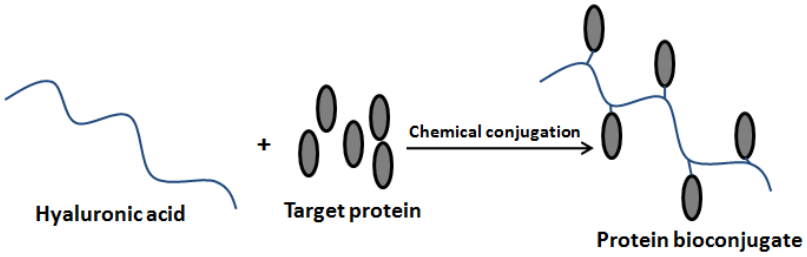

Figure 15. Formation of an HA-Protein bioconjugate. The reactive groups of hyaluronic acid are used to chemically link the protein to the polymer.

Table 8. Examples of peptide/protein-HA-based bioconjugates: drug loading and release properties

Type of nanocarrier	Peptide / Protein	Size (nm)	AE (%)	LC (%)	≤ 1 h burst / cumulative release (time) - pH medium	Ref.
Nanogel-Physical crosslinking	GrB	160	n.a.	n.a.	n.a.	[75]
Nanogel-Physical crosslinking	BSAO	120	20	9	n.a.	[76]
Nanogel-Chemical crosslinking	GrB and CC	150	CC : 89 GrB: n.a.	CC: 10 GrB: n.a.	CC: >5%/30% (48 h) pH 7.4 GrB: not made	[78]
PECs	VEGF and PDGF-BB	180-220	VEGF: 94 PDGF-BB: 54	VEGF: 0.3 PDGF-BB: 0.1	VEGF: 80%/100% (24 h) pH 7 PDGF-BBF: 5%/100% (7 h) pH 7	[98]
PECs	rHBsAg	100-400	>90	2.5-5	n.a.	[96]
PECs	Salmon calcitonin	100-500	>90	10-36	50%/80% (24 h) pH 7.4	[93]
HA bioconjugate	Insulin, RNAse A and trypsin	n.a.	n.a.	Insulin: 17-32 RNAse: 21 Trypsin: 15	n.a.	[126]
HA bioconjugate	Trypsin and EGF	n.a.	n.a.	Trypsin: 2.5 EGF: 1	n.a.	[129]

AE: association efficiency (100 x associated peptide mass / total peptide mass); LC: loading capacity (100 x peptide mass /total formulation mass); VEGF: Vascular endothelial growth factor; PDGF-BB: plateled derived growth factor; GrB: Grandzyme B; BSAO; Bovin Serum Albumin Oxidase; CC: Cytoctrome c; rHBsAg: Recombinant hepatitis B surface antigen; EGF: epidermal growth factor; n.a.: not applicable; Ref.: references;

Bibliography

[1] I. Santalices, A. Gonella, D. Torres, M. Jos, Advances on the formulation of proteins using nanotechnologies, J. Drug Deliv. Sci. Technol. 42 (2017) 155–180. doi:10.1016/j.jddst.2017.06.018.

[2] K. Jelonek, J. Kasperczyk, Polyesters and polyester carbonates for controlled drug delivery, Polimery/Polymers. 58 (2013) 858–863. doi:10.14314/polimery.2013.858.

[3] M. Tobío, R. Gref, A. Sanchez, R. Langer, M.J. Alonso, Stealth PLA-PEG nanoparticles as protein carriers for nasal administration, Pharm. Res. 15 (1998) 270–275. doi:10.1023/A:1011922819926.

[4] M. Tobío, A. Sánchez, A. Vila, I. Soriano, C. Evora, J.. J. Vila-Jato, M.. M. Alonso, The role of PEG on the stability in digestive fluids and in vivo fate of PEG-PLA nanoparticles following oral administration, Colloids Surfaces B Biointerfaces. 18 (2000) 315–323. doi:10.1016/S0927-7765(99)00157-5.

[5] P. Kocbek, N. Obermajer, M. Cegnar, J. Kos, J. Kristl, Targeting cancer cells using PLGA nanoparticles surface modified with monoclonal antibody, J. Control. Release. 120 (2007) 18–26. doi:10.1016/j.jconrel.2007.03.012.

[6] R.H. Ansary, M.B. Awang, M.M. Rahman, Biodegradable poly (D,L-lactic-co-glycolic acid)-based micro/nanoparticles for sustained release of protein drugs - A review, Trop. J. Pharm. Res. 13 (2014) 1179–1190. doi:10.4314/tjpr.v13i7.24.

[7] Y. Wang, W. Qu, S.H. Choi, FDA's regulatory science program for generic PLA/PLGA-based drug products, Am. Pharm. Rev. (2016).

[8] L.-H. Hung, S.-Y. Teh, J. Jester, A.P. Lee, PLGA micro/nanosphere synthesis by droplet microfluidic solvent evaporation and extraction approaches, Lab Chip. 10 (2010) 1820–1825. doi:10.1039/C002866E.

[9] H. Xie, J.W. Smith, Fabrication of PLGA nanoparticles with a fluidic nanoprecipitation system, J. Nanobiotechnology. 8 (2010) 18. doi:10.1186/1477-3155-8-18.

[10] P.M. Valencia, O.C. Farokhzad, R. Karnik, R. Langer, Microfluidic technologies for accelerating the clinical translation of nanoparticles, Nat. Nanotechnol. 7 (2012) 623–629. doi:10.1038/nnano.2012.168.

[11] M.D. Blanco, M.J. Alonso, Development and characterization of protein-loaded poly(lactide-co-glycolide) nanospheres, Eur. J. Pharm. Biopharm. 43 (1997) 287–294. doi:10.1016/S0939-6411(97)00056-8.

[12] J.P. Rao, K.E. Geckeler, Polymer nanoparticles: preparation techniques and size-control parameters, Prog. Polym. Sci. 36 (2011) 887–913. doi:10.1016/j.progpolymsci.2011.01.001.

[13] S. Schubert, J.T. Delaney, Jr, U.S. Schubert, Nanoprecipitation and nanoformulation of polymers: from history to powerful possibilities beyond poly(lactic acid), Soft Matter. 7 (2011) 1581–1588. doi:10.1039/C0SM00862A.

[14] N. Csaba, L. González, A. Sánchez, M.J. Alonso, Design and characterisation of new nanoparticulate polymer blends for drug delivery, J. Biomater. Sci. Polym. Ed. 15 (2004) 1137–1151. doi:10.1163/1568562041753098.

[15] I. D'Angelo, M. Garcia-Fuentes, Y. Parajó, A. Welle, T. Vántus, A. Horváth, G. Bökönyi, G. Kéri, M.J. Alonso, Nanoparticles based on PLGA: poloxamer blends for the delivery of proangiogenic growth factors, Mol. Pharm. 7 (2010) 1724–1733. doi:10.1021/mp1001262.

[16] M.J. Santander-Ortega, D. Bastos-González, J.L. Ortega-Vinuesa, M.J. Alonso, Insulin-loaded PLGA nanoparticles for oral administration: an in vitro physico-chemical characterization, J. Biomed. Nanotechnol. 5 (2009) 45–53. doi:10.1166/jbn.2009.022.

[17] U. Bilati, E. Allémann, E. Doelker, Nanoprecipitation versus emulsion-based techniques for the encapsulation of proteins into biodegradable nanoparticles and process-related stability issues, AAPS PharmSciTech. 6 (2005) E594–E604. doi:10.1208/pt060474.

[18] M.M. Morales-Cruz, G.M. Flores-Fernández, M.M. Morales-Cruz, E.A. Orellano, J.A. Rodriguez-Martinez, M. Ruiz, K. Griebenow, Two-step nanoprecipitation for the production of protein-loaded PLGA nanospheres, Results Pharma Sci. 2 (2012) 79–85. doi:10.1016/j.rinphs.2012.11.001.

[19] J. Vandervoort, K. Yoncheva, A. Ludwig, Influence of the homogenisation procedure on the

physicochemical properties of PLGA nanoparticles, Chem. Pharm. Bull. (Tokyo). 52 (2004) 1273–1279. doi:10.1248/cpb.52.1273.

[20] M.C. Julienne, M.J. Alonso, J.L. Gómez Amoza, J.P. Benoit, Preparation of poly (D,L-lactide/ glycolide) nanoparticles of controlled particle size distribution: application of experimental designs, Drug Dev. Ind. Pharm. 18 (1992) 1063–1077. doi:10.3109/03639049209069315.

[21] M.J. Santander-Ortega, N. Csaba, L. González, D. Bastos-González, J.L. Ortega-Vinuesa, M.J. Alonso, Protein-loaded PLGA-PEO blend nanoparticles: encapsulation, release and degradation characteristics, Colloid Polym. Sci. 288 (2010) 141–150. doi:10.1007/s00396-009-2131-z.

[22] M.M. Gaspar, D. Blanco, M.E.M. Cruz, M. José Alonso, Formulation of L-asparaginase-loaded poly(lactide-co-glycolide) nanoparticles: influence of polymer properties on enzyme loading, activity and in vitro release, J. Control. Release. 52 (1998) 53–62. doi:10.1016/S0168-3659(97)00196-X.

[23] M. Alonso-Sande, A. des Rieux, V. Fievez, B. Sarmento, A. Delgado, C. Evora, C. Remuñán-López, V. Préat, M.J. Alonso, Development of PLGA-mannosamine nanoparticles as oral protein carriers, Biomacromolecules. 14 (2013) 4046–4052. doi:10.1021/bm401141u.

[24] P.S. Kumar, T.R. Saini, D. Chandrasekar, V.K. Yellepeddi, S. Ramakrishna, P. V Diwan, Novel approach for delivery of insulin loaded poly(lactide-co-glycolide) nanoparticles using a combination of stabilizers, Drug Deliv. 14 (2007) 517–523. doi:10.1080/10717540701606467.

[25] J. Hines, D. Kaplan, Poly (lactic-co-glycolic acid) controlled release systems: experimental and modeling insights, Crit. Rev. Ther. Drug Carr. Syst. 30 (2013) 257–276. doi:10.1615/CritRevTherDrugCarrierSyst.2013006475.

[26] M. Tobío, M.J. Alonso, Study of the inactivation process of the tetanus toxoid in contact with poly(lactic/glycolic acid) degrading microspheres, STP Pharma Sci. 8 (1998) 303–310.

[27] M. Tobío, S.P. Schwendeman, Y. Guo, J. McIver, R. Langer, M.J. Alonso, Improved immunogenicity of a core-coated tetanus toxoid delivery system, Vaccine. 18 (1999) 618–622. doi:10.1016/S0264-410X(99)00313-8.

[28] V.D. Wagh, D.U. Apar, Cyclosporine A loaded PLGA nanoparticles for dry eye disease: in vitro characterization studies, J. Nanotechnol. 2014 (2014) 683153. doi:10.1155/2014/683153.

[29] M.F. Zambaux, F. Bonneaux, R. Gref, P. Maincent, E. Dellacherie, M.J. Alonso, P. Labrude, C. Vigneron, Influence of experimental parameters on the characteristics of poly(lactic acid) nanoparticles prepared by a double emulsion method, J. Control. Release. 50 (1998) 31–40. doi:10.1016/S0168-3659(97)00106-5.

[30] J.G. Eley, P. Mathew, Preparation and release characteristics of insulin and insulin-like growth factor-one from polymer nanoparticles, J. Microencapsul. 24 (2007) 225–34. doi:10.1080/02652040601162335.

[31] G. Birrenbach, P.P. Speiser, Polymerized micelles and their use as adjuvants in immunology, J. Pharm. Sci. 65 (1976) 1763–1766. doi:10.1002/jps.2600651217.

[32] A. Patel, M. Patel, X. Yang, A.K. Mitra, Recent advances in protein and Peptide drug delivery: a special emphasis on polymeric nanoparticles, Protein Pept. Lett. 21 (2014) 1102–20. doi:10.2174/0929866521666140807114240.

[33] V.G. Kadajji, G. V. Betageri, Water soluble polymers for pharmaceutical applications, Polymers (Basel). 3 (2011) 1972–2009. doi:10.3390/polym3041972.

[34] M.G. Han, S. Kim, S.X. Liu, Synthesis and degradation behavior of poly (ethyl cyanoacrylate), Polym. Degrad. Stab. J. 93 (2008) 1243–1251. doi:10.1016/j.polymdegradstab.2008.04.012.

[35] C. Vauthier, C. Dubernet, E. Fattal, H. Pinto-Alphandary, P. Couvreur, Poly(alkylcyanoacrylates) as biodegradable materials for biomedical applications, Adv. Drug Deliv. Rev. 55 (2003) 519–548. doi:10.1016/S0169-409X(03)0004l-3.

[36] Y. Barkan, M. Levinman, I. Veprinsky-Zuzuliya, T. Tsach, E. Merqioul, G. Blum, A.J. Domb, A. Basu, Comparative evaluation of polycyanoacrylates, Acta Biomater. 48 (2017) 390–400.

doi:10.1016/j.actbio.2016.11.011.
[37] C. Vauthier, K. Bouchemal, Methods for the preparation and manufacture of polymeric nanoparticles, Pharm. Res. 26 (2009) 1025–1058. doi:10.1007/s11095-008-9800-3.
[38] P. Couvreur, G. Barratt, E. Fattal, P. Legrand, C. Vauthier, Nanocapsule technology: a review, Crit. Rev. Ther. Drug Carr. Syst. 19 (2002) 99–134. doi:10.1615/CritRevTherDrugCarrierSyst.v19.i2.10.
[39] J.L. Grangier, M. Puygrenier, J.C. Gautier, P. Couvreur, Nanoparticles as carriers for growth hormone releasing factors, J. Control. Release. 15 (1991) 3–13. doi:10.1016/0168-3659(91)90098-X.
[40] M. Gallardo, G. Couarraze, B. Denizot, L. Treupel, P. Couvreur, F. Puisieux, Study of the mechanisms of formation of nanoparticles and nanocapsules of polyisobutyl-2-cyanoacrylate, Int. J. Pharm. 100 (1993) 55–64. doi:10.1016/0378-5173(93)90075-Q.
[41] C. Damge, C. Michel, M. Aprahamian, P. Couvreur, New approach for oral administration of insulin with polyalkylcyanoacrylate nanocapsules as drug carrier, Diabetes. 37 (1988) 246–251. doi:10.2337/diab.37.2.246.
[42] S. Watnasirichaikul, T. Rades, I.G. Tucker, N.M. Davies, Effects of formulation variables on characteristics of poly(ethylcyanoacrylate) nanocapsules prepared from w/o microemulsions, Int. J. Pharm. 235 (2002) 237–246. doi:10.1016/S0378-5173(02)00002-9.
[43] S. Watnasirichaikul, T. Rades, I.G. Tucker, N.M. Davies, In-vitro release and oral bioactivity of insulin in diabetic rats using nanocapsules dispersed in biocompatible microemulsion, J. Pharm. Pharmacol. 54 (2002) 473–480. doi:10.1211/0022357021778736.
[44] S. Li, Y. He, C. Li, X. Liu, In vitro release of protein from poly(butylcyanoacrylate) nanocapsules with an aqueous core, Colloid Polym. Sci. 283 (2005) 480–485. doi:10.1007/s00396-004-1173-5.
[45] S. Watnasirichaikul, N.M. Davies, T. Rades, I.G. Tucker, Preparation of biodegradable insulin nanocapsules from biocompatible microemulsions, Pharm. Res. 17 (2000) 684–689. doi:10.1023/A:1007574030674.
[46] V. Reukov, V. Maximov, A. Vertegel, Proteins conjugated to poly(butyl cyanoacrylate) nanoparticles as potential neuroprotective agents, Biotechnol. Bioeng. 108 (2011) 243–252. doi:10.1002/bit.22958.
[47] Q. Zhang, Z. Shen, T. Nagai, Prolonged hypoglycemic effect of insulin-loaded polybutylcyanoacrylate nanoparticles after pulmonary administration to normal rats, Int. J. Pharm. 218 (2001) 75–80. doi:10.1016/S0378-5173(01)00614-7.
[48] M.A. Radwant, H.Y. Aboul-Enein, The effect of oral absorption enhancers on the in vivo performance of insulin-loaded poly(ethylcyanoacrylate) nanospheres in diabetic rats, J. Microencapsul. 19 (2002) 225–235. doi:10.1080/02652040110081406.
[49] C. Kusonwiriyawong, V. Lipipun, Q. Zhang, G.C. Ritthidej, Poly(α-butyl cyanoacrylate) nanoparticles for intracellular delivery of protein: physicochemical properties, cytotoxicity study and cellular uptake in dendritic cells, in: Proc. Tenth Eur. Symp. Control. Drug Deliv., 2008: pp. e6–e8. doi:10.1016/j.jconrel.2008.09.043.
[50] S. Kim, K. Evans, A. Biswas, Production of BSA-poly(ethyl cyanoacrylate) nanoparticles as a coating material that improves wetting property, Colloids Surfaces B Biointerfaces. 107 (2013) 68–75. doi:10.1016/j.colsurfb.2013.01.064.
[51] W. Leobandung, H. Ichikawa, Y. Fukumori, N.A. Peppas, Preparation of stable insulin-loaded nanospheres of poly(ethylene glycol) macromers and N-isopropyl acrylamide, J. Control. Release. 80 (2002) 357–363. doi:10.1016/S0168-3659(02)00028-7.
[52] A.C. Foss, T. Goto, M. Morishita, N.A. Peppas, Development of acrylic-based copolymers for oral insulin delivery, Eur. J. Pharm. Biopharm. 57 (2004) 163–169. doi:10.1016/S0939-6411(03)00145-0.
[53] N. Kamaly, B. Yameen, J. Wu, O.C. Farokhzad, C. Kusonwiriyawonga, V. Lipipuna, Q. Zhangb,

G.C. Ritthideja, Degradable controlled-release polymers and polymeric nanoparticles: mechanisms of controlling drug release, Chem. Rev. 116 (2016) 2602–2663. doi:10.1021/acs.chemrev.5b00346.

[54] L. Boguslavsky, S. Baruch, S. Margel, Synthesis and characterization of polyacrylonitrile nanoparticles by dispersion/emulsion polymerization process, J. Colloid Interface Sci. 289 (2005) 71–85. doi:10.1016/j.jcis.2005.03.063.

[55] G. Wu, C. Wang, Z. Tan, H. Zhang, Effect of temperature on emulsion polymerization of n-butyl acrylate, Procedia Eng. 18 (2011) 353–357. doi:10.1016/j.proeng.2011.11.056.

[56] S.J. Douglas, L. Illum, S.S. Davis, K. Kreuter, Particle size and size distribution of poly(butyl-2-cyanoacrylate) nanoparticles I. Influence of physicochemical factors, J. Colloid Interface Sci. 101 (1984) 149–158. doi:10.1016/0021-9797(84)90015-8.

[57] H.E. Shahmabadi, S.K.B. Doun, S.E. Alavi, M. Mortazavi, Z. Saffari, M. Farahnak, A. Akbarzadeh, An investigation into the parameters affecting preparation of polybutyl cyanoacrylate nanoparticles by emulsion polymerization, Indian J. Clin. Biochem. 29 (2014) 357–361. doi:10.1007/s12291-013-0325-0.

[58] N. Behan, C. Birkinshaw, N. Clarke, Poly n-butyl cyanoacrylate nanoparticles: a mechanistic study of polymerisation and particle formation, Biomaterials. 22 (2001) 1335–1344. doi:10.1016/S0142-9612(00)00286-6.

[59] M. Durán-Lobato, B. Carrillo-Conde, Y. Khairandish, N.A. Peppas, Surface-modified P(HEMA-co-MAA) nanogel carriers for oral vaccine delivery: design, characterization, and in vitro targeting evaluation, Biomacromolecules. 15 (2014) 2725–2734. doi:10.1021/bm500588x.

[60] J.L. Grangier, M. Puygrenier, J.C. Gauthier, P. Couvreur, Nanoparticles as carriers for growth hormone releasing factors (GRF), J. Control. Rel. 15 (1991) 3–13.

[61] E.S. De Alvarenga, Characterization and properties of chitosan, in: M. Elnashar (Ed.), Biotechnol. Biopolym., InTech, 2011: pp. 91–108. doi:10.5772/17020.

[62] M. Rinaudo, Chitin and chitosan: properties and applications, Prog. Polym. Sci. 31 (2006) 603–632. doi:10.1016/j.progpolymsci.2006.06.001.

[63] M. Cegnar, J. Ker, Self-assembled polyelectrolyte nanocomplexes of alginate, chitosan and ovalbumin, Acta Chim. Slov. 57 (2010) 431–441.

[64] K. Lee, D. Mooney, Alginate: properties and biomedical applications, Prog. Polym. Sci. 37 (2013) 106–126. doi:10.1016/j.progpolymsci.2011.06.003.

[65] J.P. Paques, E. Van Der Linden, C.J.M. Van Rijn, L.M.C. Sagis, Preparation methods of alginate nanoparticles, Adv. Colloid Interface Sci. 209 (2014) 163–171. doi:10.1016/j.cis.2014.03.009.

[66] H. Zhao, Z.Y. Lin, L. Yildirimer, A. Dhinakar, X. Zhao, J. Wu, Polymer-based nanoparticles for protein delivery: design, strategy and applications, J. Mater. Chem. B. 4 (2016) 4060–4071. doi:10.1039/C6TB00308G.

[67] R.K. Purama, P. Goswami, A.T. Khan, A. Goyal, Structural analysis and properties of dextran produced by Leuconostoc mesenteroides NRRL B-640, Carbohydr. Polym. 76 (2009) 30–35. doi:10.1016/j.carbpol.2008.09.018.

[68] J. Varshosaz, Dextran conjugates in drug delivery, Expert Opin. Drug Deliv. 9 (2012) 509–523. doi:10.1517/17425247.2012.673580.

[69] H. Katas, Z. Hussain, S.A. Awang, Bovine serum albumin-loaded chitosan/dextran nanoparticles: preparation and evaluation of ex vivo colloidal stability in serum, J. Nanomater. 2013 (2013) 536291. doi:10.1155/2013/536291.

[70] Y. Chen, V.J. Mohanraj, F. Wang, H. a E. Benson, Designing chitosan-dextran sulfate nanoparticles using charge ratios, AAPS PharmSciTech. 8 (2007) 131–139. doi:10.1208/pt0804098.

[71] W. Tiyaboonchai, J. Woiszwillo, R.C. Sims, C.R. Middaugh, Insulin containing polyethylenimine-dextran sulfate nanoparticles, Int. J. Pharm. 255 (2003) 139–151. doi:10.1016/S0378-5173(03)00055-3.

[72] K.Y. Choi, G. Saravanakumar, J.H. Park, K. Park, Hyaluronic acid-based nanocarriers for intracellular targeting: interfacial interactions with proteins in cancer, Colloids Surfaces B Biointerfaces. 99 (2012) 82–94. doi:10.1016/j.colsurfb.2011.10.029.

[73] P. Calvo, C. Remuñan-López, J.L. Vila-Jato, M.J. Alonso, Chitosan and chitosan/ethylene oxide-propylene oxide block copolymer nanoparticles as novel carriers for proteins and vaccines, Pharm. Res. 14 (1997) 1431–1436. doi:10.1023/A:1012128907225.

[74] P. Calvo, C. Remuñán-López, J.L. Vila-Jato, M.J. Alonso, Novel hydrophilic chitosan-polyethylene oxide nanoparticles as protein carriers, J. Appl. Polym. Sci. 63 (1997) 125–132. doi:10.1002/(SICI)1097-4628(19970103)63:1<125::AID-APP13>3.0.CO;2-4.

[75] K. Liang, S. Ng, F. Lee, J. Lim, J.E. Chung, S.S. Lee, M. Kurisawa, Targeted intracellular protein delivery based on hyaluronic acid-green tea catechin nanogels, Acta Biomater. 33 (2016) 142–152. doi:10.1016/j.actbio.2016.01.011.

[76] E. Montanari, S. Capece, C. Di Meo, M. Meringolo, T. Coviello, E. Agostinelli, P. Matricardi, Hyaluronic acid nanohydrogels as a useful tool for BSAO immobilization in the treatment of melanoma cancer cells, Macromol. Biosci. 13 (2013) 1185–1194. doi:10.1002/mabi.201300114.

[77] T. Vermonden, R. Censi, W.E. Hennink, Hydrogels for protein delivery, Chem. Rev. 112 (2012) 2853–2888. doi:10.1021/cr200157d.

[78] J. Chen, Y. Zou, C. Deng, F. Meng, J. Zhang, Z. Zhong, Multifunctional click hyaluronic acid nanogels for targeted protein delivery and effective cancer treatment in vivo, Chem. Mater. 28 (2016) 8792–8799. doi:10.1021/acs.chemmater.6b04404.

[79] C.P. Reis, A.J. Ribeiro, F. Veiga, R.J. Neufeld, C. Damgé, Polyelectrolyte biomaterial interactions provide nanoparticulate carrier for oral insulin delivery, Drug Deliv. 15 (2008) 127–39. doi:10.1080/10717540801905165.

[80] C.P. Reis, A.J. Ribeiro, S. Houng, F. Veiga, R.J. Neufeld, Nanoparticulate delivery system for insulin: design, characterization and in vitro/in vivo bioactivity, Eur. J. Pharm. Sci. 30 (2007) 392–397. doi:10.1016/j.ejps.2006.12.007.

[81] A. Bernkop-Schnürch, S. Dünnhaupt, Chitosan-based drug delivery systems, Eur. J. Pharm. Biopharm. 81 (2012) 463–469. doi:10.1016/j.ejpb.2012.04.007.

[82] W. Tiyaboonchai, Chitosan nanoparticles: a promising system for drug delivery, Naresuan Univ. J. 11 (2003) 51–66. doi:10.1248/cpb.58.1423.

[83] F. Saraei, N. Mohamadpour Dounighi, H. Zolfagharian, S. Moradi Bidhendi, P. Khaki, F. Inanlou, Design and evaluate alginate nanoparticles as a protein delivery system, Arch. Razi Inst. 68 (2013) 139–146. doi:10.7508/ari.2013.02.008.

[84] Y. Parajó, I. D'Angelo, A. Horváth, T. Vantus, K. György, A. Welle, M. Garcia-Fuentes, M.J. Alonso, PLGA: poloxamer blend micro- and nanoparticles as controlled release systems for synthetic proangiogenic factors, Eur. J. Pharm. Sci. 41 (2010) 644–649. doi:10.1016/j.ejps.2010.09.008.

[85] R.K. Das, N. Kasoju, U. Bora, Encapsulation of curcumin in alginate-chitosan-pluronic composite nanoparticles for delivery to cancer cells, Nanomedicine Nanotechnology, Biol. Med. 6 (2010) 153–160. doi:10.1016/j.nano.2009.05.009.

[86] C. Ankerfors, S. Ondaral, L. Wågberg, L. Ödberg, Using jet mixing to prepare polyelectrolyte complexes: complex properties and their interaction with silicon oxide surfaces, J. Colloid Interface Sci. 351 (2010) 88–95. doi:10.1016/j.jcis.2010.07.027.

[87] S.L. Patwekar, A.P. Potulwar, S.R. Pedewas, M.S. Gaikwad, S.A. Khan, A.B. Suryawanshi, Review on polyelectrolyte complex as novel approach for drug delivery system, Int. J. Pharm. Pharm. Res. 5 (2016) 97–109.

[88] J.H. Hamman, Chitosan based polyelectrolyte complexes as potential carrier materials in drug delivery systems, Mar. Drugs. 8 (2010) 1305–1322. doi:10.3390/md8041305.

[89] N. Csaba, M. Köping-Höggård, M.J. Alonso, Ionically crosslinked chitosan/tripolyphosphate

nanoparticles for oligonucleotide and plasmid DNA delivery, Int. J. Pharm. 382 (2009) 205–214. doi:10.1016/j.ijpharm.2009.07.028.

[90] K.A. Janes, M.J. Alonso, Depolymerized chitosan nanoparticles for protein delivery: preparation and characterization, J. Appl. Polym. Sci. 88 (2003) 2769–2776. doi:10.1002/app.12016.

[91] M. Alonso-Sande, M. Cuña, C. Remuñán-López, D. Teijeiro-Osorio, J.L. Alonso-Lebrero, M.J. Alonso, Formation of new glucomannan - chitosan nanoparticles and study of their ability to associate and deliver proteins, Macromolecules. 39 (2006) 4152–4158. doi:10.1021/ma060230j.

[92] R. Fernández-Urrusuno, P. Calvo, C. Remuñán-López, J.L. Vila-Jato, M.J. Alonso, Enhancement of nasal absorption of insulin using chitosan nanoparticles, Pharm. Res. 16 (1999) 1576–1581. doi:10.1023/A:1018908705446.

[93] A. Umerska, K.J. Paluch, M.J.S. Martinez, O.I. Corrigan, C. Medina, L. Tajber, Self-assembled hyaluronate/protamine polyelectrolyte nanoplexes: synthesis, stability, biocompatibility and potential use as peptide carriers, J. Biomed. Nanotechnol. 10 (2014) 3658–3673. doi:10.1166/jbn.2014.1878.

[94] B. Sarmento, S. Martins, A. Ribeiro, F. Veiga, R. Neufeld, D. Ferreira, Development and comparison of different nanoparticulate polyelectrolyte complexes as insulin carriers, Int. J. Pept. Res. Ther. 12 (2006) 131–138. doi:10.1007/s10989-005-9010-3.

[95] M. Cetin, Y. Aktas, I. Vural, Y. Capan, L.A. Dogan, M. Duman, T. Dalkara, Preparation and in vitro evaluation of bFGF-loaded chitosan nanoparticles, Drug Deliv. 14 (2007) 525–529. doi:10.1080/10717540701606483.

[96] J.V. González-Aramundiz, M. Peleteiro Olmedo, Á. González-Fernández, M.J. Alonso Fernández, N.S. Csaba, Protamine-based nanoparticles as new antigen delivery systems, Eur. J. Pharm. Biopharm. 97 (2015) 51–59. doi:10.1016/j.ejpb.2015.09.019.

[97] B. Azimi, P. Nourpanah, M. Rabiee, S. Arbab, Producing gelatin nanoparticles as delivery system for bovine serum albumin, Iran. Biomed. J. 18 (2014) 34–40. doi:10.6091/ibj.1242.2013.

[98] Y. Parajó, I. D'Angelo, A. Welle, M. Garcia-Fuentes, M.J. Alonso, Hyaluronic acid/chitosan nanoparticles as delivery vehicles for VEGF and PDGF-BB, Drug Deliv. 17 (2010) 596–604. doi:10.3109/10717544.2010.509357.

[99] M. Zohri, A. Nomani, T. Gazori, I. Haririan, S.S. Mirdamadi, S.K. Sadjadi, M.R. Ehsani, Characterization of chitosan/alginate self-assembled nanoparticles as a protein carrier, J. Dispers. Sci. Technol. 32 (2011) 576–582. doi:10.1080/01932691003757314.

[100] E. Bahreini, K. Aghaiypour, R. Abbasalipourkabir, A.R. Mokarram, M. Taghi Goodzari, Preparation and nanoencapsulation of L-asparaginase II in chitosan-tripolyphosphate nanoparticles and in vitro release study, Nanoscale Res. Lett. 9 (2014). doi:10.1186/1556-276X-9-340.

[101] S.J. Na, S.Y. Chae, S. Lee, K. Park, K. Kim, J.H. Park, I.C. Kwon, S.Y. Jeong, K.C. Lee, Stability and bioactivity of nanocomplex of TNF-related apoptosis-inducing ligand, Int. J. Pharm. 363 (2008) 149–154. doi:10.1016/j.ijpharm.2008.07.013.

[102] B. Sarmento, A. Ribeiro, F. Veiga, P. Sampaio, R. Neufeld, D. Ferreira, Alginate/chitosan nanoparticles are effective for oral insulin delivery, Pharm. Res. 24 (2007) 2198–2206. doi:10.1007/s11095-007-9367-4.

[103] C.P. Reis, F.J. Veiga, A.J. Ribeiro, R.J. Neufeld, C. Damgé, Nanoparticulate biopolymers deliver insulin orally eliciting pharmacological response, J. Pharm. Sci. 97 (2008) 5290–5305. doi:10.1002/jps.21347.

[104] Y. Chen, V.J. Mohanraj, J.E. Parkin, Chitosan-dextran sulfate nanoparticles for delivery of an anti-angiogenesis, Lett. Pept. Sci. 10 (2003) 621–629. doi:10.1007/BF02442596.

[105] L.P. Herrera Estrada, J.A. Champion, Protein nanoparticles for therapeutic protein delivery,

Biomater. Sci. 3 (2015) 787–799. doi:10.1039/C5BM00052A.
[106] H.J. Lee, H.H. Park, J.A. Kim, J.H. Park, J. Ryu, J. Choi, J. Lee, W.J. Rhee, T.H. Park, Enzyme delivery using the 30Kc19 protein and human serum albumin nanoparticles, Biomaterials. 35 (2014) 1696–1704. doi:10.1016/j.biomaterials.2013.11.001.
[107] L. Herrera Estrada, S. Chu, J.A. Champion, Protein nanoparticles for intracellular delivery of therapeutic enzymes, J. Pharm. Sci. 103 (2014) 1863–1871. doi:10.1002/jps.23974.
[108] S. Zhang, G. Wang, X. Lin, M. Chatzinikolaidou, H.P. Jennissen, M. Laub, H. Uludağ, Polyethylenimine-coated albumin nanoparticles for BMP-2 delivery, Biotechnol. Prog. 24 (2008) 945–956. doi:10.1002/btpr.12.
[109] J. Kundu, Y.-I. Chung, Y.H. Kim, G. Tae, S.C. Kundu, Silk fibroin nanoparticles for cellular uptake and control release, Int. J. Pharm. 388 (2010) 242–250. doi:10.1016/j.ijpharm.2009.12.052.
[110] R. Kaintura, P. Sharma, S. Singh, K. Rawat, P.R. Solanki, Gelatin nanoparticles as a delivery system for proteins, J. Nanomedicine Res. 2 (2015) 18. doi:10.15406/jnmr.2015.02.00018.
[111] E.J. Oh, K. Park, K.S. Kim, J. Kim, J.A. Yang, J.H. Kong, M.Y. Lee, A.S. Hoffman, S.K. Hahn, Target specific and long-acting delivery of protein, peptide, and nucleotide therapeutics using hyaluronic acid derivatives, J. Control. Release. 141 (2010) 2–12. doi:10.1016/j.jconrel.2009.09.010.
[112] B. Delpech, N. Girard, P. Bertrand, M. Courel, C. Chauzy, A. Delpech, C. Chauzy, D.A.C. Henri-becquerel, Hyaluronan : fundamental principles and applications in cancer, J. Intern. Med. (1997) 41–48.
[113] T. Chanmee, P. Ontong, N. Itano, Hyaluronan : A modulator of the tumor microenvironment, Cancer Lett. 375 (2016) 20–30. doi:10.1016/j.canlet.2016.02.031.
[114] D.G. Jackson, R. Prevo, S. Clasper, S. Banerji, LYVE-1, the lymphatic system and tumor lymphangiogenesis, TRENDS Immunol. 22 (2001) 317–321.
[115] R. Racine, M.E. Mummert, Hyaluronan Endocytosis : Mechanisms of Uptake and Biological Functions, 2012.
[116] K.Y. Choi, H. Chung, K.H. Min, Y.Y. Hong, K. Kim, J.H. Park, I.C. Kwon, S.Y. Jeong, Biomaterials Self-assembled hyaluronic acid nanoparticles for active tumor targeting, Biomaterials. 31 (2010) 106–114. doi:10.1016/j.biomaterials.2009.09.030.
[117] H.S.S. Qhattal, X. Liu, Characterization of CD44-Mediated Cancer Cell Uptake and Intracellular Distribution of Hyaluronan-Grafted Liposomes, Mol. Pharm. 8 (2012) 1233–1246. doi:10.1021/mp2000428.Characterization.
[118] A. Cadete, M.J. Alonso, Targeting cancer with hyaluronic acid- based nanocarriers : recent advances and translational perspectives, Futur. Med. 11 (2016) 2341–2357. doi:10.2217/nnm-2016-0117.
[119] R. Racine, M.E. Mummert, Hyaluronan Endocytosis: Mechanisms of Uptake and Biological Functions, in: Mol. Regul. Endocytosis, 2012: pp. 377–390. doi:10.5772/45976.
[120] G. Tripodo, A. Trapani, M. Luisa, G. Giammona, G. Trapani, D. Mandracchia, Hyaluronic acid and its derivatives in drug delivery and imaging : Recent advances and challenges, Eur. J. Pharm. Biopharm. 97 (2015) 400–416. doi:10.1016/j.ejpb.2015.03.032.
[121] S. Yin, J. Huai, X. Chen, Y. Yang, X. Zhang, Y. Gan, G. Wang, X. Gu, J. Li, Intracellular delivery and antitumor effects of a redox-responsive polymeric paclitaxel conjugate based on hyaluronic acid, Acta Biomater. 26 (2015) 274–285. doi:10.1016/j.actbio.2015.08.029.
[122] G. Kogan, S. Ladislav, R. Stern, P. Gemeiner, Hyaluronic acid : a natural biopolymer with a broad range of biomedical and industrial applications, Biotechnol. Lett. 29 (2007) 17–25. doi:10.1007/s10529-006-9219-z.
[123] F. Sultana, Manirujjaman, Imran-Ul-Haque, M. Arafat, S. Sharmin, An overview of nanogel drug delivery system, J. Appl. Pharm. Sci. 3 (2013) 95–105. doi:10.7324/JAPS.2013.38.S15.
[124] Y. Parajo, I. D'Angelo, A. Welle, M. Garcia-Fuentes, M.J. Alonso, Hyaluronic acid/Chitosan nanoparticles as delivery vehicles for VEGF and PDGF-BB, Drug Deliv. 17 (2010) 596–604.

doi:10.3109/10717544.2010.509357.
[125] R.J. Verheul, B. Slütter, S.M. Bal, J.A. Bouwstra, W. Jiskoot, W.E. Hennink, Covalently stabilized trimethyl chitosan-hyaluronic acid nanoparticles for nasal and intradermal vaccination, J. Control. Release. 156 (2011) 50–56. doi:10.1016/j.jconrel.2011.07.014.
[126] A. Mero, M. Campisi, Hyaluronic acid bioconjugates for the delivery of bioactive molecules, Polymers (Basel). 6 (2014) 346–369. doi:10.3390/polym6020346.
[127] C.E. Schanté, G. Zuber, C. Herlin, T.F. Vandamme, Chemical modifications of hyaluronic acid for the synthesis of derivatives for a broad range of biomedical applications, Carbohydr. Polym. 85 (2011) 469–489. doi:10.1016/j.carbpol.2011.03.019.
[128] A. Mero, M. Pasqualin, M. Campisi, D. Renier, G. Pasut, Conjugation of hyaluronan to proteins, Carbohydr. Polym. 92 (2013) 2163–2170. doi:10.1016/j.carbpol.2012.11.090.
[129] E.L. Ferguson, A.M.J. Alshame, D.W. Thomas, Evaluation of hyaluronic acid-protein conjugates for polymer masked-unmasked protein therapy, Int. J. Pharm. 402 (2010) 95–102. doi:10.1016/j.ijpharm.2010.09.029.

Background

USC
UNIVERSIDADE
DE SANTIAGO
DE COMPOSTELA

During the last years, it has been shown that protein therapeutics offers significant advantages in the treatment of cancers in term of specificity and selectivity for the targets. The use of proteins and, notably, mAbs helps reducing the side effects inherent to chemotherapy [1–3]. Examples of FDA approved antibodies for cancer treatment are herceptin [4], cetuximab [5] or bevacizumab (BVZ) [6]. The use of BVZ for treating breast cancer is still under investigation due to the side effects developed by the patients upon the treatment with this drug [7].

The nanoencapsulation of anticancer proteins confers significant advantages from the point of view of their intracellular delivery to cancer cells. The nanocarriers are able to increase the proteins circulation time, protect them from degradation, reduce their immunogenicity and increase their tumor penetration, allowing a better accumulation of these therapeutics in the tumor tissue [8,9]. Moreover, if surface-decorated with specific ligands, they could favor the targeting of specific tumor cells or the internalization of the associated proteins [10,11]. The cytoplasmic proteins targeting could also help in overcoming the mechanisms which often cancer cells use for resisting to anti-cancer therapies. This is particularly true with BVZ, where the VEGF-A intracellular pool has a key role in cancer cell survival, invasion and migration [12,13]. In this regard, the nanoencapsulation of BVZ has been studied as a strategy for delivering the antibody intracellularly and for reducing its side effects [14–17].

A variety of polymers have already been used for the encapsulation of therapeutic proteins, being PLGA the most used. Our lab pioneered the encapsulation of proteins within PLGA [18] and PLA-PEG [19] nanoparticles as well as within nanoparticles made of natural polymers, i.e. chitosan [20] and glucomannan [21]. We have also produced HA-based nanocapsules, which facilitated the access of monoclonal antibodies to cancer cells [22].

Bibliography

[1] E. Pérez-Herrero, A. Fernández-Medarde, Advanced targeted therapies in cancer: Drug nanocarriers, the future of chemotherapy, Eur. J. Pharm. Biopharm. 93 (2015) 52–79. doi:10.1016/j.ejpb.2015.03.018.

[2] V.P. Torchilin, A.N. Lukyanov, Peptide and protein drug delivery to and into tumors: challenges and solutions, Drug Discov. Today. 8 (2003) 259–266. doi:10.1016/S1359-6446(03)02623-0.

[3] A.M. Scott, J.D. Wolchok, L.J. Old, Antibody therapy of cancer, Nature. 12 (2012) 278–287. doi:10.1038/nrc3236.

[4] https://www.herceptin.com/.

[5] T.T. Hansel, H. Kropshofer, T. Singer, J.A. Mitchell, A.J.T. George, The safety and side effects of monoclonal antibodies, Nat. Rev. Drug Discov. 9 (2010) 325–338. doi:10.1038/nrd3003.

[6] https://www.avastin.com/patient/mcrc.html.

[7] A.J. Montero, M. Escobar, G. Lopes, S. Gluck, C. Vogel, Bevacizumab in the Treatment of Metastatic Breast Cancer: Friend or Foe?, Curr. Oncol. Rep. 14 (2013) 1–11. doi:10.1007/s11912-011-0202-z.

[8] T.A.S. Aguirre, D. Teijeiro-Osorio, M. Rosa, I.S. Coulter, M.J. Alonso, D.J. Brayden, Current status of selected oral peptide technologies in advanced preclinical development and in

clinical trials, Adv. Drug Deliv. Rev. 106 (2016) 223–241. doi:10.1016/j.addr.2016.02.004.
[9] H. Zhao, Z.Y. Lin, L. Yildirimer, A. Dhinakar, X. Zhao, J. Wu, Polymer-based nanoparticles for protein delivery: design, strategy and applications, J. Mater. Chem. B. 4 (2016) 4060–4071. doi:10.1039/C6TB00308G.
[10] W.C. Chen, A.X. Zhang, S. Li, Limitations and niches of the active targeting approach for nanoparticle drug delivery, Eur. J. Nanomedicine. 4 (2012) 89–93. doi:10.1515/ejnm-2012-0010.
[11] D.A. Ossipov, Nanostructured hyaluronic acid-based materials for active delivery to cancer, Expert Opin. Drug Deliv. 7 (2010) 681–703. doi:10.1517/17425241003730399.
[12] R. Bhattacharya, F. Fan, R. Wang, X. Ye, L. Xia, D. Boulbes, L.M. Ellis, Intracrine VEGF signalling mediates colorectal cancer cell migration and invasion, Br. J. Cancer. 117 (2017) 848–855. doi:10.1038/bjc.2017.238.
[13] R. Bhattacharya, X. Ye, R. Wang, X. Ling, M. Mcmanus, F. Fan, D. Boulbes, L.M. Ellis, Intracrine VEGF Signaling Mediates the Activity of Pro-survival Pathways in Human Colorectal Cancer Cells, Cancer Res. 76 (2017) 3014–3024. doi:10.1158/0008-5472.CAN-15-1605.
[14] S. Tangutoori, B.Q. Spring, Z. Mai, A. Palanisami, L.B. Mensah, T. Hasan, Simultaneous delivery of cytotoxic and biologic therapeutics using nanophotoactivatable liposomes enhances treatment efficacy in a mouse model of pancreatic cancer, Nanomedicine Nanotechnology, Biol. Med. 12 (2016) 223–234. doi:10.1016/j.nano.2015.08.007.
[15] B. Spring, Z. Mai, P. Rai, S. Chang, T. Hasan, Theranostic Nanocells for Simultaneous Imaging and Photodynamic therapy of Pancreatic Cancer, Opt. Methods Tumor Treat. Detect. Mech. Tech. Photodyn. Ther. 7551 (2010) 1–11. doi:10.1117/12.843725.
[16] A.R. Srinivasan, A. Lakshmikuttyamma, S.A. Shoyele, Investigation of the Stability and Cellular Uptake of Self-Associated Monoclonal Antibody (MAb) Nanoparticles by Non-Small Lung Cancer Cells, Mol. Pharm. 10 (2013) 3275–3284. doi:10.1021/mp3005935.
[17] Y. Zhang, J. Guo, X. Zhang, D. Li, T. Zhang, Antibody fragment-armed mesoporous silica nanoparticles for the targeted delivery of bevacizumab in ovarian cancer cells, Int. J. Pharm. 496 (2015) 1026–1033. doi:10.1016/j.ijpharm.2015.10.080.
[18] M.D. Blanco, M.J. Alonso, Development and characterization of protein-loaded poly(lactide-co-glycolide) nanospheres, Eur. J. Pharm. Biopharm. 43 (1997) 287–294. doi:10.1016/S0939-6411(97)00056-8.
[19] P. Quellec, R. Gref, L. Perrin, E. Dellacherie, F. Sommer, J.M. Verbavatz, M.J. Alonso, Protein encapsulation within polyethylene glycol-coated nanospheres. I. Physicochemical characterization, J. Biomed. Mater. Res. 42 (1998) 45–54. doi:10.1002/(SICI)1097-4636(199810)42:1<45::AID-JBM7>3.0.CO;2-O.
[20] P. Calvo, C. Remuñán-López, J.L. Vila-Jato, M.J. Alonso, Novel hydrophilic chitosan-polyethylene oxide nanoparticles as protein carriers, J. Appl. Polym. Sci. 63 (1997) 125–132. doi:10.1002/(SICI)1097-4628(19970103)63:1<125::AID-APP13>3.0.CO;2-4.
[21] M. Alonso-Sande, M. Cuña, C. Remuñán-López, D. Teijeiro-Osorio, J.L. Alonso-Lebrero, M.J. Alonso, Formation of new glucomannan - chitosan nanoparticles and study of their ability to associate and deliver proteins, Macromolecules. 39 (2006) 4152–4158. doi:10.1021/ma060230j.
[22] Á. Molina-Crespo, A. Cadete, D. Sarrio, M. Gámez-Chiachio, L. Martinez, K. Chao, A. Olivera, A. Gonella, E. Díaz, J. Palacios, P.K. Dhal, M. Besev, M. Rodríguez-Serrano, M.L. García Bermejo, J.C. Triviño, A. Cano, M. García-Fuentes, O. Herzberg, D. Torres, M.J. Alonso, G. Moreno-Bueno, Intracellular Delivery of an Antibody Targeting Gasdermin-B Reduces HER2 Breast Cancer Aggressiveness, Clin. Cancer Res. (2019). doi:10.1158/1078-0432.CCR-18-2381.
[23] G.R. Rivera-rodríguez, M.J. Alonso, D. Torres, Poly- L-asparagine nanocapsules as anticancer drug delivery vehicles, Eur. J. Pharm. Biopharm. 85 (2013) 481–487. doi:10.1016/j.ejpb.2013.08.001.

[24] D.R. Wise, C.B. Thompson, Glutamine Addiction: A New Therapeutic Target in Cancer, Trend Biochem. Sci. 35 (2011) 427–433. doi:10.1016/j.tibs.2010.05.003.Glutamine.

[25] R.J. DeBerardinis, J.J. Lum, G. Hatzivassiliou, C.B. Thompson, The Biology of Cancer : Metabolic Reprogramming Fuels Cell Growth and Proliferation, Cell Press. 7 (2008) 11–20. doi:10.1016/j.cmet.2007.10.002.

USC
UNIVERSIDADE
DE SANTIAGO
DE COMPOSTELA

Hypothesis

USC
UNIVERSIDADE
DE SANTIAGO
DE COMPOSTELA

1. HA, a well-known biomaterial in the drug delivery field, can form drug nanocarriers by assembling it with cationic surfactants, e.g. LAE.

2. HA-based nanocomplexes could be suitable for the association of proteins, through the formation of multiple distinct interactions with the proteins (hydrophobic, electrostatic, Van der Waals, etc.). This can be obtained thanks to the polymer and surfactant characteristics and by tuning the production methods based on protein's features.

3. HA-based nanocomplexes can be able to interact with cancer cells trough the recognition of the HA polymer by the CD44 receptor. This interaction could allow the internalization of the nanocarriers by an endocytic process. This internalization could be also favored by the use of a cationic surfactant.

4. The nanocomplexes can be useful carriers for the intra and extracellular delivery of the monoclonal antibody BVZ, thereby improving its anticancer efficacy.

USC
UNIVERSIDADE
DE SANTIAGO
DE COMPOSTELA

Objectives

USC
UNIVERSIDADE
DE SANTIAGO
DE COMPOSTELA

Considering the presented background information and hypothesis, the objective of this doctoral thesis has been the development of a novel HA-based nanosystem with the capacity to associate proteins with different properties, mainly antibodies, for their delivery to tumors. This goal has been achieved through the following experimental steps:

Development of a new HA-based nanosystem for intracellular protein delivery

1. Development of nanocomplexes made by HA and the cationic surfactant LAE, enveloped by a protective polymer layer.
2. Association of two model proteins (BSA and IgG) to the developed nanocomplexes and assessment of their structural stability during the formulation process, as well as their stability and release in simulated biological fluids.
3. Evaluation of the storage stability of the nanocarriers in different conditions.

The results corresponding to this step will be shown in Chapter III: “Hyaluronic acid-based nanocomplexes for the delivery of proteins to cancer cells”

Development of HA- based nanosystems for the intracellular delivery of BVZ

1. Development of BVZ-loaded enveloped HA/LAE nanocomplexes (BVZ-loaded HA ENCPs).
2. Evaluation of the association efficiency and functional stability of BVZ.
3. Study of the nanocomplexes stability in simulated biological fluids and of the BVZ release upon the dilution of the nanosystem in the same media.
4. Evaluation of the BVZ-loaded nanocomplexes stability upon their storage in different conditions.
5. Understanding the interaction of the BVZ-loaded nanocarriers with a breast cancer cell line. Experiments of toxicity, internalization and gene expression will be done.
6. Evaluation of the *in vivo* efficacy of the developed formulation containing BVZ.

The results of these studies will be presented in Chapter IV: “Bevacizumab-loaded hyaluronic acid enveloped nanocomplexes for the treatment of breast cancer”.

This work was done in collaboration with Institute Galien Paris Sud (Université Paris Sud) and Sylentis S.A. (Madrid) .

USC
UNIVERSIDADE
DE SANTIAGO
DE COMPOSTELA

Chapter III

Hyaluronic acid-based nanocomplexes for the delivery of proteins to cancer cells

USC
UNIVERSIDADE
DE SANTIAGO
DE COMPOSTELA

ABSTRACT

It is known that chemotherapeutic agents classically used for the treatment of cancer generally lead to important side effects that are accompanied of a limited efficacy. This poor performance has encouraged researchers to design more selective therapies. The use of protein therapeutics, highly specific, associated to nanoparticles, able to protect and deliver them to the target site, is raising as one of the most important alternatives to classical chemotherapy. The objective of this work was to produce hyaluronic acid (HA)-based nanoparticles and to assess their potential for the delivery of proteins. The nanoparticles consisted of complexes of the protein with HA and the surfactant ethyl lauroyl arginate (LAE), finally enveloped by two layers of polyarginine and HA, respectively. Two different model proteins, BSA and an IgG, were successfully associated to the developed nanosystems, thus showing the feasibility of the nanocarriers for the association of different kinds of proteins. The formulation conditions were found to strongly influence both the physico-chemical properties of the nanosystems, and their stability in simulated biological fluids (SBF). In particular, it was found that the association of BSA and the presence of the multiple polymer coatings were necessary for preventing the stability in SBF supplemented with FBS. The nanocomplexes could be freeze-dried. Overall, this work presents critical information for the formulation of proteins and notably antibodies using nanotechnology.

Keywords: therapeutic proteins; monoclonal antibodies; hyaluronic acid; cancer; nanocomplexes; nanomedicine

USC
UNIVERSIDADE
DE SANTIAGO
DE COMPOSTELA

1. Introduction

Nowadays, cancer is one of the most important causes of human death. As estimated by the World Health Organization, 9.6 millions of death have been estimated in 2018 [1]. The most common approaches to treat cancer, include surgery, radiation therapy and chemotherapy [2,3]. Unfortunately, the efficacy of these treatments is often limited whereas the associated side effects are remarkable. To solve this problem, researchers have looked at new strategies, some of which involve the use of proteins and monoclonal antibodies. Proteins and, notably, monoclonal antibodies are specific and selective as compared to chemically synthesized compounds (e.g. receptors, inhibitors, etc.) [3,4]. Approximately, 35 monoclonal antibody therapeutics have been approved for clinical use in the United States and many are in various stages of clinical trials [5]. Unfortunately, their exploitation is being limited by their poor tumor penetration, instability and intrinsic immunogenicity (typical of high molecular weight proteins) [6–8]. These draw-backs have stimulated research in the area of drug delivery and nanotechnology with the final goal of making the administration of these powerful drugs more efficient [9–11].

Encapsulating proteins into nanocarriers could be a practical way to deliver proteins inside cancer cells and protect them from enzymatic degradation [12]. Liposomes were the first nanocarriers proposed for protein delivery in the early 70's [13,14]. Meanwhile, Speiser and co-workers investigated the possibility to encapsulate drugs or antigens into polyacrylic nanoparticles using micelle polymerization techniques [15]. A decade later, poly(alkyl)cyanoacrylate nanocapsules were proposed as carriers for the oral administration of insulin [16]. Finally, over the 90's Gasco et al. produced peptide-loaded solid lipid nanoparticles [17–19] and within the same decade our group pioneered the development of nanoparticles made of PLGA [20], PLA-PEG [21] and chitosan [22] for the delivery of proteins and antigens. Overall, the tendency has been towards the use of biodegradable and biocompatible biomaterials that can form nanostructures based on friendly and easily scalable techniques.

On the other hand, the idea of making particles with polymers that can be recognized by specific groups of cells started at the beginning of 2000 [23–25]. In this regard, we have reported that hyaluronic acid (HA)
2-based nanocapsules are able to reach the tumor and be internalized by cancer cells [26]. This was justified by the fact that HA binds specifically to cancer cells which overexpress the CD44 receptor (e.g. breast, colon, ovarian, lung etc.), allowing the active targeting of the tumor. Most important, when the interaction between CD44 and its ligand takes place, an internalization process endocytosis mediated occurs [27,28].

Based on this background information, the objective of this work was to develop a new HA-based nanocarrier and evaluate its capacity for the association of two different model proteins, BSA and IgG. Different formulation strategies were employed and the developed nanocarriers were characterized for their physicochemical properties, encapsulation efficiency, stability in simulated biological fluids, storage stability and release. Studies related to the structural stability of the encapsulated proteins were also performed in order to assess the protein functionality.

2. Materials and Methods

2.1 Chemicals

BSA (66 kDa) and IgG (150 kDa) were purchased from Sigma – Aldrich (Spain). Ethyl Lauryl Arginate (LAE) was a gift from Vedeqsa (Spain) and Hyaluronic Acid (HA, 47 – 57 kDa) was purchased from Lifecore Biomedical (USA). Poly-L-Ariginine was purchased from PTS (Spain) while FITC and the Centripure mini desalt Z-50 spin columns from emp BIOTECH (Spain). α-trehalose have been purchased by Pfanstiehl (USA).

2.2. Preparation of blank HA nanocomplexes with the film hydration technique

Nanocomplexes were prepared with the well-known film hydration technique. Briefly, 4 mg of LAE were dissolved in ethanol, and a film of the surfactant was formed on the walls of a bottom round flask using rotaevaporation. The formed film was then hydrated with 1 mL of a HA solution (different concentrations have been tested). The HA solution have been dissolved in different media before the hydration of the film (i.e. milliQ water, HEPES buffer 5 mM-pH 7.2 and acetate buffer 5mM-pH 4.5) for understanding if the osmolarity and changes in pH could affect particles properties.

2.3 Preparation of blank, BSA-loaded, IgG-loaded and BSA/IgG-loaded HA nanocomplexes with the injection technique

Nanocomplexes were prepared adding 250 µL of LAE solution to 500 µL of an HA solution. The suspension was stirred (900 rpm) for 15 minutes at room temperature. Different w/w ratios between LAE and HA and different formulating media (i.e. water, HEPES buffer-5 mM-pH 7.2, acetate buffer-5mM-pH 4.5 and phosphate buffer 10 mM-pH 7.2) were tested and the results compared. It is thought the nanocomplexes are made both by electrostatic interaction between the positively charged head of LAE and the negative charges of the HA and by the hydrophobic interactions between the LAE tails. After the selection of the more suitable blank particles, the protein have been introduced into the formulation mixture, as indicted as follow.

a) BSA-loaded HA nanocomplexes

The protein was dissolved in the corresponding formulating media and added (drop by drop, 200 µL, different concentrations tested) to the LAE solution. The suspension was stirred (300 rpm) for 15 minutes at room temperature and a complex between the surfactant and the protein is formed. The LAE is interacting both with electrostatic and hydrophobic interactions with the protein. The protein/LAE complex was then added to 500 µL of HA solution under stirring (900 rpm). Particles are immediately formed.

b) IgG-loaded HA nanocomplexes

The same protocol used to produce the BSA-loaded HA nanocomplexes have been used with the IgG (previously dissolved in NaCl 150 mM). In this case, the effect of adding the IgG to the solution of LAE or HA was also studied. Briefly, 200 µL of the protein solution (different concentrations tested) has been added drop by drop to the LAE or the HA solution (I phase). After 15 minutes stirring, the I phase was added on the top of the II phase (HA or LAE solution, based on the used I phase).

c) BSA/IgG-loaded HA nanocomplexes

30 µL of the IgG (previously dissolved in NaCl 150 mM and then diluted to a concentration of 5.3 mg/mL) were added to 200 µL of a BSA solution (10 mg/mL) and stirred for 15 minutes (300 rpm). The proteins solutions were then added to the LAE solution (drop by drop) and further stirred for 15 minutes (300 rpm). Finally all the mixture was added to the HA solution and again stirred for 15 minutes (900 rpm) to form the nanocomplexes.

d) Layer-by-layer PArg/HA enveloped nanocomplexes (layer-by-layer PArg/HA ENCPs)

The layer-by-layer ENCPs were prepared attaching multiple polymer layers on the surface of the prototype developed before (BSA/IgG-loaded HA nanocomplexes). Briefly, 30 µL of IgG (5.3 mg/mL) were added to 200 µL of a BSA solution at a concentration of 10 mg/mL and stirred for 15 min (300 rpm). The proteins solution was then added drop by drop to 250 µL of a LAE solution (8mg/mL) and further stirred (300 rpm). After 15 minutes, the proteins/LAE mixture was added to 500 µL of an HA solution (4 mg/mL) under stirring (900 rpm, 15 minutes) forming negatively charged nanocomplexes (HA I layer). Then, 450 µL of the nanoformulation were placed under stirring (500 rpm) and 450 µL of a poly-L-Arginine (PArg) solution (PArg II layer-different molar ratios tested) were then added on the top of the negatively charged complex under stirring (500 rpm). After 15 minutes, 200 µL of the PArg coated nanocomplexes were taken and further 200 µL of an HA solution (HA III layer-different molar ratios tested) were added on the top and the obtained PArg/HA coated formulation and stirred for further 15 min. All the solutions were prepared in milliQ water.

The final PArg II layer and HA III layer concentrations selected (after the optimization procedure) are 1.3 mg/mL and 3.1 mg/mL, respectively.

2.4 Physicochemical characterization of the nanoformulations

The size and zeta potential of the colloidal systems were determined by photon correlation spectroscopy and laser Doppler anemometry using a Zetasizer Nano-ZS (Malvern Instruments, Worcestershire, United Kingdom). The zeta potential of the formulations was measured in KCl 1 mM (as suggested by Malvern). TEM (Transmission Electron Microscopy) and SEM (scanning electron microscopy) was also used to better characterize the particles from the point of view of their shape and size.

2.5 Simulated biological fluids (PBS and RPMI) stability studies

All the synthesized nanocomplexes have been characterized from the point of view of their stability in PBS, RPMI or FBS supplemented RPMI (10% FBS concentration). Briefly, the nanosystems were diluted in the media and were incubated at 37°C. At different time points (from 0 to 24h) size and mean count rate were measured with Zetasizer Nano-ZS.

2.6 Association efficiency, AE (%), studies

a) BSA-loaded HA nanocomplexes

Two different methods were used to evaluate the AE of the protein into the nanosystems. With the first method (method 1) the BSA-loaded formulation was isolated by centrifugation (10000g – 15°C – 30 minutes), a pellet was formed and the supernatant withdrawn. If no protein was encapsulated, all

the BSA must have been found in the supernatant. Hence, 150 µL of the supernatant were withdrawn and the protein was precipitated with the methanol – chloroform method (in order to clean the suspension from interfering compounds). Briefly, 600 µL of methanol were added to the 150 µL of supernatant and the suspension was vortexed for 30 s. Then, 150 µL of chloroform were also added and vortexed, again. Finally, 450 µL of water were added, the suspension vortexed and centrifuged at 19500g - 4°C - 5.30 min. The aqueous top layer was removed and 600 µL of methanol were added again. After vortexing, the solution was centrifuged again at 19500g – 4°C – 5.30 minutes and a protein precipitate was obtained. The excess of solvent was taken out and the pellet was dried for few minutes. The pellet was then resuspended in 500 µL of Tween20 0.1% (vortex and sonication for 30 min helped its resuspention). The amount of BSA precipitated was evaluated with a Bradford assay.
With the second encapsulation efficiency method (method 2) particles were isolated in the same way as before. The supernatant was withdrawn and the amount of protein in the supernatant was directly evaluated with a Bradford assay (i.e. the supernatant of blank HA nanocomplexes was used to build the calibration line in order to consider all the interferences).

b) BSA/IgG-loaded HA nanocomplexes
Both the total amount of associated proteins (BSA and IgG) and the association of just the IgG have been evaluated for this formulation with two different approaches. The total protein (BSA+IgG) have been measured with method 1 described above. In order to specifically know the AE (%) of the IgG in this nanosystem, the antibody was previously labeled with FITC (see paragraph 2.7). The complexes were then formulated with the labeled IgG and isolated as described before. The residual fluorescence in the supernatant was evaluated and utilized to calculate the AE (%).

c) Layer-by-layer PArg/HA ENCPs
The AE (%) of the IgG was evaluated measuring the amount of residual fluorescence in the supernatant. Briefly, the IgG was labeled with FITC and was associated to the ENCPs. The nanosystem was then isolated by centrifugation (10000g – 15°C – 30 minutes) and the amount of fluorescence in the supernatant was evaluated.

2.7 FITC labeling of the IgG
To 66 µL of the IgG solution (previously dissolved in a 150 mM NaCl at a concentration of 15.2 mg/mL), 13.2 µL of a sodium bicarbonate solution 1M pH 8.5 were added. Then, 10 µL of a 2 mM FITC solution (prepared in DMSO) were added to the protein solution and stirred for 2h. Centripure mini desalt Z-50 spin columns were used to purify the labeled antibody.

2.8 Release assay
In order to evaluate the amount of BSA and of BSA+IgG released from the nanosystems (respectively from the BSA-loaded HA nanocomplexes and from the BSA/IgG-loaded HA nanocomplexes), the formulations were diluted in PBS and incubated at 37°C. At different time points (0 to 24 hours), 500 µL of the suspensions were centrifuged (10000g – 30 min – 15°C) and a pellet is formed. The supernatant was taken and the amount of protein/s released was evaluated with a Bradford assay using method 2 (see paragraph 2.6).

For specifically understand the amount of IgG released from the BSA/IgG-loaded HA nanocomplexes, the IgG was labeled with FITC (as previously described). At different time points (0 to 24 hours) the nanoformulation was centrifuged and the amount of residual fluorescence in the supernatant evaluated.

2.9 Storage stability studies

Both the storage stability of the nanoformulations in suspension and upon freeze drying have been performed. For the storage in suspension, the selected formulations were stored at 4°C and size, polydispersity index (PDI) and mean count rate (MCR) measured at different time points (1 - 2 - 4 - 7 days).

For the freeze-drying studies, trehalose was chosen as cryo-protectant agent. Different concentrations were tested (1, 5, 10 or 15%, final concentration after resuspension) in order to understand the most suitable condition for storing the nanocarriers as dry powder. Size, PDI and MCR were evaluated after the resuspension of the powder.

2.10 Circular dichroism (CD) of the used proteins

CD experiments have been done in order to understand if the presence of the surfactant (i.e. LAE) affect the structural stability of the proteins. In this regard, the LAE was mixed with the target proteins (BSA, IgG or BSA+IgG) in the same way it was mixed when particles are formed. The LAE/proteins solution was then diluted to perform the CD analysis (to 0.1 mg/mL or 0.02 mg/mL when the BSA or the IgG structure has to be evaluated, respectively). The far-UV CD spectra was measured with a Jasco J-810 spectropolarimeter (Jasco) and a quartz cuvette of 1 cm path have been used. The analysis have been done under the following conditions: data pitch = 0.2 nm, scanning speed = 50 nm/min, D.I.T. = 1s; band width = 1 nm, accumulation = 3.

3. Results

HA and LAE were selected as main components for producing the nanocomplexes. The HA was chosen because it can be recognized by the CD44 receptor, overexpressed in different cancer types, a process that is followed by an endocytic uptake [29,30]. LAE is a positively charged surfactant which can easily interact with HA through electrostatic interactions and with proteins with both hydrophobic and electrostatic interactions. It could also help the penetration of the protein into the cancer cells [31].

The formation of the nanocomplexes and their characterization is presented below. First, the formation of protein-loaded nanocomplexes based on the use of LAE and HA is described using different techniques and, in a second part of this section, the coating of the nanocomplexes with additional polymers is presented as a strategy to improve the stability of the nanosystems upon contact with biological fluids. The sequence on the formulation optimization process is presented in Figure 3.1.

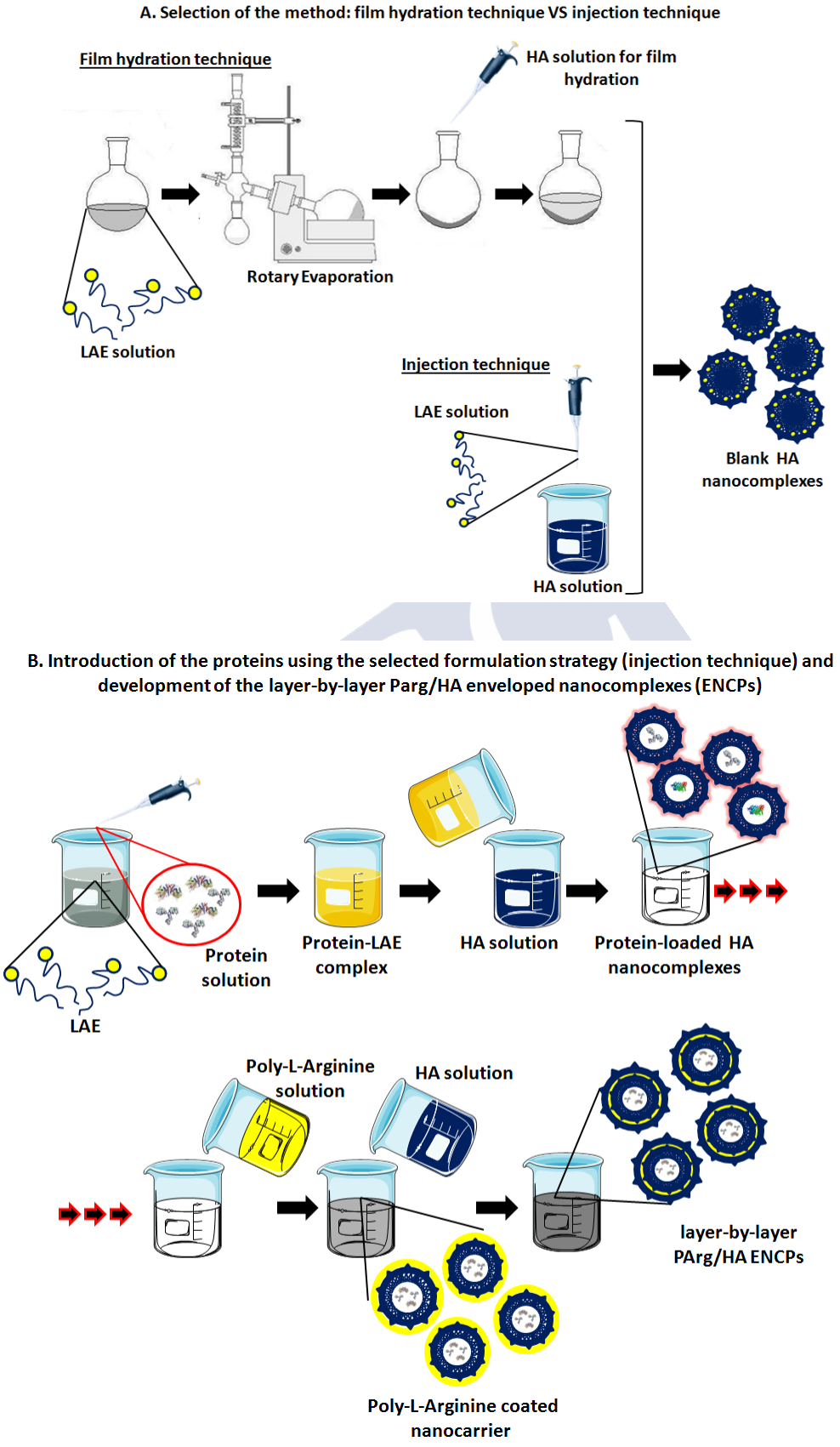

Figure 3.1. A) selection of the most suitable technique for producing the blank HA nanocomplexes (non loaded with any protein). The film hydration and the injection techniques have been tested. B) After the selection of the injection technique

the proteins have been incorporated in the formulation, obtaining the protein-loaded HA nanocomplexes (coated by an HA layer). The layer-by-layer PArg/HA ENCPs, made by a second poly-L-Arginine and a third HA layers, have been developed for stabilizing the formulation in biological media.

3.1 Film hydration technique vs. injection technique for the production of protein-loaded HA nanocomplexes

3.1.1 Formation of the blank HA nanocomplexes

The film hydration technique has been frequently used to produce liposomes or micelles. A fix amount of LAE was selected (4 mg) and different amounts of HA (from 0.1 to 1 mg) were tested in order to find the ratio that leads to the formation of reproducible nanocomplexes (Table 3.1). The final volume of the suspension was 1 mL. On the other hand, three different aqueous solvents were employed for preparing the formulations. As shown in Figure 3.2, nanocomplexes were formed at all ratios except for 1mg of HA dissolved in MilliQ water or HEPES buffer, while with the use of acetate buffer as a dissolving medium, nanocomplexes could be formed at any of the ratios investigated. On the other hand, as expected, the increase of the HA amount led to an inversion of the zeta potential from positive to negative values.

Table 3.1. Tested LAE/HA amounts for the formation of the nanocomplexes through the film hydration technique. The amount of LAE was fixed to 4 mg and different amounts of HA were used for hydrating the film. The components were dissolved in different aqueous solvents (MilliQ water, HEPES buffer pH 7.2 and Acetate buffer pH 4.5) at all the tested ratios.

LAE (mg)	HA (mg)	HA hydration volume (mL)
4	0.1	1
4	0.25	1
4	0.5	1
4	0.75	1
4	1	1

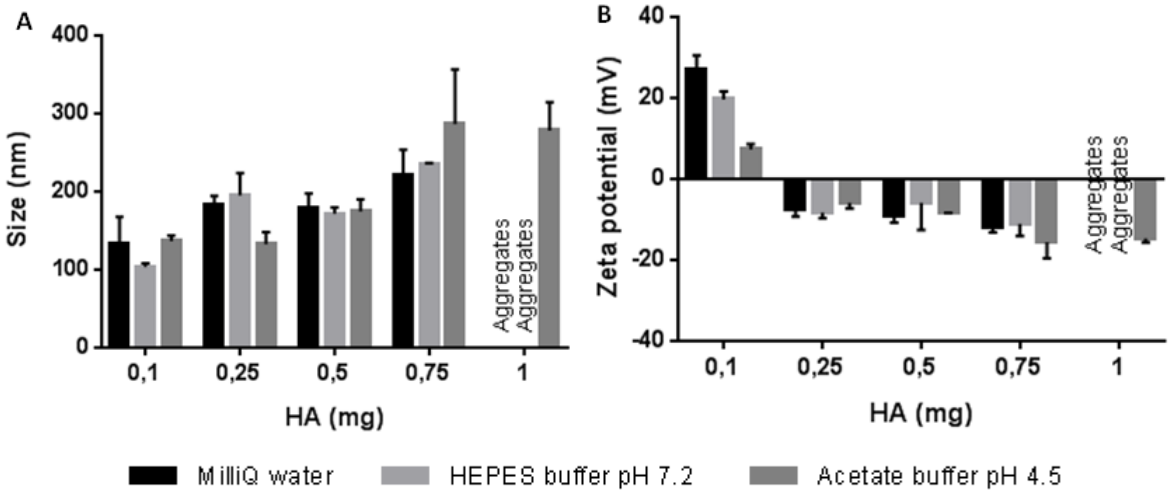

Figure 3.2. Size and zeta potential of the nanocomplexes produced by film hydration using a fix amount of LAE (4 mg) and a variable amounts of HA. The final volume of suspension was in all the cases 1 mL. A: size; B: zeta potential.

In parallel, another technique was adopted to prepare nanocomplexes with the same components. This technique involved the injection of the LAE solution into a HA solution under stirring. This is a faster, simpler and more scalable method as compared to film hydration technique. Three different LAE concentrations were tested in order to select the suitable amount of positively charged surfactant, while the amount of HA was fixed to 0.5 mg (500 µL – 1 mg/mL) (Table 3.2). MilliQ water was the dissolution medium tested in this case. With 1 mg of LAE (250 µL – 4 mg/mL), the particles were not formed, while using 0.5 mg (250 µL – 2 mg/mL) and 2 mg (250 µL – 8 mg/mL) the particles could be formed. Particles of 90 nm and a negative zeta potential could be obtained when 0.5 mg of LAE was used, however these nanoparticles were unstable upon dilution in water. In theory, these particles are expected to be micellar clusters in association with HA. Our hypothesis is that, after dilution these clusters lose their structure due to the weakness of the interacting forces among the different ingredients [32].

Once 2 mg was selected as an adequate amount of LAE (see Table 3.2), different amounts of HA were tested in order to produce nanocomplexes with the appropriate properties for our purposes. Three different amounts and four different formulation media were used in this case in order to understand if changes in osmolarity or pH of the formulation could influence the particle's properties. As shown in Figure 3.3, when MilliQ water was employed, nanocomplexes could only be formed for HA amounts of 1 mg (500 µL – 2 mg/ml) and 2 mg (500 µL – 4 mg/mL) and the resulting nanocomplexes had a negative charge. Unexpectedly, when HEPES pH 7.2 and acetate buffer pH 4.5 were used, nanocomplexes could be formed for 0.5 mg (500 µL – 1 mg/mL) and 2 mg (500 µL – 4 mg/mL) of HA but they aggregated when the amount of HA was 1 mg (500 µL – 2 mg/mL). The explanation could be found in the higher ionic strength of the buffers which allow the formation of the nanocomplexes with 0.5 mg of HA, but not with 1 mg. In fact, salts have an influence on the electrostatic interactions between LAE and HA (i.e. charges are shielded), hence on the behavior of the system at the different LAE/HA ratios. The same result was observed with particles formed in phosphate buffer. The ionic strength of this buffer is higher (0.022 M) that the one of the others (0.001 M) and particles were only formed when the amount of HA was 2 mg (see Figure 3.3).

Table 3.2. Selection of the LAE amount for producing the blank HA nanocomplexes by the injection technique.

LAE amount (mg)	LAE volume (µL)	LAE concentration (mg/mL)	HA amount (mg)	HA volume (µL)	HA concentration (mg/mL)	Size (nm)	ζ (mV)	PDI
0.5	250	2	0.5	500	1	91±2	-29±5	0.2
1	250	4	0.5	500	1		Aggregates	
2	250	8	0.5	500	1	143±9	-17±6	0.1

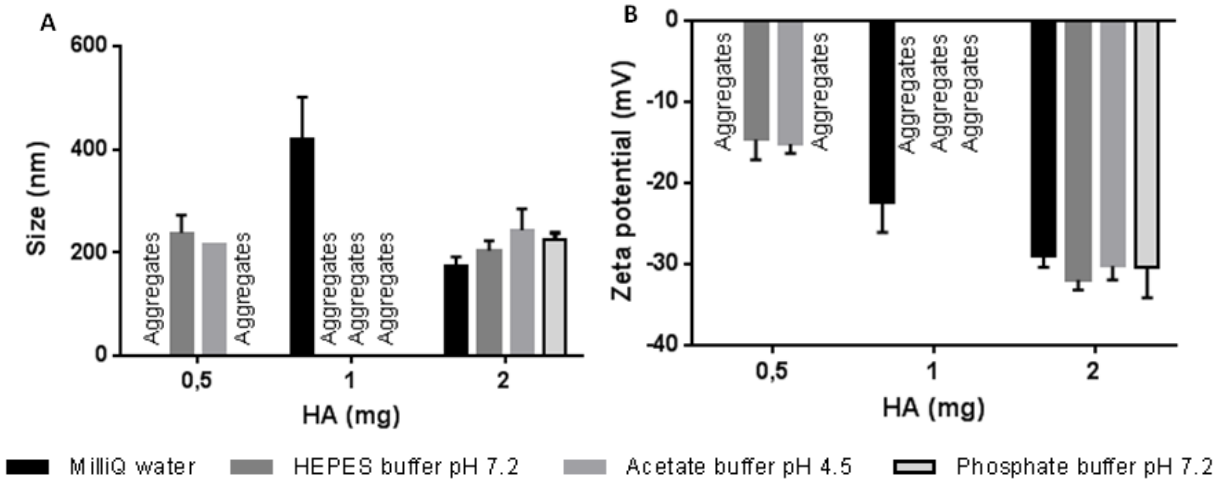

Figure 3.3. Selection of the HA amount for the production of the blank HA nanocomplexes by the injection technique. 250 µL of LAE at a concentration of 8 mg/mL were used for producing the nanocomplexes and the HA amounts tested were dissolved in 500 µL, corresponding to concentrations of 1, 2 and 4 mg/mL. A: size; B: zeta potential.

Due to the simplicity and scalability of the method and to the good properties of the particles, the injection method was selected to proceed with the studies. MilliQ water and phosphate buffer were selected as formulation media and 2 mg HA (500 µL – 4 mg/mL) as the amount of polymer per formulation, due to the good reproducibility of the nanoparticles and their small size.

3.1.2 Protein association (BSA and IgG) to the nanocomplexes

In a first step the complexation of BSA with LAE was investigated using either milliQ water and phosphate buffer. The results in Figure 3.4 indicate that in both formulation media an increase of the BSA amount resulted in a decrease of the positive zeta potential. This is probably due to the negative charge of BSA (isoelectric point: 4.7-4.8) at neutral pH of the medium in which the complex formation takes place. In contrast, the trend observed for the size was very different depending on the complex formation medium. In fact, an increase in the amount of BSA led to a size reduction when the interaction of the complexing species occurred in water and the opposite was observed when complexes were formed in phosphate buffer. This could be due to the interference of the phosphate buffer ions in the complex formation.

In a second step, HA was added in order to coat the nanocomplexes. The results in Figure 3.5 show the negative zeta potential of the resulting nanocomplexes, a fact that was mainly attributed to the HA coating. When using milliQ water for complex formation, the size of the nanocomplexes was similar for amounts of BSA lower than 4 mg. However, when the BSA amount reached this value a size increase and a slight reduction in the negative value of the zeta potential was observed. In contrast, when phosphate buffer is used, a size increase was observed when the amount of BSA varied from 0.1 mg to 0.5 mg and from 2 mg to 4 mg. Slightly less negative zeta potential values were found when increasing the BSA amounts. In general, the particles formulated in milliQ water are smaller than the ones formulated in phosphate buffer, meaning that the presence of ions could influence the physicochemical properties of the particles. Based on this information the amount of BSA selected for subsequent studies was 2 mg of BSA (theoretical loading of 33%). The properties of

the selected particles and a comparison with blank ones (i.e. non loaded with BSA) are shown in Table 3.3.

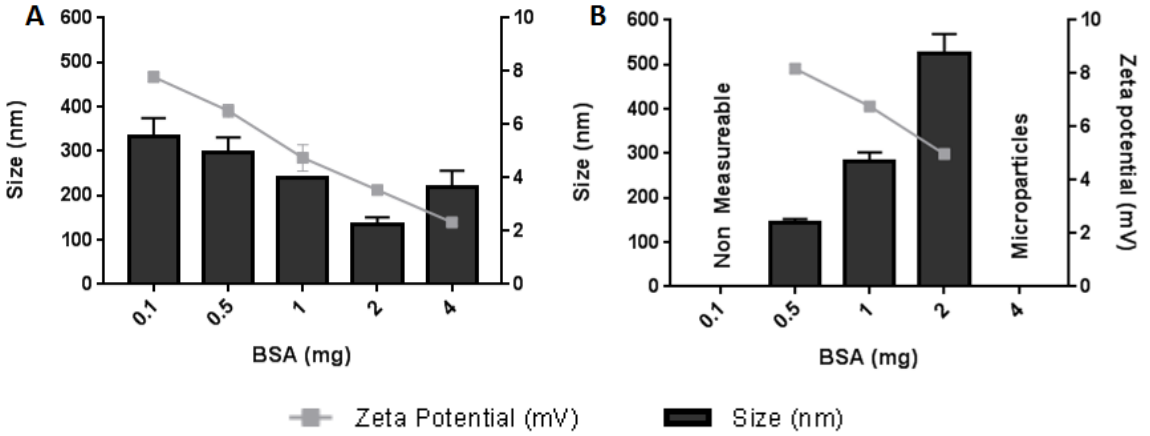

Figure 3.4. Size and zeta potential of the BSA/LAE complexes produced in milliQ water (A) or phosphate buffer pH 7.2 (B) using a fixed amount of LAE (2 mg in 250 µL) and variable amounts of BSA (from 0.1 to 4 mg dissolved in 200 µL). The final LAE/BSA complexes volume is 450 µL.

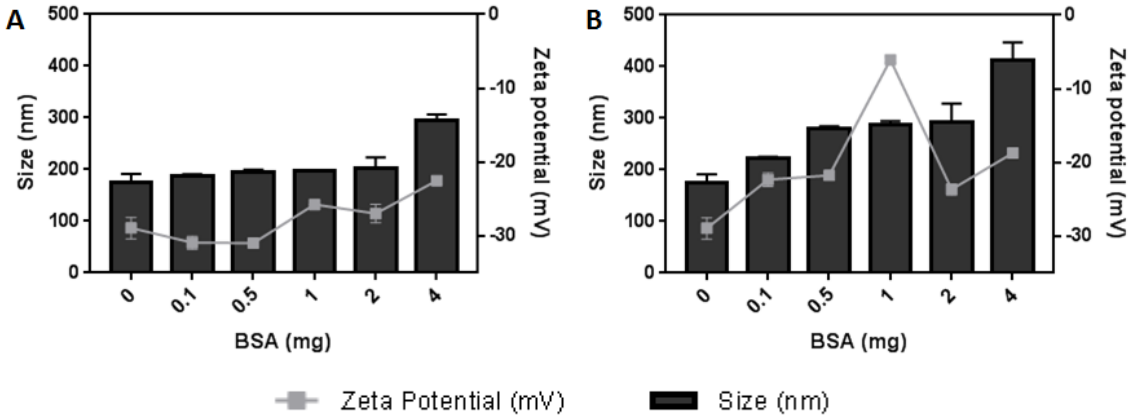

Figure 3.5. Size and zeta potential of the BSA-loaded HA nanocomplexes. The amounts of LAE and HA used to produce the particles are for both the components 2 mg. The final formulation volume is 950 µL (250 µL of LAE solution at a concentration of 8 mg/mL, 500 µL of HA solution at a concentration of 4 mg/mL and 200 µL of protein solution at different concentrations based on the used amount of protein). MilliQ water (A) or phosphate buffer pH 7.2 (B) have been used as formulation media.

Table 3.3. Selected BSA-loaded HA nanocomplexes prototypes and comparison with the blank systems

Prototype	Formulation media	LAE amount (mg)	LAE volume (µL)	LAE concentration (mg/mL)	HA amount (mg)	HA volume (µL)	HA concentration (mg/mL)	Size (nm)	PDI	ζ (mV)
Blank HA nanocomplexes	MilliQ water	2	250	8	2	500	4	174 ± 17	0.1	-29±1
	Phosphate buffer	2	250	8	2	500	4	226 ± 12	0.1	-31±4
BSA-loaded HA nanocomplexes*	MilliQ water	2	250	8	2	500	4	196 ± 11	0.2	-27±1
	Phosphate buffer	2	250	8	2	500	4	292 ± 36	0.1	-24±1

** The selected amount of BSA is 2 mg for both the prototypes produced in MilliQ water and Phosphate buffer (in final formulation volume of 950 µL)*

BSA: Bovine serum albumin; ζ: zeta potential; PDI: polydispersity index

In a third step, the association of an IgG to the selected nanosystems was investigated. For this purpose, variable amounts of IgG were introduced either in the aqueous LAE or HA solutions. MilliQ water was the only formulation medium used in this case, because when the components were

dissolved in phosphate buffer aggregates were obtained upon their mixture. The results in Figure 3.6 indicate that the association of the IgG was higher when added to the LAE solution. In fact, when the IgG is incorporated into the HA phase, the maximum amount of antibody which could be loaded without any aggregation was 50 µg, while, when the IgG was added to the LAE solution, up to 400 µg could be associated without any significant change in size. Due to the lower size, good reproducibility and macroscopic properties, particles loaded with 150 µg or 400 µg (IgG added to the LAE aqueous phase) were selected for subsequent experiments (theoretical loading of respectively, 3.6% and 9.1%).

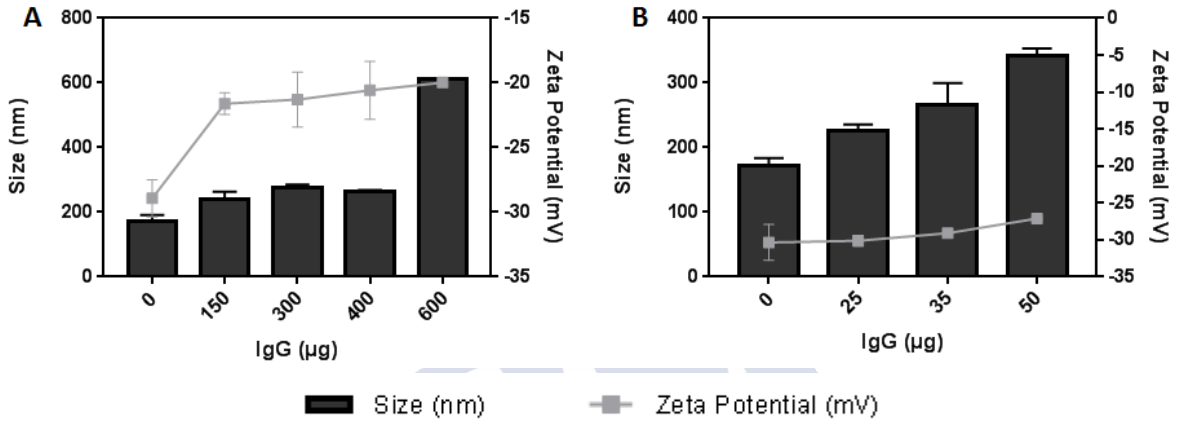

Figure 3.6. Size and zeta potential of the nanocomplexes associating the IgG and formulated in milliQ water. The amounts of LAE and HA used to produce the particles are for both the components 2 mg. The final formulation volume is 950 µL (250 µL of LAE solution at a concentration of 8 mg/mL, 500 µL of HA solution at a concentration of 4 mg/mL and 200 µL of IgG solution at different concentrations based on the used amount of protein). A: IgG dropped into the LAE aqueous phase. B: IgG dropped into the HA aqueous phase.

Based on the fact that BSA-containing nanocomplexes were more stable in simulated biological fluids than those containing only IgG (discussed in section 3.1.3), the association of different amounts of IgG in the presence of 2 mg of BSA was investigated. The results in Figure 3.7 indicate that the presence of BSA does not influence the antibody loading, although a slight neutralization was observed when the amount of IgG increased. The selected formulations were the ones loaded with 150 µg and 400 µg respectively, due to the good macroscopic properties of the system.

A resume of the selected prototypes is shown in Table 3.4.

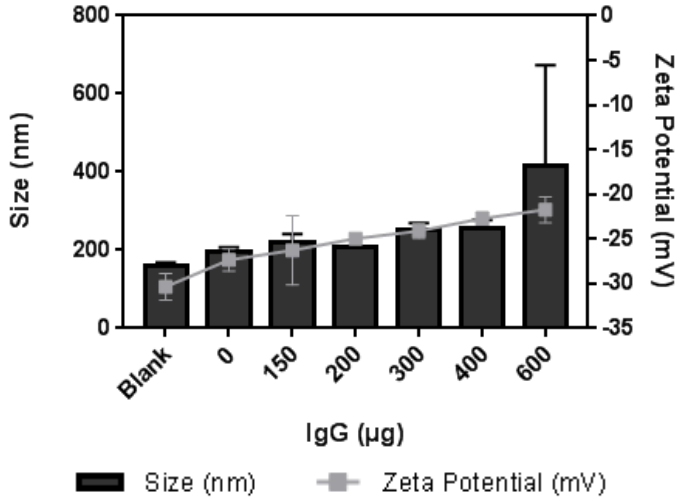

Figure 3.7. Size and zeta potential of the nanocomplexes formulated with both BSA and IgG (BSA/IgG-loaded HA nanocomplexes). The IgG (30 µL) was firstly mixed with the BSA solution (2 mg in 200 µL) and the proteins were then added to 2 mg of LAE (250 µL of LAE solution at a concentration of 8 mg/mL). The proteins/LAE mixture was then injected into 2 mg of HA solution (500 µL of HA solution at a concentration of 4 mg/mL), forming the BSA/IgG-loaded HA nanocomplexes. The final formulation volume is 980 µL.

Table 3.4. Resume of the selected nanocomplexes. For all the selected prototypes, the same amounts of LAE and HA were used for producing the nanocomplexes (2 mg of each component). MQ and BP are used to indicate the medium used for dissolving the components, i.e. MilliQ water (MQ) and phosphate buffer (BP).

Prototype	Formulation media	BSA loaded amount (mg)	IgG loaded amount (mg)	Theoretical LC (%)
BSA/BP-loaded HA nanocomplexes	Phosphate buffer	2	/	33.3
BSA/MQ-loaded HA nanocomplexes	MilliQ water	2	/	33.3
IgG/MQ loaded HA nanocomplexes (400 µg)	MilliQ water	/	0.4	9.1
IgG/MQ loaded HA nanocomplexes (150 µg)	MilliQ water	/	0.15	3.6
BSA/IgG/MQ-loaded HA nanocomplexes (400 µg)	MilliQ water	2	0.4	BSA: 31.3; IgG: 6.3
BSA/IgG/MQ loaded HA nanocomplexes (150 µg)	MilliQ water	2	0.15	BSA: 32.5; IgG: 2.4

BSA: Bovine serum albumin; BP: nanocomplexes formulated in phosphate buffer; MQ: nanocomplexes formulated in milliQ water; Theoretical LC (%): theoretical protein loading (100 x protein mass loaded /total formulation mass).

3.1.3 Stability of the selected protein-loaded HA nanocomplexes in simulated biological fluids (SBF)

The stability of the systems incubated in PBS and in cell culture medium (RPMI) at 37ºC was evaluated by monitoring their size and mean count rate (MCR) over the time. MCR is usually used as an indication of the stability of the nanosystems, since a decrease in MCR values is indicative for nanoparticles aggregation or disassembling.

a) BSA containing nanocomplexes prepared in phosphate buffer (BP) (BSA/BP-loaded HA nanocomplexes)

The stability of BSA-containing nanocomplexes composed by BSA, LAE and HA (2 mg of each one of the components) and formulated in BP was evaluated. The results in Figure 3.8.A indicate that these nanocomplexes are stable at least 24 hours in PBS. In fact, the particles maintained a size of around 300 nm and a MCR of 200 kcps during the incubation time. A good stability was also observed in

RPMI (Figure 3.9.A). In fact, even if a slight increase in size was observed after 24 hours, the size was kept around 300 nm. The MCR values remained close to 200 kcps.

b) BSA containing nanocomplexes prepared in milliQ water (MQ) (BSA/MQ-loaded HA nanocomplexes)

The stability of BSA-containing nanocomplexes composed by BSA, LAE and HA (2 mg of each one of the components) and formulated in MQ was evaluated. The results in Figure 3.8.B indicate that once diluted in PBS, an initial decrease of the MCR and a gradual increase of the size were observed reaching a maximum size of 350 nm at 24 hours. Similar results can be seen with RPMI, since the size doubled after 24 hours and a high variability between the triplicates is observed (Figure 3.9.B).

c) IgG containing nanocomplexes prepared in milliQ water (MQ) (IgG/MQ-loaded HA nanocomplexes)

For the two IgG amounts tested (150 and 400 µg, see Table 3.4) the nanocomplexes were completely unstable upon their dilution in PBS or RPMI (i.e. the nanocarriers were disassembled after their dilution in the media).

d) BSA/IgG containing HA nanocomplexes prepared in milliQ water (MQ) (BSA/IgG/MQ-loaded HA nanocomplexes)

The stability of BSA/IgG-containing HA nanocomplexes composed by LAE, HA and BSA (2 mg of each one of the components) and 150 or 400 µg of IgG (see Table 3.4) was evaluated. An amount of 2 mg of BSA had to be included in the formulation since those lacking of BSA were not stable, as indicated above. BSA/IgG/MQ-loaded HA nanocomplexes (150 µg) were found to be stable in PBS, since they keep a constant size around 225 nm for, at least, 24 hours (Figure 3.10.A). The same conclusion was obtained from BSA/IgG/MQ-loaded HA nanocomplexes (400 µg), although in this case a bigger decrease of MCR values was observed immediately upon dilution of the nanocomplexes and this was followed by a high variability in the MCR (Figure 3.10.B). A similar conclusion could be drawn from the data obtained after incubation of the nanocomplexes in RPMI. BSA/IgG/MQ-loaded HA nanocomplexes (150 µg) were more stable than those with a higher IgG loading (400 µg), where an increase in size values and a higher variability was measured (Figure 3.11).

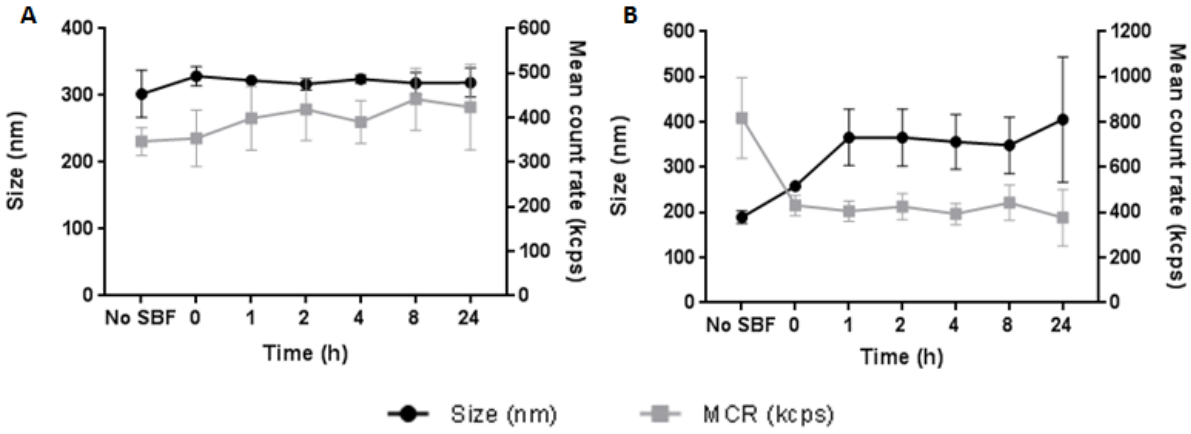

Figure 3.8. Stability of BSA-loaded HA nanocomplexes prepared in phosphate buffer (BP) (A) or milliQ water (MQ) (B) after their dilution in PBS at 37°C. *Size (black circles) and MCR (grey squares) are represented.*

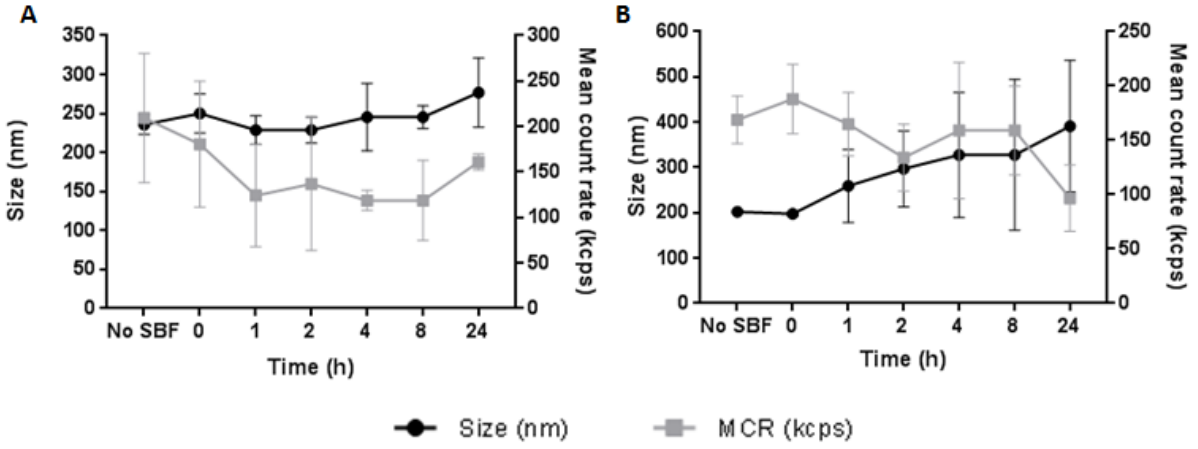

Figure 3.9. Stability of BSA-loaded HA nanocomplexes prepared in phosphate buffer (BP) (A) or milliQ water (MQ) (B) after their dilution in RPMI at 37°C. *Size (black circles) and MCR (grey squares) are represented.*

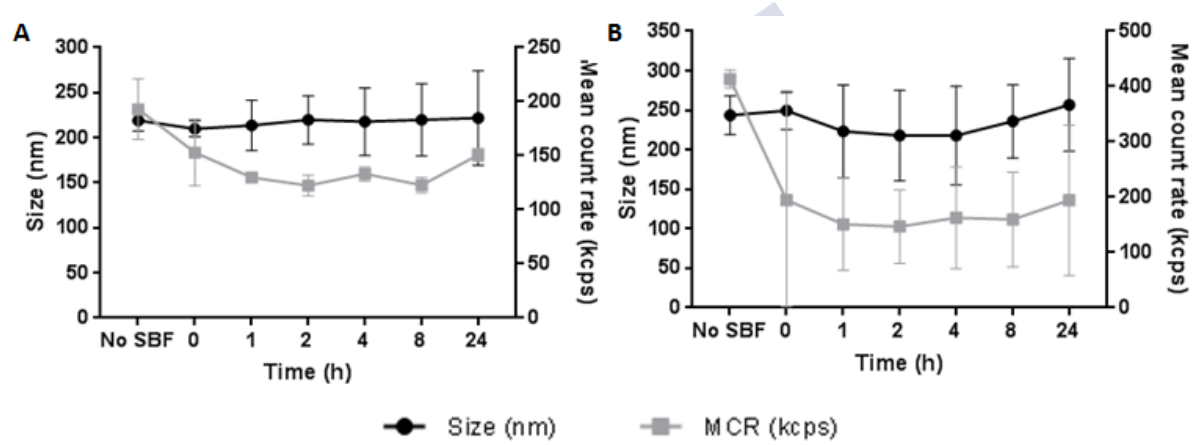

Figure 3.10. Stability of BSA/IgG/MQ-loaded HA nanocomplexes (150 µg of IgG) *(A) and* BSA/IgG/MQ-loaded HA nanocomplexes (400 µg of IgG) (B) after their dilution in PBS at 37ºC*. Size (black circles) and MCR (grey squares) are represented.*

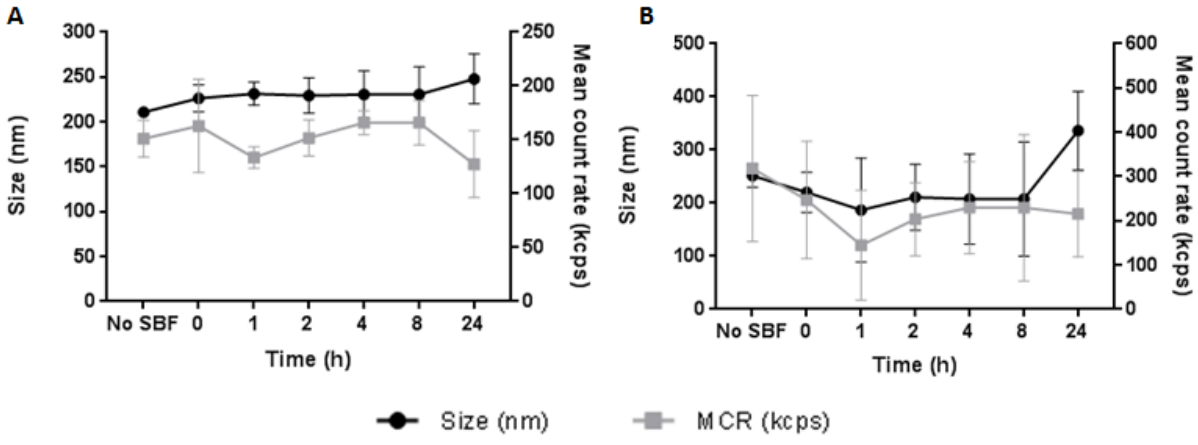

Figure 3.11. Stability of BSA/IgG/MQ-loaded HA nanocomplexes (150 µg IgG) (A) and BSA/IgG/MQ-loaded HA nanocomplexes (400 µg IgG) (B) after their dilution in RPMI at 37ºC. *Size (black circles) and MCR (grey squares) are represented.*

Overall, the stability results indicate that the formulation of the nanocomplexes in phosphate buffer (BSA/BP-loaded HA nanocomplexes) and in the presence of BSA (BSA/IgG/MQ-loaded HA

nanocomplexes) helps preserving the stability of the nanoparticles in simulated biological fluids (either PBS or RPMI). They also indicate that the association of a high amount of IgG leads to the destabilization of the nanosystem. Hence, the amount of IgG and BSA were fixed to 150 µg and 2 mg, respectively, being this amount of BSA necessary for stabilizing the formulation in PBS (Figure 3.12).

In Table 3.5 the nanocomplexes selected for proceeding with the studies and their properties are indicated. The particles were further characterized using TEM. The images presented in Figure 3.13 indicate that they have a spherical shape and a size comparable to the one measured by the Zetasizer Nano-ZS.

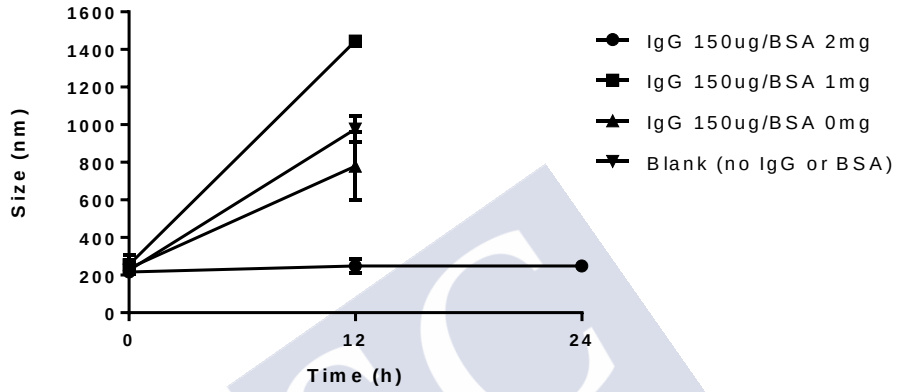

Figure 3.12. Stability of the BSA/IgG/MQ-loaded HA nanocomplexes produced with differet amounts of BSA, after their incubation in PBS. The minimum amount of BSA necessary for stabilizing the nanocomplexes is 2 mg.

Table 3.5. Properties of the BSA/BP-loaded and BSA/IgG/MQ-loaded HA nanocomplexes selected.

Prototype	BSA (mg)	IgG (mg)	LC (%) BSA	LC (%) IgG
BSA/BP-loaded HA nanocomplexes	2	/	33.3	/
BSA/IgG/MQ-loaded HA nanocomplexes	2	0.15	32.5	2.4

BSA: Bovine serum albumin; %LC: loading capacity (100 x protein mass loaded /total formulation mass); BP: nanocomplexes formulated in phosphate buffer; MQ: nanocomplexes formulated in milliQ water.

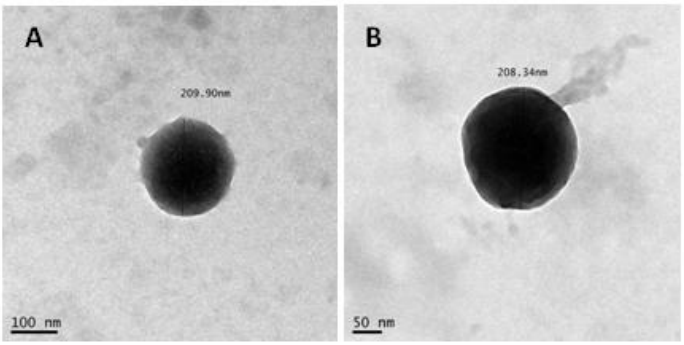

Figure 3.13 TEM images of the selected nanocarriers. A: BSA/BP-loaded HA nanocomplexes; B: BSA/IgG/MQ-loaded HA nanocomplexes.

3.1.4 Study of the proteins conformation with Circular Dichroism (CD)

One of the main drawbacks of using ionic surfactants is their ability in denaturating proteins. For example, the surfactant used for SDS PAGE gels is sodium dodecyl sulphate, SDS (a negatively charged surfactant), with a negative head and a C12 carbon chain. Also LAE has a charged head (positive) and C12 carbon chain (Figure 3.14).

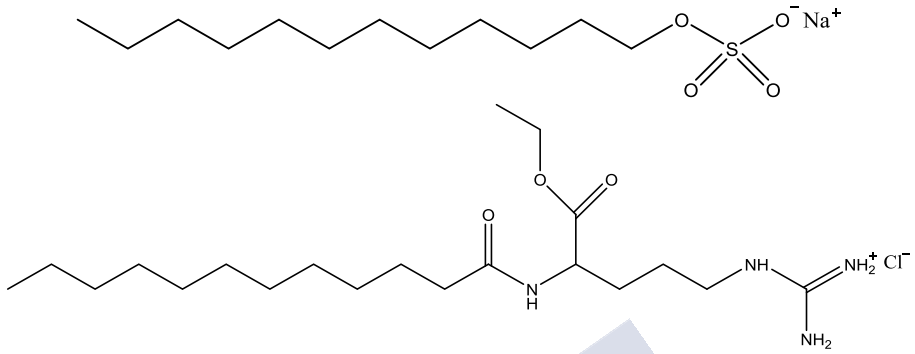

Figure 3.14. Chemical structure of SDS (up) and LAE (down).

In order to obtain information regarding the structural stability of the proteins when mixed with LAE, CD experiments were performed. LAE was mixed with the proteins in the ratio used to produce the nanocarriers. The CD signal was measured and a comparison with the signal of the protein and of the surfactant alone has been done (Figure 3.15). As shown in Figure 3.15.A, the spectra of BSA alone and the one of BSA+LAE are the same, meaning that no denaturation occurs when BSA is mixed with the surfactant. If some denaturation would have occurred, a random coil signal should have been obtained. In fact, both curves are typical of the alpha helix structure, meaning that the secondary structure of the protein was maintained. The LAE alone (control) shows a typical random coil curve, illustrative of a no secondary structure. On the other hand, when the structural stability of the IgG was studied in the presence of the surfactant (IgG+LAE, Figure 3.15.B), a typical random coil signal was detected, similar to the one of LAE alone. If the protein keeps its structure, a beta sheet signal must be measured, as the one of the IgG control alone. The fact that a random coil was detected in the presence of LAE does not necessarily indicate that IgG was denaturated. This could be simply related to the limited amount of IgG in the formulation (150 µg) as compared to the amount of LAE (2 mg), which may overlap the typical signal of IgG. Something similar happen when the mixture BSA/IgG+LAE (mixed in the same protein ratio used for producing BSA/IgG/MQ-loaded HA nanocomplexes) is considered, but in this case is the signal of BSA covering the one of the IgG (Figure 3.15.C).

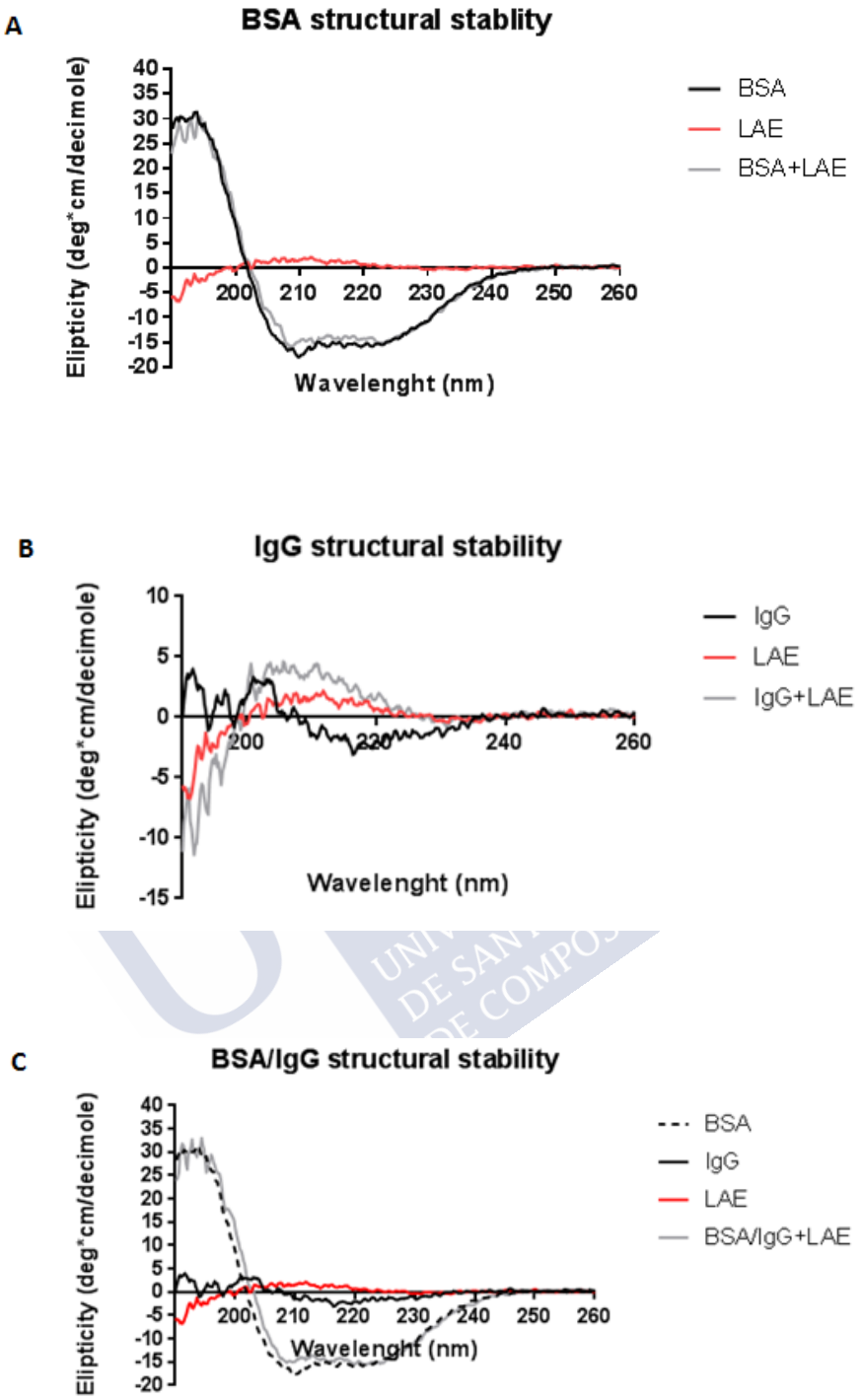

Figure 3.15. Circular Dichroism (CD) signals of BSA (A), IgG (B) or the mixture of BSA/IgG (C) alone or in presence of LAE. All the components have been used in the same ratios utilized to produce the nanocomplexes.

3.1.5 Protein association efficiency and release

The association efficiency, AE (%), of the different proteins to the nanocomplexes was evaluated using different methods as described in paragraph 2.6. The loading properties of the two model proteins are summarized below.

a) BSA/BP-loaded HA nanocomplexes

As indicated in the materials and methods (*paragraph 2.6, a)*), both, method 1 and method 2 were used to measure the association of the protein to the nanosystem. As shown in Table 3.6, both the methods rendered similar results, confirming the high AE (%) for the BSA.

b) BSA/IgG/MQ-loaded HA nanocomplexes (150 µg)

Both, the total association of proteins (BSA+IgG) and the specific association of the IgG to the system, were evaluated (Table 3.6). In both the cases, the AE (%) was found to be very high, confirming the suitability of the system in encapsulating these proteins.

Table 3.6. AE (%) of the proteins for the selected nanosystems. The amount of BSA and IgG were 2 mg and 0.15 mg, respectively. Method 1 is based on the precipitation of the proteins in the supernatant after centrifuging the formulation and the following proteins quantification by Bradford. Method 2 is based on the direct protein quantification in the supernatant without precipitating the proteins. The media used for producing the different prototypes is also indicated in the table: phosphate buffer (BP) and milliQ water (MQ).

Prototype	AE (%) BSA	AE (%) IgG	AE (%) BSA+ IgG (total)	Method
BSA/BP-loaded HA nanocomplexes	98.1±1.0	NA	NA	Method 1
BSA/BP-loaded HA nanocomplexes	95.4±1.1	NA	NA	Method 2
BSA/IgG/MQ-loaded HA nanocomplexes	NA	NA	98.3±2.1	Method 1
BSA/IgG/MQ-loaded HA nanocomplexes	NA	97.7±4.1	NA	Fluorescence

%AE: % association efficiency (*100 x associated peptide mass/total peptide mass)*; BSA: bovine serum albumin; *BP: nanocomplexes formulated in phosphate buffer; MQ: nanocomplexes formulated in milliQ water.*

Overall, the conclusion is that the system is suitable for the association of proteins, since proteins with different properties have been associated with high efficiency. The fact of having both ionic interactions (with the HA or the LAE head) and hydrophobic anchors (LAE hydrophobic tail) probably increase the affinity of the proteins for the nanosystems, enabling the high association.

The release profile of the proteins from the nanosystems was also evaluated. As shown in Figure 3.16, the release behavior was similar for the different formulations. The profile shows an initial burst release, which varied depending on the type of formulation, followed by the absence of release for up to 24 hours. The maximum burst (60%) was observed for the BSA loaded in the BSA/IgG/MQ-loaded HA nanocomplexes. On the contrary, a 40% burst was measured from the system produced in phosphate buffer (BP). The osmolarity of the media in which the release was evaluated (i.e. PBS) and of the formulation media used for producing the particles is, probably, playing a role regarding the release of the proteins. In fact, the BSA/IgG/MQ-loaded nanocomplexes are produced in milliQ water, and when diluted in PBS they move from a zero osmolarity to a high osmolarity condition, which might highly perturb the nanosystem causing the huge burst. On the other hand, the BSA/BP-loaded nanocomplexes are already produced in a salt containing media (i.e. phosphate buffer) and the perturbation of the nanosystem after its dilution in PBS is lower, resulting in a lower burst.

The release of IgG from the nanosystem containing both BSA and IgG, (i.e. BSA/IgG/MQ-loaded HA nanocomplexes) was measured using FITC-labeled IgG (Figure 3.16). The observed burst release is similar to the one of BSA from the BSA/BP-loaded nanocomplexes (40%).

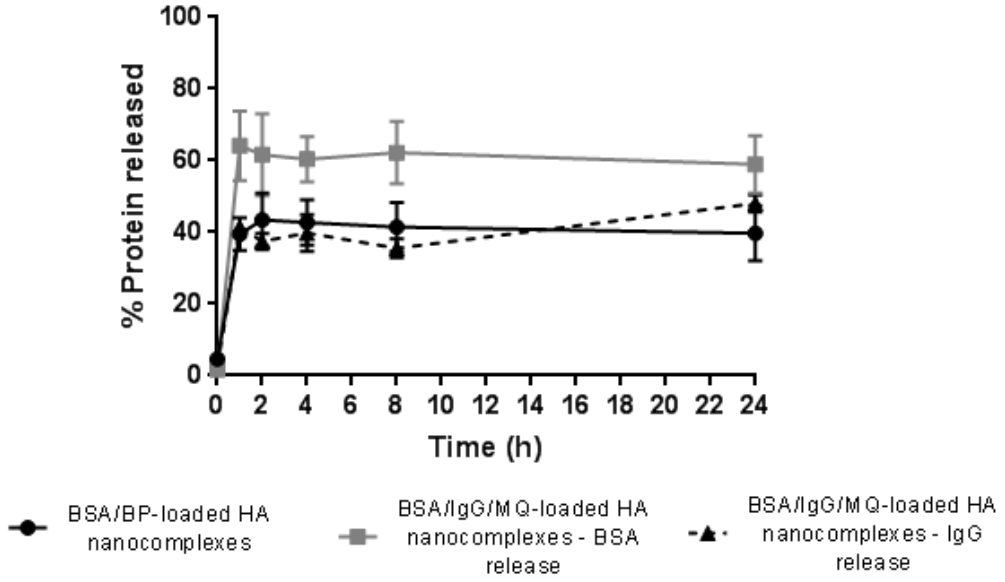

Figure 3.16. Release of the BSA (black circles), BSA/IgG (grey squares) or IgG (black triangles with dashed line) from the selected nanocomplexes.

3.1.6 Storage stability of the nanocomplexes

The storage stability of the particles in suspension (stored at 4°C) and upon freeze drying was studied. The BSA/BP-loaded and blank HA nanocomplexes prepared in phosphate buffer were found to be unstable upon incubation in suspension at 4°C. In fact, already after one day the nanocomplexes suffered a size increase accompanied by a reduction of the MCR (Figure 3.17). This is due to the presence of salts in the formulation media.

A less pronounced aggregation behavior was observed for BSA/IgG/MQ-loaded HA nanocomplexes (produced in milliQ water), where after 7 days a 25% particles size increase is measured (Figure 3.18.A). The size increase was, also in this case, accompanied by a reduction of the MCR values (Figure 3.18.B). Interestingly, the blank nanosystem (non loaded with any protein) and the one loaded with only BSA (BSA/MQ-loaded HA nanocomlexes), both prepared in milliQ water, were stable at least 7 days at 4°C. This means that the main source of instability is the IgG.

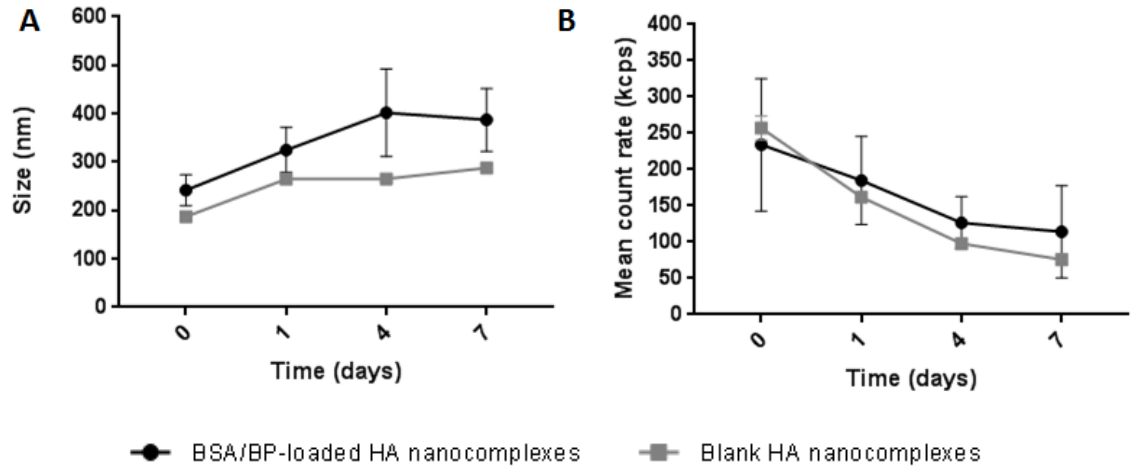

Figure 3.17. Stability of BSA/BP-loaded and blank HA nanocomplexes upon storage in suspension at 4°C. Blank HA nanocomplexes do not contain any protein. The nanocomplexes (both protein loaded or blank) were produced in phosphate buffer (BP). Size (A) and MCR (B) are considered as indicator for the stability.

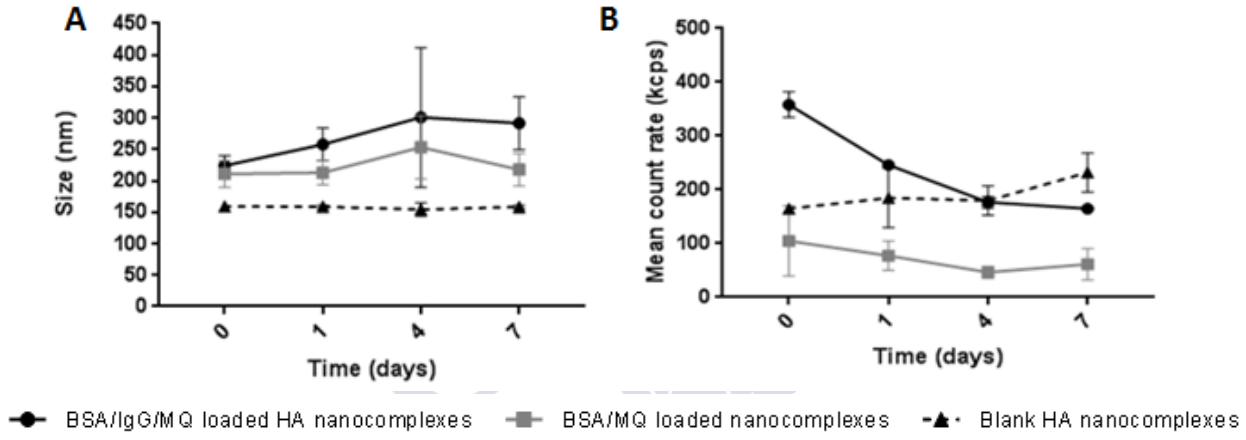

Figure 3.18. Stability of BSA/IgG/MQ-loaded, BSA/MQ-loaded and blank HA nanocomplexes upon storage in suspension at 4°C. Blank HA nanocomplexes do not contain any protein. The nanocomplexes (both blank or protein/s loaded) were produced in milliQ water (MQ). Size (A) and MCR (B) are considered as indicator for the stability.

Freeze drying studies were performed in order to improve the stability of the nanocomplexes. Trehalose was chosen as a cryoprotectant at different concentrations (1%, 5%, 10% and 15% w/v; final concentration after re-suspension). Both BSA/BP-loaded HA nanocomplexes and BSA/IgG/MQ-loaded HA nanocomplexes could not be properly resuspended when using 1 and 5% trehalose concentration (Table 3.7). In the case of BSA/BP-loaded HA nanocomplexes, resuspension was achieved using 10 and 15% trehalose, although the best properties were obtained when using 15% trehalose. In the case of BSA/IgG/MQ-loaded HA nanocomplexes, both 10% and 15% trehalose concentrations were found to be suitable for preserving the stability of the nanocomplexes upon storage. For this reason, the 10% trehalose concentration was chosen as optimal storage condition. Data are shown in Table 3.7, and the selected conditions are highlighted (bold).

*Table 3.7. Freeze drying studies made on the BSA/BP-loaded HA nanocomplexes (BP) or BSA/IgG/MQ-loaded HA nanocomplexes. The selected freeze drying conditions are highlighted (bold). Statistical analysis using t-test have been done to understand if the size increase measured after resuspension was significant (**p<0.01).*

	Cryoprotector	**Before freeze-drying**		**After freeze-drying**		
Prototype	**Trehalose (%)**	**Size (nm)**	**PDI**	**Size (nm)**	**PDI**	**Size increase (%)**
BSA/BP-loaded HA nanocomplexes	1	243±39	0.2	Aggregates		NA
	5	249±36	0.2	Aggregates		NA
	10	243±39	0.2	303±29	0.2	25**
	15	**249±36**	**0.2**	**281±19**	**0.2**	13
BSA/IgG/MQ-loaded HA nanocomplexes	1	222±28	0.2	Aggregates		NA
	5	222±31	0.2	Aggregates		NA
	10	**222±28**	**0.2**	**221±24**	**0.2**	0
	15	222±31	0.2	220±16	0.2	0

MCR: mean count rate; PDI: polydispersity index. Size increase (%) = 100 x size after freeze-drying-size before freeze drying/size before freeze-drying

3.2 Layer-by-layer PArg/HA enveloped HA nanocomplexes (ENCPs): development and characterization

3.2.1 Characterization of the ENCPs

The studies presented above showed the stability profiles of the nanocomplexes in simple media, i.e. PBS or RPMI, however, the stability of nanocomplexes in serum is a key parameter in order to assess the value of the nanocomplexes for intravenous administration. For this reason, the stability of BSA/IgG/MQ-loaded nanocomplexes was tested in RPMI supplemented with fetal bovine serum (FBS) (10% v/v). Unfortunately, the nanocomplexes were unstable in this medium, a result that encouraged us to design new strategies for improving their stability. With this objective in mind, we developed a layer-by-layer process that enabled the envelopment of the protein-LAE complex with a protective coating (see Figure 3.1.B). The original BSA/IgG-LAE nanocomplexes were already enveloped by HA (layer I). A positively charged polymer, poly-L-arginine (PArg), was, then, added to the system, which become positively charged (layer II) (see Figure 3.1.B). Different amounts of poly-L-Arginine (i.e. different molar ratios between the I HA and the II PArg layers) were investigated, in order to find the best coating conditions (Table 3.8). The only condition in which particles were obtained was an HA:PArg molar ratio of 1:1. Finally, the nanosystem was coated by an additional layer of HA, a fact that reverted the charge to negative values (layer III). Different amounts of HA were tested (different molar ratios between the II PArg and the III HA layers). The results shown in Table 3.8 indicate that the 1:3 molar ratio PArg:HA was the one producing more homogeneous particles. The obtained formulation (layer-by-layer PArg/HA ENCPs) was monodispersed and its final size was slightly smaller than the original one (Figure 3.19), a fact that could be attributed to the electrostatic compression of the structure.

Table 3.8. Molar ratios studies made for attaching the PArg II layer and HA III layer to the BSA/IgG/MQ-loaded HA nanocomplexes (already coated by an HA I layer). These starting nanocomplexes showed a size of 240 nm and a zeta potential of -27 mV (as shown in Figure 3.19.B - HA I layer). These nanocomplexes were then coated with further layers of PArg and HA, as indicated in the table.

II PArg layer			**III HA layer**	
HA:PArg Molar ratio	**Size (nm)**	**ζ (mV)**	**PArg:HA Molar ratio**	**Size (nm)** **ζ (mV)**
1/5	Aggregates		1/5	214±31 -25.1
1/3	Aggregates		1/3	191 ±16 -24.5
1/1	225±25	+20.1	1/1	249±84 -22.0
3/1	Aggregates		3/1	No particles
5/1	Aggregates		5/1	No particles

ζ=zeta potential

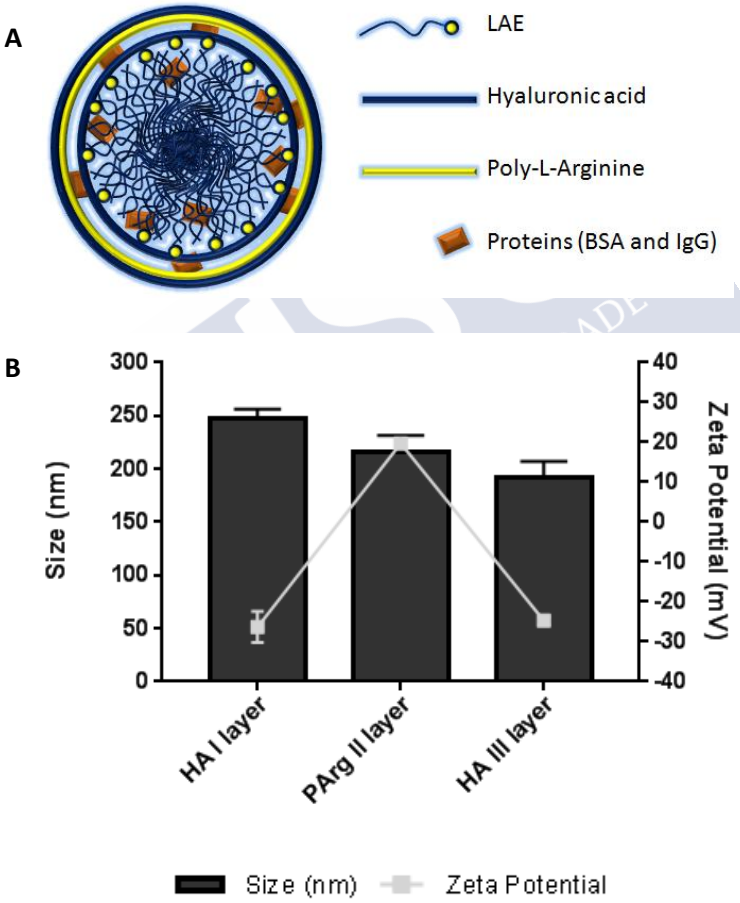

Figure 3.19. A) Schematic representation of the layer-by-layer PArg/HA ENCPs. B) Particle size and zeta potential of BSA/IgG/MQ-loaded HA nanocomplexes enveloped by HA/PArg/HA layers for forming the ENCPs.

3.2.2 Stability of the ENCPs in simulated biological fluids

The stability of the ENCPs in the RPMI supplemented with FBS (10% v/v) was evaluated. As shown in Figure 3.20, the ENCPs were significantly more stable than the original nanocomplexes (that were totally destroyed in this media). A first decrease of the MCR value was due to the dilution of the system in the medium. The small size increase observed after dilution in the medium could be due to

the swelling of the nanostructures upon contact with media or to the attachment of plasma protein to the nanostructures.

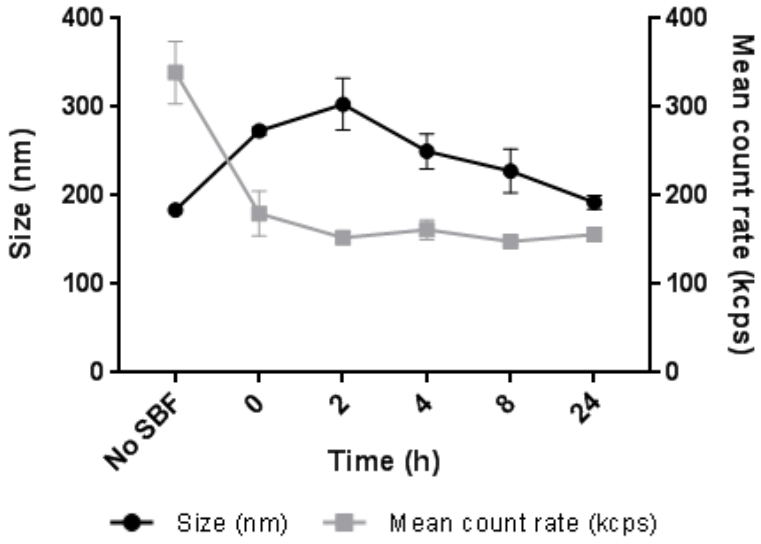

Figure 3.20. Size and MCR of the ENCPs: stability in RPMI supplemented with FBS (10% v/v).

3.2.3 Proteins association efficiency

The association efficiency, AE (%), of the ENCPs was evaluated using fluorescence (FITC-labeled IgG) resulting in 85 % AE. With regard to the final IgG loading, the values moved from 2.4% for the original formulations to 1.7% in the ENCPs. In Table 3.9 a comparison of the properties of the original and optimized formulation are shown.

Table 3.9. Properties of BSA/IgG-loaded formulation before (nanocomplexes) and after the enveloping process (ENCPs).

Prototype	Size (nm)	ζ (mV)	PDI	Stable in PBS	Stable in FBS-RPMI
BSA/IgG/MQ-loaded HA nanocomplexes	220±22	-26±3.9	0.2	Yes	No
Layer-by-layer PArg/HA ENCPs	191±16	-25±1.0	0.2	No	Yes

ζ: zeta potential; BSA: bovine serum albumin; PDI: polydispersity index; PBS: phosphate buffer saline; FBS: fetal bovine serum; RPMI: Roswell park memorial institute medium

4. Discussion

The possibility of delivering highly specific and selective drugs, i.e. therapeutic proteins, to cancer cells, through the use of nanotechnology, is opening new frontiers in the treatment of cancer [33]. Moreover, the decoration of nanocarriers with polymers that are able to target intracellular oncoproteins open novel therapeutic windows (e.g. intracellular drug targeting) [5,34]. With this objective in mind, here we present a new type of nanostructure based on HA. The nanostructure is formed upon the interaction of a positively charged surfactant (LAE) with the negatively charged HA. It is reported that the strength of the binding depends on several properties like the charge density of the polyelectrolyte, the presence of salts, the pH and the concentration of both surfactant and polyelectrolyte [35]. Based on this premise, we have explored different formulation strategies (film

hydration and injection techniques). Using the injection technique, which involved the simple injection of the LAE solution into the HA solution, particles with a negative zeta potential were obtained (Figure 3.3). After selecting the proper amounts of HA and LAE, two different model proteins, BSA and IgG, were incorporated into the nanosystem with high efficiencies (Table 3.6). In the case of BSA, a loading capacity as high as 33% could be obtained (Table 3.5). According to the procedure, first a protein/LAE positively charged complex is formed that is, then, coated with the HA. The ionic head group of the surfactant interacts with the proteins through electrostatic interactions, while the hydrophobic tails could bind the non-polar motifs of the proteins, forming protein/surfactant complexes [36]. With milliQ water a decrease in the size of the BSA/LAE complex is observed when the amount of BSA increased. This corresponded to a decrease of zeta potential values, respectively, probably due to the association of BSA to the surfactant, since at neutral pHs BSA is negatively charged (pI=4.7-4.8) (Figure 3.4) [37]. A similar trend in zeta potential is observed when particles are formulated in phosphate buffer, however, in terms of size an increase of the BSA amount led to the formation of larger particles. The ions of the buffer could have played a role in this case. It is well known that proteins properties depend on the presence of salt ions in the surrounding aqueous solution. The presence of the phosphate ions could favor the protein salting out process, strengthening the hydrophobic interactions of the BSA molecules between each other and with the surfactant. At a higher protein concentration this could lead to the formation of bigger protein molecules/surfactant aggregates. Moreover, the phosphate ions reduce the critical micellar concentration of the LAE itself, buffering the positive charges on the head of the surfactant, further promoting hydrophobic interactions with the protein [38,39]. When the IgG was then introduced into the system it was observed that the antibody association was highly dependent on the aqueous phase in which the antibody was dissolved (i.e. LAE or HA phase). Higher loadings were reached when the IgG was introduced into the LAE aqueous phase, suggesting that both ionic and hydrophobic interactions are occurring between the surfactant and the antibody (Figure 3.6). Water was the only formulation media used in this case, because when phosphate buffer was employed aggregates were obtained. This is probably due to the reduction of the ionic forces as a consequence of the ion screening [38–40].

Knowing that ionic surfactants can destabilize proteins [36,41], the structural stability of the proteins in the presence of the surfactant was measured by circular dichroism (CD). The results showed that BSA was able to maintain its structure once in contact with LAE.

With regard to the stability of the developed particles in SBF, different pattern was observed for BSA-loaded and IgG-loaded HA nanocomplexes. In the case of BSA-loaded HA nanocomplexes, their stability was favorable when formulated in phosphate buffer (BSA/BP-loaded HA nanocomplexes). As commented above, the presence of phosphate ions screen the repulsion between the LAE heads, decreasing its critical micellar concentration, helping in stabilizing the nanosystem [42,43]. However, in the case of IgG, the presence of BSA was necessary in order to preserve the stability of the nanocomplexes in PBS (BSA/IgG/MQ-loaded HA nanocomplexes, Figure 3.12). We speculated that the BSA could form a protective shell around the nanocomplexes (similar to the well known protein corona) and work as an anchor for both the IgG and the LAE. In fact, due to its amphiphilic

properties, BSA could have interacted with the hydrophobic tails of the surfactant, forming a more compact core which might have stabilized the formulation in SBF [44].

Unfortunately, the stability of the BSA/IgG/MQ-loaded HA nanocomplexes in a more complex media, i.e. RPMI supplemented FBS (10% v/v), was compromised. Then, an optimization process that involved the envelopment of the nanocomplexes with multiple polymer layers (HA/poly-L-Arginine/HA) was adopted. Poly-L-Arginine was selected based on its low cytotoxicity and penetration enhancing properties [45]. The attachments of multi layers was proved by the inversion of zeta potential after attaching each polymer layer (Figure 3.19) [45,46]. A size compression of the nanosystem was detected, being the size of the ENCPs smaller than the one of the original nanocomplexes. This compression could be attributed to the formation of a more compact structure after the addition of the layers [46,47]. The presence of the double layer helped to stabilize the particles in the complex media for at least 24 hours.

The release of the proteins from the nanocomplexes (once diluted in PBS) was also evaluated (Figure 3.16). A similar release profile was observed for the tested formulations, with an initial burst, typical of polymeric based nanosystems [48]. For the particles formulated in milliQ water and associating both BSA and IgG (BSA/IgG/MQ-loaded HA nanocomplexes) the burst is higher compare to the ones formulated in phosphate buffer and encapsulating just BSA (BSA/BP-loaded HA nanocomplexes). This could be due to the higher perturbation of the milliQ water formed system once diluted in PBS, since it goes from a condition with the total absence of salts to one with a high osmolarity. The salts could have modified the physico-chemical properties of the nanosystem, partially destroying the interactions of the polymer with both the surfactant and the proteins [49]. This is also a confirmation of the electrostatic interactions of the proteins with the HA/LAE nanosystem [49,50].

In agreement with the limited stability of proteins in liquid formulations [51,52], the stability of the complexes during storage at 4°C in suspension was deficient. Storing protein formulations as a dry powder is a reliable alternative to preserve the stability of the protein-containing nanocomplexes [51,53]. For this reason, the liquid formulations were freeze-dried in the presence of trehalose. The high glass transition temperature and the high flexibility of trehalose molecules (due to the lack of intramolecular hydrogen bonds) favor the formation of hydrogen bonds with the protein nanocomplexes, thus leading to a good long term storage stability [53,54]. Table 3.7 shows the results for the freeze-drying studies on our developed formulations. For the particles loaded with both the IgG and BSA (BSA/IgG/MQ-loaded HA nanocomplexes), 10% trehalose was found to be the optimal concentration that led to the preservation of the original physico-chemical properties, while for the ones loaded with only BSA (BSA/BP-loaded HA nanocomplexes) a 15% trehalose concentration was selected as optimal storage condition.

5. Conclusion

Here a new protein nanoformulation approach is presented. The approach involves the interaction of proteins with a cationic surfactant, LAE, and HA, thus forming HA-coated nanocomplexes. Two different proteins, BSA and IgG were associated to the nanosystem with very high efficiency. The

protein-loaded nanoformulations could be freeze-dried in the presence of trehalose. The nanocomplexes were enveloped by a double layer of poly-L-Arginine and HA, which made them stable in the presence of biologically relevant media containing serum proteins. In conclusion, this work may provide readers with relevant insights when using nanotechnology for protein formulation.

Acknowledgments

This work was supported by the European Union's Horizon 2020 - Research and Innovation Framework Programme under the Marie Sklodowska - Curie Grant agreement No. 642028 (NABBA) and by the Grant Nº SAF2017-86634-R (Nano-inmunoterapias integradas dirigidas a dianas intracelulares relevantes en cancer) from the Ministry of Economy of Spain.

Bibliography

[1] World Health Organization-Cancer. https://www.who.int/news-room/fact-sheets/detail/cancer.

[2] American Cancer Society. https://www.cancer.org/.

[3] E. Pérez-Herrero, A. Fernández-Medarde, Advanced targeted therapies in cancer: Drug nanocarriers, the future of chemotherapy, Eur. J. Pharm. Biopharm. 93 (2015) 52–79. doi:10.1016/j.ejpb.2015.03.018.

[4] V.P. Torchilin, A.N. Lukyanov, Peptide and protein drug delivery to and into tumors: challenges and solutions, Drug Discov. Today. 8 (2003) 259–266. doi:10.1016/S1359-6446(03)02623-0.

[5] A. Gdowski, A. Ranjan, A. Mukerjee, J. Vishwanatha, Development of Biodegradable Nanocarriers Loaded with a Monoclonal Antibody, Int. J. Mol. Sci. 16 (2015) 3990–3995. doi:10.3390/ijms16023990.

[6] T.A.S. Aguirre, D. Teijeiro-Osorio, M. Rosa, I.S. Coulter, M.J. Alonso, D.J. Brayden, Current status of selected oral peptide technologies in advanced preclinical development and in clinical trials, Adv. Drug Deliv. Rev. 106 (2016) 223–241. doi:10.1016/j.addr.2016.02.004.

[7] M. Hofmann, M. Guschel, A. Bernd, J. Bereiter-Hahn, R. Kaufmann, C. Tandi, H. Wiig, S. Kippenberger, Lowering of Tumor Interstitial Fluid Pressure Reduces Tumor Cell Proliferation in a Xenograft Tumor Model 1, Neoplasia. 8 (2006) 89–95. doi:10.1593/neo.05469.

[8] P. Chames, M. Van Regenmortel, E. Weiss, D. Baty, Therapeutic antibodies : successes, limitations and hopes for the future, Br. J. Pharmacol. 157 (2009) 220–233. doi:10.1111/j.1476-5381.2009.00190.x.

[9] D.S. Pisal, M.P. Kosloski, S. V. Balu-Iyer, Delivery of therapeutic proteins, J. Pharm. Sci. 99 (2010) 2557–2575. doi:10.1002/jps.22054.

[10] C.F. Van Der Walle, O. Olejnik, An overview of the field of peptide and protein delivery, in: C.F. Van Der Walle (Ed.), Pept. Protein Deliv., First, Academic Press, 2011: pp. 1–22. doi:10.1016/b978-0-12-384935-9.10001-x.

[11] B.J. Bruno, G.D. Miller, C.S. Lim, Basics and recent advances in peptide and protein drug delivery, Ther. Deliv. 4 (2013) 1443–1467. doi:10.4155/tde.13.104.

[12] H. Zhao, Z. Lin, L. Yildirimer, A. Dhinakar, X. Zhaoa, J. Wub, Polymer-based nanoparticles for protein delivery: design, strategy and applications, J. Mater. Chem. B. 4 (2016) 4060–4071. doi:10.1039/C6TB00308G.

[13] G. Gregoriadis, P. Leathwood, B.E. Ryman, Enzyme entrapment in liposomes, FEBS Lett. 14 (1971) 95–99. doi:10.1016/0014-5793(71)80109-6.

[14] G. Gregoriadis, B.E. Ryman, Fate of protein containing liposomes injected into rats - An approach to the treatment of storage diseases, Eur. J. Biochem. 24 (1972) 485–491. doi:10.1111/j.1432-1033.1972.tb19710.x.

[15] G. Birrenbach, P.P. Speiser, Polymerized micelles and their use as adjuvants in immunology, J. Pharm. Sci. 65 (1976) 1763–1766. doi:10.1002/jps.2600651217.

[16] C. Damge, C. Michel, M. Aprahamian, P. Couvreur, New approach for oral administration of insulin with polyalkylcyanoacrylate nanocapsules as drug carrier, Diabetes. 37 (1988) 246–251. doi:10.2337/diab.37.2.246.

[17] S. Morel, M. Rosa Gasco, R. Cavalli, Incorporation in lipospheres of [D-Trp-6] LHRH, Int. J. Pharm. 105 (1994) R1–R3. doi:10.1016/0378-5173(94)90466-9.

[18] S. Morel, E. Ugazio, R. Cavalli, M.R. Gasco, Thymopentin in solid lipid nanoparticles, Int. J. Pharm. 132 (1996) 259–261. doi:https://doi.org/10.1016/0378-5173(95)04388-8.

[19] M.R. Gasco, Method for producing solid lipid microspheres having a narrow size distribution, US5250236, 1993.

[20] A. Sánchez, J. Vila-Jato, M.J. Alonso, Development of biodegradable microspheres and nanospheres for the controlled release of cyclosporin A, Int. J. Pharm. 99 (1993) 263–273. doi:10.1016/0378-5173(93)90369-Q.

[21] P. Quellec, R. Gref, L. Perrin, E. Dellacherie, F. Sommer, J.M. Verbavatz, M.J. Alonso, Protein encapsulation within polyethylene glycol-coated nanospheres. I. Physicochemical characterization, J. Biomed. Mater. Res. 42 (1998) 45–54. doi:10.1002/(SICI)1097-4636(199810)42:1<45::AID-JBM7>3.0.CO;2-O.

[22] P. Calvo, C. Remuñán-López, J.L. Vila-Jato, M.J. Alonso, Novel hydrophilic chitosan-polyethylene oxide nanoparticles as protein carriers, J. Appl. Polym. Sci. 63 (1997) 125–132. doi:10.1002/(SICI)1097-4628(19970103)63:1<125::AID-APP13>3.0.CO;2-4.

[23] J. Kreuter, Nanoparticles — A historical perspective, Int. J. Pharm. 331 (2007) 1–10. doi:10.1016/j.ijpharm.2006.10.021.

[24] H. Wartlick, B. Spankuch-Schmitt, K. Strebhardt, J. Kreuter, K. Langer, Tumour cell delivery of antisense oligonucleotides by human serum albumin nanoparticles, J. Control. Release. 96 (2004) 483–495. doi:10.1016/j.jconrel.2004.01.029.

[25] S. Balthasar, K. Michaelis, N. Dinauer, H. Von Briesen, K. Langer, Preparation and characterisation of antibody modified gelatin nanoparticles as drug carrier system for uptake in lymphocytes, Biomaterials. 26 (2005) 2723–2732. doi:10.1016/j.biomaterials.2004.07.047.

[26] A. Cadete, M.J. Alonso, Targeting cancer with hyaluronic acid- based nanocarriers : recent advances and translational perspectives, Futur. Med. 11 (2016) 2341–2357. doi:10.2217/nnm-2016-0117.

[27] Y. Parajo, I. D'Angelo, A. Welle, M. Garcia-Fuentes, M.J. Alonso, Hyaluronic acid/Chitosan nanoparticles as delivery vehicles for VEGF and PDGF-BB, Drug Deliv. 17 (2010) 596–604. doi:10.3109/10717544.2010.509357.

[28] F.A. Oyarzun-Ampuero, F.M. Goycoolea, D. Torres, M.J. Alonso, A new drug nanocarrier consisting of polyarginine and hyaluronic acid, Eur. J. Pharm. Biopharm. 79 (2011) 54–57. doi:10.1016/j.ejpb.2011.04.008.
[29] D.A. Ossipov, Nanostructured hyaluronic acid-based materials for active delivery to cancer, Expert Opin. Drug Deliv. 7 (2010) 681–703. doi:10.1517/17425241003730399.
[30] G. Tzircotis, R.F. Thorne, C.M. Isacke, Chemotaxis towards hyaluronan is dependent on CD44 expression and modulated by cell type variation in CD44-hyaluronan binding, J. Cell Sci. 118 (2005) 5119–5128. doi:10.1242/jcs.02629.
[31] S. Inàcio, K.A. Mesquita, M. Baptista, In Vitro Surfactant Structure-Toxicity Relationships : Implications for Surfactant Use in Sexually Transmitted Infection Prophylaxis and Contraception, PLoS One. 6 (2011) 1–15. doi:10.1371/journal.pone.0019850.
[32] P.U. Singare, J.D. Mhatre, Cationic Surfactants from Arginine : Synthesis and Physicochemical Properties, Am. J. Chem. 2 (2012) 186–190. doi:10.5923/j.chemistry.20120204.02.
[33] A. Patel, K. Cholkar, A.K. Mitra, Recent developments in protein and peptide parenteral delivery approaches, Ther. Deliv. 5 (2014) 337–365. doi:10.4155/tde.14.5.
[34] G.Y. Berguig, A.J. Convertine, S. Frayo, H.B. Kern, E. Procko, D. Roy, S. Srinivasan, D.H. Margineantu, G. Booth, M.C. Palanca-wessels, D. Baker, O.W. Press, P.S. Stayton, G.Y. Berguig, A.J. Convertine, S. Frayo, H.B. Kern, An intracellular delivery system for antibody-peptide drug conjugates, Mol. Ther. 23 (2015) 907–917. doi:10.1038/mt.2015.22.
[35] J. Koetz, S. Kosmella, Polyelectrolyte and Nanoparticles, 2007.
[36] D. Kelley, D.J. McClements, Interactions of bovine serum albumin with ionic surfactants in aqueous solutions, Kelley, D. McClements, D.J. 17 (2003) 73–85. doi:10.1016/S0268-005X(02)00040-1.
[37] T.J. Su, J.R. Lu, R.K. Thomas, Effect of pH on the Adsorption of Bovine Serum Albumin at the Silica / Water Interface Studied by Neutron Reflection, J. Phys. Chem. B. 103 (1999) 3727–3736. doi:10.1021/jp983580j.
[38] M. Lund, R. Vacha, P. Jungwirth, Specific Ion Binding to Macromolecules : Effects of Hydrophobicity and Ion Pairing, Langmuir. 24 (2008) 3387–3391. doi:10.1021/la7034104.
[39] P. Mukerjee, K. Mysels, P. Kapadan, Counterion Specificity in the Formation of Ionic Micelles — Size , Hyadration, and Hydrophobic Bonding Effect, 71 (1966) 4166–4175. doi:10.1021/j100872a702.
[40] H. Dautzenberg, Polyelectrolyte Complex Formation in Highly Aggregating Systems. 1. Effect of Salt: Polyelectrolyte Complex Formation in the Presence of NaCl, 30 (1997) 7810–7815. doi:10.1021/ma970803f.
[41] D. Otzen, Protein–surfactant interactions: A tale of many states, Biochim. Biophys. Acta. 1814 (2011) 562–591. doi:10.1016/j.bbapap.2011.03.003.
[42] X. Wang, Y. Li, J. Li, J. Wang, Y. Wang, Z. Guo, Salt Effect on the Complex Formation between Polyelectrolyte and Oppositely Charged Surfactant in Aqueous Solution, J. Phisical Chem. B. 109 (2005) 10807–10812. doi:10.1021/jp0450585.
[43] P. Palladino, R. Ragone, Ionic Strength Effects on the Critical Micellar Concentration of Ionic and Nonionic Surfactants: The Binding Model, Langmuir. 27 (2011) 14065–

14070. doi:10.1021/la202897q.

[44] A. Valstar, M. Almgren, W. Brown, The Interaction of Bovine Serum Albumin with Surfactants Studied by Light Scattering, Langmuir. 16 (2000) 922–927. doi:10.1021/la990423i.

[45] Z.J. Deng, S.W. Morton, E. Ben-akiva, E.C. Dreaden, K.E. Shopsowitz, P.T. Hammond, Layer-by-Layer Nanoparticles for Systemic Codelivery of an Anticancer Drug and siRNA for Potential Triple-Negative Breast Cancer Treatment, 7 (2013) 9571–9584. doi:10.1021/nn4047925.

[46] T. Ramasamy, T. Hiep, J. Yeon, H. Jun, J. Hwan, C. Soon, H. Choi, J. Oh, Layer-by-layer coated lipid – polymer hybrid nanoparticles designed for use in anticancer drug delivery, 102 (2014) 653–661. doi:10.1016/j.carbpol.2013.11.009.

[47] J. Crecente-campo, S. Lorenzo-abalde, A. Mora, J. Marzoa, N. Csaba, J. Blanco, Á. González-fernández, M. José, Bilayer polymeric nanocapsules : A formulation approach for a thermostable and adjuvanted E . coli antigen vaccine, J. Control. Release. 286 (2018) 20–32. doi:10.1016/j.jconrel.2018.07.018.

[48] I. Santalices, A. Gonella, D. Torres, M. Jos, Advances on the formulation of proteins using nanotechnologies, J. Drug Deliv. Sci. Technol. 42 (2017) 155–180. doi:10.1016/j.jddst.2017.06.018.

[49] M. Alonso-Sande, M. Cuña, C. Remuñán-López, D. Teijeiro-Osorio, J.L. Alonso-Lebrero, M.J. Alonso, Formation of new glucomannan - chitosan nanoparticles and study of their ability to associate and deliver proteins, Macromolecules. 39 (2006) 4152–4158. doi:10.1021/ma060230j.

[50] W. Tiyaboonchai, J. Woiszwillo, R.C. Sims, C.R. Middaugh, Insulin containing polyethylenimine-dextran sulfate nanoparticles, Int. J. Pharm. 255 (2003) 139–151. doi:10.1016/S0378-5173(03)00055-3.

[51] B.R. Sloat, M.A. Sandoval, Z. Cui, Towards Preserving the Immunogenicity of Protein Antigens Carried by Nanoparticles While Avoiding the Cold Chain, Int. J. Pharm. 393 (2011) 197–202. doi:10.1016/j.ijpharm.2010.04.003.Towards.

[52] W. Wang, S. Singh, D.L. Zeng, K. King, S. Nema, W.E.T. Al, Antibody Structure , Instability , and Formulation, J. Pharm. Sci. 96 (2007) 1–26. doi:10.1002/jps.

[53] F. Sousa, A. Cruz, I. Mendes, B. Sarmento, Nanoparticles provide long-term stability of bevacizumab preserving its antiangiogenic activity, Acta Biomater. 78 (2018) 285–295. doi:10.1016/j.actbio.2018.07.040.

[54] L.M. Crowe, D.S. Reid, J.H. Crowe, Is Trehalose Special for Preserving Dry Biomaterials ?, Biophys. J. 71 (1996) 2087–2093. doi:10.1016/S0006-3495(96)79407-9.

USC
UNIVERSIDADE
DE SANTIAGO
DE COMPOSTELA

Chapter IV

Bevacizumab-loaded hyaluronic acid enveloped nanocomplexes for the treatment of breast cancer

USC
UNIVERSIDADE
DE SANTIAGO
DE COMPOSTELA

This work was done in collaboration with Institute Galien Paris Sud (Université Paris Sud, Paris, France) and Sylentis S.A. (Madrid, Spain)

ABSTRACT

Bevacizumab (BVZ), a monoclonal antibody designed to target the vascular endothelia growth factor-A (VEGF-A), is currently indicated in the treatment of different types of cancer. However, despite the recognized value of this targeted therapy, its limited accumulation in the tumor and the resistance mechanisms triggered by tumor cells make its clinical exploitation far from optimum. Besides, BVZ does not have the ability to enter the tumor cells, where its target is generated. The objective of this work was to develop a new nanocarrier with the capacity to deliver BVZ not only in the tumor extracellular matrix but also inside the cancer cells. The nanomedicine candidate consisted of nanocomplexes of BVZ with HA and the surfactant lauroyl arginate (LAE), enveloped by a hyaluronic acid (HA) shell. The enveloped nanocomplexes (ENCPs) were able to associate BVZ (50% association efficiency) and were stable for 24 hours in SBF (PBS supplemented with FBS). The ENCPs provided a bi-phasic release of BVZ, with an initial burst followed by the absence of release for at least 24 hours. The ENCPs could be freeze-dried while preserving their physicochemical properties. Cell studies on MDA-MB-231 breast cancer cells indicated that the ENCPs could potentially enter the cells and that their toxicity was concentration-dependent. The measurement of the mRNA expression of the h-VEGF protein family and h-KDR (one of the VEGF receptors) in the presence of the ENCPs indicated that the mAb-loaded ENCPs could slightly modulate the levels of expression of the genes. Finally, the *in vivo* efficacy experiment in breast cancer bearing mice showed no significant differences in terms of tumor growth between the free and the ENCPs-associated drug. In conclusion, these results suggest that despite the ENCPs suitability in terms of BVZ association and apparent cell internalization and plasma stability, other factors not considered in this work, might be responsible for the limited in vivo performance of the formulation.

Keywords: bevacizumab; hyaluronic acid; breast cancer; nanomedicine

USC
UNIVERSIDADE
DE SANTIAGO
DE COMPOSTELA

1. Introduction

The development of the hybridoma technology and the possibility of producing antibodies in large scale have opened new doors to the treatment of cancer [1]. The high specificity and selectivity of therapeutic antibodies compared to the one of chemotherapeutic agents used so far, has drastically reduce the side effects of the anti-cancer therapies [2]. Moreover, the possibility of tuning antibodies immunogenicity and pharmacokinetic through protein engineering based techniques and formulation strategies, increased the interest around the use of these molecules as anti-cancer agents [3,4].

Bevacizumab (BVZ) was approved in 2004 for the treatment of solid tumors which overexpress VEGF-A, a pro-angiogenic factor necessary for tumor development, migration and invasion [5]. Tumor cells need to sustain their rapid growth through the influx of blood for the delivery of nutrients and oxygen [6]. In order to increase the blood supply, they overexpress the hypoxia-inducible factor-1 (HIF-1) which lead to a higher production of VEGF-A and the faster formation of new abnormal blood vessels [5,7]. Bevacizumab acts by recognizing the VEGF-A making it un-available for the recognition by its receptor. This leads to tumor starvation and blood vessels normalization and to a more efficient penetration of chemotherapeutic agents [8,9]. Despite the good results obtained with combination of BVZ and chemotherapeutic drugs for the treatment of several types of cancers, problems related to the resistance of cancer cells to the BVZ molecules, their low tumor penetration and their toxicity have encouraged researchers to explore the value of delivery strategies [10,11]. In fact, after a first approval of a combination of BVZ and paclitaxel in 2008, the FDA reversed this decision, indicating that the side effects of bevacizumab for treating breast cancer (hypertension, proteinuria, gastrointestinal perforation, vomit, thromboembolic events, etc.) outweigh the benefits in prolonging the progression-free survival [12].

In our view the use of nanotechnology could be a reliable solution for overcoming the poor biological outcome (resistances and tumor targeting) and for reducing the safety issues that BVZ-based therapies suffer nowadays. The nanocarriers could also favor the accumulation of BVZ at the tumor site enhancing its anti-cancer effect, as already shown for other nano-encapsulated antibodies [2,13–15].

Some nanocarriers, mostly liposomes, have already been used for the in vivo delivery of BVZ in combination with chemotherapy or photodynamic therapy, obtaining promising results [15–17]. It was also reported that the intracellular delivery of BVZ could have a beneficial effect in terms of blocking of the VEGF-A intracellular pool, indicated as a source of resistance to common BVZ therapies [15]. For example, Tangutoori and co-workers developed a nanocarrier able to deliver both BVZ and BDP (benzoporphyrin derivative monoacid A, a compound used in photo-dynamic therapies) in the cytoplasm of pancreatic cancer cells, demonstrating the anti-cancer efficacy of the nanosystem in vivo. They hypothesized that the intracellular delivery of BVZ could have enhanced the effects of the therapy, avoiding the development of resistance mechanisms [15]. A similar approach have been used by Spring and co-workers, which demonstrated in vivo that the co-delivery of BVZ and BDP in the cytoplasm of pancreatic cells significantly reduced tumor burden compared to the extracellular

co-delivery of BVZ along and BDP, probably due to the blockage of the intracellular VEGF signalling [17]. In another work the co-delivery of two liposomes, one associating BVZ and the other encapsulating doxorubicin, drastically reduced tumor growth compared to the single administration of the liposomal formulations in a breast cancer mice model [16].

Based on this back-ground information, the main objective of this work was to develop and characterize an alternative nanocarrier for BVZ, based on its controlled complexation with HA. The selection of HA was based on its reported capacity to target the CD44 receptors present in cancer cells and facilitate the internalization of the systems [18,19], thereby avoiding resistance, as already indicated by other authors [15,17,20]. The design of the nanocarriers was based on a number of targeted properties: (i) reproducible small size and low-negative zeta potential; (ii) high BVZ loading and sustained release capacity (iii) stability in simulated biological fluids. The resulting nanocarriers were evaluated in vitro in order to assess their toxicity and internalization, and to investigate their capacity to affect the mRNA expression of the h-VEGF family and h-KDR. Finally, the selected prototype was also evaluated in vivo, in a triple negative breast cancer model.

2. Materials and methods

2.1 Chemicals

Bevacizumab was a gift from mAbxience (Spain). Ethyl Lauryl Arginate (LAE) was a gift from Vedeqsa (Spain) and Hyaluronic Acid (HA, 47 – 57 kDa) was purchased from Lifecore Biomedical (USA). The peroxidase-conjugated AffiniPure Goat Anti-Human IgG, Fcy Fragment Specific, was purchased from Jackson ImmunoResearch (UK) and the Human $VEGF_{165}$ (Cat # 100-20) from Peprotech (Spain). The 96 multiwells plate (medisorp) were purchased from Thermofisher scientific (Spain). ABTS (2,2'-azino-di-(3-ethylbenzthiazoline sulfonic acid) solution was purchased by Roche diagnostic (Spain). RNEasy RNA extraction kit (74106) was purchased from QIAGEN while the High-Capacity cDNA Archive Kit (4368813) for reverse transcription as well as the Taqman 2x Universal master mix (4364338) from Applied Biosystems. FITC and Centripure mini desalt Z-50 spin columns were purchase from emp BIOTECH.

2.2 Synthesis of blank and BVZ-loaded HA enveloped nanocomplexes (ENCPs)

Blank HA ENCPs were synthesized mixing 250 µL of LAE (8 mg/mL) with 500 µL of HA under stirring (15 minutes – 900 rpm). Different concentrations of HA have been tested and positively charged nanocomplexes were formed. Then, 500 µL were withdrawn and further 500 µL of an HA solution were added on the top of the LAE/HA positively charged nanocomplex under stirring (500 rpm – 15 minutes), forming the ENCPs with the wanted properties (also in this case different HA concentrations were tested).

BVZ was then associated to the ENCPs. Briefly, 260 µL of the antibody (different concentrations were tested) were dropped into 250 µL of LAE solution (8 mg/mL) under stirring (300 rpm – 15 minutes). The BVZ/LAE solution was then added into the one of HA, as made for the formation of the blank HA ENCPs. The addition of the second HA solution was then done as for the blank HA ENCPs.

2.3 Physicochemical characterization of the nanocomplexes

The size and zeta potential of the colloidal systems were determined by photon correlation spectroscopy and laser Doppler anemometry using a Zetasizer Nano-ZS (Malvern Instruments, Worcestershire, United Kingdom). The zeta potential was measured in KCl 1 mM (as suggested by Malvern).

STEM (Scanning Transmission Electron Microscopy) and SEM (Scanning Electron Microscopy) were also used to characterize the selected ENCPs from the point of view of their shape and size.

2.4 BVZ association efficiency, AE (%)

The AE (%) of the BVZ was evaluated with an ELISAs assays. A 96 multiwell plate was coated with 0.005 µg antigen/well (i.e. recombinant Human $VEGF_{165}$) at a concentration of 0.05 µg/mL (100 µL/well). The antigen was prepared in coating buffer (0.015mol/L Na_2CO_3, 0.035mol/L $NaHCO_3$, 0.0077mol/L NaN_3, pH 9.59) and the coating of the plate was done overnight at 4°C. After the antigen attachment, the plate was washed four times with 300 µL/well of washing buffer (0.05% Tween20 in PBS, pH7.4, 5 minutes per wash). The blocking was then performed with 300 µL/well of blocking buffer (2% dry milk powder prepared in Washing Buffer) for 2 hours at 37°C. A further washing step is done and the antigen coated plate is ready to use.

BVZ-loaded HA ENCPs were isolated by centrifugation (10000g – 30 minutes – 15°C) on a 20 µL glycerol bed and the amount of BVZ in the supernatant, in the pellet and in the non isolated formulation was evaluated. The pellets were destroyed with a mixture of Tween20 0.05% and BSA 50 mg/mL (1:1, v/v) while the non-isolated formulation was treated with Tween20 0.05% (1/10 dilution). The resulting samples were then loaded onto the previously prepared antigen coated plate and incubated for 1 hour at 37°C. Then, the plate was washed with washing buffer, coated by the secondary HRP-goat anti-human antibody (0.08 µg/mL, prepared in coating buffer) and incubated for 30 minutes at 37°C. The plate was washed again and the detection substrate (ABTS) was added to each well (50 µL/well).

2.5 Simulated biological fluids (SBF) stability

The formulation was diluted in PBS supplemented with 10% (v/v) of FBS and incubated at 37°C. At different time points (2, 4, 8 and 24 hours) part of the samples were withdrawn and size and mean count rate (MCR) were measured with Zetasizer Nano-ZS (Malvern Instruments, Worcestershire, United Kingdom).

2.6 FITC labeling of BVZ

A volume of 13.2 µL of 1M sodium bicarbonate solution, pH 8.5, was added to 66 µL of the BVZ solution (15.2 mg/mL). Then, 10 µL of a 2 mM FITC solution (prepared in DMSO) were pipetted into the protein solution and stirred for 2 hours. Centripure mini desalt Z-50 spin columns were used to purify the labeled antibody.

2.7 Release of BVZ from the BVZ-loaded HA ENCPs

FITC-labeled BVZ (see paragraph 2.6) was used to produce FITC-BVZ-loaded HA ENCPs. The particles were diluted in PBS supplemented with 10% (v/v) of FBS and at different time points (2, 4, 8 and 24 hours) the formulations were isolated by centrifugation and the release of FITC-labeled BVZ was

evaluated by fluorimetry. For this purpose, a calibration curve was built using blank nanostructures as controls containing the desired amounts of FITC-labeled -BVZ.

2.8 Storage stability of the HA ENCPs

The selected nanosystems were evaluated for their storage stability in both suspension at 4°C and upon in a freeze-dried form. For the 4°C storage stability, size and MCR of the HA ENCPs have been measured at different time points (1, 4 and 7 days). In the case of freeze-drying, different cryoprotectant and stabilizers have been tested (see Table 3.4).

2.9 Cell line and culture conditions

Human breast basal epithelial cancer cells (MDA-MB-231) were obtained from ATCC (France) and maintained in Leibovitz's L15 medium supplemented with 15% (v/v) fetal bovine serum (FBS), glutamine (2 mM) and sodium hydrogen carbonate (20 mM). Cells were maintained in a humid atmosphere at 37 °C with 5% CO_2.

2.10 Cytotoxicity assay

Cytotoxicity studies were performed using the 3-(4,5-dimethylthiazol-2-yl)-2,5-diphenyl tetrazolium bromide (MTT) test using the MDA-MB-231 cells. Briefly, 100µL/well of a cell dispersion ($5x10^4$ cells/mL) was seeded in 96-well plates 24 hours before the treatment with the different samples (i.e. BVZ-loaded HA ENCPs, blank HA ENCPs, LAE and free BVZ). Several concentrations, ranging from 1 to 124 µg/mL (BVZ based concentrations) were tested. After 72h incubation, 20 µL of a 5 mg/mL MTT solution in phosphate buffered saline was added to each well for 2 hours. Then, culture medium was removed, and the formed crystals were dissolved in 200 µL of dimethyl sulfoxide (DMSO). Spectrophotometric measurements of the solubilized dye absorbance were performed on a microplate reader at 570 nm.

2.11 Uptake of the BVZ associated to the ENCPs by MDA-MB-231 cells

The uptake of the BVZ by the MDA-MB-231 cells was evaluated by confocal laser scan microscopy (SP5 Leica AOBS-SP5). Briefly, 24 hours before the experiments, cells were seeded at a density of 100.000 cell/mL on 12 mm diameter treated coverslips, previously placed in a 24 wells plate. The BVZ was then FITC-labeled and the ENCPs produced. Cells were then incubated with the samples (i.e. BVZ-loaded HA ENCPs, free BVZ, LAE+free BVZ) for 1 and 3 hours and the cells fixed with PFA 4 % (15 minutes, room temperature), permeabilized with Triton-X 0.2 % (v/v) (10 minutes, room temperature) and counterstained with DAPI (1 µg/mL in PBS for 30 minutes). The samples were then analyzed with the microscope.

2.12 Gene expression profile of human h-VEGF-A, h-VEGF-B, h-VEGF-C and h-KDR genes after the treatment with BVZ-loaded HA ENCPs.

MDA-MB-231 were seeded at a density of 200.000 cell/well with a 90% confluence to maintain the cell growth in exponential phase. 24 hours after the seeding, cells were treated for 1 hour with different samples: free BVZ, blank HA ENCPs, BVZ-loaded HA ENCPs and LAE. The BVZ concentration used for these experiments was 15 µg/mL. After 1 hour, cells were washed with PBS and the medium was replaced. Thereafter, cells were collected at different time points (24, 48 and 72 hours) and

analyzed for gene expression. RNA was extracted using RNEasy RNA extraction kit in the automatic extractor QIACUBE, according to manufacturer's instructions. RNA was quantified and analyzed for signs of degradation using Agilent 2100 Bioanalizer following standard procedures. Total RNA (4µg) was reversely transcribed in 80 µl reactions using High-Capacity cDNA Archive Kit, following the manufactures instructions. Real time PCR was performed using StepOnePlus detection systems (Applied Biosystems). Gene-specific primers and probes available as Taqman Gene Expression assays were used for all target genes and internal controls. The internal standards were chosen regarding the previous expression analysis which indicated that each of the chosen internal standards showed the most stable expression across samples for each target gene and cell line, and because the amplification had a comparable efficiency to that of the target gene. 100 ng of cDNA were amplified in a Taqman 2x Universal master mix under the following conditions: 95ºC for 10 minutes, followed by 40 cycles of 95ºC for 15s and 60ºC for 1minute. All real time quantitative PCR experiments were performed in triplicate and repeated in three independent experiments, always including reverse transcription and no template controls. In order to quantify the results obtained by real-time RT-PCR, the Comparative Threshold (Ct) method was used. This involves comparing the Ct values of the samples of interest with a control or calibrator such as a non-treated sample. The Ct values of both the calibrator and the samples of interest are normalized to an appropriate endogenous housekeeping gene. The comparative Ct method is also known as the $2^{-\Delta\Delta Ct}$ method (Livak and Schmittgen 2001).

2.13 Anticancer efficacy of BVZ-loaded HA ENCPs upon intraperitoneal injection

Six-week old female mice (athymic nude) were purchased from Envigo Laboratory (France). All animals were housed in appropriate animal care facilities during the experimental period. The experimental protocols were approved by the Animal Care Committee of the Université Paris-Sud in agreement with the principles of laboratory animal care and legislation in force in France (n°APAFIS#13238-2018012911422090v1).

The anticancer efficacy of the formulation was evaluated on MDA-MB-231 tumor-bearing mice. A volume of 50 µL of MDA-MB-231 cell suspension in PBS (5 x 10^6 cells/mice) was injected subcutaneously into the left third mammary gland. Tumors were allowed to grow for two weeks until reaching a volume ~100 mm^3 before initiating the treatment. Tumor length (a) and width (b) were measured with calipers and the tumor volume was calculated using the following equation: tumor volume (V) = (a x b^2)/2. Tumor-bearing mice were randomly divided into 4 groups of 8 mice each. Mice were injected intraperitoneally and received three injections per week, for a total of nine injections of either *(i)* BVZ-loaded HA ENCPs at a BVZ equivalent dose of 6.2 mg/kg, *(ii)* free BVZ at 6.2 mg/kg, (iii) blank HA ENCPs or *(iv)* dextrose 5%.

Mice were monitored regularly for changes in tumor size, body weight and health status. Mice were humanely sacrificed on day 33.

2.14 Statistical analysis.

Differences were statistically evaluated by a two-ways ANOVA followed by a Fisher's LSD test. All statistical analysis were conducted using GraphPad Prism (Version 7.0 software). A p value < 0.05 was considered to be significant.

3. Results

The main objective of the work was to develop a new nanocarrier for the intracellular delivery of monoclonal antibodies. HA was selected as main biomaterial of the nanocarrier due to its excellent safety profile and the capacity to target the CD44 receptors [10,18,19]. BVZ was selected as a model monoclonal antibody, which could potentially benefit from the intracellular delivery. In fact, an intracellular pool of VEGF-A, the target of BVZ, has been indicated as a cause of resistance to BVZ-based therapies. In addition, the nano-encapsulation of BVZ could potentially reduce the side effects observed with free BVZ treatments and favor the penetration of the drug across the tumor.
Here we describe, step by step, the development and in vitro/in vivo characterization of the said nanoformulation.

3.1 Blank and BVZ-loaded HA ENCPs development and characterization

Based on a previous work (see Chapter III) we selected HA and LAE as the main ingredients of the nanocarrier. In a first set of experiments, the amount of HA necessary for the formation of HA-LAE nanocomplexes was investigated by fixing the amount of LAE in 2 mg (250 µL of an 8 mg/mL solution prepared in milliQ water). The results in Table 3.1 indicate that the nanocomplexes are formed when using the lowest amount of HA (0.25 mg in 500 µL). In these conditions, the resulting nanocomplexes exhibited a positive zeta potential. In a second set of experiments, the BVZ solution (260 µL – different concentration tested) was then added to the LAE solution (250 µL – 8 mg/mL) under stirring and the resulting mixture was then injected into the HA solution (500 µL – 0.5 mg/mL). As shown in Figure 3.1.A., the addition of increasing amounts of BVZ led to a certain increase in particle size and a small reduction of the positive zeta potential of the nanocomplexes, changes that might be related to the association of BVZ to the nanostructure. Unfortunately, these positively charged complexes were sensitive to dilution. To avoid this problem the nanocomplexes were enveloped with a HA layer, thus forming the enveloped nanocomplexes (ENCPs). A schematic representation of the ENCPs formation is given in Figure 3.2. As expected, the ENCPs showed a negative zeta potential (Figure 3.1.B), due to the external exposure of the HA coating. The results in Figure 3.1.B also indicate that a minimum amount of 0.5 mg of HA was necessary for the enveloping process in order to obtain well-defined and stable ENCPs. The amount of BVZ in this composition was 75 µg, which corresponds to a final theoretical loading of 3.4% (Figure 3.1.B). Higher loadings (up to 375 µg of BVZ, corresponding to 15.1% theoretical loading) and stable nanocomplexes were achieved by increasing the amount of HA up to 1 mg/mL. The physico-chemical properties of these ENCPs are indicated in table 3.2. The ENCPs and their appearance and particle size were also observed by STEM and SEM (Figure 3.3). A spherical shape and a size of around 200 nm were observed irrespective of the technique. However, the presence of small nanostructures of less than 100 nm was also detected using SEM, an observation that was attributed to the formation of surfactant micelles formed due to the excess of surfactant used to produce the nanosystem.

Table 3.1. Optimization of the HA amount for the formation of the blank HA nanocomplexes.

						Blank nanocomplexes		
LAE amount (mg)	**LAE volume (µL)**	**LAE concentration (mg/mL)**	**HA amount (mg)**	**HA volume (µL)**	**HA concentration (mg/mL)**	**Size (nm)**	**ζ (mV)**	**PDI**
2	250	8	0.25	500	0.5	111±4	24±1	0.1
2	250	8	0.5	500	1	Aggregates		
2	250	8	1	500	2	Aggregates		

LAE: ethyl lauroyl arginate; HA: hyaluronic acid; ζ: zeta potential; PDI: polydispersity index.

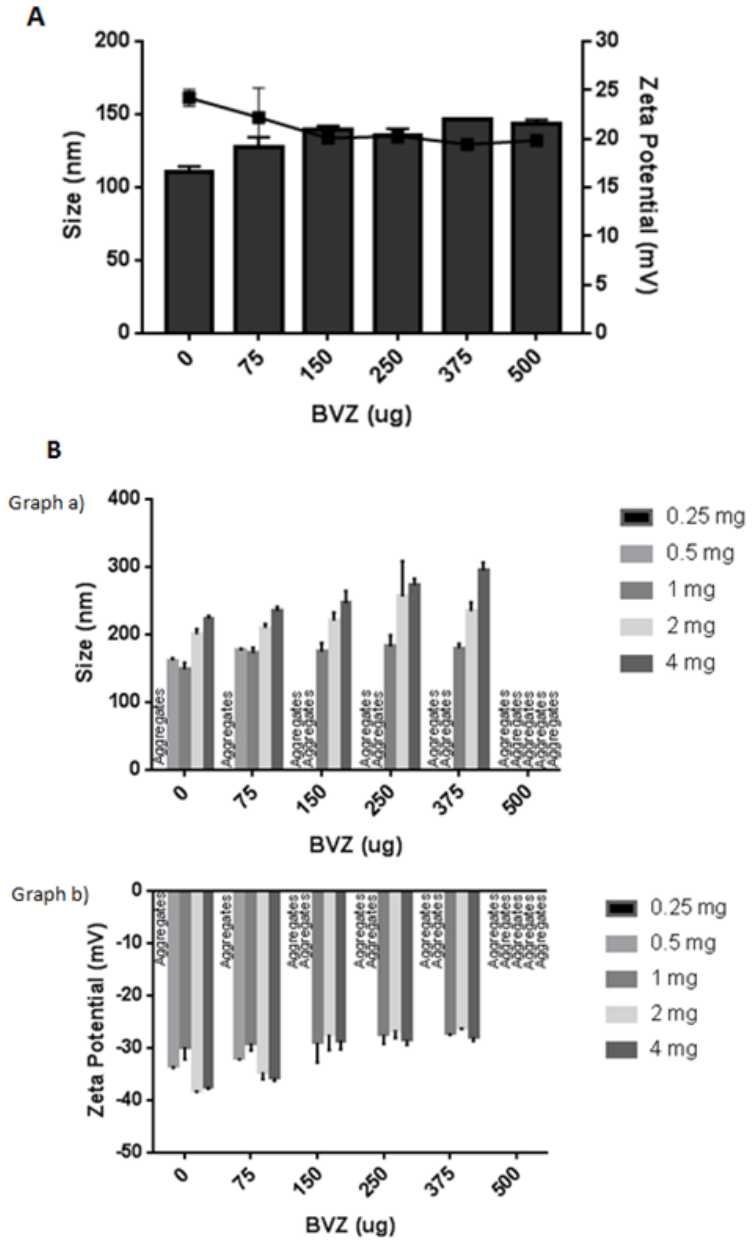

Figure 3.1. A) Size and zeta potential of the positively charged LAE/HA nanocomplexes loaded with BVZ. Increasing amounts of BVZ have been tested. The resulted formulations are made by 2 mg of LAE, 0.25 mg of HA and variable amounts of BVZ in

a final volume of 1.01 mL. B) Influence of the amount of HA (0.25, 0.5, 1, 2, 4 mg) on size (Graph a)) and zeta potential (Graph b)) of the enveloped nanocomplexes (ENCPs).

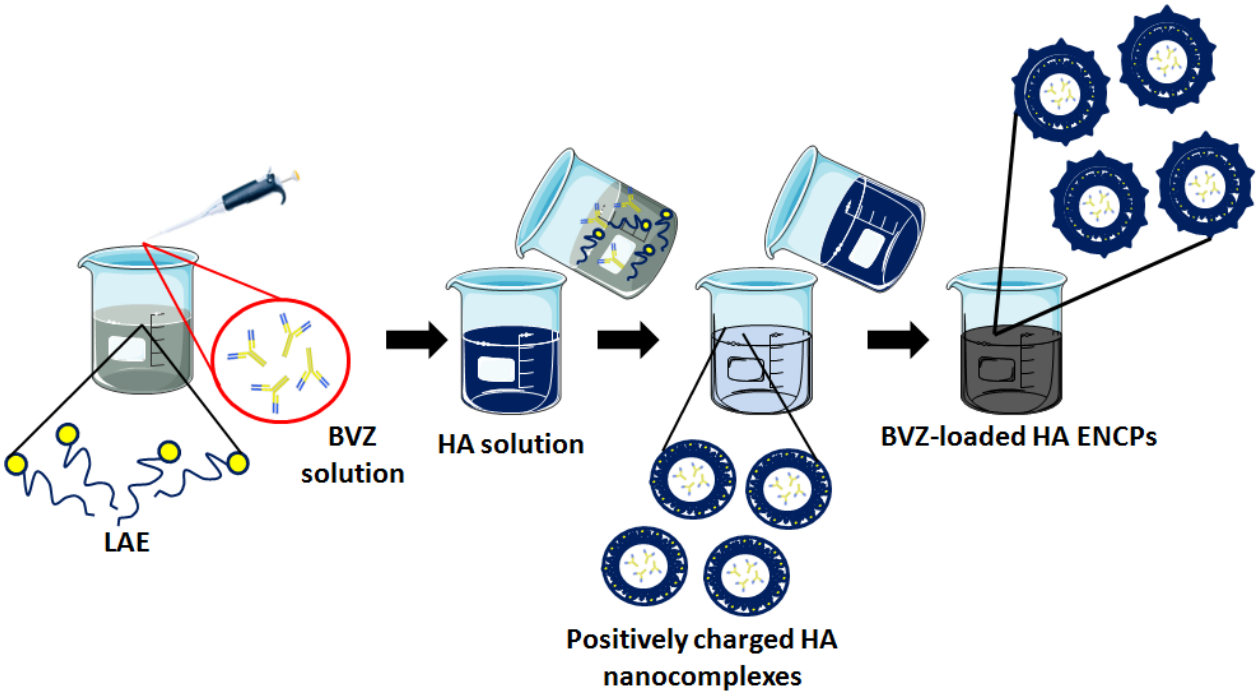

Figure 3.2. Schematic representation of the BVZ-loaded HA ENCPs formation.

Table 3.2. Amounts of LAE, HA and physico-chemical properties of the selected BVZ-loaded HA ENCPs."I HA amount" is referred to the amount of HA used to form the positively charged nanocomplexes; "II HA amount" is referred to the amount of HA used to coat the positively charged nanocomplexes, forming the ENCPs.

				BVZ-loaded HA ENCPs		
Sample	**LAE (mg)**	**I HA amount (mg)**	**II HA amount (mg)**	**Size (nm)**	**ζ (mV)**	**PDI**
BVZ-loaded HA ENCPs (75 µg)	2	0.25	1	173±8	-29.0±1.4	0.1
BVZ-loaded HA ENCPs (375 µg)	2	0.25	1	179±8	-27.0±0.3	0.1

LAE: ethyl lauroyl arginate; HA: hyaluronic acid; ζ: zeta potential; PDI: polydispersity index

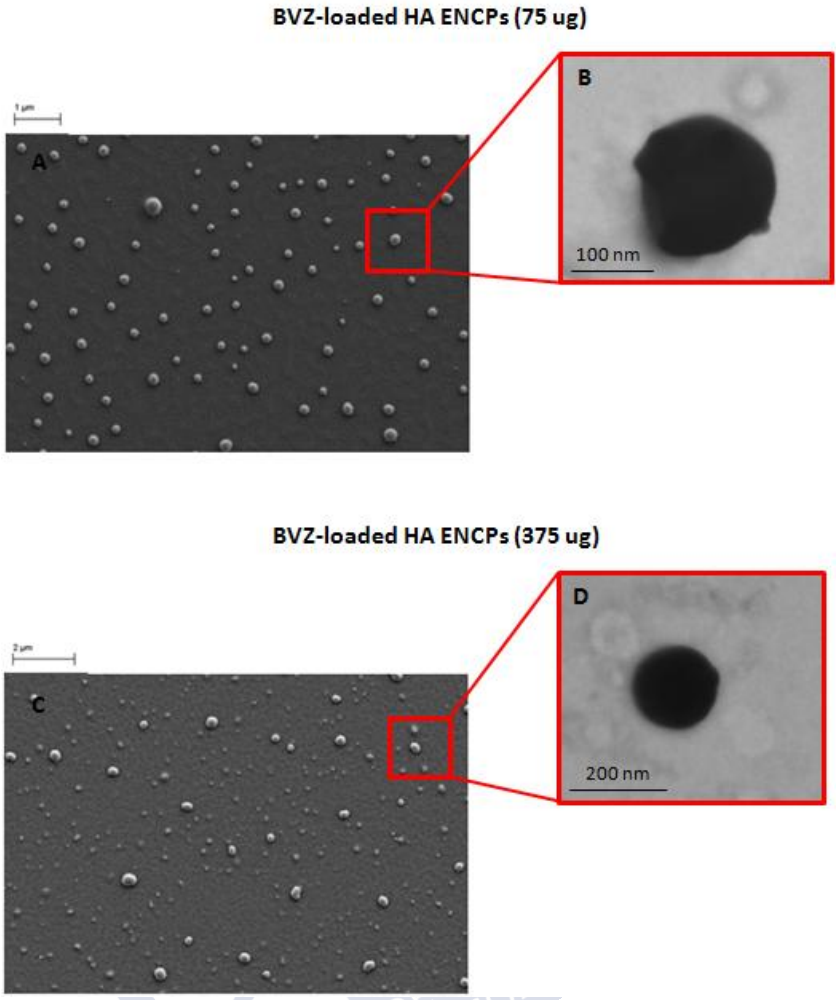

Figure 3.3. SEM (images A and C) and sTEM (images B and D) of the selected BVZ-loaded HA ENCPs. The upper panels refer to an amount of the BVZ of 75 µg (3.4% theoretical loading) per formulation, while the bottom ones correspond to 375 µg of BVZ (15.1% theoretical loading). A) size bar: 1 µm; B) size bar: 100 nm; C) size bar: 2 µm; D) size bar: 200 nm.

3.2 BVZ association efficiency AE (%) and loading capacity LC (%)

The amount of BVZ encapsulated into the selected prototypes was measured by ELISA. Irrespective of the amount of BVZ (75 µg and 375 µg) an AE value of around 40-50% was measured (Table 3.3). The LC (%) of the BVZ-loaded HA ENCPs (375 µg) is higher, since a higher amount of protein was used to form the ENCPs (Table 3.3). The ELISA results indicate that the formulated BVZ was able to recognize its antigen and, hence, that its functional capacity was preserved.

Table 3.3. Comparison of the AE (%) and the LC (%) of the BVZ-loaded HA ENCPs (75 µg) and BVZ-loaded HA ENCPs (375 µg).

Prototype	AE (%)	LC (%)
BVZ-loaded HA ENCPs (75 µg)	42.4	1.5
BVZ-loaded HA ENCPs (375 µg)	48.1	7.3

AE (%): association efficiency (%) (100 x associated peptide mass/total peptide mass); LC (%): loading capacity (%) (100 x protein mass loaded /total formulation mass)

3.3 BVZ release and ENCPs stability in simulated biological fluids (SBF)

The release of the antibody from the *ENCPs* was evaluated after incubation of the ENCPs in PBS supplemented with FBS 10% (v/v) at 37°C. For this purpose, BVZ was labeled with FITC and the amount of FITC-labeled BVZ released was measured by fluorescence. The results in Figure 3.4 indicate that BVZ was released in a bi-phasic manner with an initial burst release, followed by the absence of release for up to 24 hours. The immediate release could be attributed to the BVZ molecules that are not well entrapped within the nanocarrier. This is in agreement with the fact that the highest burst was observed for the nanocomplexes with a higher BVZ loading.

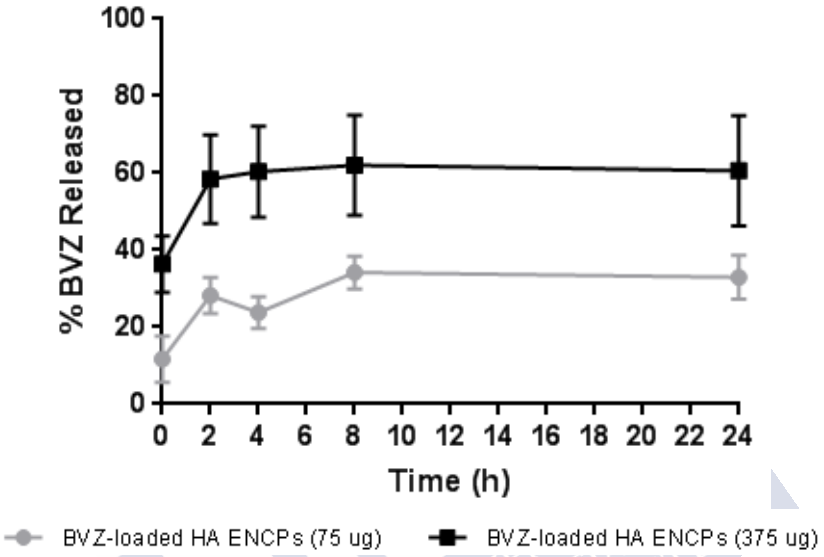

Figure 3.4. Release of BVZ from the BVZ-loaded HA ENCPs (75 µg) and BVZ-loaded HA ENCPs (375 µg).

The stability of the selected nanosystems was evaluated in the same buffer used for the release (PBS supplemented with FBS 10% (v/v)). The behavior of BVZ-loaded HA ENCPs was similar irrespective of the amount of BVZ loading. As shown in Figure 3.5, a first drop in size was observed immediately after the particles were diluted in the media. The initial decrease in the particle size could be attributed to the partial detachment of the antibody (as shown in Figure 3.4 with the burst release) and/or to the formation of additional nanostructures due to the interaction of LAE and free BVZ with serum proteins. Following this initial size reduction both the particle size and the MCR were maintained for up to 24 hours, thus suggesting that the ENCPs are stable in the selected SBF.

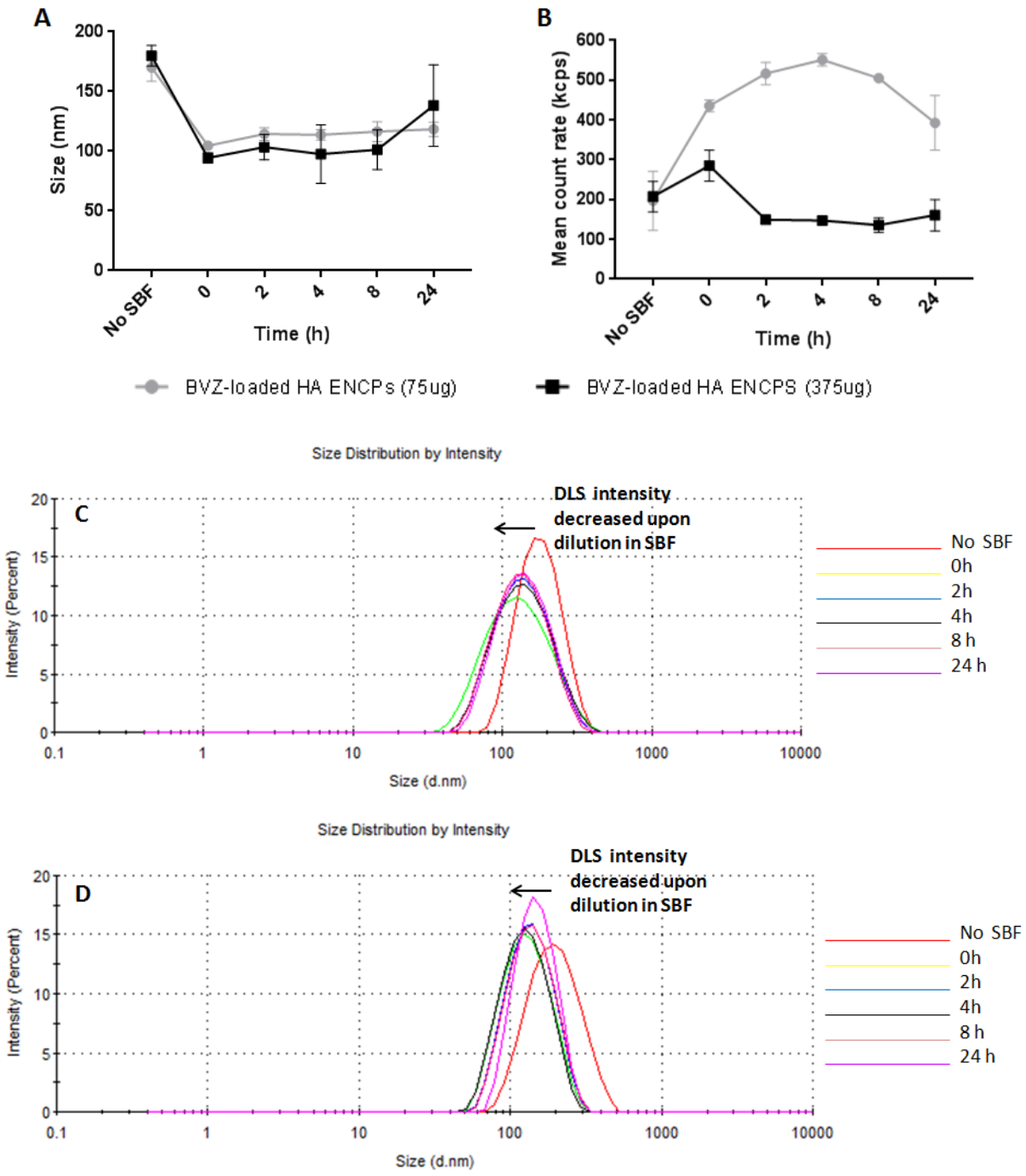

Figure 3.5. Stability of BVZ-loaded HA ENCPs (75 µg) and BVZ-loaded HA ENCPs (375 µg) in PBS (supplemented with FBS 10% (v/v)). Size (A) and mean count rate (B) are indicated in the graphs. An example of the ENCPs distribution profiles upon the dilution in the SBF is also indicated: C) BVZ-loaded HA ENCPs (75 µg) and D) BVZ-loaded HA ENCPs (375 µg).

3.4 Stability of ENCPs during storage

To preserve the stability of nanocarriers is a critical issue for their utility as pharmaceutical products. Blank and BVZ-loaded nanocarriers with different drug loading were stored at 4°C and their size and mean count rate were monitored over the time. The results in Figure 3.6 show that the ENCPs loaded with high amounts of BVZ suffered a significant size increase during storage (from 180 to 250 nm), whereas the mean count rate decreased (which is an indication of the ENCPs instability). This

instability problem was just relatively observed for the formulation with a low BVZ loading or the blank formulation, where the size increase after 7 days is minimum.

Typically, colloidal formulations are stored in the form of powder. Different cryoprotectors and stabilizers at different concentrations were tested for freeze drying the formulation and the best results are reported in Table 3.4. The results indicated that the low BVZ-loaded nanocarriers (BVZ-loaded HA ENCPs (75 µg)) were stable when trehalose 10% was used as a cryoprotectant, however, in the case of the high BVZ-loaded nanocarriers (BVZ-loaded HA ENCPs (375 µg)) stabilization were only achieved when trehalose 2.5% and PEG 2.5% were added to the formulation. However, in this condition, an increase in the particle size variability of the formulation was observed.

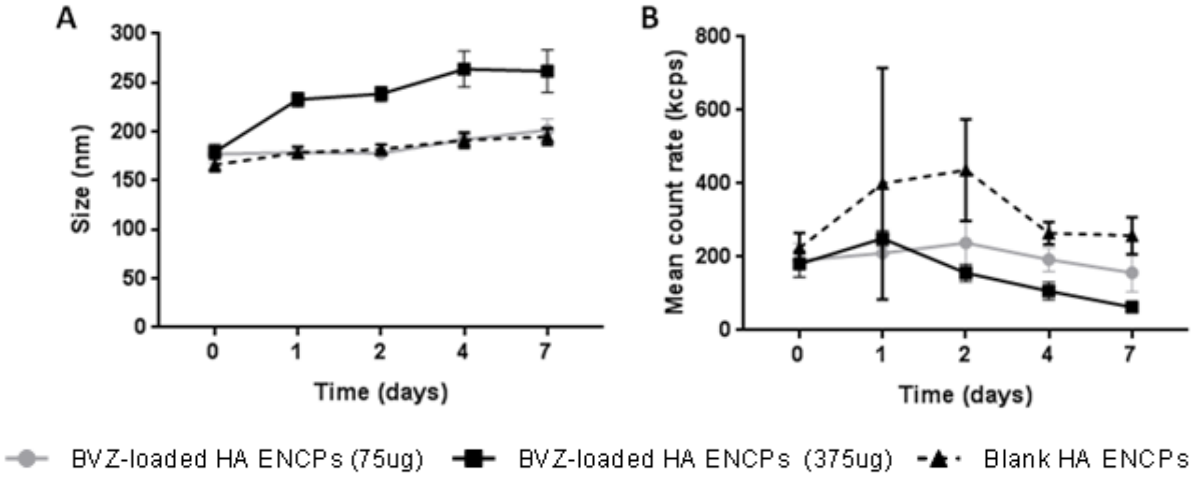

Figure 3.6. Liquid storage stability (4°C) of BVZ-loaded HA ENCPs (75 µg) and BVZ-loaded HA ENCPs (375 µg). Size (A) and MCR (B) were used as stability indicators.

*Table 3.4. Freeze drying conditions used for the BVZ-loaded HA ENCPs. Size and PDI before and after freeze drying are indicated. Statistical analysis using t-test have been done to understand if the size increase was significant (*p<0.05 and **p<0.01).*

	Cryo-protectors			Before freeze-drying		After freeze-drying		
Prototype	**Trehalose (%)**	**PEG-400 (%)**	**PVP (%)**	**Size (nm)**	**PDI**	**Size (nm)**	**PDI**	**Size increase (%)**
BVZ-loaded HA ENCPs (75µg)	10	-	-	170±12	0.1	189±5	0.1	11*
	5	-	2.5	175±3	0.1	208±14	0.2	19**
BVZ-loaded HA ENCPs (375µg)	10	-	-	179±8	0.1	Aggregates		NA
	5	2.5	-	179±8	0.1	214±4	0.2	20*
	2.5	2.5	-	179 ±1	0.1	205±35	0.2	15

PEG400: Polyethylene glycol 400; PVP: polyvinylpirrolidone; PDI: Polydispersity index
Size increase (%) = 100 x (size after freeze drying-size before freeze drying)/size before freeze drying

Due to the higher AE (%) and LC (%) and their good SBF and storage stability profiles, BVZ-loaded HA ENCPs (375 µg) have been selected for proceeding with the studies.

3.5 Cell viability assays

Cell toxicity assays were performed for blank and BVZ-loaded nanocarriers with a high BVZ loading (7.3%), using different concentrations of BVZ and nanocarrier (Table 3.5). The results in Figure 3.7 show a significant decrease in cell viability when cells were exposed to the ENCPs at BVZ concentrations higher than 15 µg/mL (127 µg/mL of nanocarrier), for up to 72 hours. A similar toxicity profile was observed for the blank HA ENCPs and for the surfactant (LAE), a result that suggests that LAE is the main cause of cytotoxicity. IC50 was above 25 µg/mL of BVZ (212 µg/mL of nanocarrier).

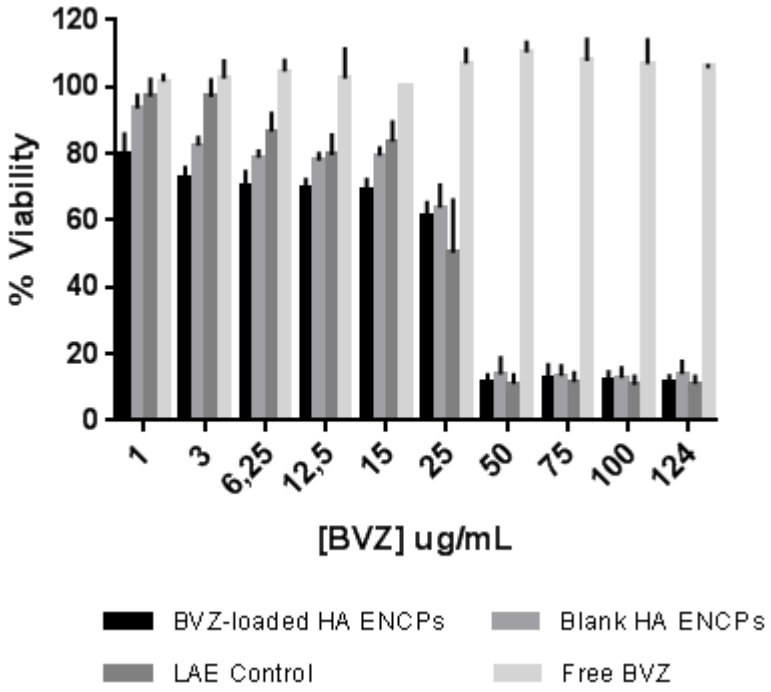

Figure 3.7. MTT viability assays on MDA-MB-231 breast cancer cell line. BVZ-loaded HA ENCPs *(375 µg), blank HA* ENCPs*, LAE and free BVZ have been tested and compared (72 hours contact of samples with the cells). An ANOVA was used for detecting significant differences (***p<0.001 and ****p<0.0001). At all the selected concentrations there is significant difference between the BVZ-loaded HA ENCPs and the free BVZ (p<0.001 at 1 µg/mL and p<0.0001 at all the other concentrations). When blank HA ENCPs are considered, the only concentration at which a significant difference is not observed is the lowest one (1 µg/mL). In all the other cases the differences are statistically significant (p<0.0001). A similar behavior is observed with LAE, where starting from the concentration of 6.25 µg/mL the differences are statistically significant (p<0.001 or p<0.0001).*

Table 3.5. Concentrations of BVZ and the corresponding HA ENCPs used for the MTT assays.

[BVZ] µg/mL	1	3	6.25	12.5	15	25	50	75	100	124
[ENCPs] µg/mL	8.5	25.4	52.3	106	127.2	212	424	636	848	1051.2

3.6 Uptake of the BVZ-loaded HA ENCPs by MDA-MB-231 cells

The internalization of FITC-labeled BVZ (75 µg/mL of BVZ corresponding to 636 µg/mL of nanocarrier) by the breast cancer cells was evaluated after the incubation of the BVZ-loaded HA ENCPS for up to 1 and 3 hours at 37°C. As shown in Figure 3.8, after 1 hour of incubation with the FITC-labeled BVZ-loaded HA ENCPs, fluorescent spots could be identified, potentially inside the cells. Studies aiming in

understanding the real localization of BVZ (i.e. inside the cells or on their surface) would be needed. In contrast, no internalization was observed for the free BVZ. A similar pattern was observed after a 3 hours incubation time. On the other hand, the images show that the presence of LAE facilitated the apparent internalization of the antibody. Taking into account that the ENCPs formulations contained a significant amount of free LAE and free BVZ, we cannot conclude from these studies that the potential BVZ internalization is due to its association to the ENCPs.

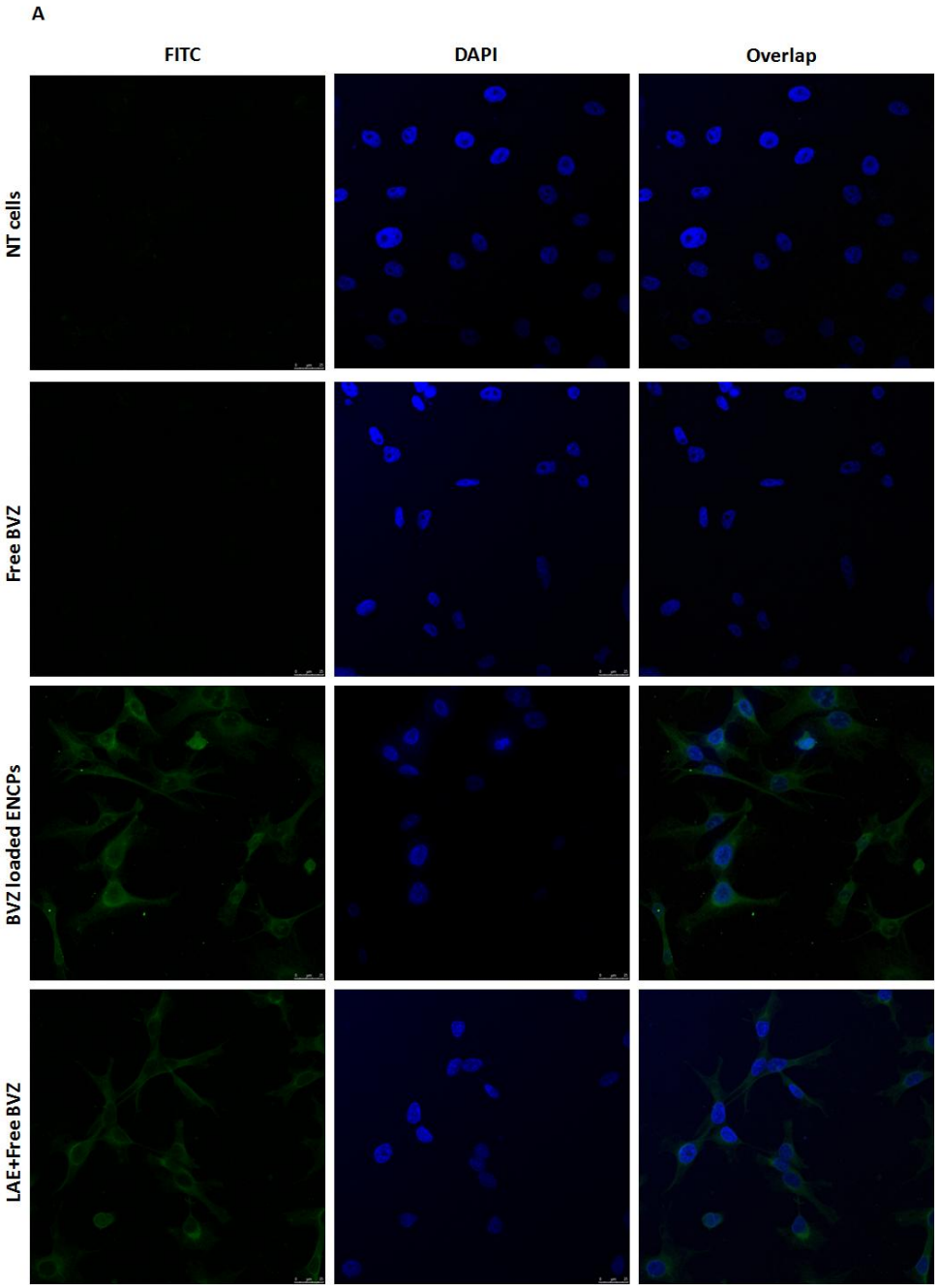

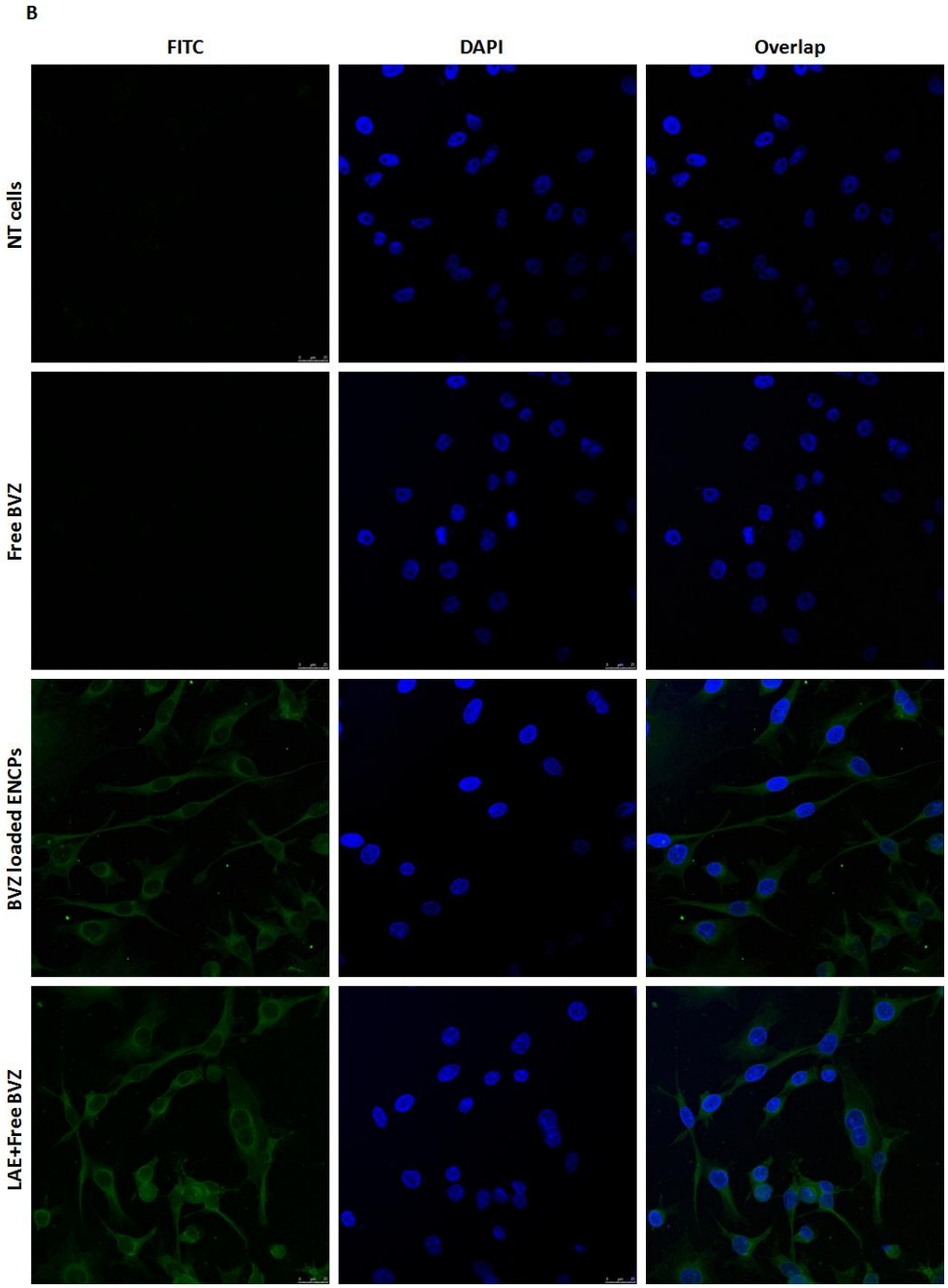

Figure 3.8. Apparent internalization of FITC-labeled BVZ in MDA-MB-231 cells observed by confocal laser microscopy after 1 hour incubation (Panel A) or 3 hours incubation (Panel B) with the FITC-labeled BVZ-loaded ENCPs. Controls of non-treated cells (NT cells), free BVZ and the physical mixture of BVZ and LAE (LAE+FreeBVZ) are also shown. DAPI was used for labeling the nucleus of the cells.

3.7 Study on the mRNA expression of h-VEGF-A, h-VEGF-B, h-VEGF-C and h-KDR genes upon the treatment of MDA-MB-231 cells with the ENCPs

The effect of the free BVZ, the BVZ-loaded HA ENCPs (375 μg), the blank HA ENCPs and the LAE on the mRNA expression of some of the genes involved in the VEGF pathway, was evaluated. Specifically, the changes in mRNA expression of three genes belonging to the human VEGF protein

family (i.e. VEGF-A, VEGF-B, VEGF-C) and of one of the receptors involved in the h-VEGF-A, h-VEGF-C and h-VEGF-D recognition (i.e. KDR, also called VEGFR-2, [21]) were studied. Differences with a $p<0.01$ (**) are indicated in Figure 3.9.

As shown in Figure 3.9.A, 24 hours after the treatment, a first slight increase in VEGF-A mRNA levels was measured when cells were exposed to BVZ-loaded HA ENCPs, blank HA ENCPs, and a LAE control solution. This behavior was not observed when the free BVZ was used, thus suggesting that the increase in gene expression was due to a component of the HA ENCPs, probably LAE. However, at 48 hours post-exposure, BVZ-loaded HA ENCPs significantly reduced the VEGF-A expression levels (30% reduction) as compared to the other experimental groups. After 72 hours, the expression levels returned to the basal ones or increase (the free BVZ increase up to 120%), meaning that the decrement observed after 48 hours was transient.

With regard to the level of expression of VEGF-B *(*Figure 3.9.B*)*, it was found that free BVZ increased the VEGF-B expression levels while the ENCPs or the surfactant significantly reduced the mRNA levels down to 20-30% compared to the non-treated cells. This effect was transient as the mRNA expression levels returned to the basal ones in 72 hours.

With regard to the level of expression of *VEGF-C*, the results in figure 3.9.C show a progressive increase of VEGF-C gene expression levels of cells treated with free BVZ (a 25% gene expression increase was detected after 72 hours). However, no significant changes were observed in this gene expression when cells were exposed to the rest of the formulations for up to 72 hours.

Finally, with regard to the expression of KDR (figure 3.9.D), no significant differences ($p<0.01$) were found for KDR gene expression levels for all the experimental conditions (figure 3.9.D). Interestingly, 48 hours after the treatment with the BVZ-loaded HA ENCPs, KDR gene decreased its expression as compared to the non treated control ($p<0.05$).

Overall, it could be concluded that the levels of expression of different genes were reduced in a transient manner upon exposure to BVZ-loaded HA ENCPs. The expression levels returned to their normal values at 72 hours post-incubation.

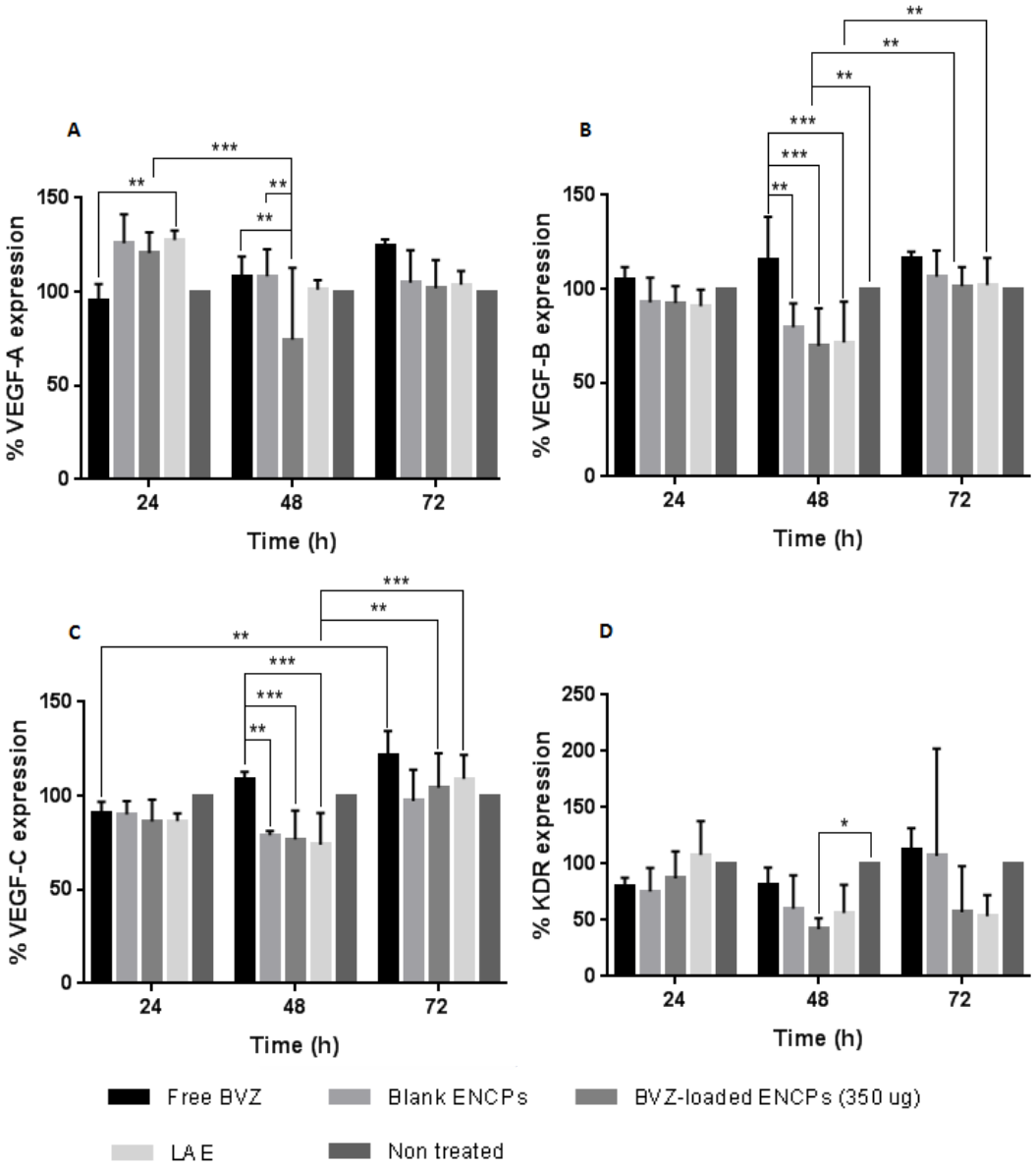

*Figure 3.9. mRNA expression upon treatment of MDA-MB-231 cells with free BVZ (15 µg/mL), BVZ-loaded HA ENCPs (BVZ concentration of 15 µg/mL corresponding to a ENCPs concentration of 127.2 µg/mL), blank ENCPs (127.2 µg/mL), and LAE (59.3 µg/mL, i.e. theoretical concentration based on the amount in the ENCPs). The expression of the following genes was studied: VEGF-A (A), VEGF-B (B), VEGF-C (C) and KDR (D). An ANOVA was used for detecting significant differences (**p<0.01 and ***p<0.001).*

3.8 In vivo efficacy of the BVZ-loaded HA ENCPs

The BVZ-loaded HA ENCPs, free BVZ, blank HA ENCPs and 5% dextrose solution were administered intraperitoneally to 4 groups of mice (n=8) for a time period of 3 weeks (BVZ dose of 6.2 mg/kg). The results in Figure 3.10 indicate that the faster tumor growth was observed for the control-treated mice (blank HA ENCPs and dextrose). In these groups a high tumor necrosis occurred at day 25 post-tumor induction and these mice had to be sacrificed. Although tumor growth is slower in groups treated with the free drug and drug-loaded HA ENCPs, the differences among these groups were not

statistically significant. The beginning of tumor necrosis was observed only at the end of the monitoring phase in both these groups.

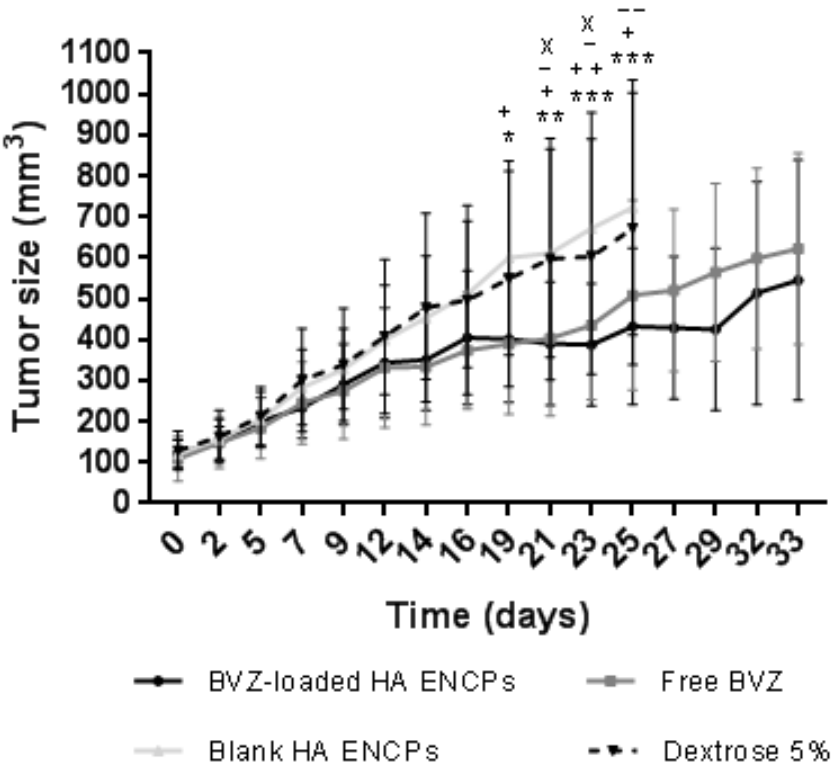

Figure 3.10. Tumor volume growth in MDA-MB-231 tumor-bearing mice after intraperitoneal administration of BVZ-loaded HA ENCPs, free BVZ, blank HA ENCPs and dextrose solution 5% (Dextrose 5%). The statistically significant differences among the groups are presented below:

** = BVZ-loaded HA ENCPs and blank HA ENCPs (*p<0.05 , **p<0.01 and ***p<0.001)*

+ = free BVZ and blank HA ENCPs (; $^{+}$p<0.05 and $^{++}$p<0.01)

- = BVZ-loaded HA ENCPs and dextrose 5% ($^{-}$p<0.05 and $^{--}$p<0.01)

x = free BVZ and dextrose 5% (; ^{x}p<0.05 and ^{xx}p<0.01)

No significant differences have been found among the BVZ-loaded HA ENCPs and the free BVZ groups.

4. Discussion

Despite the high selectivity and specificity of monoclonal antibodies (mAbs), there are still some problems that hinder their indication in some cancer therapies. Indeed, their high molecular weight, their huge specificity (binding site barrier effect, i.e. the stackness of these molecules at the tumor periphery) and the high interstitial tumor pressure make the penetration of the these macromolecules into the tumor mass very poor, a fact that limits their success in some pathological situations [22]. A further limitation of mAbs in anti-cancer therapies is that they only target secreted antigens, whereas a huge number of targets can be found in the cytoplasm of cells [20,23]. Finally, these molecules exhibit problems related to the resistance mechanisms, associated to repeated treatments, and specific side effects, as it is the case of BVZ. Therefore, there is room for improving the performance of monoclonal antibodies and the solution may be found on the use of nanotechnology. Several examples can be given regarding the increase of mAbs performances once

encapsulated. For example, Deng and co-workers reported in vivo studies showing an increase in the efficacy of doxorubicin when delivered along with a mAb (i.e. anti-S100A4 antibody) inside the cancer cells thanks to the use of a liposome. The antibody blocked the S100A4 protein, reducing cells motility, and boosts the effect of doxorubicin [24]. In another interesting work, an anti-IL6 antibody was delivered to the cytoplasm of breast cancer cells in vivo, blocking the IL6R-Stat3 signalling, causing a delay in tumor growth and the inhibition of the formation of metastasis [2]. Other studies have also disclosed the benefit of delivering BVZ at the intracellular level. In one of them, BVZ was co-encapsulated with BDP (a compound used in phodynamic therapies) in a liposomal formulation. The authors hypothesized that the intracellular delivery of BVZ could block the signal cascade before it starts, avoiding tumor re-growth and overcoming the effect of potential resistance mechanisms [15,17]. Finally, Tang and co-workers showed the enhanced in vivo anti-cancer efficacy of delivering two independent liposomes to breast cancer, one encapsulating BVZ and the other encapsulated doxorubicin and decorated with a anti-HER2 antibody [16].

Overall, based on these previous studies and on the recognized problems associated to monoclonal antibodies-based cancer treatments, the aim to this work was to develop and characterize a nanocarrier that would potentially help BVZ to overcome the previously described biological barriers. For this purpose, we chose hyaluronic acid-based ENCPs. These ENCPs were expected to protect the drug from degradation, reduce its side effects and bypass the typically observed resistance mechanisms, thanks to the BVZ intracellular delivery. Positively charged nanocomplexes were formed through a simple surfactant/polyelectrolyte complexation procedure, and where then coated with a layer of HA, thus forming the ENCPs. A similar approach was reported for Trastuzumab, which was complexed with a catechin derivative (a PEG modified natural phenol) through both, hydrophobic interactions and hydrogen bonds. The results of the in vivo studies indicated the performance of the nano-complexes in terms of reducing tumor growth and favoring tumor accumulation. The nanocarrier also increased the half-life of the antibody [13].
The ENCPs described here exhibit the capacity to associate significant amounts of BVZ (up to 375 µg, Figure 3.2) while preserving its functionality. A release behavior typical of polyelectrolytes complexes was observed with an initial burst release in the first two hours [25,26]. This burst effect could be related to the release of the protein located on the surface of the ENCPs, as observed for other nanosystems [27,28]. The osmolarity and/or the presence of proteins in the incubation medium (SBF) in which the release was evaluated could have also played a role in the release of the antibody [29–31].

The HA ENCPs with a high BVZ content (375 µg) resulted unstable upon storage at 4°C in suspension whereas those with a lower BVZ content (75 µg) were stable at least one week (Figure 3.6). This is in line with literature, where a concentration dependent aggregation upon the storage of antibodies formulations is described [32]. Freeze-drying was also tested as an option for storing the ENCPs. Trehalose was used as cryo-protectant agent based on its ability to form a glass that slows down the molecular mobility of proteins, avoiding their degradation and aggregation [33]. A 10% trehalose concentration was found to preserve the physico-chemical properties of BVZ-loaded HA ENCPs (75 µg). The same conditions could not be used for storing BVZ-loaded HA ENCPs (375 µg) (aggregates

were obtained after resuspension). In this case, a combination of trehalose and PEG-400 was needed in order to preserve the physico-chemical properties (Table 3.4).

BVZ-loaded HA ENCPs (375 µg) were then selected and tested for their in vitro cytotoxicity on breast cancer VEGF producing cells (MDA-MB-231). When both the HA ENCPs (BVZ-loaded or not) and the LAE were used, a concentration-dependent toxicity was observed. Since the only common component between the three groups is the LAE, it is highly probable that this surfactant is the principal source of toxicity. It is well known that cationic surfactants are more cytotoxic than the anionic or non-ionic ones [34–36]. A straight-forward way to reduce the toxicity of the formulation may involve its purification by tangential filtration in order to eliminate the excess of LAE present in the formulation.

In vitro internalization assays have also been done for evaluating the ability of the nanocarrier for the delivery of BVZ inside the cells. It is well documented that the VEGF-A intracellular pool is fundamental for cancer cells growth, survival, migration and invasion [37–40]. Blocking this target could also avoid the recruitment of bone marrow-derived cells progenitors, indicated as a source of resistance to BVZ therapy [15]. The results of this study showed that both the ENCPs and the physical mixture of LAE and BVZ, are able to facilitate the apparent internalization of the antibody by the cancer cells. Since the ability of cationic surfactants to enhance cellular permeation is known [41,42], more studies are needed in order to understand the real effect of the ENCPs on the cellular uptake of BVZ and for discriminating the fraction of antibody internalized or attached to the surface of the cells. It would be also interesting to understand the potential mechanism of uptake of the nanosystems and to evaluate the role of hyaluronic acid in the process.

The effect of free BVZ and BVZ-loaded HA ENCPs on the mRNA expression of specific genes (the h-VEGF family and of one of the receptors involved in their recognition, h-KDR) referred to the BVZ targeted molecular pathways was also evaluated. This was also done for understanding if the apparent internalization of BVZ influences the expression of these genes.

VEGF-A is the principal protein involved in angiogenic processes. It is released by tumor cells, macrophages and endothelial cells and binds to specific receptors. i.e. KDR and Flt-1, with KDR being the mainly used signaling receptor [43]. These receptors are located on the surface of endothelial cells and upon the binding of VEGF-A activate a series of downstream signals which stimulate endothelial cells proliferation (i.e. angiogenesis) [44]. Some works also reported the presence of Flt-1 on breast cancer cells membrane and its role in promoting their growth [45]. The other VEGF isoforms are involved in biological pathways like cell survival (VEGF-B) and lymphoangiogenesis (VEGF-C and VEGF-D) [46]. We also decided to study the expression of these isoforms, since it is recognized that may replace the function of VEGF-A when blocked [47–49]. Based on this information in this study we investigated the potential effects of the ENCPs on the mRNA expression of VEGF-A, VEGF.B, VEGF C and KDR. The results showed that some minor effects were observed at 48 hours post-treatment, however these effects reverted at 72 hours. Probably, the most interesting result from this set of experiments was the one observed for BVZ-loaded HA ENCPs on the expression of VEGF-A (Figure 3.9.A). After a 48 hours exposure the expression levels of the gene decrease

compared to the time 24 hours, while the same effect was not observed for control groups (free BVZ and blank HA ENCPs). More detailed experiments using DNA microarrays would be necessary for confirming the observed variations and their relation with the protein expression pattern [50,51]. It would be also interesting to quantify the amount of soluble and intracellular h-VEGF-A before and after the treatment with the BVZ-loaded HA ENCPs in order to assess the capacity of the antibody to block the intracellular pool of h-VEGF-A and, hence, to overcome resistance and enhance anti-cancer effects [20,52].

An in vivo efficacy experiment was also performed. The results showed that after the intraperitoneal treatment of tumor-bearing mice with BVZ, either in a free form or associated to HA ENCPs, a minor but statistically significant reduction in the tumor growth was observed (from the day 19, $p<0.05$ or lower, see Figure 3.10). However, no significant differences were observed when treating the tumor bearing mice with the BVZ-loaded HA ENCPs or the free drug. Several explanations could be given to the limited response observed, one of which could be related to the modality of administration. In humans, BVZ is administered intravenously at a high dose (10-20 mg/kg), while in the experiment reported here we use an intraperitoneal administration of a relatively low dose (6.3 mg/kg). In such a situation, part of the drug could be lost due its passage to the liver and also to the lymphatic system [53,54]. Overall, the subsequent biodistribution and access to the tumor tissue might explain the limited efficacy of both, the free and the encapsulated BVZ [55,56]. The abnormal tumor vasculature and stromal matrix could have also been a reason for the inefficient tumor drug accumulation [57–59]. For example, it has been reported that breast cancer's extracellular matrix is 10 time stiffer than in a normal breast tissue [59,60]. Interestingly, Ho and co-workers analyzed in detail the blood vessels and extracellular matrix structures for MDA-MB-231 orthotopic mammary fat pad tumors (the same used in our in vivo model). They showed the presence of small, sparse and thick blood vessels, which lead to low accumulation of nanocarriers in the tumor [61]. Also, they observed an accumulation of interstitial fluid at the tumor level and a thicker basement membrane, facts which further limit the penetration of macromolecules and nanocarriers. In this regard, biodistribution experiments should be done to study the accumulation of the BVZ-loaded HA ENCPs at the tumor level.

Finally, the development of resistance mechanisms by the tumor could also be a reasonable explanation to the unsuccessful therapy. Several works proved the initial benefits of the anti-angiogenic therapies, followed by the further re-growth of the tumor [11,62,63]. An example is given by the work of Hanahan and co-workers, that after measuring a first decrease in vascular density 10 days after the treatment with an anti-VEGF antibody, observed new angiogenic events. They showed that the tumor vessels re-growth is due to the increased expression of other pro-angiogenc factors belonging to the FGF family [64]. In a different work, it was shown that the early treatment of glioblastoma with BVZ induces the late proliferation of TAMs (tumor associated macrophages), which cause resistance to the antibody [65]. Finally, a work by Becheritat and Valamanesh, showed that colorectal cancer-bearing mice treated with BVZ developed an increased pericytes coverage of the blood vessels, which resulted in an increased resistance [66]. Further experiments should be done to investigate if and which type of resistance mechanisms is implicated here and how to improve the properties of the nanocarrier for overcoming this issue.

It is worth to mention that even if no effects have been shown regarding tumor growth and size, it would be interesting to measure parameters like the amount of VEGF-A in the tumor tissue, the vascular density and normalization and the pericytes coverage of the vessels, to understand if the treatment confer advantages which cannot be appreciated only measuring the tumor size [67]. A longer monitoring of the tumor size could have also been necessary, since often the effect of an anticancer drug is observed after a longer time period [16,68,69]

Finally, it could be concluded that the use of a higher dose (the used one was 6.3 mg/kg), an earlier treatment (e.g. 1 or 2 days post-tumor cells-injection) or a combination therapy could provide more satisfactory data in terms of the efficacy of the ENCPs-based treatment. In fact, the few in vivo works showing a successful results with nano-encapsulated BVZ use the antibody in combination with other drugs and report that the intracellular delivery of BVZ could be the reason for the efficacious treatment [15–17].

5. Conclusions

A potential nanocarrier for the delivery of BVZ consisting of a nanocomplex of HA and LAE, surrounded by a HA coating is reported. The resulting nanostructure named as HA ENCPs was able to hold a significant amount of BVZ. The HA ENCPs were stable in simulated biological fluids and could be free-dried in order to preserve their stability. Despite these appealing pharmaceutical properties, the resulting BVZ formulation did not result more efficacious that the free BVZ after intraperitoneal administration to mice. Subsequent biodistribution and high dose *in vivo* response experiments are expected in order to assess the value of this formulation.

Acknowledgments

This work was supported by the European Union's Horizon 2020 - Research and Innovation Framework Programme under the Marie Sklodowska - Curie Grant agreement No. 642028 (NABBA) and by the Grant Nº SAF2017-86634-R (Nano-inmunoterapias integradas dirigidas a dianas intracelulares relevantes en cancer) from the Ministry of Economy of Spain.

Bibliography

[1] A. Coulson, A. Levy, Monoclonal Antibodies in Cancer Therapy : Mechanisms, Successes and Limitations, West Indian Med. J. 63 (2014) 650–654. doi:10.7727/wimj.2013.241.

[2] C. Guo, Y. Chen, W. Gao, A. Chang, Y. Ye, W. Shen, Y. Luo, S. Yang, P. Sun, R. Xiang, N. Li, Liposomal Nanoparticles Carrying anti-IL6R Antibody to the Tumour Microenvironment Inhibit Metastasis in Two Molecular Subtypes of Breast Cancer Mouse Models, Theranostics. 7 (2017) 775–778. doi:10.7150/thno.17237.

[3] A. Kim, Y. Miura, T. Ishii, O. Mutaf, N. Nishiyama, H. Cabral, K. Kataoka, Intracellular Delivery of Charge-Converted Monoclonal Antibodies by Combinatorial Design of Block/Homo Polyion Complex Micelles, Biomacromolecules. (2016) 446–453. doi:10.1021/acs.biomac.5b01335.

[4] A.M. Scott, J.D. Wolchok, L.J. Old, Antibody therapy of cancer, Nature. 12 (2012) 278–287. doi:10.1038/nrc3236.

[5] L.M. Ellis, Mechanisms of Action of Bevacizumab as a Component of Therapy for Metastatic Colorectal Cancer, Semin. Oncol. 33 (2006) S1–S7. doi:10.1053/j.seminoncol.2006.08.002.

[6] D.M. Gilkes, G.L. Semenza, D. Wirtz, Hypoxia and the extracellular matrix: drivers of tumour metastasis, Nat. Rev. Cancer. 14 (2014) 430–439. doi:10.1038/nrc3726.

[7] H. Gerber, N. Ferrara, Pharmacology and Pharmacodynamics of Bevacizumab as Monotherapy or in Combination with Cytotoxic Therapy in Preclinical Studies, Cancer Res. 65 (2005) 671–681.

[8] P. Carmeliet, R.K. Jain, Principles and mechanisms of vessel normalization for cancer and other angiogenic diseases, Nat. Rev. Drug Discov. 10 (2011) 417–427. doi:10.1038/nrd3455.

[9] J. Folkman, Tumor angiogenesis: therapeutic implications, N. Engl. J. Med. 285 (1971) 1182–1186.

[10] F. Sousa, A. Cruz, P. Fonte, I.M. Pinto, M.T. Neves, B. Sarmento, A new paradigm for antiangiogenic therapy through controlled release of bevacizumab from PLGA nanoparticles, Nat. Sci. Reports. 7 (2017) 1–13. doi:10.1038/s41598-017-03959-4.

[11] G. Bergers, D. Hanahan, Modes of resistance to anti-angiogenic therapy, Nat. Rev. Drug Discov. 8 (2008) 592–603. doi:10.1038/nrc2442.

[12] A.J. Montero, M. Escobar, G. Lopes, S. Gluck, C. Vogel, Bevacizumab in the Treatment of Metastatic Breast Cancer: Friend or Foe?, Curr. Oncol. Rep. 14 (2013) 1–11. doi:10.1007/s11912-011-0202-z.

[13] J.E. Chung, S. Tan, S.J. Gao, N. Yongvongsoontorn, S.H. Kim, J.H. Lee, H.S. Choi, H. Yano, L. Zhuo, M. Kurisawa, J.Y. Ying, Self-assembled micellar nanocomplexes comprising green tea catechin derivatives and protein drugs for cancer therapy, Nat. Nanotechnol. 9 (2014) 907–912. doi:10.1038/nnano.2014.208.

[14] F. Ordikhani, M. Uehara, V. Kasinath, L. Dai, S.K. Eskandari, B. Bahmani, M. Yonar, J.R. Azzi, Y. Haik, P.T. Sage, G.F. Murphy, N. Annabi, T. Schatton, I. Guleria, R. Abdi, Targeting antigen-presenting cells by anti – PD-1 nanoparticles augments antitumor immunity, JCI Insight. 3 (2018) 1–17. doi:doi: 10.1172/jci.insight.122700.

[15] S. Tangutoori, B.Q. Spring, Z. Mai, A. Palanisami, L.B. Mensah, T. Hasan, Simultaneous delivery of cytotoxic and biologic therapeutics using nanophotoactivatable liposomes enhances treatment efficacy in a mouse model of pancreatic cancer, Nanomedicine Nanotechnology, Biol. Med. 12 (2016) 223–234. doi:10.1016/j.nano.2015.08.007.

[16] Y. Tang, F. Soroush, Z. Tong, M.F. Kiani, B. Wang, Targeted multidrug delivery system to overcome chemoresistance in breast cancer, Int. J. Nanomedicine. 12 (2017) 671–681. doi:10.2147/IJN.S124770.

[17] B. Spring, Z. Mai, P. Rai, S. Chang, T. Hasan, Theranostic Nanocells for Simultaneous Imaging and Photodynamic therapy of Pancreatic Cancer, Opt. Methods Tumor Treat. Detect. Mech. Tech. Photodyn. Ther. 7551 (2010) 1–11. doi:10.1117/12.843725.

[18] D.A. Ossipov, Nanostructured hyaluronic acid-based materials for active delivery to cancer, Expert Opin. Drug Deliv. 7 (2010) 681–703. doi:10.1517/17425241003730399.

[19] G. Tzircotis, R.F. Thorne, C.M. Isacke, Chemotaxis towards hyaluronan is dependent on CD44 expression and modulated by cell type variation in CD44-hyaluronan binding, J. Cell Sci. 118 (2005) 5119–5128. doi:10.1242/jcs.02629.

[20] A.R. Srinivasan, A. Lakshmikuttyamma, S.A. Shoyele, Investigation of the Stability and Cellular Uptake of Self-Associated Monoclonal Antibody (MAb) Nanoparticles by Non-Small Lung Cancer Cells, Mol. Pharm. 10 (2013) 3275–3284. doi:10.1021/mp3005935.

[21] Uniprot, VEGFR-2 protein. https://www.uniprot.org/uniprot/P35968.

[22] R.A. Beckman, L.M. Weiner, H.M. Davis, Antibody constructs in cancer therapy. Protein Engineering Strategies to Improve Exposure in Solid Tumors, Cancer. 109 (2007) 170–179.

doi:10.1002/cncr.22402.
[23] A. Gdowski, A. Ranjan, A. Mukerjee, J. Vishwanatha, Development of Biodegradable Nanocarriers Loaded with a Monoclonal Antibody, Int. J. Mol. Sci. 16 (2015) 3990–3995. doi:10.3390/ijms16023990.
[24] H. Deng, K. Song, X. Zhao, Y. Li, F. Wang, J. Zhang, A. Dong, Z. Qin, Tumor Microenvironment Activated Membrane Fusogenic Liposome with Speedy Antibody and Doxorubicin Delivery for Synergistic Treatment of Metastatic Tumor, ACS Appl. Mater. Interfaces. 9 (2017) 9315–9326. doi:10.1021/acsami.6b14683.
[25] Y. Parajo, I. D'Angelo, A. Welle, M. Garcia-Fuentes, M.J. Alonso, Hyaluronic acid/Chitosan nanoparticles as delivery vehicles for VEGF and PDGF-BB, Drug Deliv. 17 (2010) 596–604. doi:10.3109/10717544.2010.509357.
[26] A. Umerska, K.J. Paluch, M.J.S. Martinez, O.I. Corrigan, C. Medina, L. Tajber, Self-assembled hyaluronate/protamine polyelectrolyte nanoplexes: synthesis, stability, biocompatibility and potential use as peptide carriers, J. Biomed. Nanotechnol. 10 (2014) 3658–3673. doi:10.1166/jbn.2014.1878.
[27] Y. Yeo, K. Park, Control of Encapsulation Efficiency and Initial Burst in Polymeric Microparticle Systems, Arch. Pharm. Res. 27 (2004) 1–12.
[28] Q. Gan, T. Wang, Chitosan nanoparticle as protein delivery carrier — Systematic examination of fabrication conditions for efficient loading and release, Colloids Surfaces B. 59 (2007) 24–34. doi:10.1016/j.colsurfb.2007.04.009.
[29] I. Santalices, A. Gonella, D. Torres, M. Jos, Advances on the formulation of proteins using nanotechnologies, J. Drug Deliv. Sci. Technol. 42 (2017) 155–180. doi:10.1016/j.jddst.2017.06.018.
[30] W. Tiyaboonchai, J. Woiszwillo, R.C. Sims, C.R. Middaugh, Insulin containing polyethylenimine-dextran sulfate nanoparticles, Int. J. Pharm. 255 (2003) 139–151. doi:10.1016/S0378-5173(03)00055-3.
[31] M. Alonso-Sande, M. Cuna, C. Remunàn-Lopez, D. Teijeiro-Osorio, J.L. Alonso-Lebrero, M. Alonso, Formation of New Glucomannan - Chitosan Nanoparticles and Study of Their Ability To Associate and Deliver Proteins, Macromolecules. 39 (2006) 4152–4158.
[32] W. Wang, S. Singh, D.L. Zeng, K. King, S. Nema, W.E.T. Al, Antibody Structure , Instability , and Formulation, J. Pharm. Sci. 96 (2007) 1–26. doi:10.1002/jps.
[33] S. Singh, P. Kolhe, A.P. Mehta, S.C. Chico, A.L. Lary, M. Huang, Frozen State Storage Instability of a Monoclonal Antibody: Aggregation as a Consequence of Trehalose Crystallization and Protein Unfolding, Pharm. Res. 28 (2011) 873–885. doi:10.1007/s11095-010-0343-z.
[34] N. Vlachy, D. Touraud, J. Heilmann, W. Kunz, Determining the cytotoxicity of catanionic surfactant mixtures on HeLa cells, Colloids Surfaces B Biointerfaces. 70 (2009) 278–280. doi:10.1016/j.colsurfb.2008.12.038.
[35] R.L. Grant, C. Yao, D. Gabaldon, D. Acosta, Evaluation of surfactant cytotoxicity potential by primary cultures of ocular tissues: I . Characterization of rabbit corneal epithelial cells and initial injury and delayed toxicity studies, Toxicology. 76 (1992) 153–176. doi:10.1016/0300-483X(92)90162-8.
[36] S. Inàcio, K.A. Mesquita, M. Baptista, In Vitro Surfactant Structure-Toxicity Relationships : Implications for Surfactant Use in Sexually Transmitted Infection Prophylaxis and Contraception, PLoS One. 6 (2011) 1–15. doi:10.1371/journal.pone.0019850.
[37] M. Björndahl, R. Cao, A. Eriksson, Y. Cao, Blockage of VEGF-Induced Angiogenesis by Preventing VEGF Secretion, Circ. Res. 94 (2004) 1443–50. doi:10.1161/01.RES.0000129194.61747.bf.
[38] R. Bhattacharya, X. Ye, R. Wang, X. Ling, M. Mcmanus, F. Fan, D. Boulbes, L.M. Ellis, Intracrine VEGF Signaling Mediates the Activity of Pro-survival Pathways in Human Colorectal Cancer Cells, Cancer Res. 76 (2017) 3014–3024. doi:10.1158/0008-5472.CAN-15-1605.

[39] T. Lee, S. Seng, M. Sekine, C. Hinton, Y. Fu, H.K. Avraham, S. Avraham, Vascular Endothelial Growth Factor Mediates Intracrine Survival in Human Breast Carcinoma Cells through Internally Expressed VEGFR1/ FLT1, Plos Med. 4 (2007) 1101–1116. doi:10.1371/journal.pmed.0040186.

[40] R. Bhattacharya, F. Fan, R. Wang, X. Ye, L. Xia, D. Boulbes, L.M. Ellis, Intracrine VEGF signalling mediates colorectal cancer cell migration and invasion, Br. J. Cancer. 117 (2017) 848–855. doi:10.1038/bjc.2017.238.

[41] A. Xu, M. Yao, G. Xu, J. Ying, W. Ma, B. Li, Y. Jin, A physical model for the size-dependent cellular uptake of nanoparticles modified with cationic surfactants, Int. J. Nano. 7 (2012) 3547–3554.

[42] C. Peetla, V. Labhasetwar, Effect of Molecular Structure of Cationic Surfactants on Biophysical Interactions of the Surfactant-modified Nanoparticles with a Model Membrane and Cellular Uptake, Int. J. Nanomedicine. 25 (2010) 2369–2377. doi:10.1021/la803361y.Effect.

[43] D. Donovan, J.H. Harmey, D. Toomey, TGFβ-1 Regulation of VEGF Production by Breast Cancer Cells, Ann. Surg. Oncol. 4 (1997) 621–627.

[44] M. Shibuya, Vascular Endothelial Growth Factor (VEGF) and Its Receptor (VEGFR) Signaling in Angiogenesis : A Crucial Target for, Genes Cancer. 2 (2011) 1–5. doi:10.1177/1947601911423031.

[45] Y. Wu, A.T. Hooper, Z. Zhong, L. Witte, P. Bohlen, S. Rafii, D.J. Hicklin, The vascular endothelial growth factor receptor (VEGFR-1) supports growth and survival of human breast carcinoma, Int. J. Cancer. 1529 (2006) 1519–1529. doi:10.1002/ijc.21865.

[46] V. Gardner, O.M. Chikezie, Y. Lu, Anti-VEGF Therapy in Cancer: A Double-Edged Sword, in: Physiol. Pathol. Angiogenesis-Signalling Mech. Target. Ther., 2016: pp. 385–410.

[47] M. Chien, C. Ku, G. Johansson, M. Chen, M. Hsiao, J. Su, K. Hua, L. Wei, M. Kuo, Vascular endothelial growth factor-C (VEGF-C) promotes angiogenesis by induction of COX-2 in leukemic cells via the VEGF-R3/JNK/AP-1 pathway, Carcinogeneis. 30 (2013) 2005–2013. doi:10.1093/carcin/bgp244.

[48] A.J. Weickhardt, D.S. Williams, C.K. Lee, F. Chionh, J. Simes, C. Murone, K. Wilson, M.M. Parry, K. Asadi, A.M. Scott, C.J. Punt, I.D. Nagtegaal, T.J. Price, J.M. Mariadason, N.C. Tebbutt, Vascular endothelial growth factor D expression is a potential biomarker of bevacizumab benefit in colorectal cancer, Br. J. Cancer. 113 (2015) 37–45. doi:10.1038/bjc.2015.209.

[49] F. Zhang, Z. Tang, X. Hou, J. Lennartsson, Y. Li, A.W. Koch, P. Scotney, C. Lee, P. Arjunan, L. Dong, A. Kumar, T.T. Rissanen, B. Wang, N. Nagai, P. Fons, R. Fariss, Y. Zhang, E. Wawrousek, G. Tansey, J. Raber, G. Fong, H. Ding, D.A. Greenberg, K.G. Becker, J. Herbert, A. Nash, S. Yla-herttuala, Y. Cao, R.J. Watts, X. Li, VEGF-B is dispensable for blood vessel growth but critical for their survival , and VEGF-B targeting inhibits pathological angiogenesis, PNAS. 106 (2009) 6152–6157.

[50] G. Pentheroudakis, V. Kotoula, E. Fountzilas, G. Kouvatseas, G. Basdanis, I. Xanthakis, T. Makatsoris, E. Charalambous, D. Papamichael, E. Samantas, P. Papakostas, D. Bafaloukos, E. Razis, C. Christodoulou, I. Varthalitis, P. Nicholas, G. Fountzilas, A study of gene expression markers for predictive significance for bevacizumab benefit in patients with metastatic colon cancer: a translational research study of the Hellenic Cooperative Oncology Group (HeCOG), BMC Cancer. 14 (2014) 1–10. doi:10.1186/1471-2407-14-111.

[51] M. Filali, L. V Ly, G.P.M. Luyten, M. Versluis, H.E. Grossniklaus, P.A. Van, Bevacizumab and intraocular tumors : an intriguing paradox, Mol. Vis. 12 (2012) 2454–2467.

[52] F. Sousa, A. Cruz, P. Fonte, I.M. Pinto, M.T. Neves-, A new paradigm for antiangiogenic therapy through controlled release of bevacizumab from PLGA nanoparticles, (2017) 1–13. doi:10.1038/s41598-017-03959-4.

[53] K. Hirano, C.A. Hunt, Lymphatic Transport of Liposome-Encapsulated Agents: Effects of Liposome Size Following Intraperitoneal administration, J. Pharm. Sci. 74 (1985) 915–921.

doi:10.1002/jps.2600740902.
[54] Y. Deng, F. Yang, E. Cocco, E. Song, J. Zhang, J. Cui, M. Mohideen, S. Bellone, A.D. Santin, W.M. Saltzman, Improved i. p. drug delivery with bioadhesive nanoparticles, PNAS. 113 (2016) 11453–11458. doi:10.1073/pnas.1523141113.
[55] F. Marcucci, M. Bellone, C. Rumio, A. Corti, Approaches to improve tumor accumulation and interactions between monoclonal antibodies and immune cells, MAbs. 5 (2013) 34–46.
[56] D. Rosenblum, N. Joshi, W. Tao, J.M. Karp, D. Peer, Progress and challenges towards targeted delivery of cancer therapeutics, Nat. Commun. 9 (2018) 1–12. doi:10.1038/s41467-018-03705-y.
[57] Y. Nakamura, A. Mochida, P.L. Choyke, H. Kobayashi, Nanodrug Delivery: Is the Enhanced Permeability and Retention Effect Sufficient for Curing Cancer?, Bioconjug. Chem. 27 (2016) 2225–2238. doi:10.1021/acs.bioconjchem.6b00437.
[58] F. Marcucci, A. Corti, How to improve exposure of tumor cells to drugs — Promoter drugs increase tumor uptake and penetration of effector drugs, Adv. Drug Deliv. Rev. 64 (2011) 53–68. doi:10.1016/j.addr.2011.09.007.
[59] I. Choi, R. Strauss, M. Richter, C. Yun, A. Lieber, Strategies to increase drug penetration in solid tumors, Front. Oncol. 3 (2013) 1–18. doi:10.3389/fonc.2013.00193.
[60] A.E. Place, S.J. Huh, K. Polyak, The microenvironment in breast cancer progression : biology and implications for treatment, Breast Cancer Res. 13 (2011) 1–11.
[61] K.S. Ho, P.C. Poon, S.C. Owen, M.S. Shoichet, Blood vessel hyperpermeability and pathophysiology in human tumour xenograft models of breast cancer: a comparison of ectopic and orthotopic tumours, BMC Cancer. 12 (2012) 1. doi:10.1186/1471-2407-12-579.
[62] L.M. Ellis, D.J. Hicklin, Pathways Mediating Resistance to Vascular Endothelial Growth Factor-Targeted Therapy, Mol. Pathways. 14 (2008) 6371–6376. doi:10.1158/1078-0432.CCR-07-5287.
[63] S. Loges, T. Schmidt, P. Carmeliet, Mechanisms of Resistance to Anti- Angiogenic Therapy and Development of Third-Generation Anti-Angiogenic Drug Candidates, Genes Cancer. 1 (2010) 12–25. doi:10.1177/1947601909356574.
[64] O. Casanovas, D.J. Hicklin, G. Bergers, D. Hanahan, Drug resistance by evasion of antiangiogenic targeting of VEGF signaling in late-stage pancreatic islet tumors, Cancer Cell. 8 (2005) 299–309. doi:10.1016/j.ccr.2005.09.005.
[65] B.A. Castro, P. Flanigan, A. Jahangiri, D. Hoffman, W. Chen, R. Kuang, M. De Lay, G. Yagnik, J.R. Wagner, S. Mascharak, M. Sidorov, S. Shrivastav, G. Kohanbash, H. Okada, M.K. Aghi, Macrophage migration inhibitory factor downregulation: a novel mechanism of resistance to anti-angiogenic therapy, Oncogene. 36 (2017) 3749–3759. doi:10.1038/onc.2017.1.
[66] S. Becherirat, F. Valamanesh, Discontinuous Schedule of Bevacizumab in Colorectal Cancer Induces Accelerated Tumor Growth and Phenotypic Changes, Transl. Oncol. 11 (2018) 406–415. doi:10.1016/j.tranon.2018.01.017.
[67] N. Zhang, G. Zhang, Y. Zheng, T. Wang, H. Wang, Effect of Avastin on the number and structure of tumor blood vessels of nude mice with A549 lung adenocarcinoma, Exp. Ther. Med. 8 (2014) 1723–1726. doi:10.3892/etm.2014.1991.
[68] E. Pham, M. Yin, C.G. Peters, C.R. Lee, D. Brown, P. Xu, S. Man, L. Jayaraman, E. Rohde, A. Chow, D. Lazarus, S. Eliasof, F.S. Foster, R.S. Kerbel, Preclinical Efficacy of Bevacizumab with CRLX101, an Investigational Nanoparticle – Drug Conjugate, in Treatment of Metastatic Triple-Negative Breast Cancer, Cancer Res. 76 (2016) 4493–4504. doi:10.1158/0008-5472.CAN-15-3435.
[69] S. Mollard, J. Ciccolini, D. Imbs, R. El Cheikh, D. Barbolosi, S. Benzekry, Model driven optimization of antiangiogenics+cytotoxics combination: application to breast cancer mice treated with bevacizumab+paclitaxel doublet leads to reduced tumor growth and fewer metastasis, Oncotarget. 8 (2017) 23087–23098.

Chapter V
General discussion

USC
UNIVERSIDADE
DE SANTIAGO
DE COMPOSTELA

Therapeutic proteins and peptides are highly specific and selective drugs whose importance has incredibly increased in the pharmaceutical market during the last decade [1]. Huge efforts have been made for developing protein-based anticancer drugs in order to reduce the side effects of classical chemotherapeutics and increase the specificity of the cancer therapy [2]. Lagassé and co-workers interestingly showed that between 2011 and 2016, 26% of the approved therapeutic proteins were developed for oncology (Figure 1) [1]. Moreover, around 48% of these approved drugs are monoclonal antibodies (mAbs), thus indicating the enormous potential of these biologics [1]. In fact, mAbs offer advantages in terms of specificity, potency, tolerance and dosing frequency, compared to conventional therapeutics [3]. Indeed, the production of biologicals has been optimized in the last years, enabling their cost-effective large scale production [4]. The good safety profile of these drugs as compared to that of chemotherapeutics has contributed to their rapid commercialization [4].

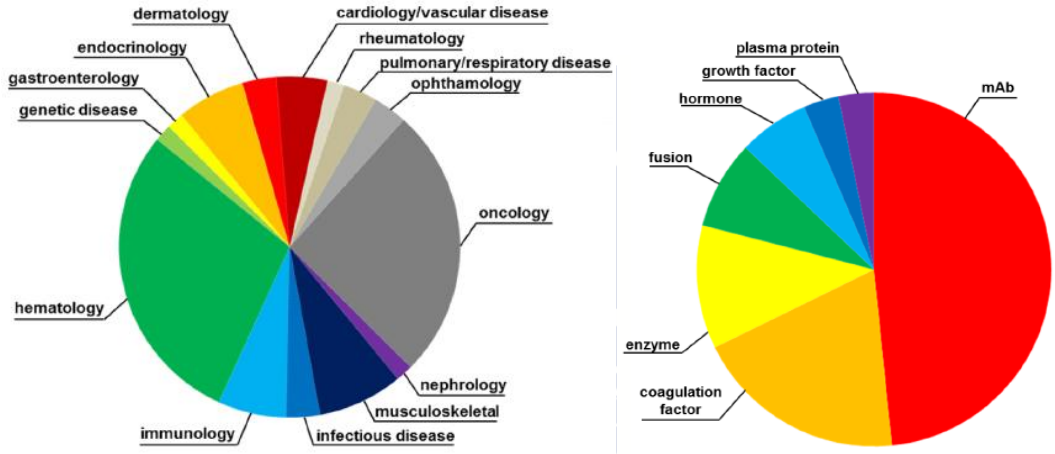

Figure 1. FDA approved therapeutic proteins between 2011 and 2016. The therapeutic areas and type of approved proteins are indicated. Image extracted from [1] *(creative commons license).*

However, several problems still need to be solved for the adequate exploitation of anti-cancer protein therapeutics. The **limited half-life** of some of these molecules is still one of the major drawbacks and the majority of the strategies explored up to now for extending their bioavailability include chemical modifications [5]. For example, a fusion protein based product (i.e. Zaltrap®) made by VEGFR1 and VEGFR2 fragments joined to an Fc domain (which extend their half-life) was approved by the FDA for the treatment of colorectal cancer [6].

Protein aggregation upon the contact with human serum has also been reported as one of the drawbacks for protein administration, as well as their **limited stability** in the certain biological conditions (i.e. low pH or presence of enzymes) [7,8].

Besides these problems, the major limitations of anti-cancer mAbs are related to their **poor tumor penetration** and **inability to target intracellular antigens**, to the development of **resistance mechanisms** and to their **immunogenicity** [9–14]. In fact, even if humanized antibodies are less immunogenic compared to other type of drugs or to their murine counterpart, they can still activate the immune system. [15–18].

The nanoencapsulation of therapeutic proteins appears as a promising solution for overcoming these problems. Indeed, the use of a nanocarrier may facilitate the targeting and penetration of proteins across the tumor tissue, enhancing the proteins accumulation at the target site, even at the intracellular level. It could also help to overcome the typically observed resistance mechanisms which cancer cells use for by-passing the effect of the anticancer drugs [19–22].

The main objective of this work has been to develop new HA-based nanocarriers, which could potentially help to solve the above indicated problems. Different nanocarriers were produced, all of them having in common two key components, i.e. ethyl lauroyl arginate (LAE) and hyaluronic acid (HA). LAE was chosen due to its amphiphilic properties and, hence, for the possibility of interacting with proteins through hydrophobic and electrostatic forces. Moreover, it is well known the ability of the surfactant in helping the cell membrane penetration of molecules and favor their endosomal escape [23–25]. On the other hand, HA was chosen because of its known protective role and its ability to interact with the CD44 receptors, overexpressed on the surface of some cancer cell lines (e.g. breast, lung, colorectal, gastric). This interaction was expected to facilitate the cell internalization of the nanocarriers by endocytosis [26–29].

Several formulation strategies were developed using model proteins (i.e. Bovine Serum Albumin, BSA, and an IgG) and the knowledge generated was, then, applied to the encapsulation of bevacizumab (BVZ). This formulation was intended to facilitate the targeting of the extracellular and intracellular pool of VEGF-A, the last one being partially responsible for the resistance to BVZ therapies [20,30,31]. Also, the nanocarrier could potentially reduce the side effects observed with the usual BVZ therapy [32,33] and could help the penetration of the drug at the tumor site, as shown for other nano-associated mAbs [22,34].

The developed nanocarriers were characterized for their physico-chemical properties, encapsulation efficiency, stability in simulated biological fluids, storage stability and release. Studies related to the structural stability of the encapsulated proteins were also performed in order to assess the protein functionality.

Initially, two different formulation strategies, film hydration and injection technique, were investigated for the production of the blank HA nanocomplexes (Figure 2). The injection technique was chosen over the film hydration due to its mildness (no solvents used) and simplicity. After selecting the proper amounts of HA and LAE (i.e. no aggregates formation, negative zeta potential and size around 200 nm or below), the way in which the components are added and the proper formulation media (MilliQ water or phosphate buffer), two different model proteins (i.e. BSA and IgG) were incorporated into the nanocomplexes. Subsequently, the coating of the nanocomplexes with additional polymers was evaluated as a strategy to improve the stability of the nanosystems upon contact with biological fluids (layer-by-layer PArg/HA ENCPs). As a result, three different prototypes associating the two model proteins were produced. Finally, the nanocarrier containing BVZ was developed based on the strategies developed for associating the two model proteins (Table 1).

The formulation strategies needed to be adapted for each specific protein associated [14,35]. For example, when the protocol used for producing BSA/BP-loaded HA nanocomplexes or BSA/IgG/MQ-loaded HA nanocomplexes (Figure 3.A) was used for the association of BVZ, aggregates were obtained. The adaptation of the procedure, decreasing the amount of HA and coating the nanocomplexes with an additional HA layer (Figure 3.C) was necessary for forming stable nanocomplexes.

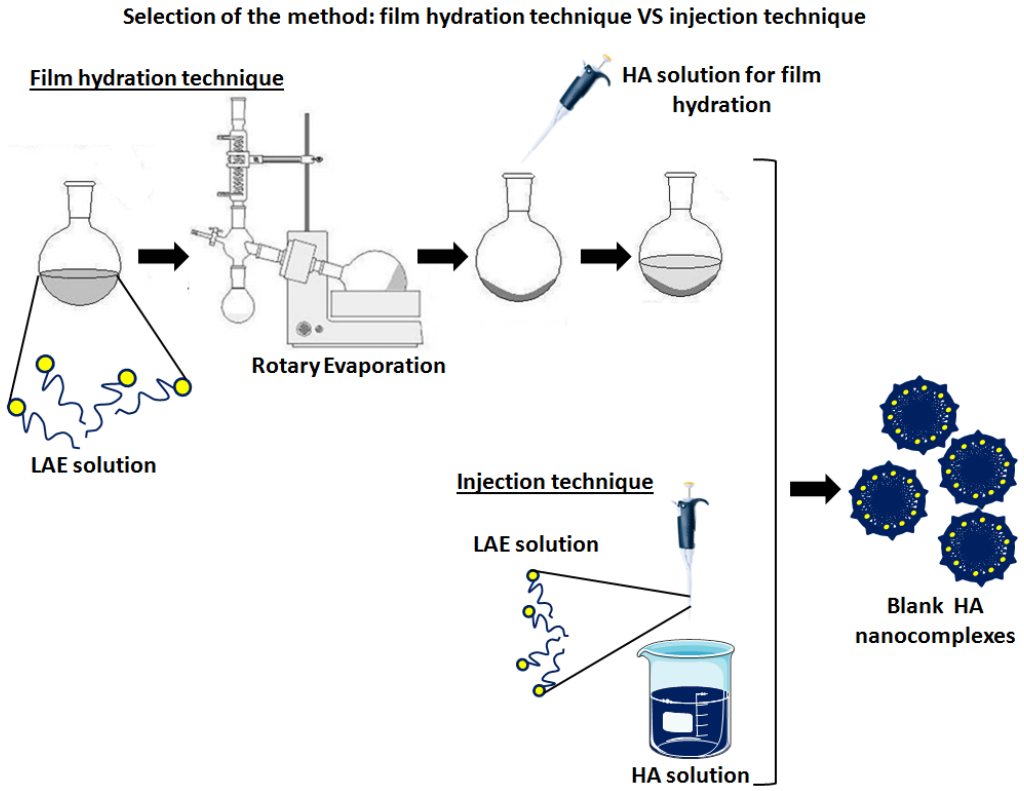

Figure 2. Scheme for the production of the blank HA nanocomplexes by the film hydration or the injection technique.

Table 1. Comparison of the characteristics of BSA/BP-loaded HA nanocomplexes, BSA/IgG/MQ-loaded HA nanocomplexes, layer-by-layer PArg/HA ENCPs and BVZ-loaded HA ENCPs. The formulation medium, the amounts and volumes of LAE and HA and the physico-chemical properties of the formulations are here indicated.

Formulation prototype	Formulation media	LAE amount (mg)	LAE volume (µL)	HA amount (mg)	HA volume (µL)	II HA layer	Size (nm)	ζ (mV)	% AE	% LC
BSA/BP-loaded HA nanocomplexes	Phosphate buffer pH 7.2	2	250	2	500	No	292 ± 36	-31±4	97	33
BSA/IgG/MQ-loaded HA nanocomplexes	MilliQ water	2	250	2	500	No	220 ± 22	-26±4	98*	2.4*
Layer-by-layer PArg/HA ENCPs	MilliQ water	2	250	2	500	Yes**	191±16	-25±1	85*	1.7*
BVZ-loaded HA ENCPs	MilliQ water	2	250	0.25	500	Yes***	179±8	-27±1	42 or 48****	7.3 or 1.5****

AE (%): Association efficiency (%); LC (%): Loading capacity (%) (experimental); BSA: bovine serum albumin; BP: nanocomplexes formulated in phosphate buffer; MQ: nanocomplexes formulated in milliQ water; BVZ: bevacizumab; ENCPs: enveloped nanocomplexes

**AE (%) and LC (%) related to the IgG*

*** The BSA/IgG/MQ-loaded HA nanocomplexes were coated firstly with poly-L-arginine (PArg) and then with a further layer of HA (forming the layer-by-layer PArg/HA ENCPs) for stabilizing the particles in serum containing biological fluids (RPMI supplemented with FBS). 450 µL of Poly-L-Arginine (1.3 mg/mL) were added over 450 µL of the BSA/IgG/MQ-loaded nanocomplexes forming the PArg-coated HA nanocomplexes; 200 µL of this nanoformulation were withdrawn and 200 uL of a HA solution (3.1 mg/mL) was then added on the top, forming the layer-by-layer PArg/HA ENCPs.*

****500 µL of an HA solution (2 mg/mL) were added over 500 µL of the positively charged nanocomplexes containing BVZ for forming the BVZ-loaded ENCPs (see Figure 3.C here below).*

*****Two different BVZ-loaded HA ENCPs have been used for performing the experiments, BVZ-loaded HA ENCPs (75 µg) (corresponding to a AE (%) of 42% and protein LC (%) of 1.5%) and BVZ-loaded ENCPs (375 µg) (corresponding to a AE (%) of 48% and a protein LC (%) of 7.3%).*

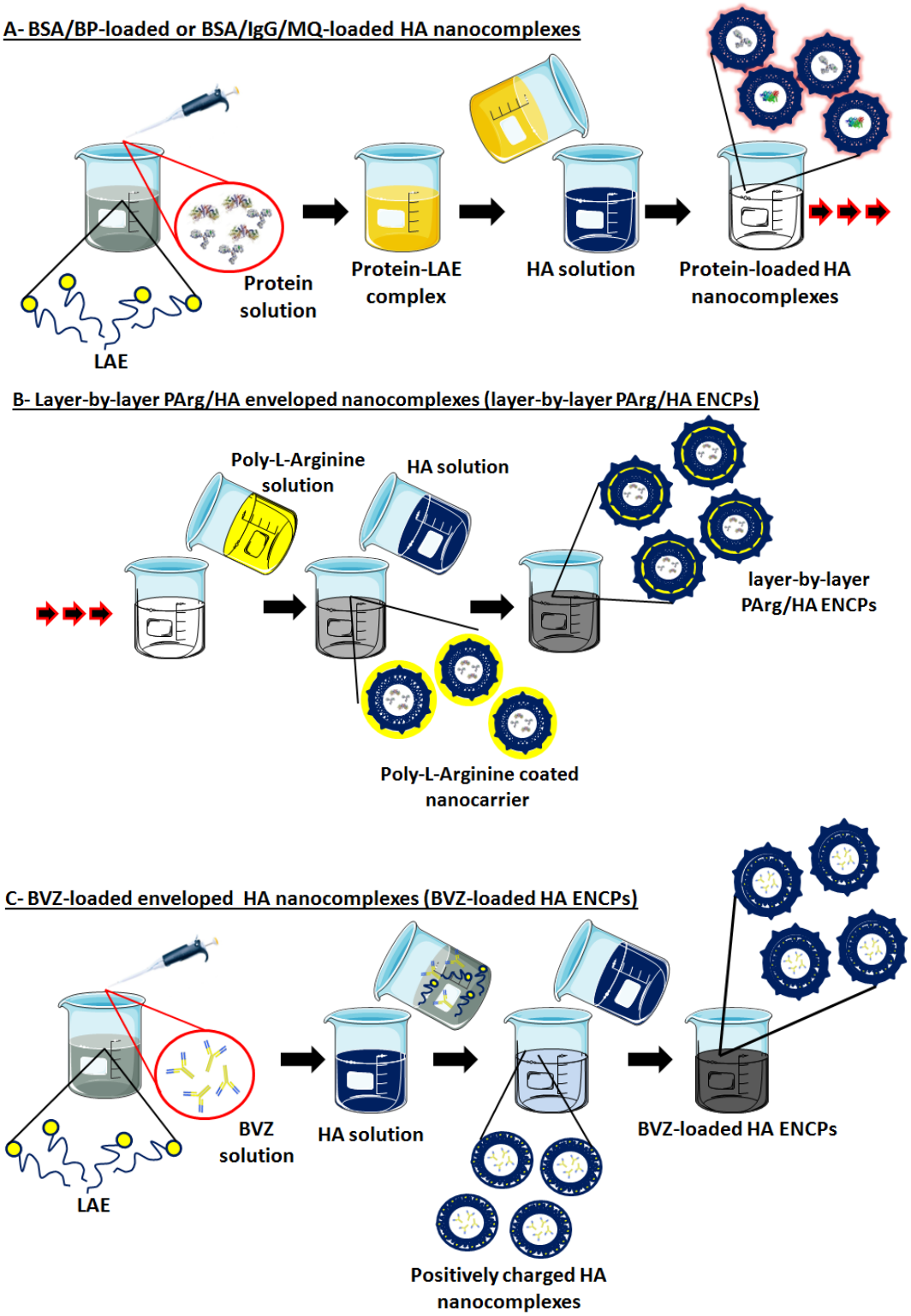

Figure 3. Formulation strategies used for producing the protein-loaded HA nanocarriers. The injection technique was used for producing all the nanosystems and it was adapted based on the influence of the different proteins on the formulation strategy. A) formation of the BSA/BP or BSA/IgG/MQ-loaded HA nanocomplexes; B) formation of the layer-by-layer PArg/HA ENCPs; the BSA/IgG/MQ-loaded nanocomplexes (A) are the core of this formulation which were further coated with multiple polymer layers (Poly-L-Arginine and HA). C) BVZ- loaded enveloped HA nanocomplexes (BVZ-loaded HA ENCPs).

Size of the nanosystems

Table 1 reports the main differences among the strategies used for producing the different nanocarriers' prototypes. It also highlights how the size of the selected prototypes varies based on the used formulation strategy. For example, the presence of salts in the formulation media increases the size of the nanocomplexes (as it is the case of BSA/BP-loaded HA nanocomplexes, produced in phosphate buffer). The presence of ions screens the charges on both LAE and HA, and leads to the co-precipitation of the protein and the polymers in the form of bigger complexes [36–38].

Interestingly, when BSA was used, a complex between the protein and LAE was formed (see Figure 4), while it did not happen with BVZ. This is probably due to the different properties of the proteins (Table 2) and, hence, their different interaction with the polymers. At neutral pHs, BSA is more prone than antibodies to interact with the cationic head of LAE (e.g. the pI of BSA is 4.7, while the one of BVZ is 8.3). In addition, BSA may interact through hydrophobic forces (i.e. in the human body works as a fatty acid transporter) [39]. These are probably the reasons for the formation of a measurable complex with the nanosystems containing BSA.

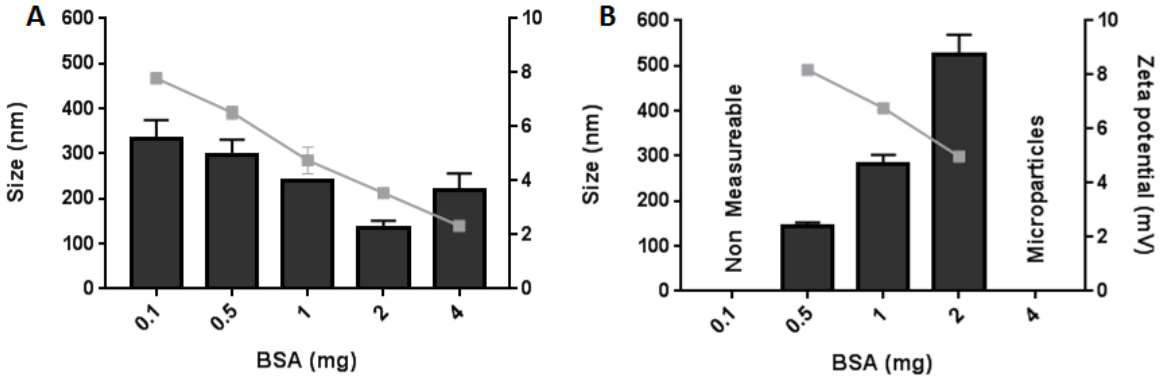

Figure 4. Formation of positively charged nanocomplexes between the BSA and the LAE when the components were dissolved in milliQ water, MQ, (graph A) or phosphate buffer, BP, (graph B).

The presence of multiple layers (layer-by-layer PArg-HA ENCPs) decreased the size of the nanosystem, compared to the non-coated one (BSA/IgG/MQ-loaded HA nanocomplexes). This is probably due to the electrostatic compression exerted by the surface attached polymer layers which leads to the formation of a more compact structure, as already observed with other multiple layered nanoparticles [40,41].

Interestingly, the BVZ-loaded HA ENCPs showed the lowest size, probably due to the absence of BSA and to the lower HA amount used for forming the core of the nanocomplexes.

With all the developed formulation strategies, round shaped nanocarriers were formed, suggesting that the interaction between LAE and HA leads to spherical systems, irrespective to the used formulation strategy (Figure 5).

Stability of the formulations in simulated biological fluids (SBF)

Differences related to the stability of the formulations in simulated biological fluids (SBF) were also detected. In fact, BSA resulted fundamental for conferring stability to the IgG-encapsulating HA

nanocomplexes once diluted in SBF containing salts (i.e. PBS). We speculated that the BSA could form a protective shell around the nanocomplexes (similar to the well known protein corona) and work as an anchor for both IgG and LAE. In fact, due to its amphiphilic properties, BSA could have interacted with the hydrophobic tails of the surfactant, forming a more compact core which might have stabilized the formulation in SBF [42].

Moreover, the double layered formulation (layer-by-layer PArg/HA ENCPs) was developed for stabilizing the particles in a more complex media containing proteins (10% (v/v) FBS supplementation).

With the BVZ-loaded HA ENCPs the size decreased upon their dilution in the SBF containing FBS, however it remained stable for at least 24 hours without the necessity of BSA or multiple layers.

Table 2. Main characteristics and structures of BVZ and BSA. The properties of BVZ were obtained from [43,44] *and* [45]*, while those of BSA from* [46] *and* [47].

Protein	pI	MW (kDa)	Structure
BVZ	8.3	149	Mostly β-Sheet 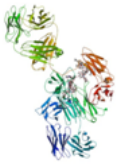
BSA	4.7	66	Mostly α-elix 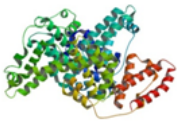

pI=isoelectric point; MW=molecular weight

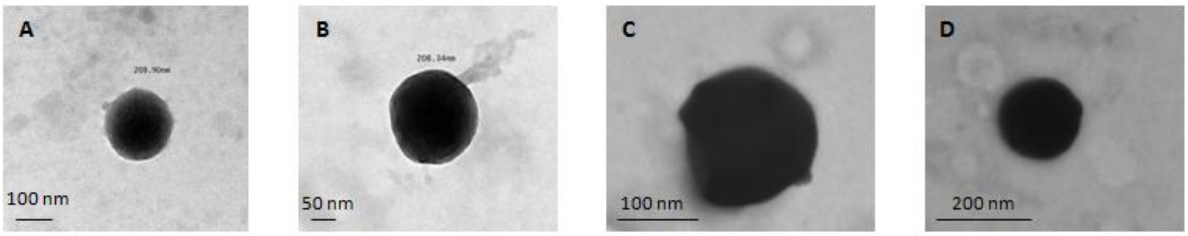

Figure 5. STEM and TEM images of the developed prototypes. (A) BSA/BP-loaded HA nanocomplexes (TEM); (B) BSA/IgG/MQ-loaded HA nanocomplexes (TEM); (C) BVZ-loaded HA ENCPs (75 µg) (STEM); (D) BVZ-loaded HA ENCPs (375 µg) (sTEM). Unfortunately, no microscope pictures related to the layer-by-layer PArg/HA ENCPs are available.

Protein association and loading capacity

It was also observed that the aqueous phase in which the proteins are added strongly influences the association and loading capacity of the nanosystems. In fact, it was shown that when the IgG was

dissolved in the HA aqueous phase, lower protein loadings were obtained as compared to those obtained when the protein was dissolved in the LAE aqueous phase (Figure 6). It becomes apparent that IgG interacts more favorably with LAE than with HA. This is probably due to the capacity of the antibody of interacting with the LAE both through hydrophobic and electrostatic forces, while with the HA no hydrophobic interactions are possible. Similar approaches have been used for forming self-assembled micelles associating lysozyme and trastuzumab through hydrophobically modified polymers. It was shown that the proteins can interact both through electrostatic and hydrophobic interactions with the polymers and that the hydrophobic interactions are the driving force for the association [22,48].

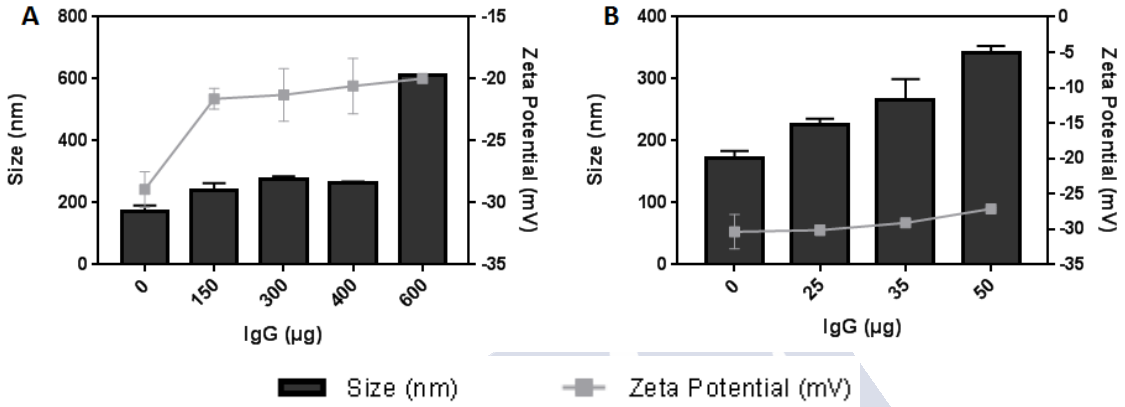

Figure 6. Size and zeta potential of the HA nanocomplexes associating different amounts of IgG and formulated in milliQ water (no BSA was used here, since it was added later for stabilizing the nanocomplexes in SBF). A: IgG was dissolved in the LAE aqueous phase and then added to the HA water phase for forming the nanocomplexes. B: IgG was dissolved in the HA aqueous phase and then added to the LAE water phase for forming the nanocomplexes. The protein loading is clearly higher when the antibody is in the LAE water phase.

The surface charge of the formulations was also affected by the association of the antibodies (both IgG and BVZ). As shown in Figure 6 and Figure 7.A, the negative zeta potential values decreased upon increase of the IgG amount. The same tendency (although less p pronounced) was observed for the BVZ-loaded HA ENCPs (Figure 7.B and Figure 8), in which the negative values of the zeta potential become smaller upon addition of increasing amounts of BVZ. This neutralization of the negative change caused by the presence of the mAb is obviously due to the interaction of the mAb with the negatively charged carrier.

Protein release from the nanosystems

With regard to the release of the proteins (Figures 7 and 9) a biphasic profile characterized by an initial burst followed by a very slow release is shown. The burst release, typically observed for protein-loaded nanocarriers, could be attributed to the detachment of the protein molecules located near the surface of the nanosystems, as already indicated by other authors [49,50]. This detachment could be motivated by the high osmolarity of the media. This corroborates the idea that the interaction of the protein with the nanocarrier is, at least in part, mediated by electrostatic forces [51,52]. However, other type of interactions (i.e. hydrophobic, hydrogen bonding, dipole-dipole interactions, etc.) may participate in the formation of the nanosystems, since stable size and mean count rate (MCR) are maintained for at least 24 hours in the complex media.

On the other hand, it has been reported that the formation of complexes in a high osmolarity media (i.e. refer to the BSA/BP-loaded HA nanocomplexes, formulated in phosphate buffer) could help in stabilizing the formulation and decreasing the burst release effect (Figure 9) in salts-containing media. In this sense it has been suggested that the phosphate ions could reduce the repulsion between the LAE heads, thus stabilizing the nanosystem [36–38]. However, the presence of salts did not allow the formation of the nanocomplexes when the IgG was introduced into the formulation (aggregates were obtained).

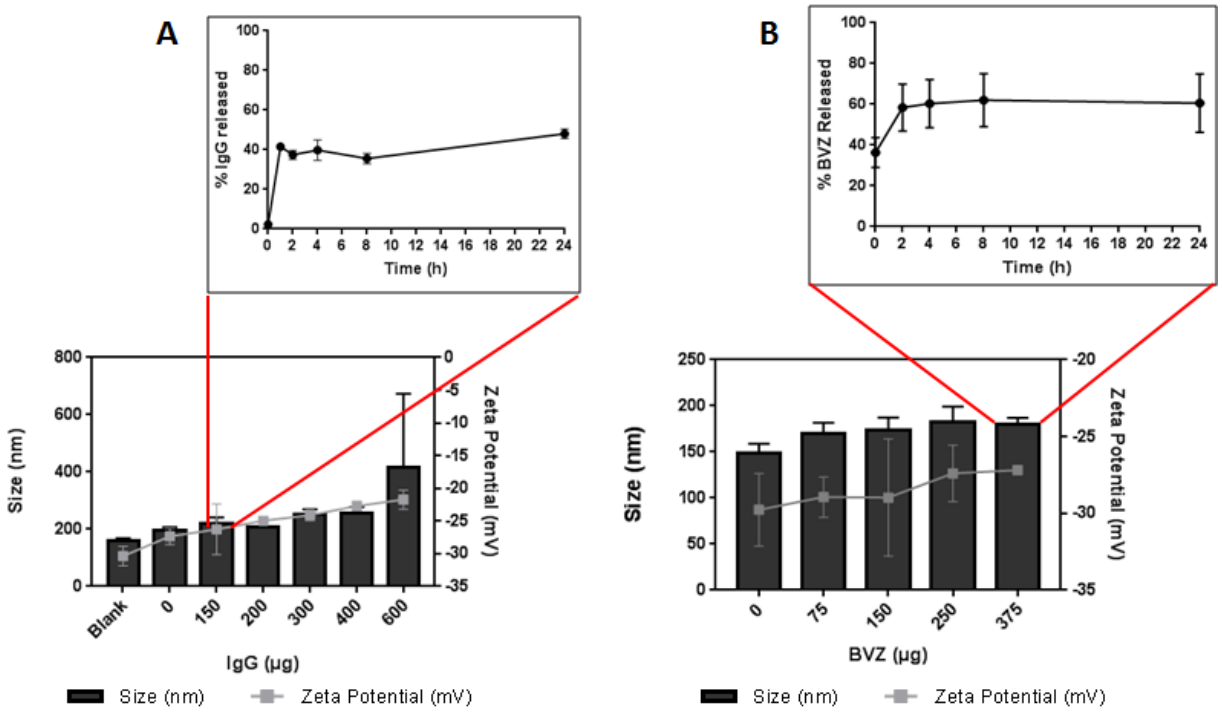

Figure 7. Size, zeta potential and release profile in simulated biological fluids (SBFs) of A) BSA/IgG/MQ-loaded HA nanocomplexes and B) BVZ-loaded HA ENCPs, containing different amounts of IgG and BVZ, respectively. PBS was used as release medium for the BSA/IgG/MQ-loaded HA nanocomplexes, while PBS supplemented with FBS (10% v/v concentration) as release medium for the BVZ-loaded HA ENCPs.

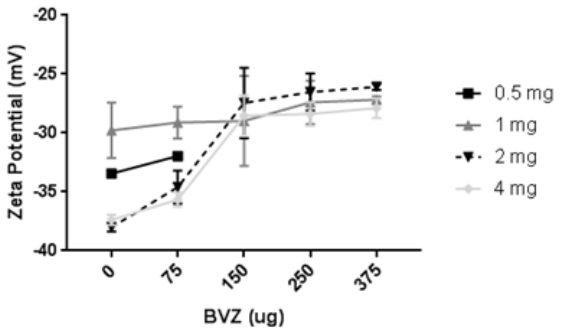

Figure 8. Zeta potential of the BVZ-loaded HA ENCPs prepared with different HA and BVZ amounts. The used HA amounts are indicated on the left in the graph (0.5, 1, 2 and 4 mg). The decrease of the zeta potential negative values is higher when higher amounts of HA were used.

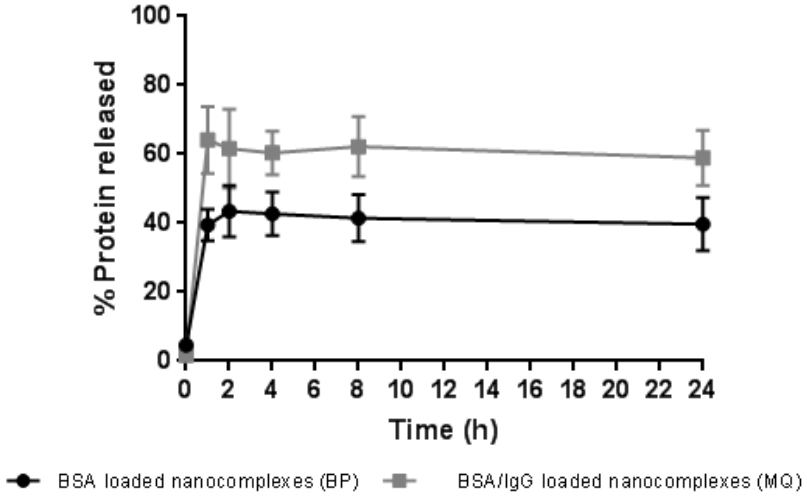

Figure 9. BSA released from the nanosystems prepared in phosphate buffer (BSA/BP-loaded HA nanocomplexes) and in milliQ water (BSA/IgG/MQ-loaded HA nanocomplexes).

Structural and functional stability of the associated proteins

Knowing the capacity of ionic surfactants to destabilize protein structures [53,54], we evaluated the structural and functional stability of the proteins formulated in the form of nanocomplexes using circular dichroism and the ELISA techniques. The results indicated that the structural stability of BSA was unaffected by the presence of the cationic surfactant. Similarly, the functional stability of BVZ was found to be unaltered upon the association to the nanosystems.

Freeze-drying of the nanocomplexes

As shown in Table 3 the size of the nanosystems shows a tendency to increase upon storage, especially when stored in the form of suspension (Table 3.A). Being aware of the necessity to preserve the stability of the formulations [55], we freeze-dried the nanocomplexes using different cryoprotectants. Trehalose was found to be the most suitable for all the prototypes, probably due to its high glass transition temperature and its high molecular flexibility [56,57]. However, in the case of the BVZ-loaded HA ENCPs (375 µg) (i.e. the ENCPs with the highest amount of antibody), it was necessary to add PEG-400 in order to preserve the stability of the formulation. Further studies on the long-term stability of the freeze-dried formulations must be conducted.

*Table 3. Mean size of the antibodies-loaded nanosystems upon storage in suspension at 4°C for 7 days (Table A) or after freeze-drying (Table B). For the storage in suspension, the size at day 0 and day 7 are compared, while for the freeze-drying, the size before and after freeze-drying are compared. BSA/IgG/MQ HA nanocomplexes and BVZ-loaded HA ENCPs (75 µg) were freeze-dried in the presence of trehalose as cryoprotectant (10% w/w). BVZ-loaded HA ENCPs (375 µg) were freeze-dried using both trehalose (2.5% w/w) and PEG-400 (2.5% w/w). Statistical differences using t-test are shown (*p<0.05 and **p<0.01).*

A

Type of nanocarrier	Day 0	Day 7
BSA/IgG/MQ-loaded HA nanocomplexes	224±16	292±42
BVZ-loaded HA ENCPs (75 µg)	178±9	202±11**
BVZ loaded HA ENCPs (375 µg)	179±8	262±22**

B

Type of nanocarrier	Before	After
BSA /IgG/MQ-loaded HA nanocomplexes	222±28	221±24
BVZ-loaded HA ENCPs (75 µg)	170±12	189±5*
BVZ-loaded HA ENCPs (375 µg)	179±1	205±35

% Size increase (storage in suspension) = 100 x (size day 7-size day 0)/size day 0; % Size increase (after freeze drying) = 100 x (size after freeze drying-size before freeze drying)/size before freeze drying.

***In vitro* cell culture studies**

The toxicity of the BVZ-loaded ENCPs and the internalization of the BVZ associated was evaluated in a breast cancer VEGF producing cell line (MDA-MB-231). ENCPs with the higher loading of BVZ (7.3%) were tested in these experiments.

The results showed a significant decrease in cell viability when cells were exposed to the BVZ-loaded HA ENCPs at BVZ concentrations higher than 15 µg/mL (127 µg/mL of nanocarrier) for 72 hours (Figure 10). The toxicity was probably due to the presence of the positively charged surfactant, since comparable toxicity profiles were shown when the cells were treated with the blank HA ENCPs or the LAE alone. In fact, it is well known that cationic surfactants exhibit cytotoxicity, normally attributed to their capacity to disrupt the cell membrane [58–63]. A straight-forward way to reduce the toxicity of the formulation may involve its purification by tangential filtration in order to eliminate the excess of LAE present in the formulation.

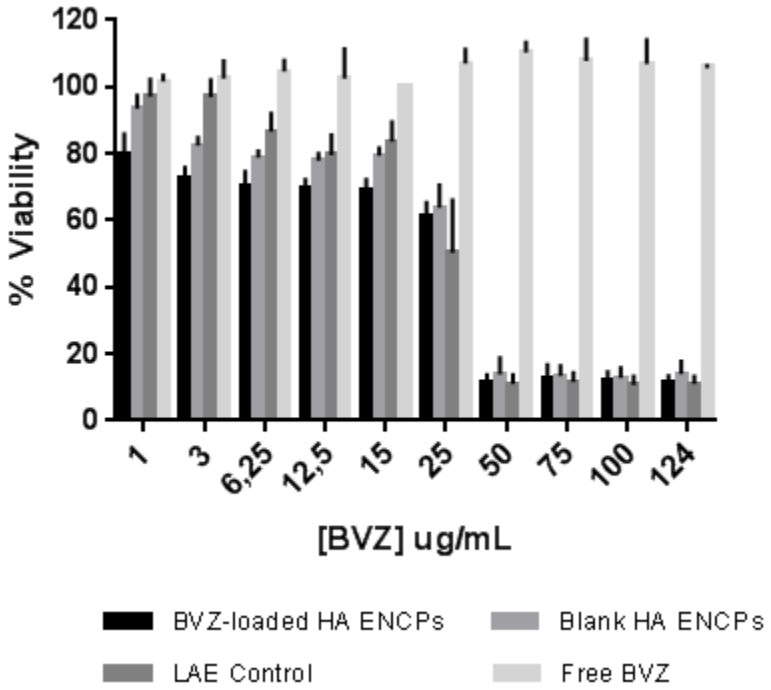

Figure 10. MTT viability assays on MDA-MB-231 breast cancer cell line. BVZ-loaded HA ENCPs *(375 µg), blank HA* ENCPs*, LAE and free BVZ have been tested and compared (72 hours contact of samples with the cells). An ANOVA was used for detecting significant differences (***p<0.001 and ****p<0.0001). At all the selected concentrations there were significant differences between the BVZ-loaded HA ENCPs and the free BVZ (p<0.001 at 1 µg/mL and p<0.0001 at all the other concentrations). When blank HA ENCPs are considered, the only concentration at which significant differences were not observed was the lowest one (1 µg/mL). In all the other cases the differences were statistically significant (p<0.0001). A similar behavior was observed with LAE, where starting from the concentration of 6.25 µg/mL the differences were statistically significant (p<0.001 or p<0.0001).*

It is well documented that the VEGF-A intracellular pool is fundamental for cancer cell growth, migration and invasion [30,64] as well as for recruiting bone marrow-derived cells progenitors, a possible source of resistance to BVZ therapies [34,65]. Based on this, our hypothesis has been that the association of BVZ to a nanocarrier may facilitate the access to the intracellular VEGF-A. Several attempts have been made so far towards achieving this goal, and some of them have given positive results. For example, when BVZ was incorporated into liposomes and co-administered with a photosensitizing agent a decrease in the tumor growth was observed in a pancreatic cancer mice model [34,66]. The authors hypothesized that the intracellular delivery of BVZ could block the signal cascade before it starts, avoiding tumor re-growth and overcoming the effect of potential resistance mechanisms.

In this manuscript we have shown that the apparent penetration of BVZ into the breast cancer cell line MDA-MB-231 would be possible when the antibody is associated to the ENCPs (Figure 11). In fact, after 1 hour of incubation with the FITC-labeled BVZ-loaded HA ENCPs, fluorescent spots could be identified, potentially inside the cells. However, more experiments are needed for understanding if the BVZ penetrate the cells or is simply attached to their surface. In contrast, no internalization was observed for the free BVZ. These results were counterbalanced by the fact that the only presence of LAE facilitated the apparent internalization of the free antibody (see Figure 11, BVZ+LAE). Therefore,

we cannot conclude from these studies that the potential internalization of BVZ is due to its association to the ENCPs. Further experiments aimed at understanding the mechanistic issues involved in the antibody internalization should be performed. Uptake experiments on tumor explants after the in vivo treatment could be also planned for demonstrating the internalization of the antibody in vivo [66].

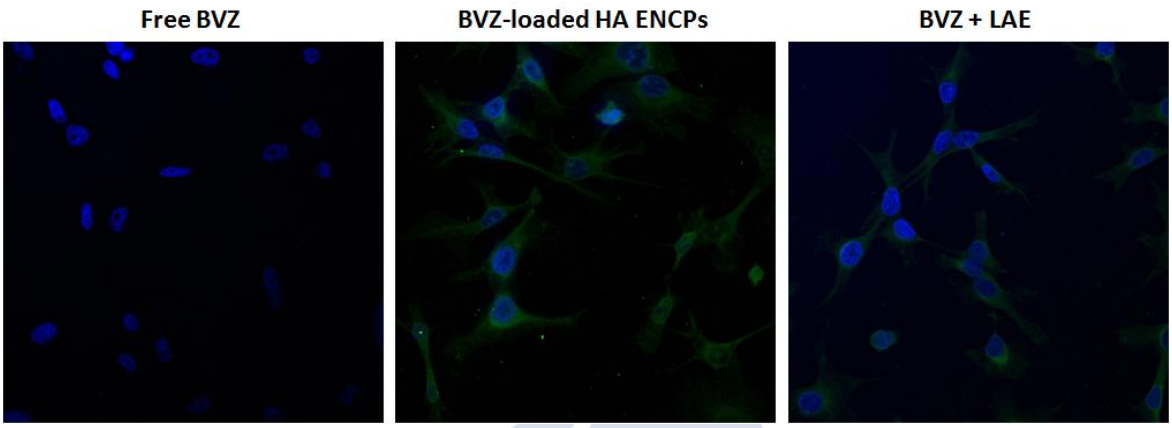

Figure 11. Examples of confocal microscopy images after the treatment of cells for 1 hour with free FITC-labeled BVZ (green color), FITC-labeled BVZ associated to ENCPs and the physical mixture of FITC-labeled BVZ with LAE. DAPI (blue color) was used for labeling the nucleus of the cells.

Experiments related to the influence of the BVZ-loaded HA ENCPs on the expression of some of the genes involved in the VEGF pathway were also carried out. Even if the natural target of BVZ is VEGF-A, it has been reported that the function of VEGF-A could be replaced by the other VEGFs [67–69], therefore the expression of the other genes belonging to the same protein family (VEGF-B, VEGF-C and VEGF-D) was also investigated. The results showed no significant variations in the mRNA expression which could be attributed to the internalization of the antibody. Probably, the most interesting result from this set of experiments was the one observed for BVZ-loaded HA ENCPs on the expression of VEGF-A. After a 48 hours exposure, the expression levels of the gene decreased compared to the time 24 hours, while the same effect was not observed for control groups (free BVZ and blank HA ENCPs). More experiments correlating the gene to the protein expression pattern and aimed at studying a higher number of genes (i.e. gene chip based analysis) could be interesting for understanding the effect of the intracellular delivery of BVZ and if more genes, different from the ones of the VEGF pathway, are involved in the VEGF-A blockage response [70,71].

***In vivo* efficacy studies**

Finally, an in vivo efficacy experiment was performed. The results showed that after the intraperitoneal treatment of tumor-bearing mice with BVZ, either in a free form or associated to ENCPs, a minor but statistically significant reduction in the tumor growth was observed (from the day 19). However, no significant differences were observed among the two groups of animals (Figure 12). As expected, the tumor growth and necrosis were shown to be faster for the groups non treated with BVZ.

Several explanations can be given for the limited response to the treatment. One of them could be related to the modality of injection and the dose injected. In humans BVZ is given intravenously at a high dose (10-20 mg/kg), while in the experiment reported here we used an intraperitoneal administration of a relatively low dose (6.3 mg/kg). An earlier stage mice treatment might also be a reliable option for increasing the efficacy of the therapy. Several papers indicate that a BVZ treatment 1 or 2 days post-tumor cells-injection significantly reduced tumor growth compared to the control groups [72–74]. On the other hand, biodistribution studies will need to be performed in order to elucidate the potential biodistribution problems of the antibody associated to the nanosystem. Also, studies of the degree of vascular density and pericytes coverage would be interesting in order to elucidate a potential problem of diffusion across the tumor stroma [75,76]. Finally, a combination therapy would also be reliable alternative for improving the efficiency of the anticancer therapy. In fact, the few in vivo studies showing significant effects with nanoencapsulated BVZ, administered the antibody along with a chemotherapeutic or a photosensitizing agent, claiming that the enhanced anticancer therapy is hypothetically due to the internalization of both the drugs [34,66].

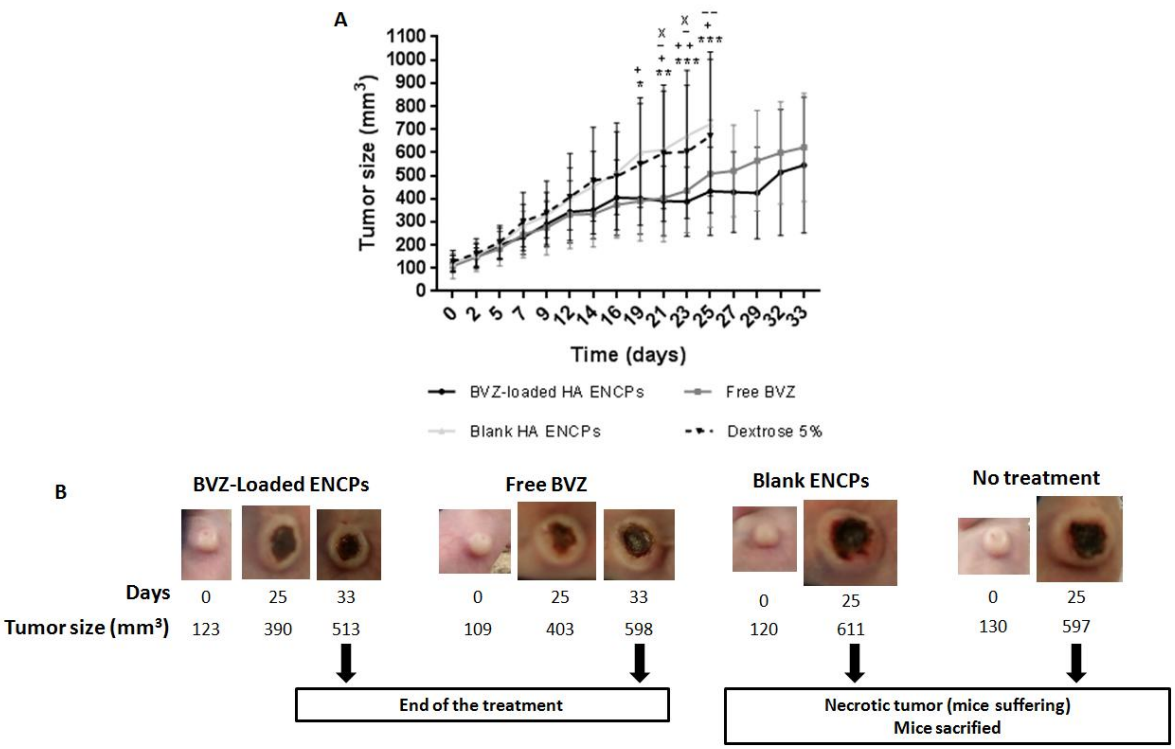

Figure 12. A) Tumor growth over the course of the treatment

A) Tumor volume growth in MDA-MB-231 tumor-bearing mice after intraperitoneal administration of BVZ-loaded HA ENCPs, free BVZ, blank HA ENCPs and dextrose solution 5% (Dextrose 5%). The statistically significant differences among the groups are presented below:

** = BVZ-loaded HA ENCPs and blank HA ENCPs (*p<0.05 , **p<0.01 and ***p<0.001)*

+ = free BVZ and blank HA ENCPs (; $^{+}$p<0.05 and $^{++}$p<0.01)

- = BVZ-loaded HA ENCPs and dextrose 5% ($^{-}$p<0.05 and $^{--}$p<0.01)

x = free BVZ and dextrose 5% (; ^{x}p<0.05 and ^{xx}p<0.01)

No significant differences have been found among the BVZ-loaded HA ENCPs and the free BVZ groups.

B) Pictures of the tumor in the different stages of its development (the pictures are referred to only one mouse per group). The indicated tumor sizes are the average of all the mice belonging to the same group in the indicated day. The tumor

growth of the control groups (i.e. blank HA ENCPs and no treatment) was faster and the tumor got into necrosis before compared to the groups treated with BVZ

Bibliography

[1] H.A.D. Lagassé, A. Alexaki, V.L. Simhadri, N.H. Katagiri, W. Jankowski, Z.E. Sauna, C. Kimchi-sarfaty, Recent advances in (therapeutic protein) drug development, F1000 Res. 6 (2017) 1–17. doi:10.12688/f1000research.9970.1.

[2] E. Pérez-Herrero, A. Fernández-Medarde, Advanced targeted therapies in cancer: Drug nanocarriers, the future of chemotherapy, Eur. J. Pharm. Biopharm. 93 (2015) 52–79. doi:10.1016/j.ejpb.2015.03.018.

[3] A.L. Catapano, N. Papadopoulos, The safety of therapeutic monoclonal antibodies : Implications for cardiovascular disease and targeting the PCSK9 pathway, Atherosclerosis. 228 (2013) 18–28. doi:10.1016/j.atherosclerosis.2013.01.044.

[4] D.M. Ecker, S.D. Jones, H.L. Levine, The therapeutic monoclonal antibody market, MAbs. 7 (2015) 9–14. doi:10.4161/19420862.2015.989042.

[5] J.R. Kintzing, M. V. Filsinger Interrante, J.R. Cochran, Emerging Strategies for Developing Next-Generation Protein Therapeutics for Cancer Treatment, Trends Pharm. Sci. 37 (2016) 1–16.

[6] P.A. Tang, M.J. Moore, Aflibercept in the treatment of patients with metastatic colorectal cancer : latest findings and interpretations, Therap. Adv. Gastroenterol. 6 (2013) 459–473. doi:10.1177/1756283X13502637.

[7] T. Arvinte, C. Palais, E. Green-trexler, S. Gregory, H. Mach, C. Narasimhan, M. Shameem, Aggregation of biopharmaceuticals in human plasma and human serum. Implications for drug research and development, MAbs. 5 (2013) 491–500. doi:10.4161/mabs.24245.

[8] M. Leeman, J. Choi, S. Hansson, M.U. Storm, L. Nilsson, Proteins and antibodies in serum , plasma , and whole blood — size characterization using asymmetrical flow field-flow fractionation (AF4), Anal. Bioanal. Chem. 410 (2018) 4867–4873.

[9] R.A. Beckman, L.M. Weiner, H.M. Davis, Antibody constructs in cancer therapy. Protein Engineering Strategies to Improve Exposure in Solid Tumors, Cancer. 109 (2007) 170–179. doi:10.1002/cncr.22402.

[10] O. Casanovas, D.J. Hicklin, G. Bergers, D. Hanahan, Drug resistance by evasion of antiangiogenic targeting of VEGF signaling in late-stage pancreatic islet tumors, Cancer Cell. 8 (2005) 299–309. doi:10.1016/j.ccr.2005.09.005.

[11] P. Chames, M. Van Regenmortel, E. Weiss, D. Baty, Therapeutic antibodies: successes , limitations and hopes for the future, Br. J. Pharmacol. 157 (2009) 220–233. doi:10.1111/j.1476-5381.2009.00190.x.

[12] M.J. Miller, Cancer Immunotherapy: Present Status, Future Perspective, and a New Paradigm of Peptide Immunotherapeutics, Discov. Med. 15 (2013) 166–176.

[13] T.A.S. Aguirre, D. Teijeiro-Osorio, M. Rosa, I.S. Coulter, M.J. Alonso, D.J. Brayden, Current status of selected oral peptide technologies in advanced preclinical development and in clinical trials, Adv. Drug Deliv. Rev. 106 (2016) 223–241. doi:10.1016/j.addr.2016.02.004.

[14] I. Santalices, A. Gonella, D. Torres, M. Jos, Advances on the formulation of proteins using nanotechnologies, J. Drug Deliv. Sci. Technol. 42 (2017) 155–180. doi:10.1016/j.jddst.2017.06.018.

[15] J.K.H. Liu, The history of monoclonal antibody development e Progress , remaining challenges and future innovations, Ann. Med. Surg. 3 (2014) 113–116. doi:10.1016/j.amsu.2014.09.001.

[16] F.C. Breedveld, Therapeutic monoclonal antibodies, New Drug Classes. 355 (2000) 735–740. doi:10.1016/S0140-6736(00)01034-5.

[17] K. Bloem, B. Hernandez-Breijo, A. Martìnez-Feito, T. Rispens, Immunogenicity of therapeutic

antibodies: monitoring anti-drug antibodies in a clinical context, Ther. Drug Monit. 39 (2017) 327–332. doi:10.1097/FTD.0000000000000404.

[18] M.P. Baker, H.M. Reynolds, B. Lumicisi, C.J. Bryson, Immunogenicity of protein therapeutics The key causes , consequences and challenges, Self. Nonself. 1 (2010) 314–322. doi:10.4161/self.1.4.13904.

[19] F. Sousa, A. Cruz, P. Fonte, I.M. Pinto, M.T. Neves, B. Sarmento, A new paradigm for antiangiogenic therapy through controlled release of bevacizumab from PLGA nanoparticles, Nat. Sci. Reports. 7 (2017) 1–13. doi:10.1038/s41598-017-03959-4.

[20] S. Tangutoori, B.Q. Spring, Z. Mai, A. Palanisami, L.B. Mensah, T. Hasan, Simultaneous delivery of cytotoxic and biologic therapeutics using nanophotoactivatable liposomes enhances treatment efficacy in a mouse model of pancreatic cancer, Nanomedicine Nanotechnology, Biol. Med. 12 (2016) 223–234. doi:10.1016/j.nano.2015.08.007.

[21] A.R. Srinivasan, A. Lakshmikuttyamma, S.A. Shoyele, Investigation of the Stability and Cellular Uptake of Self-Associated Monoclonal Antibody (MAb) Nanoparticles by Non-Small Lung Cancer Cells, Mol. Pharm. 10 (2013) 3275–3284. doi:10.1021/mp3005935.

[22] J.E. Chung, S. Tan, S.J. Gao, N. Yongvongsoontorn, S.H. Kim, J.H. Lee, H.S. Choi, H. Yano, L. Zhuo, M. Kurisawa, J.Y. Ying, Self-assembled micellar nanocomplexes comprising green tea catechin derivatives and protein drugs for cancer therapy, Nat. Nanotechnol. 9 (2014) 907–912. doi:10.1038/nnano.2014.208.

[23] S. Li, Z. Su, M. Sun, Y. Xiao, F. Cao, A. Huang, H. Li, Q. Ping, C. Zhang, An arginine derivative contained nanostructure lipid carriers with pH-sensitive membranolytic capability for lysosomolytic anti-cancer drug delivery, Int. J. Pharm. 436 (2012) 248–257. doi:10.1016/j.ijpharm.2012.06.040.

[24] K. Patel, M. Tyagi, J. Monpara, L. Vora, S. Gupta, P. Vavia, Arginoplexes : an arginine-anchored nanoliposomal carrier for gene delivery, J. Nanoparticle Res. 16 (2014) 1–10. doi:10.1007/s11051-014-2345-y.

[25] C. Liu, S.-Y. Yu, Cationic nanoemulsions as non-viral vectors for plasmid DNA delivery, Colloids Surfaces B Biointerfaces. 79 (2010) 509–515. doi:10.1016/j.colsurfb.2010.05.026.

[26] R. Racine, M.E. Mummert, Hyaluronan Endocytosis: Mechanisms of Uptake and Biological Functions, in: Mol. Regul. Endocytosis, 2012: pp. 377–390. doi:10.5772/45976.

[27] G. Tripodo, A. Trapani, M. Luisa, G. Giammona, G. Trapani, D. Mandracchia, Hyaluronic acid and its derivatives in drug delivery and imaging : Recent advances and challenges, Eur. J. Pharm. Biopharm. 97 (2015) 400–416. doi:10.1016/j.ejpb.2015.03.032.

[28] S. Yin, J. Huai, X. Chen, Y. Yang, X. Zhang, Y. Gan, G. Wang, X. Gu, J. Li, Intracellular delivery and antitumor effects of a redox-responsive polymeric paclitaxel conjugate based on hyaluronic acid, Acta Biomater. 26 (2015) 274–285. doi:10.1016/j.actbio.2015.08.029.

[29] H.S.S. Qhattal, X. Liu, Characterization of CD44-Mediated Cancer Cell Uptake and Intracellular Distribution of Hyaluronan-Grafted Liposomes, Mol. Pharm. 8 (2012) 1233–1246. doi:10.1021/mp2000428.Characterization.

[30] R. Bhattacharya, F. Fan, R. Wang, X. Ye, L. Xia, D. Boulbes, L.M. Ellis, Intracrine VEGF signalling mediates colorectal cancer cell migration and invasion, Br. J. Cancer. 117 (2017) 848–855. doi:10.1038/bjc.2017.238.

[31] T. Lee, S. Seng, M. Sekine, C. Hinton, Y. Fu, H.K. Avraham, S. Avraham, Vascular Endothelial Growth Factor Mediates Intracrine Survival in Human Breast Carcinoma Cells through Internally Expressed VEGFR1/ FLT1, Plos Med. 4 (2007) 1101–1116. doi:10.1371/journal.pmed.0040186.

[32] F. Saffari, A. Jafarzadeh, B.K. Khandani, F. Saffari, S. Soleimanyamoli, M. Mohammadi, Immunogenicity of Rituximab , Trastuzumab, and Bevacizumab Monoclonal Antibodies in Patients with Malignant Diseases, Int. J. Cancer Manag. 11 (2018) 4–8. doi:10.5812/ijcm.64983.Research.

[33] Y. Zhang, J. Guo, X. Zhang, D. Li, T. Zhang, Antibody fragment-armed mesoporous silica nanoparticles for the targeted delivery of bevacizumab in ovarian cancer cells, Int. J. Pharm. 496 (2015) 1026–1033. doi:10.1016/j.ijpharm.2015.10.080.

[34] S. Tangutoori, B.Q. Spring, Z. Mai, A. Palanisami, L.B. Mensah, T. Hasan, Simultaneous delivery of cytotoxic and biologic therapeutics using nanophotoactivatable liposomes enhances treatment efficacy in a mouse model of pancreatic cancer, Nanomedicine Nanotechnology, Biol. Med. 12 (2016) 223–234. doi:10.1016/j.nano.2015.08.007.

[35] O. V Salata, Applications of nanoparticles in biology and medicine, J. Nanobiotechnology. 2 (2004) 1–6. doi:10.1186/1477-3155-2-3.

[36] M. Lund, R. Vacha, P. Jungwirth, Specific Ion Binding to Macromolecules : Effects of Hydrophobicity and Ion Pairing, Langmuir. 24 (2008) 3387–3391. doi:10.1021/la7034104.

[37] P. Mukerjee, K. Mysels, P. Kapadan, Counterion Specificity in the Formation of Ionic Micelles — Size , Hyadration, and Hydrophobic Bonding Effect, 71 (1966) 4166–4175. doi:10.1021/j100872a702.

[38] H. Dautzenberg, Polyelectrolyte Complex Formation in Highly Aggregating Systems. 1. Effect of Salt: Polyelectrolyte Complex Formation in the Presence of NaCl, 30 (1997) 7810–7815. doi:10.1021/ma970803f.

[39] G. Van der Vusse, Albumin as Fatty Acid Transporter, Drug Metab. Pharmacokinet. 24 (2009) 300–307. doi:10.2133/dmpk.24.300.

[40] J. Crecente-Campo, S. Lorenzo-Abalde, A. Mora, J. Marzoa, N. Csaba, J. Blanco, Á. González-Fernández, M. José, Bilayer polymeric nanocapsules: A formulation approach for a thermostable and adjuvanted E. coli antigen vaccine, J. Control. Release. 286 (2018) 20–32. doi:10.1016/j.jconrel.2018.07.018.

[41] T. Ramasamy, T. Hiep, J. Yeon, H. Jun, J. Hwan, C. Soon, H. Choi, J. Oh, Layer-by-layer coated lipid – polymer hybrid nanoparticles designed for use in anticancer drug delivery, 102 (2014) 653–661. doi:10.1016/j.carbpol.2013.11.009.

[42] A. Valstar, M. Almgren, W. Brown, The Interaction of Bovine Serum Albumin with Surfactants Studied by Light Scattering, Langmuir. 16 (2000) 922–927. doi:10.1021/la990423i.

[43] C. Qiu, S. Arzhantsev, Secondary structure assessment of formulated bevacizumab in the presence of SDS by deep ultraviolet resonance Raman (DUVRR) spectroscopy, Anal. Biochem. 15 (2018) 26–32. doi:10.1016/j.ab.2018.06.003.

[44] S. Kaja, J. Hulgenberg, E. Everett, S. Olitsky, J. Gossage, P. Koulen, Effects of dilution and prolonged storage with preservative in a polyethylene container on Bevacizumab (Avastin™) for topical delivery as a nasal spray in anti-hereditary hemorrhagic telangiectasia and related therapies, Hum. Antibodies. 20 (2012) 95–101. doi:10.3233/HAB-2011-0244.Effects.

[45] Bevacizumab-drug data bank.

[46] T.J. Su, J.R. Lu, R.K. Thomas, Effect of pH on the Adsorption of Bovine Serum Albumin at the Silica / Water Interface Studied by Neutron Reflection, J. Phys. Chem. B. 103 (1999) 3727–3736. doi:10.1021/jp983580j.

[47] BSA-protein data bank (PDB).

[48] K. Liang, S. Ng, F. Lee, J. Lim, J.E. Chung, S.S. Lee, M. Kurisawa, Targeted intracellular protein delivery based on hyaluronic acid-green tea catechin nanogels, Acta Biomater. 33 (2016) 142–152. doi:10.1016/j.actbio.2016.01.011.

[49] Y. Yeo, K. Park, Control of Encapsulation Efficiency and Initial Burst in Polymeric Microparticle Systems, Arch. Pharm. Res. 27 (2004) 1–12. doi:10.1007/BF02980037.

[50] Q. Gan, T. Wang, Chitosan nanoparticle as protein delivery carrier — Systematic examination of fabrication conditions for efficient loading and release, Colloids Surfaces B. 59 (2007) 24–34. doi:10.1016/j.colsurfb.2007.04.009.

[51] M. Alonso-Sande, M. Cuna, C. Remunàn-Lopez, D. Teijeiro-Osorio, J.L. Alonso-Lebrero, M. Alonso, Formation of New Glucomannan - Chitosan Nanoparticles and Study of Their Ability

To Associate and Deliver Proteins, Macromolecules. 39 (2006) 4152–4158.
[52] W. Tiyaboonchai, J. Woiszwillo, R.C. Sims, C.R. Middaugh, Insulin containing polyethylenimine-dextran sulfate nanoparticles, Int. J. Pharm. 255 (2003) 139–151. doi:10.1016/S0378-5173(03)00055-3.
[53] D. Kelley, D.J. McClements, Interactions of bovine serum albumin with ionic surfactants in aqueous solutions, Kelley, D. McClements, D.J. 17 (2003) 73–85. doi:10.1016/S0268-005X(02)00040-1.
[54] D. Otzen, Protein–surfactant interactions: A tale of many states, Biochim. Biophys. Acta. 1814 (2011) 562–591. doi:10.1016/j.bbapap.2011.03.003.
[55] World Health Organization, Stability testing of active pharmaceutical ingredients and finished pharmaceutical products, 2009.
[56] F. Sousa, A. Cruz, I. Mendes, B. Sarmento, Nanoparticles provide long-term stability of bevacizumab preserving its antiangiogenic activity, Acta Biomater. 78 (2018) 285–295. doi:10.1016/j.actbio.2018.07.040.
[57] L.M. Crowe, D.S. Reid, J.H. Crowe, Is Trehalose Special for Preserving Dry Biomaterials ?, Biophys. J. 71 (1996) 2087–2093. doi:10.1016/S0006-3495(96)79407-9.
[58] N. Vlachy, D. Touraud, J. Heilmann, W. Kunz, Determining the cytotoxicity of catanionic surfactant mixtures on HeLa cells, Colloids Surfaces B Biointerfaces. 70 (2009) 278–280. doi:10.1016/j.colsurfb.2008.12.038.
[59] R.L. Grant, C. Yao, D. Gabaldon, D. Acosta, Evaluation of surfactant cytotoxicity potential by primary cultures of ocular tissues: I . Characterization of rabbit corneal epithelial cells and initial injury and delayed toxicity studies, Toxicology. 76 (1992) 153–176. doi:10.1016/0300-483X(92)90162-8.
[60] S. Inàcio, K.A. Mesquita, M. Baptista, In Vitro Surfactant Structure-Toxicity Relationships: Implications for Surfactant Use in Sexually Transmitted Infection Prophylaxis and Contraception, PLoS One. 6 (2011) 1–15. doi:10.1371/journal.pone.0019850.
[61] M.K. Dymond, G.S. Attard, Cationic Type I Amphiphiles As Modulators of Membrane Curvature Elastic Stress in Vivo, Langmuir. 24 (2008) 11743–11751. doi:10.1021/la8017612.
[62] B. Vieira, A.M. Carmona-ribeiro, U. De Sa, A. Lineu, P. Butanta, Cationic lipids and surfactants as antifungal agents : mode of action, J. Antimicrob. Chemother. 58 (2006) 760–767. doi:10.1093/jac/dkl312.
[63] A. Patrzykat, C.L. Friedrich, L. Zhang, V. Mendoza, R.E.W. Hancock, Sublethal Concentrations of Pleurocidin-Derived Antimicrobial Peptides Inhibit Macromolecular Synthesis in Escherichia coli, Antimicrob. Agents Chemother. 46 (2002) 605–614. doi:10.1128/AAC.46.3.605.
[64] M. Björndahl, R. Cao, A. Eriksson, Y. Cao, Blockage of VEGF-Induced Angiogenesis by Preventing VEGF Secretion, Circ. Res. 94 (2004) 1443–50. doi:10.1161/01.RES.0000129194.61747.bf.
[65] R. Bhattacharya, X. Ye, R. Wang, X. Ling, M. Mcmanus, F. Fan, D. Boulbes, L.M. Ellis, Intracrine VEGF Signaling Mediates the Activity of Pro-survival Pathways in Human Colorectal Cancer Cells, Cancer Res. 76 (2017) 3014–3024. doi:10.1158/0008-5472.CAN-15-1605.
[66] B. Spring, Z. Mai, P. Rai, S. Chang, T. Hasan, Theranostic Nanocells for Simultaneous Imaging and Photodynamic therapy of Pancreatic Cancer, Opt. Methods Tumor Treat. Detect. Mech. Tech. Photodyn. Ther. 7551 (2010) 1–11. doi:10.1117/12.843725.
[67] M. Chien, C. Ku, G. Johansson, M. Chen, M. Hsiao, J. Su, K. Hua, L. Wei, M. Kuo, Vascular endothelial growth factor-C (VEGF-C) promotes angiogenesis by induction of COX-2 in leukemic cells via the VEGF-R3/JNK/AP-1 pathway, Carcinogeneis. 30 (2013) 2005–2013. doi:10.1093/carcin/bgp244.
[68] A.J. Weickhardt, D.S. Williams, C.K. Lee, F. Chionh, J. Simes, C. Murone, K. Wilson, M.M. Parry, K. Asadi, A.M. Scott, C.J. Punt, I.D. Nagtegaal, T.J. Price, J.M. Mariadason, N.C. Tebbutt, Vascular endothelial growth factor D expression is a potential biomarker of bevacizumab

benefit in colorectal cancer, Br. J. Cancer. 113 (2015) 37–45. doi:10.1038/bjc.2015.209.

[69] F. Zhang, Z. Tang, X. Hou, J. Lennartsson, Y. Li, A.W. Koch, P. Scotney, C. Lee, P. Arjunan, L. Dong, A. Kumar, T.T. Rissanen, B. Wang, N. Nagai, P. Fons, R. Fariss, Y. Zhang, E. Wawrousek, G. Tansey, J. Raber, G. Fong, H. Ding, D.A. Greenberg, K.G. Becker, J. Herbert, A. Nash, S. Yla-herttuala, Y. Cao, R.J. Watts, X. Li, VEGF-B is dispensable for blood vessel growth but critical for their survival , and VEGF-B targeting inhibits pathological angiogenesis, PNAS. 106 (2009) 6152–6157. doi:10.1073/pnas.0813061106.

[70] G. Pentheroudakis, V. Kotoula, E. Fountzilas, G. Kouvatseas, G. Basdanis, I. Xanthakis, T. Makatsoris, E. Charalambous, D. Papamichael, E. Samantas, P. Papakostas, D. Bafaloukos, E. Razis, C. Christodoulou, I. Varthalitis, P. Nicholas, G. Fountzilas, A study of gene expression markers for predictive significance for bevacizumab benefit in patients with metastatic colon cancer: a translational research study of the Hellenic Cooperative Oncology Group (HeCOG), BMC Cancer. 14 (2014) 1–10. doi:10.1186/1471-2407-14-111.

[71] M. Filali, L. V. Ly, G.P.M. Luyten, M. Versluis, H.E. Grossniklaus, P.A. Van, Bevacizumab and intraocular tumors : an intriguing paradox, Mol. Vis. 12 (2012) 2454–2467.

[72] R.S. Warren, H. Yuan, M.R. Matli, N.A. Gillett, N. Ferrara, Regulation by Vascular Endothelial Growth Factor of Human Colon Cancer Tumorigenesis in a Mouse Model of Experimental Liver Metastasis, J. Clin. Invest. 95 (1995) 1789–1797. doi:10.1172/JCI117857.

[73] Y. Okada, T. Akisue, H. Hara, K. Kishimoto, T. Kawamoto, M. Imabori, S. Kishimoto, N. Fukase, Y. Onishi, M. Kurosaka, The Effect of Bevacizumab on Tumour Growth of Malignant Fibrous Histiocytoma in an Animal Model, Anticancer Res. 30 (2010) 3391–3395.

[74] Z. Zhao, X. Li, W. Liu, X. Liu, S. Wu, X. Hu, Inhibition of Growth and Metastasis of Tumor in Nude Mice after Intraperitoneal Injection of Bevacizumab, Orthop. Surg. 8 (2016) 234–240. doi:10.1111/os.12236.

[75] M.O. Stefanini, F.T.H. Wu, F. Mac Gabhann, A.S. Popel, Increase of Plasma VEGF after Intravenous Administration of Bevacizumab Is Predicted by a Pharmacokinetic Model, Cancer Res. 70 (2010) 9886–9895. doi:10.1158/0008-5472.CAN-10-1419.

[76] N. Zhang, G. Zhang, Y. Zheng, T. Wang, H. Wang, Effect of Avastin on the number and structure of tumor blood vessels of nude mice with A549 lung adenocarcinoma, Exp. Ther. Med. 8 (2014) 1723–1726. doi:10.3892/etm.2014.1991.

USC
UNIVERSIDADE
DE SANTIAGO
DE COMPOSTELA

Conclusions

USC
UNIVERSIDADE
DE SANTIAGO
DE COMPOSTELA

The aim of the present work was the design and development of new HA-based nanocarriers particularly adapted for the association and delivery of monoclonal antibodies (bevacizumab; BVZ), not only into the tumoral stroma but also inside the cancer cells. The results allowed us to withdraw the following conclusions:

1. New drug delivery nanocomplexes prepared by the simple assembling of hyaluronic acid (HA) and the cationic surfactant ethyl lauroyl arginate (LAE) were obtained using different methods and formulation conditions.

2. The feasibility of the nanosystems for the association of different kind of proteins was proven using model proteins (BSA, IgG) and the therapeutic monoclonal antibody BVZ. The developed nanoformulations were stable at least 24 hours in simulated biological fluids and could be conveniently freeze-dried. The preservation of the structural and functional stability of the encapsulated proteins was assessed by the use of circular dichroism and ELISA techniques.

3. The BVZ-loaded HA enveloped nanocomplexes (ENCPs) were potentially able to deliver the BVZ inside a breast cancer cell line. However, the role of the cationic surfactant seem relevant in this internalization process.

4. The use of BVZ (free or associated to the HA ENCPs) for treating breast cancer bearing mice resulted in a slower tumor growth. However, no significant differences were observed among the BVZ-loaded HA ENCPs and the free BVZ groups. This limited efficacy could be attributed to a variety of reasons including, the modality of administration and dosing protocol, an inefficient biodistribution and/ or the necessity of a combination therapy.

USC
UNIVERSIDADE
DE SANTIAGO
DE COMPOSTELA

Annex I

Synthesis and characterization of targeted glutamine-modified hyaluronic acid nanocarriers for the delivery of monoclonal antibodies

USC
UNIVERSIDADE
DE SANTIAGO
DE COMPOSTELA

This work was done in collaboration with the department of Biotechnology and Biosciences of the University of Milano-Bicocca (Milano, Italy).

ABSTRACT

Among the most promising nano-therapies for treating cancers there are active targeting therapies. These treatments are based on the decoration of nanocarriers' surfaces with moieties which can be specifically recognized by cancer cells (receptor-ligand interactions), reducing the common side effects observed with classical therapies. However, several advantages could be also drawn by the use of molecules for which cancer cells are addicted and, in this regard, the metabolic rearrangement of tumors could be used as an advantage. The shift from an oxidative to a fermentative metabolism is one of the main hallmarks of all the solid tumors and results in the addiction to glutamine, a fundamental aminoacid for cancer cells biosynthesis. Based on this background, the aim of this work was the development of a targeted nanocarrier decorated with glutamine-modified hyaluronic acid (HA). HA was selected due to its capacity to interact with the CD44 receptor, overexpressed on the membrane of cancer cells, while glutamine was expected to favor the accumulation of the nanocarrier at the tumor site due to the avidity of cancer cells towards this aminoacid. The newly synthesized glutamine-modified HA was characterized. The resulting nanoparticles exhibited a size of around 250 nm and a negative zeta potential. The capacity of the nanoparticles to delivery monoclonal antibodies inside cancer cells was assessed in a breast cancer model cell line. Further studies will be necessary for assessing the real value of this new targeted delivery nanosystem.

USC
UNIVERSIDADE
DE SANTIAGO
DE COMPOSTELA

1. Introduction

Among the main bottlenecks for the treatment of cancer there are the poor accumulation of the anti-cancer drugs at the tumor site and the side effects that the therapy could cause [1]. These drawbacks can be overcome with the association of the drugs to nanocarriers which increase the circulation time of the therapeutic molecules raising the probability of extravasation at the tumor level thanks to the EPR effect [2]. This also reduce the accumulation of the drug in normal tissues, decreasing the side effects of the therapy [3]. However, it is reported that the EPR effect is often not enough for guaranteeing the wanted accumulation, since less than 2-fold drug-increase amount is measured at the tumor level exploiting this effect [2]. In this regard, finding further strategies which enable the accumulation of the nanoencapsulated molecules at the tumor site became an important subject to be developed. The so called active targeting, i.e. the decoration of nanocarriers' surface with moieties which are recognized by cancer cells receptors, have been proposed and multiple efforts have been done during the last years for developing ligand-decorated based nanosystems [4]. However, it was discover that the active targeting just increase the uptake of the drug, but not its biodistribution [5]. Moreover, no nanoparticulate based products exists in the market exploiting the active targeting for treating cancer up to now [6,7]. However, the potential of this strategy is still under evaluation and good results have been obtained with pre-clinical studies. Hyaluronic acid have been often used as targeting moiety for cancer cells overexpressing the CD44 receptor, which upon the recognition of the polymer, switch on an internalization process endocytosis mediated [8]. This is particularly important when cytoplasmatic antigens need to be targeted. However, more strategies could be used for targeting tumors, and their metabolic switch from oxidative to fermentative could be one of them. In fact, one of the hallmarks of all the types of cancer cells is the so called Warburg effect, consisting in the fact that the tumor cells transform their main source of energy (glucose) to lactic acid (through fermentation) instead of oxidizing it through the Krebs cycle and the electron transport chain [9,10]. One of the consequences of this metabolic reprogramming is an un-balanced production of the building blocks which are necessary for cells survival, normally produced by the Krebs cycle. Nevertheless, cells have found strategies for refilling the cycle and the internalization of glutamine is one of them [9,11]. Several works demonstrating the addiction of cancer cells for this aminoacid can be found in the literature [12–14] and the idea of developing of a nanosystem which use the addiction of aminoacids for cancer cells is not new. In fact, a similar approach was used in our lab, developing poly-asparagine coated nanocapsules for targeting lung cancer [15]. However, a multiple bulleting strategy exploiting both the metabolic reprogramming of cancer cells (i.e. their glutamine addiction) and a receptor mediated targeting (i.e. through hyaluronic acid) has not been used, yet. We present here the development of a novel chemically synthesized HA polymer, modified by PEG spacers bearing glutamine on their top. The first step consist in the conjugation of the PEG to glutamine residues, then, the obtained conjugate was linked to the HA trough a simple coupling reaction. The polymer was then used for synthesizing blank and bevacizumab (BVZ) loaded enveloped nanocomplexes (ENCPs), with procedures previously developed by ourselves. The particles are bigger than the ones synthesized with the un-modified polymer and their size increased when the antibody is introduced in the formulation. This is an indication for the association of BVZ, even if more studies for evaluating the exact amount of associated protein should be done. The liquid storage of the formulation was also evaluated, finding that the antibody is the main source of

instability. This result is in line with the literature data and with what presented in this manuscript. Cells internalization assays have also been done for evaluating the capacity of the ENCPs for delivering the drug to the intracellular environment of breast cancer cells. Results suggest that the carrier could potentially allow the BVZ penetration inside the cells and the cationic surfactant which form the particles seem to be an important actor in the internalization process. More experiments regarding the real benefits of the glutamine-modified HA on the uptake and accumulation of the ENCPs by the cancer cells should be done.

2. Materials and Methods

2.1 Chemicals

Fmoc-L-glutamine (Fmoc-Gln), 4-(4,6-Dimethoxy-1,3,5-triazin-2-yl)-4-methylmorpholinium chloride (DMTMM), *N,N'*-Dicyclohexylcarbodiimide (DCC), piperidine, 2-(N-Morpholino) ethanesulfonic acid hydrate (MES) and 4-Dimethylaminopyridine were bought from Sigma. 1-Hydroxybenzotriazole hydrate (HOBt) was bought from Fluka while O-(N-Trt-3-aminopropyl)-O'-(3-aminpropyl)-diethyleneglycol (Trt-NH-PEG-NH_2) was bought from Novabiochem. Hyaluronic Acid (HA, 47 – 57 kDa) was purchased from Lifecore Biomedical (USA). Snakeskin dialysis membranes 16 mm-3.5 kDa were purchased from Thermofisher scientific. Bevacizumab was a gift from mAbxience (Spain). Ethyl Lauryl Arginate (LAE) was a gift from Vedeqsa (Spain). FITC and Centripure mini desalt Z-50 spin columns were purchased from emp BIOTECH.

2.2 Coupling of Trt-NH-PEG$_2$-NH$_2$ to Fmoc-L-glutamine and TrT deprotection

The aminoacid (Fmoc-glutamine, 368 Da, 0.69 mmol) was weighted in a round bottom flask and was then dissolved in 3.5 mL of anhydrous DMF. Trt-NH-PEG-NH_2 (462.62 Da, 0.23 mmol) and triethylamine (101.2 Da, 0.69 mmol) where added to the flask and stirred for 30 minutes. The reaction was then cooled to 0°C and HOBt (153.1 Da, 1.38 mmol) and DCC (206.3 Da, 0.92 mmol) were added to the reaction as coupling agents. All the reactions were performed with argon atmosphere. The reaction was left under stirring for 2 days and the dicyclohexylurea formed was filtered using the buckner funnel. The DMF was then evaporated under reduced atmosphere (stripping with methanol) and the product (812 Da) was dried under vacuum o.n. The compound was then purified by silica gel flash column chromatography (eluent used: ethyl acetate:methanol – 9:1). All the reactions and the purification steps have been monitored with thin layer chromatography (UV visible light and Dragendorff reagent). After the purification both NMR and mass spectra analysis have been performed on the product. The Trt protecting group was then cleaved in an ice cold solution (20 minutes) of 20% trifluoroacetic acid (TFA) in 2 mL of methylene chloride for 3 hours. The solution containing the final product (570 Da) was then concentrated under reduced pressure and the excess of TFA stripped two times with toluene at 30°C and two times with chloroform. After the compound (Fmoc-L-Glutamine-NH-PEG-NH_2) has been dried under vacuum o.n., a film is finally obtained (>90 % yield). NMR and mass spectra analysis have been done to confirm the deprotection.

2.3 Coupling of hyaluronic acid with Fmoc-L-Glutamine-NH-PEG-NH_2 (Gln-mod-HA)

The hyaluronic acid (HA 52 kDa, 9 x 10^{-4} mmol) was dissolved in 40 mL of MES buffer pH 5.5-50 mM (2 hours hydration). 4-(4,6-Dimethoxy-1,3,5-triazin-2-yl)-4-methylmorpholinium chloride (DMTMM, 276.72 Da, 0.41 mmol) was added in solid form to the HA solution and the reaction was left to proceed for 1 hour for the activation of the carboxylic acids on the HA molecules. The Fmoc-L-Glutamine-NH-$(PEG)_2$-NH_2 previously synthesized (570 Da, 0.14 mmol) was dissolved in 1 mL DMF, added to the reaction mixture and the reaction stirred o.n. DMF was then dropped until the solution became clear (reaching a total volume of 100 mL), the coupling agent was added again (0.41 mmol) and the reaction was stirred for further 24 hours. The course of the reaction was monitored using thin liquid chromatography (UV visible light).The solution was dialyzed with 14 kDa cut off dialysis membranes for 5 days. For the first hour the reaction was dialyzed against H_2O:DMF – 2:1, while for the following cycles H_2O:DMSO was used (2:1 for the first 2 days and 8:1 for the following ones). The product (Fmoc-L-Glutamine-NH-PEG modified hyaluronic acid) was then concentrated and precipitated with ethyl acetate. The amount of polymer attached to the HA was quantified both by UV and NMR (the presence of Fmoc was detected). The Fmoc was then cleaved with piperidine. Briefly, the polymer was dissolved in a mixture of H_2O:DMF – 8:1 and piperidine (29% v/v in water) was added to the polymer solution under stirring. After 1 hour, the reaction mixture was dialyzed against water for 5 days (membrane cut – off-3.5 kDa). The obtained polymer (L-Glutamine-NH-PEG modified hyaluronic acid) was analyzed by NMR.

2.6 Synthesis of blank and Gln-mod-HA BVZ-loaded ENCPs

The procedure used to produce the nanocomplexes is similar to the one used in chapter IV (paragraph 2.2). Briefly, blank ENCPs were prepared mixing 250 µL of LAE (8 mg/mL) with 500 µL of unmodified HA (0.5 mg/mL – previously selected) under stirring (15 minutes – 900 rpm). Positively charged nanocomplexes are formed. Then, 500 µL were withdrawn and 500 µL of the Gln-mod-HA solution were added on the top of the LAE/HA positively charged nanocomplex under stirring (500 rpm – 15 minutes). ENCPs with the wanted properties were formed.

BVZ was then associated to the ENCPs. Briefly, 260 µL of the antibody (corresponding to 375 µg) were dropped into the LAE solution (8 mg/mL) under stirring (300 rpm – 15 minutes). The BVZ/LAE solution was then added into the one of HA, as done when forming the blank ENCPs. The Gln-mod-HA solution was then added as for the blank ENCPs.

2.7 Storage stability of the ENCPs

The selected nanosystems have been evaluated for their storage stability in a liquid form at 4°C measuring their size and MCR for one week once stored (data at day 1, 4 and 7 were measured).

2.8 FITC labeling of BVZ

A volume of 13.2 µL of 1M sodium bicarbonate solution, pH 8.5, was added to 66 uL of the BVZ solution (15.2 mg/mL). Then, 10 µL of a 2 mM FITC solution (prepared in DMSO) were pipetted into the protein solution and stirred for 2 hours. Centripure mini desalt Z-50 spin columns were used to purify the labeled antibody.

2.9 Cell line and culture conditions

Human breast basal epithelial cancer cells (MDA-MB-231) were obtained from ATCC and maintained in Leibovitz's L15 medium supplemented with 15% (v/v) fetal bovine serum (FBS), glutamine (2 mM) and sodium hydrogen carbonate (20 mM). Cells were maintained in a humid atmosphere at 37 °C with 5% CO_2.

2.8 Uptake of the BVZ associated to the Gln-mod-HA ENCPs by MDA-MB-231 cells

The uptake of the BVZ associated to the Gln-mod-HA ENCPs has been evaluated by confocal laser scan microscopy (SP5 Leica AOBS-SP5). Briefly, 24 hours before the experiments, cells were seeded at a density of 100.000 cell/mL on 12 mm diameter treated coverslips, previously placed in a 24 wells plate. The BVZ was then labeled and the ENCPs produced. Cells were then incubated with the samples (i.e. Gln-mod-HA BVZ-loaded ENCPs, free BVZ, LAE+free BVZ) for 3 hours and the cells fixed with PFA 4% (15 minutes, room temperature), permeabilized with Triton-X 0.2 % (v/v) (10 minutes, room temperature) and counterstained with DAPI (1 µg/mL in PBS for 30 minutes). The samples were then analyzed with the microscope.

3. Results and discussion

3.1 Synthesis of Gln-mod-HA

The addiction of cancer cells for glutamine is well known and is a direct consequence of the Warburg effect. Different works in the literature investigate the effect of glutamine deprivation strategies on the cancer cells, showing that this aminoacid is fundamental for the cancer cell growth and survival [12–14]. A similar concept could be investigated exploiting the cancer glutamine avidity as a metabolic targeting for accumulating nanoparticles at the tumor site. In this regard, a glutamine modified hyaluronic has been synthesized and used to produce ENCPs. A Fmoc protected glutamine (Fmoc-Gln) was joint to a Trt-protected PEG spacer (Trt-NHPEG-NH_2) using a DCC/HOBt coupling system (Figure 3.1.A, step 1). These coupling agents have been chosen over the more common DCC/NHS chemistry since enabled better reaction performances. Glutamine could have been coupled directly to the hyaluronic acid, but we decided to use a PEG molecule as spacer for the aminoacid to be exposed and accessible for cancer cells. The Trt-protecting group was necessary for avoiding the modification of both the extremities of PEG with two molecules of glutamine. In a second step, the Trt group was removed using cold trifluoroacetic acid (Figure 3.1.A, step 2). The glutamine modified PEG have been obtained with high yield (>90 %). All the products were analyzed by MS (Figure 3.1.B and 3.1.C) and NMR (data not shown) for proving their formation.

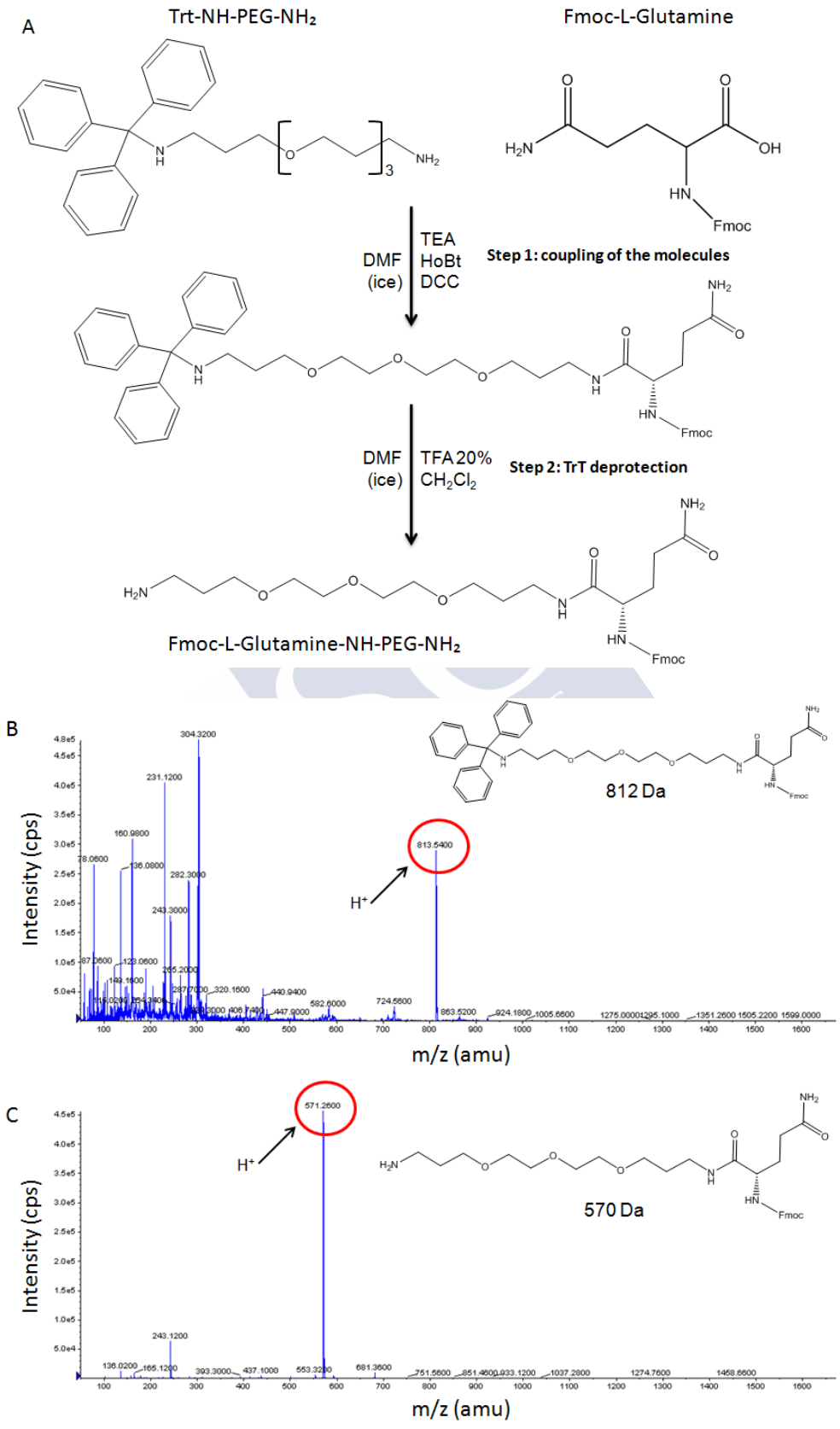

Figure 3.1. A) Reaction scheme for the synthesis of Fmoc-L-Glutamine-NH-PEG-NH_2. Step 1 indicates the coupling of the 2 molecules through the reaction of the amino group of Trt-NH-PEG-NH_2 and the carboxylic group of Fmoc -Glutamine. Step 2

indicates the deprotection of the TrT group through an acidic cleavage in order for the amine group of Fmoc-L-Glutamine-NH-PEG-NH_2 to be available for further reactions. B) Mass spectra of the Fmoc-L-Glutamine-NH-PEG-NH-TrT (molecule after step 1). C) Mass spectra of Fmoc-L-Glutamine-NH-PEG-NH_2 (molecule after step 2).

The obtained molecule was then coupled to the hyaluronic acid using DMTMM as coupling agent (Figure 3.2.A, step 1). The more common EDC/NHS chemistry have been also tested, but low reactions yields have been obtained (data not shown). In fact, one of the main problems of EDC is its instability in water, which could result in low reactions yields [16]. On the other hand, DMTMM is very stable in aqueous media and for this reason it is used for bioconjugation reactions [16,17]. Moreover, the EDC/NHS chemistry is very sensitive to pH, while DMTMM can work both at acidic and alkaline pH [16]. A double addition of the coupling agent was necessary to complete the reaction. The modification was proved by the appearance of the Fmoc signal after the analysis of the product by NMR (Figure 3.2.B, polymer dissolved in D_2O).

The degree of modification (DS) was evaluated with both fluorescence and NMR. In fact, the fluorescent properties of the Fmoc group were used for calculating the amount of glutamine attached to the hyaluronic acid polymer, resulting in 12.6% DS. On the other hand, with NMR, the signals of the anomeric protons of HA have been used as reference and compared to the ones of Fmoc for understanding the DS of the molecule, which is around 9.1% (Figure 3.2.C). The two data of degree of modification are quite close one to each other, indicating that the measured DS is a good prediction of the real one.

A

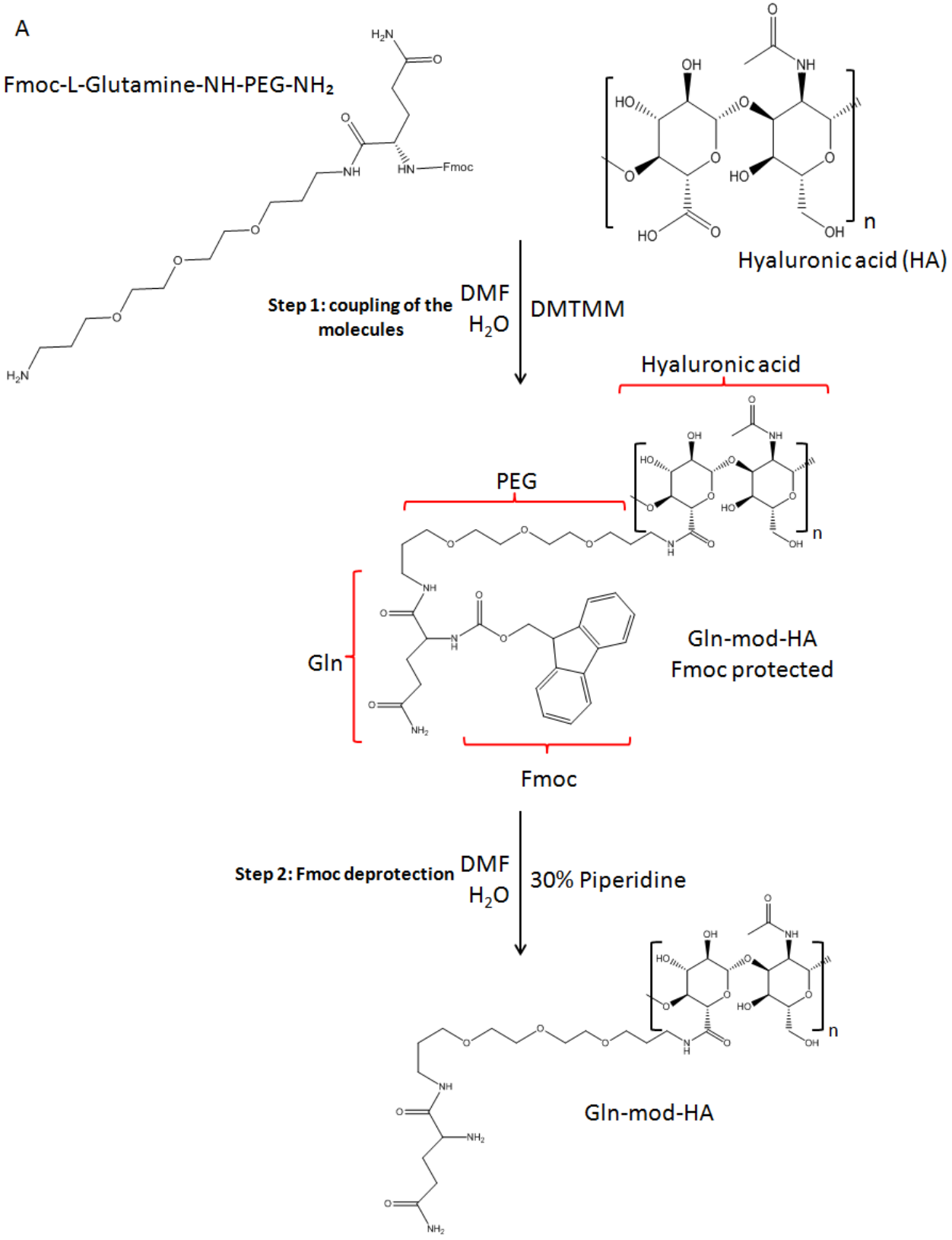
Fmoc-L-Glutamine-NH-PEG-NH2
Hyaluronic acid (HA)
Step 1: coupling of the molecules
DMF
H2O
DMTMM
Hyaluronic acid
PEG
Gln
Gln-mod-HA
Fmoc protected
Fmoc
Step 2: Fmoc deprotection
DMF
H2O
30% Piperidine
Gln-mod-HA

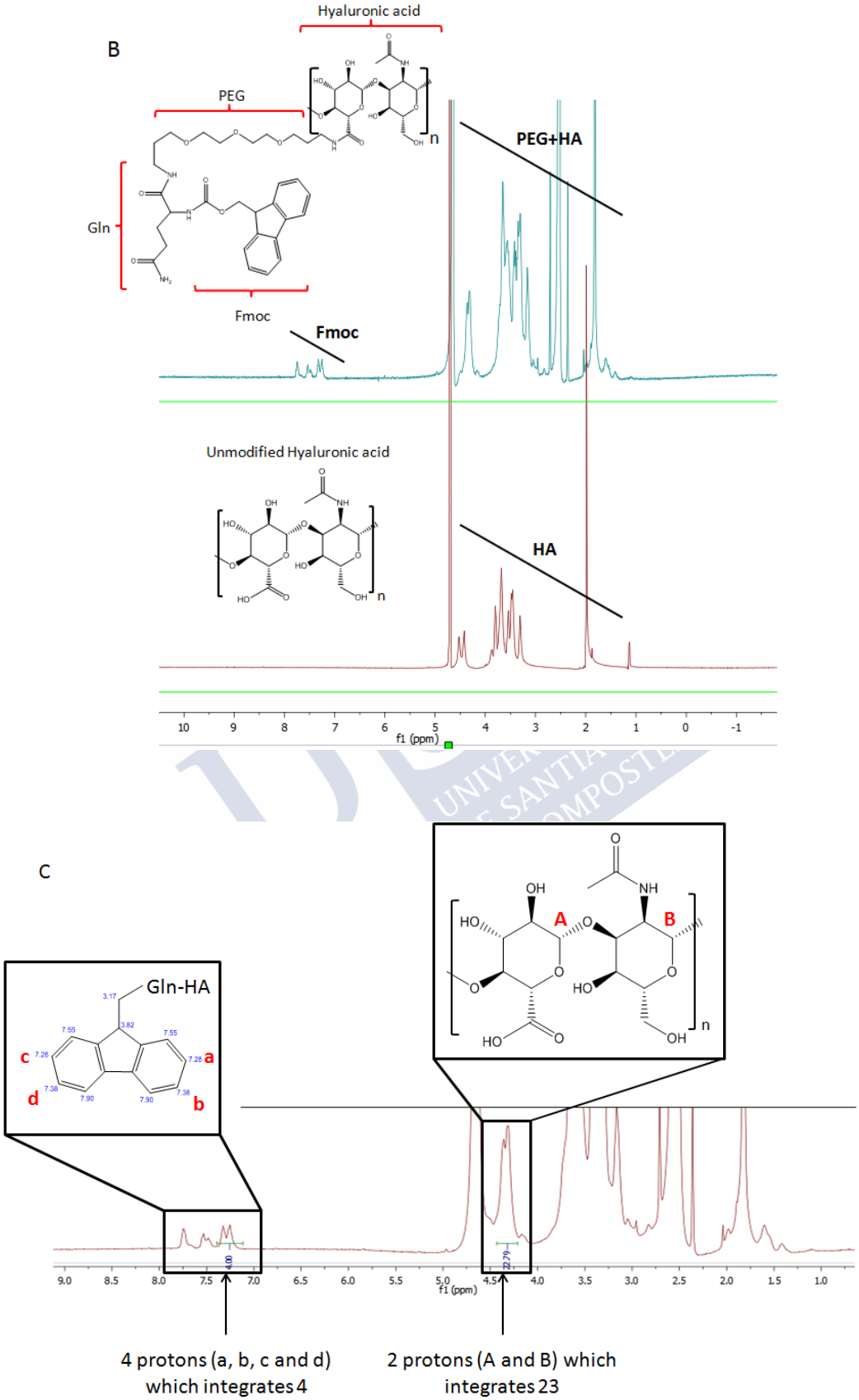

Figure 3.2. A) Reaction scheme for the synthesis of Gln-mod-HA. Step 1: coupling of the free amino group of Fmoc-L-Glutamine-NH-PEG-NH_2 with the carboxylic groups of hyaluronic acid. Step 2: Fmoc deprotection in alkaline conditions. B)

Comparison of the NMR signals of Gln-mod-HA and the unmodified HA: the typical signal of Fmoc appears between 7 and 8 ppm while the signals of the L-Glutamine and PEG fall in the 2-4.5 ppm area (difficult to distinguish due to the presence of the HA signals). The appearance of the peaks is a confirmation for the success of the reaction. The spectra were obtained using D_2O as solvent. C) Calculation of the HA degree of modification by NMR. The signals of Fmoc (the ones of protons a, b, c and d) and of the anomeric carbons of HA (the ones of protons A and B) have been used as references for calculating the degree of modification. 4 protons which integrate 4 (4/4 = 1) and 2 protons which integrate 23 (23/2 = 11.5) mean that 1 carboxylic group each 11.5 got modified by the Fmoc-L-Glutamine-NH-PEG-NH_2, suggesting an approximated degree of modification of 9.1%.

3.2 Synthesis of blank and BVZ-loaded hyaluronic acid (HA) ENCPs using the Gln-mod-HA

The same procedure used for producing the BVZ-loaded HA ENCPs (375 µg) (see Chapter IV) have been here used for the production of the Gln-mod-HA ENCPs. The amount of Gln-mod-HA to be used was optimized, discovering that 1 mg was the minimum amount for forming the nanocarrier (Table 3.1). It is interesting to note that also with the unmodified HA it was not possible to obtain ENCPs with less than 1 mg (see Chapter IV). However, ENCPs formed with 1 mg of the unmodified HA where smaller compare to the ones formed with the Gln-mod-HA (Chapter IV and Figure 3.3). This could be due to the presence of PEG and L-Glutamine, which could contribute in expanding the structure of the nanocarrier. Further investigations regarding the structure of the Gln-mod-HA BVZ-loaded ENCPs could be done using transmission and scanning electron microscopy.

The presence of the antibody led to a drastic increase of the particle size of the BVZ-loaded ENCPs, whereas the zeta potential values remained unmodified (Table 3.2). The negative zeta potential values, similar for the un-modified and modified HA-based nanocarriers, indicate that the attachment of L-Glutamine-NH-PEG-NH_2 moieties to some of the carboxylic groups of HA has a minor effect on the overall surface charge of the nanocarriers.

Table 3.1. Optimization of the amount of Gln-mod-HA for producing the blank ENCPs.

Gln-mod-HA (mg)	Size (nm)	ζ (mV)
0.25	Aggregates	
0.5	Aggregates	
1	265±36	-26

Table 3.2. Physico-chemical properties of the Gln-mod-HA blank and BVZ-loaded ENCPs.

Sample	Size (nm)	ζ (mV)	PDI
Gln-mod-HA blank ENCPs	175±1	-28	0.1
Gln-mod-HA BVZ-loaded ENCPs	257±44	-26	0.2

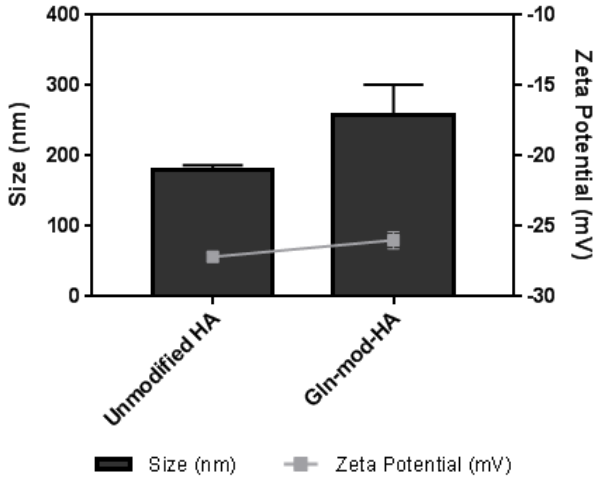

Figure 3.3. Comparison between the BVZ-loaded HA ENCPs synthesized with the unmodified HA polymer and with the Gln-mod-HA polymer. Size and zeta potential are indicated in the graph.

3.3 Storage stability of Gln-mod-HA blank and BVZ-loaded ENCPs

The liquid storage of the nanosystem has also been evaluated. As observed for the BVZ-loaded ENCPs (375 µg) produced with the unmodified HA (Chapter IV), the presence of the antibody is destabilizing the nanocarrier. In fact, the blank ENCPs are able to maintain their size for at least 7 days, while the BVZ-loaded ones increased their size after only one day (reaching values around 400 nm, as shown in Figure 3.4.A). The instability of the Gln-mod-HA BVZ-loaded ENCPs is well described by the gradual drop of the MCR, which after one week decreased to values below the 50% of the original one (Figure 3.4.B). A drop in MCR has also been measured with blank ENCPs after 7 days, even if less pronounced compare to the one of the Gln-mod-HA BVZ-loaded ENCPs.

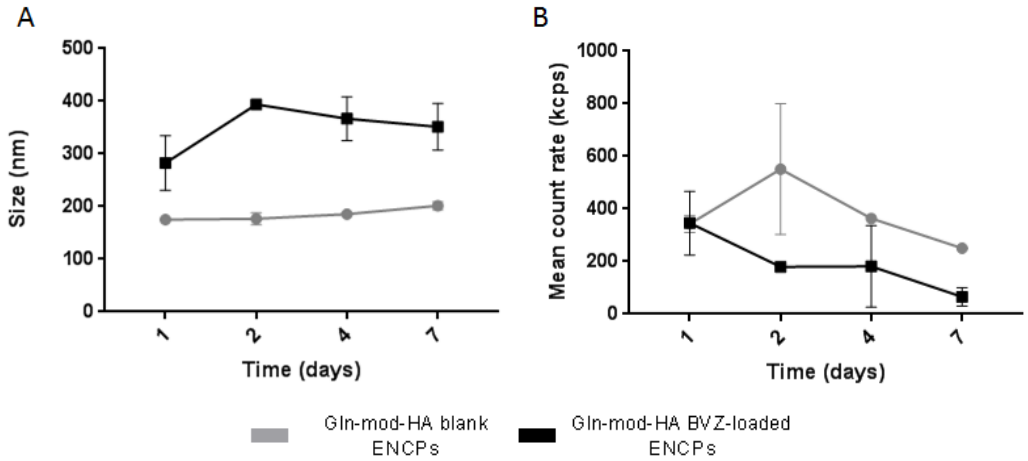

Figure 3.4. Liquid storage stability of the blank and BVZ-loaded ENCPs synthesized with the Gln-mod-HA. Size (A) and MCR (B) are represented in the graphs.

3.4 Uptake of the BVZ associated to the Gln-mod-HA ENCPs by MDA-MB-231 cells

The uptake of the BVZ associated to the Gln-mod-HA ENCPs has been evaluated by confocal microscope. The results of Figure 3.5 indicate that, apparently, the nanocarriers are able to deliver the BVZ in the intracellular environment of the cancer cells. On the other hand, the results showed

that the cationic surfactant (LAE) could be the main responsible for the delivery, since the BVZ is internalized also when given in combination with LAE (see Figure 3.5, LAE+Free BVZ). This result is in line with literature data, where it is indicated that cationic surfactants help the delivery of molecule in the intracellular environment of cells [18]. Nevertheless, further experiments are required in order to asses if the Gln-mod-HA ENCPs and the associated BVZ are internalized into the cells, or rather adsorbed onto the cell membrane. In addition, experiments aimed at evaluating the toxicity of the ENCPs should also be performed.

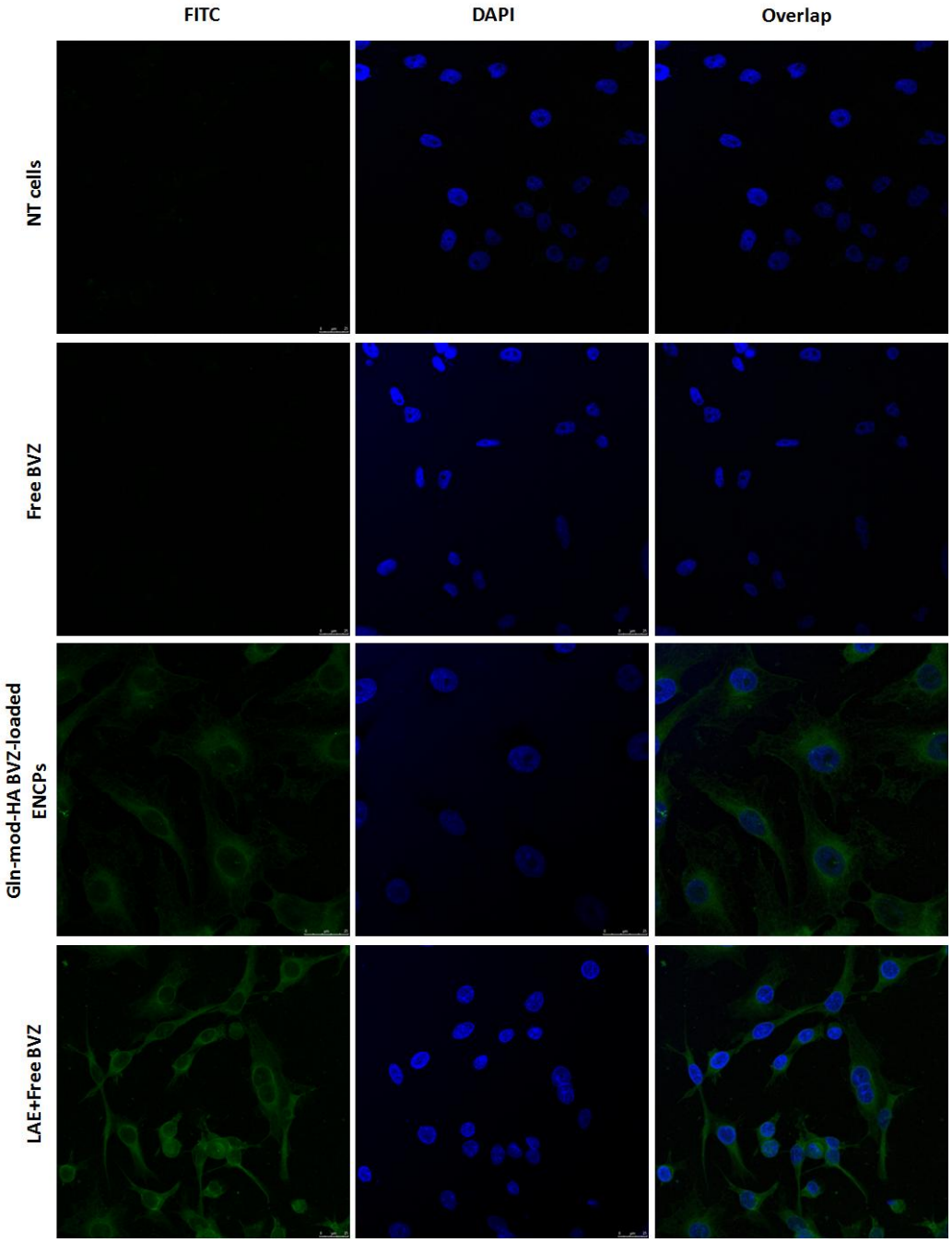

Figure 3.5. Confocal microscope images for evaluating the internalization of the BVZ associated to the Gln-mod-HA ENCPs. Controls with non treated cells and non encapsulated BVZ (free BVZ) have been done.

5. Conclusions

Here we report the synthesis of a new polymer consisting of Gln-mod-HA and the production BVZ-loaded nanoparticles made of this polymer. The degree of modification of HA with the glutamine moieties have been estimated to be between 9.1% (by NMR) and 12.6% (fluorescence). Further investigations could be done using scanning (SEM) or transmission (TEM) electron microscopy, to obtain more information related to the structure of the nanocarrier. In vitro cell culture studies showed the capacity of the nanosystem to interact with cancer cells. More detailed characterization studies together with a rigorous evaluation of the in vitro/in vivo performance of the nanocarrier would be necessary in order to assess the value of this potential new targeted delivery technology.

Acknowledgments

This work was supported by the European Union's Horizon 2020 - Research and Innovation Framework Programme under the Marie Sklodowska - Curie Grant agreement No. 642028 (NABBA).

Bibliography

[1] E. Pérez-Herrero, A. Fernández-Medarde, Advanced targeted therapies in cancer: Drug nanocarriers, the future of chemotherapy, Eur. J. Pharm. Biopharm. 93 (2015) 52–79. doi:10.1016/j.ejpb.2015.03.018.

[2] Y. Nakamura, A. Mochida, P.L. Choyke, H. Kobayashi, Nanodrug Delivery: Is the Enhanced Permeability and Retention Effect Sufficient for Curing Cancer?, Bioconjug. Chem. 27 (2016) 2225–2238. doi:10.1021/acs.bioconjchem.6b00437.

[3] A.D. Wong, M. Ye, M.B. Ulmschneider, P.C. Searson, Quantitative Analysis of the Enhanced Permeation and Retention (EPR) Effect, PLOS Oe. (2015) 1–13. doi:10.1371/journal.pone.0123461.

[4] P. Kumari, B. Ghosh, S. Biswas, Nanocarriers for cancer-targeted drug delivery, J. Drug Target. (2015) 1–13. doi:10.3109/1061186X.2015.1051049.

[5] W.C. Chen, A.X. Zhang, S. Li, Limitations and niches of the active targeting approach for nanoparticle drug delivery, Eur. J. Nanomedicine. 4 (2012) 89–93. doi:10.1515/ejnm-2012-0010.

[6] C.L. Ventola, Progress in Nanomedicine : Approved and Investigational Nanodrugs Progress in Nanomedicine :, Pharm. Ther. 42 (2017) 742–755.

[7] M.E. Davis, Z.G. Chen, D.M. Shin, Nanoparticle therapeutics : an emerging treatment modality for cancer, Nat. Rev. Drug Discov. 7 (2008) 771–782. doi:10.1038/nrd2614.

[8] H.S.S. Qhattal, X. Liu, Characterization of CD44-Mediated Cancer Cell Uptake and Intracellular Distribution of Hyaluronan-Grafted Liposomes, Mol. Pharm. 8 (2012) 1233–1246. doi:10.1021/mp2000428.Characterization.

[9] R.J. DeBerardinis, J.J. Lum, G. Hatzivassiliou, C.B. Thompson, The Biology of Cancer: Metabolic Reprogramming Fuels Cell Growth and Proliferation, Cell Press. 7 (2008) 11–20. doi:10.1016/j.cmet.2007.10.002.

[10] P.P. Hsu, D.M. Sabatini, Cancer Cell Metabolism: Warburg and Beyond, Cell. 134 (2008) 703–707. doi:10.1016/j.cell.2008.08.021.

[11] D.R. Wise, C.B. Thompson, Glutamine Addiction: A New Therapeutic Target in Cancer, Trend Biochem. Sci. 35 (2011) 427–433. doi:10.1016/j.tibs.2010.05.003.Glutamine.

[12] L. Chen, H. Cui, Targeting Glutamine Induces Apoptosis: A Cancer Therapy Approach, Int. J.

Mol. Sci. 16 (2015) 22830–22855. doi:10.3390/ijms160922830.

[13] M. Hassanein, J. Qian, M.D. Hoeksema, J. Wang, M. Jacobovitz, R. Eisenberg, P.P. Massion, Targeting SLC1A5-mediated glutamine dependence in non-small cell lung cancer Mohamed, Int. J. Cancer. 137 (2015) 1587–1597. doi:10.1002/ijc.29535.Targeting.

[14] P. Korangath, W.W. Teo, H. Sadik, L. Han, N. Mori, C.M. Huijts, F. Wildes, S. Bharti, Z. Zhang, C.A. Santa-maria, H. Tsai, C. V Dang, V. Stearns, Z.M. Bhujwalla, S. Sukumar, Targeting Glutamine Metabolism in Breast Cancer with Aminooxyacetate, Clin. Cancer Res. 21 (2015) 3263–3274. doi:10.1158/1078-0432.CCR-14-1200.

[15] G.R. Rivera-rodríguez, M.J. Alonso, D. Torres, Poly- L-asparagine nanocapsules as anticancer drug delivery vehicles, Eur. J. Pharm. Biopharm. 85 (2013) 481–487. doi:10.1016/j.ejpb.2013.08.001.

[16] M. D'Este, D. Eglin, M. Alini, A systematic analysis of DMTMM vs EDC/NHS for ligation of amines to Hyaluronan in water, Carbohydr. Polym. 108 (2014) 239–246. doi:10.1016/j.carbpol.2014.02.070.

[17] S.A. Raw, An improved process for the synthesis of DMTMM-based coupling reagents, Tetrahedron Lett. 50 (2009) 946–948. doi:10.1016/j.tetlet.2008.12.047.

[18] S. Inàcio, K.A. Mesquita, M. Baptista, In Vitro Surfactant Structure-Toxicity Relationships: Implications for Surfactant Use in Sexually Transmitted Infection Prophylaxis and Contraception, PLoS One. 6 (2011) 1–15. doi:10.1371/journal.pone.0019850.

USC
UNIVERSIDADE
DE SANTIAGO
DE COMPOSTELA

List of abbreviations

USC
UNIVERSIDADE
DE SANTIAGO
DE COMPOSTELA

AA: acrylic acid

ADCC: antibody-dependent cell-mediated cytotoxicity

AE (%): association efficiency (%), calculated as *100 x associated peptide mass/total peptide mass*

AE (%): association efficiency (%), calculated as *100 x associated peptide mass/total peptide mass*

BMP-2: bone morphogenetic protein-2

BP: phosphate buffer pH 7.2 (10mM Na_2HPO_3)

BSA/BP-loaded HA nanocomplexes: HA based nanocomplexes loaded with BSA and produced using phosphate buffer (BP) as formulation media

BSA/IgG/MQ-loaded HA nanocomplexes (150 μg): HA based nanocomplexes loaded with both BSA and 150 μg of IgG and produced using milliQ water (MQ) as formulation media

BSA/IgG/MQ-loaded HA nanocomplexes (400 μg): HA based nanocomplexes loaded with both BSA and 150 μg of IgG and produced using phosphate buffer (BP) as formulation media

BSA/MQ-loaded HA nanocomplexes: HA based nanocomplexes loaded with BSA and produced using milliQ water (MQ) as formulation media

BSA: bovine serum albumin

BSAO: Bovin Serum Albumin Oxidase

BVZ -loaded HA ENCPs (375 μg): HA enveloped nanocomplexes loaded with 375 μg of BVZ (higher amount)

BVZ: bevacizumab

BVZ-loaded HA ENCPs (75 μg): HA enveloped nanocomplexes loaded with 75 μg of BVZ (lower amount)

CC: Cytochrome C

CD: circular dichroism

CD44: cluster of differentiation 44

DCC: *N,N'*-Dicyclohexylcarbodiimide

DMF: dimethylformamide

DMSO: dimethyl sulfoxide

DMTMM: 4-(4,6-Dimethoxy-1,3,5-triazin-2-yl)-4-methylmorpholinium chloride

EGF: epidermal growth factor

EGFR: epidermal growth factor receptor

ELISA: enzyme-linked immunosorbent assay

EMA: Europeans medicines agency

ENCPs: enveloped nanocomplexes

ENCPs: enveloped nanocomplexes

FBS: fetal bovine serum

FcRn: neonatal Fc receptor

FDA: food and drug administration

FGF: fibroblast growth factor

FITC: fluorescein isothiocyanate

GFP: green fluorescent protein

Gln: glutamine

Gln-mod-HA BVZ-loaded ENCPs: nanocomplexes produced with the glutamine-modified hyaluronic acid and associating bevacizumab

Gln-mod-HA ENCPs: enveloped nanocomplexes produced with the glutamine-modified hyaluronic acid

Gln-mod-HA: glutamine modified hyaluronic acid

GrB: grandzyme-B

HA: hyaluronic acid

HIF-1: hypoxia-inducible factor-1

h-KDR: human-KDR

HOBt: 1-Hydroxybenzotriazole hydrate

HPLC: high performance liquid chromatography

HSA: human serum albumin

h-VEGF-A: human-VEGF-A

h-VEGF-B: human-VEGF-B

h-VEGF-C: human-VEGF-C

IgG/MQ-loaded nanocomplexes (150 μg): HA based nanocomplexes loaded with 150 μg of IgG and produced using milliQ water (MQ) as formulation media

IgG/MQ-loaded nanocomplexes (400 μg): HA based nanocomplexes loaded with 400 μg of IgG and produced using milliQ water (MQ) as formulation media

IgG: model antibody associated to the developed nanosystems

INF-α: interferon alpha

LAE: ethyl lauroyl arginate

Layer-by-layer PArg/HA ENCPs: multiple layer enveloped nanocomplexes resulting from the subsequent addition of a poly-L-arginine (PArg) and an HA layers on the top of the BSA/IgG/MQ-loaded HA nanocomplexes)

LC (%): loading capacity (%), calculated as *100 x protein mass loaded/total formulation mass*

LYVE-1: Lymphatic vessel endothelial hyaluronan receptor 1

MAA: methacrylic acid

mAbs: monoclonal antibodies

MCR: mean count rate

MCR: mean count rate

MES: 2-(N-Morpholino)ethanesulfonic acid hydrate

MMA: methacrylic acid

MQ: milliQ water

MW: molecular weight

NMR: nuclear magnetic resonance

OVA: ovalbumin

pAbs: polyclonal antibodies

PACA: poly(alkylcyanoacrylates)

PBS: phosphate buffer saline (137 mM NaCl, 2.7 mM KCl, 10 mM Na_2HPO_3 y 1.8 mM KH_2PO_4)

PCB: polycarboxybetadine

PDGF: platelet-derived growth factor

PDGF-BB: platelet-derived growth factor

PECs: polyelectrolytes complexes

PEG: polyethylenglycol

PEI: poly(ethylene) imine

PEO: poly(ethylene oxide)

PLA: poly-lactic acid

PLGA: poly(lactic-co-glycolic acid)

PlGF: placenta growth factor

PPO: poly(propylene oxide)

PVA: polyvinylalcohol

RHAMM: Hyaluronan-mediated motility receptor

rHBsAg: recombinant hepatitis B surface antigen

SBF: simulated biological fluids

sCT: salmon calcitonin

SDS: sodium dodecyl sulphate

SEM: scanning electron microscopy

SOD: superoxide dismutase

STEM: scanning transmission electronic microscopy

TAM: tumor associated microphages

TEM: transmission electron microscope

TFA: trifluoroacetic acid

TPP: tripolyphosphate

TRIAL: tumor necrosis factor-related apoptosis inducing ligand

v/v: volume/volume

VEGFR1: VEGF receptor 1

VEGFR2: VEGF receptor 2

W/O: water-in-oil

w/v: weight/volume

w/w: weight/weight

Ethical considerations

USC
UNIVERSIDADE
DE SANTIAGO
DE COMPOSTELA

Animal studies

The efficacy studies on animals (Chapter IV) were done in the Université Paris-Sud, authorized by the Ministére de l'enseignement supérieur (articles R.214-87 à R.214-126 of the code rural et de la pêche maritime). All the experimental protocols were approved by the Animal Care Committee of the Université Paris-Sud in accordance with the principles of laboratory animal care and with the French legislation (n°APAFIS#13238-2018012911422090v1). The study has been evaluated and approved by the ethical committee N°026 related to the animal experiments.